Al-Shihri, Marai Abdullah

BUCKLING STRENGTH OF HEAVY STEEL COLUMNS

The University of Arizona M.S. 1986

University
Microfilms
International 300 N. Zeeb Road, Ann Arbor, MI 48106

PLEASE NOTE:

In all cases this material has been filmed in the best possible way from the available copy. Problems encountered with this document have been identified here with a check mark __√__.

1. Glossy photographs or pages ______
2. Colored illustrations, paper or print ______
3. Photographs with dark background ______
4. Illustrations are poor copy ______
5. Pages with black marks, not original copy ______
6. Print shows through as there is text on both sides of page ______
7. Indistinct, broken or small print on several pages __√__
8. Print exceeds margin requirements ______
9. Tightly bound copy with print lost in spine ______
10. Computer printout pages with indistinct print ______
11. Page(s) ______ lacking when material received, and not available from school or author.
12. Page(s) ______ seem to be missing in numbering only as text follows.
13. Two pages numbered ______. Text follows.
14. Curling and wrinkled pages ______
15. Dissertation contains pages with print at a slant, filmed as received __√__
16. Other ______

BUCKLING STRENGTH OF HEAVY STEEL COLUMNS

by

Marai Abdullah Al-Shihri

A Thesis Submitted to the Faculty of the

DEPARTMENT OF CIVIL ENGINEERING AND ENGINEERING MECHANICS

In Partial Fulfillment of the Requirements
For the Degree of

MASTER OF SCIENCE
WITH A MAJOR IN CIVIL ENGINEERING

In the Graduate College

THE UNIVERSITY OF ARIZONA

1 9 8 6

STATEMENT BY AUTHOR

This thesis has been submitted in partial fulfillment of requirements for an advanced degree at The University of Arizona and is deposited in the University Library to be made available to borrowers under rules of the Library.

Brief quotations from this thesis are allowable without special permission, provided that accurate acknowledgment of source is made. Requests for permission for extended quotation from or reproduction of this manuscript in whole or in part may be granted by the head of the major department or the Dean of the Graduate College when in his or her judgment the proposed use of the material is in the interests of scholarship. In all other instances, however, permission must be obtained from the author.

SIGNED: Marai A. Al-Shihri

APPROVAL BY THESIS DIRECTOR

This thesis has been approved on the date shown below:

Reidar Bjorhovde
R. BJORHOVDE
Professor of Civil Engineering
and Engineering Mechanics

9/10/86
Date

ACKNOWLEDGMENTS

The author would like to express his deepest appreciation to Dr. Reidar Bjorhovde, who initiated and supervised this investigation.

I wish to convey my sincere gratitude to my wife, without whose patience and encouragement this research would not be completed.

TABLE OF CONTENTS

TABLE OF CONTENTS--Continued

LIST OF ILLUSTRATIONS

LIST OF ILLUSTRATIONS--Continued

LIST OF ILLUSTRATIONS--Continued

LIST OF ILLUSTRATIONS--Continued

LIST OF ILLUSTRATIONS--Continued

LIST OF ILLUSTRATIONS--Continued

LIST OF ILLUSTRATIONS--Continued

LIST OF ILLUSTRATIONS--Continued

LIST OF ILLUSTRATIONS--Continued

LIST OF ILLUSTRATIONS--Continued

LIST OF ILLUSTRATIONS--Continued

ST OF ILLUSTRATIONS--Continued

LIST OF ILLUSTRATIONS--Continued

LIST OF ILLUSTRATIONS--Continued

LIST OF TABLES

NOMENCLATURE

A	=	Area of the cross section
A_i	=	Area of element i
b	=	Width of the cross section
d	=	Depth of the cross section
e	=	Initial curvature
E		Modulus of elasticity
E_t	=	Tangent modulus
E_r	=	Reduced modulus
I	=	Moment of inertia
L, ℓ	=	Column length
M_{ext}	=	External or applied moment
M_{int}	=	Internal or resisting moment
P_{max}	=	Maximum strength load
P_{cr}	=	Buckling load (= Euler load)
P_r	=	Buckling load(= Reduced modulus load)
P_t	=	Buckling load (= Tangent modulus load)
P_y	=	Cross-sectional yield load
r	=	Radius of gyration
t	=	Flange thickness
V_p	=	Lateral member deflection due to applied load
w	=	Web width

α = Plate-factor, which is a measure of the rate of cooling after rolling $(= \frac{2(b + t)}{bt})$

β = Width-factor, which is a measure of the rate of cooling after rolling $(= \frac{\alpha}{b})$

σ_i = Stresses in element i

σ_y = Overall average yield stress of the cross section

ε_i = Strain in element i

ε_{ri} = Residual strain in element i

ε_p = Axial load strain in element i

ε_y = Overall average yield strain of the cross section

θ = Curvature of the column due to deflection, V_p

ξ_i = Distance from the element centroid to the bending axis

λ = Slenderness ratio $(= \frac{1}{\pi}\sqrt{\frac{\sigma_y}{E}}\ \frac{\ell}{r})$

δ = Sum of initial curvature and lateral displacement

ABSTRACT

The study presented in this thesis was carried out to investigate the strength and behavior of pinned-end, centrally loaded, initially curved, prismatic heavy wide-flange steel members. Both hot-rolled and welded built-up shapes were included in this evaluation, with a variety of steel grades, sizes, manufacturing methods, etc. A mathematical model based on the maximum strength approach was used in the investigation, where all of the primary column strength factors were incorporated.

The results indicate that hot-rolled shapes have a clear correlation between the relative strength and the flange thickness, t. Welded members appear to be less influenced by the flange thickness variation, particularly short and long columns. Furthermore, the initial crookedness of $\ell/1000$ is found to be a fair straightness requirement.

CHAPTER 1

INTRODUCTION

Steel is used as a construction material for a variety of structures and purposes, ranging from residential buildings to industrial plants and cranes, from transmission towers to silos, and for a variety of bridge structures.

The column is one of the primary elements of these structures. Carrying axial load, its strength and behavior have been investigated by many researchers and design engineers for a number of years. These studies have incorporated theoretical evaluations along with experimental work, aiming at determining all of the parameters that influence the column strength, and how they can be accounted for in rational design criteria.

The assumptions that the columns are perfectly straight, made of isotropic and homogenous materials and are free from any internal stresses are convenient to use in theoretical solutions. However, they do not reflect realistic characteristics of columns in structures. Actual structural steel elements display a variety of geometric and material imperfections, such as residual stresses, variation of the yield stress, and initial crookedness. It is known that these imperfections in many cases reduce the structural strength as compared to that of the idealized member. It is therefore necessary to clarify and evaluate the effect of these imperfections in order to determine the strength and behavior of the elements.

Steel columns today are available in different steel grades and shapes, as hot-rolled and welded built-up shapes, in light and heavy configuration. At the present time, the design of heavy members is not different from that of small and medium sizes. Although heavy shapes are widely used in structures such as high-rise buildings, major bridges, and off-shore structures, little information is available on their strength and behavior. The major problem associated with the design of these members is the lack of data on the residual stress distribution and magnitude, the yield stress variation throughout the cross section, and the initial geometric imperfections.

In this investigation, a column maximum strength mathematical model will be used to determine the effect of the different factors which contribute to the strength of heavy columns. In particular, rolled and welded wide-flange columns with flange thickness of 1 inch and larger were examined to provide data that are not currently available for a range of column sizes and shapes.

CHAPTER 2

SCOPE OF INVESTIGATION

The primary aim of this study is to examine the behavior and strength of pinned-end heavy columns. Both hot-rolled and welded built-up wide-flange shapes in the most common structural steel grades will be evaluated.

The major column strength parameters have been incorporated into the maximum strength model that is used in this investigation. The parameters are the residual stress, the variation of the yield stress throughout the cross section, and the initial out-of-straightness.

Data on heavy column strength are scarce. In particular, columns whose component plate thicknesses exceed 1 inch therefore will be examined. This will include development of appropriate column strength curves for heavy steel shapes.

CHAPTER 3

HISTORICAL BACKGROUND

In 1729, Musschebroek [1] conducted one of the first investigations on the stability of straight, prismatic, rectangular cross section columns. He derived a formula on the form

$$P = K \frac{bd^2}{\ell^2} \tag{3.1}$$

where

P = column critical load

K = numerical constant

b, d = width and depth of cross section, respectively

ℓ = length of column

Euler [2] developed his well-known expression in 1744 to deal with the column stability problem. He derived his formula based on the equilibrium of the buckled member, proposing an equation on the form

$$P_{cr} = \frac{\pi^2 EI}{\ell^2} \tag{3.2}$$

where

P_{cr} = buckling load

I = moment of inertia

ℓ = length of column

This formula is still used for perfectly straight columns that buckle elastically.

As the research work continued, Engesser and Considere [3, 4, 5] in 1889 independently developed the tangent modulus theory, where the deficiency of the Euler approach was removed by making it possible to take into account the behavior of materials beyond the elastic range. Engesser revised the Euler approach by replacing E with tangent modulus, E_t, in the equation for P_{cr} (Eq. 3.2).

Several researchers voiced doubt about the validity of the tangent modulus approach, which led Engesser to revise his method to one that incorporated elastic unloading of certain fibers in the cross section during column buckling [3, 4, 5].

In this fashion, two values of the modulus were applied to the cross section, and as a result the theory has later become known as the double modulus or reduced modulus approach.

Von Karman [6] derived expressions for the reduced modulus as a function of E and E_t for rectangular and I-sections. He pointed out the significance of cross section shape on the inelastic buckling behavior of columns.

Subsequent studies [4] indicated that in spite of the apparent correctness of the reduced modulus theory, actual column buckling loads turned out to lie closer to the tangent modulus values. This was confirmed by a number of carefully conducted column tests [4].

Shanley [1, 4, 5, 7] was the first to resolve the apparent contradictions between theory and tests. He proved that the reduced modulus theory gives the upper bound and the tangent modulus the lower bound of column strength, which means that the tangent modulus is a reasonable and conservative approach to the inelastic strength of perfectly straight columns.

Although the presence of residual stresses was recognized by Neuman and others [8] since the middle of the nineteenth century, the first published work was presented in 1930 by Ros [8] which was devoted to the study of the distribution and magnitude of residual stresses in hot-rolled shapes. The reduction of the column strength was attributed to the presence of this imperfection [9, 10]. Experimental verification of this effect was provided through extensive studies, primarily at Lehigh University [8, 10, 11, 12, 13, 14] to determine the distribution and magnitude of these internal stresses as well as their effect on column strength and behavior. The studies covered a great variety of steel shapes and grades.

The complexity of the mechanism of residual stress formation made the theoretical evaluation complicated and time-consuming before computers were available. However, Alpsten [8] in 1968 presented a computer model which determine the thermal residual stresses in hot-rolled shapes analytically. This was based on a finite difference solution of the governing heat flow equations.

The tangent modulus approach can be utilized to determine the buckling loads of centrally loaded, perfectly straight columns which contain residual stresses, but it does not apply to members that are initially crooked or that are subjected to end moments cause by an eccentrically applied axial load [5, 12]. Some of these effects were described by Young (1773-1829) [6] who attributed the differences between theoretical and experimental results to the presence of these imperfections. He suggested that the initial column crookedness can be described by a half sine wave which is symmetric about the mid-height of the columns. This concept has since been utilized by many researchers to represent the initial out-of-straightness of structural members.

The maximum strength approach to column buckling was developed by researchers such as Batterman and Johnston [15] Beer and Schultz [16] and Bjorhovde [5]. This solution incorporated all of the different column strength parameters, including the initial column curvature.

Bjorhovde [5] also introduced the concept of probability to study the column response in the inelastic range.

He described the column strength parameters as random variables, and developed a quasi-steady semiprobabilistic maximum strength solution that permitted a complete description of the limit states characteristics of the columns. This solution has since been made the basis for the limit states design standards [17] as well as the recent Load and Resistance Factor Design (LRFD) Specification of the American Institute of Steel Construction (AISC) [18].

The correlation between theory and experiments has become better as more of the column strength parameters have been included in the analysis. Thus, the maximum strength model of Bjorhovde [5] and others predicts the strength to within 5 percent of test values. This degree of accuracy is reflected in the higher level of resistance factors that is used in the design specifications [17, 18].

CHAPTER 4

COLUMN STRENGTH THEORY

4.1 Elastic Behavior of Columns

The Euler formula is applicable to columns which are centrally loaded, free from any internal stresses, and of elastic materials. Consider the column shown in Fig. 4.1. It is initially straight and the load is centrally applied. Equilibrium of the deflected (i.e., buckled) column at any cross section requires that the external and internal moments must be equal:

$$M_{ext} = P \cdot y = -EIy'' = M_{int} \tag{4.1}$$

where M_{ext} is the external and M_{int} is the internal moment, as established through elementary strength of materials theory. The solution for Eq. 4.1 gives the equation that describes the deflection shape of the buckled column. Thus

$$y = A \sin kx + b \cos kx \tag{4.2}$$

where A and B are constants that are found from the boundary conditions, and K is given as:

$$K = \sqrt{\frac{P}{EI}} \tag{4.3}$$

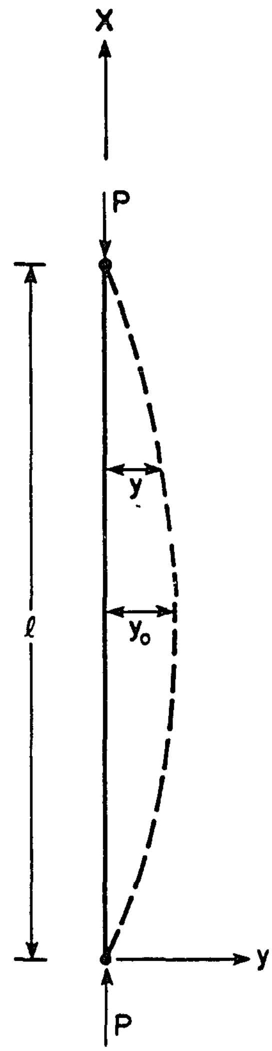

Fig. 4.1. Centrally loaded pinned-end column.

the boundary conditions give B = 0, and the only non-trivial solution results in the requirement

$$\sin k\ell = 0 \tag{4.4}$$

which gives

$$K = \frac{n\pi}{\ell} \tag{4.5}$$

For the first mode of buckling, n = 1, and Eq. 4.5 gives the buckling load as:

$$P_{cr} = \frac{\pi^2 EI}{\ell^2} \tag{4.6}$$

In terms of the average compressive stress at buckling, this becomes

$$\sigma_{cr} = \frac{P_{cr}}{A} = \frac{\pi^2 E}{(\ell/r)^2} \tag{4.7}$$

where the relationship $I = Ar^2$ has been utilized to introduce the slenderness ratio, ℓ/r.

The Euler column buckling load is the upper limit for elastic column strength.

The theory assumes that the members do not have any mechanical or geometric imperfections, while real shapes exhibit numerous deviations. This causes the strength of real columns to be substantially lower than Euler load in many cases, especially as the length gets small.

4.2 Inelastic Behavior of Columns

The previous discussion was limited to perfectly straight columns of elastic materials. in the following, the column strength will be discussed on the basis of more realistic material and member geometry assumptions. These reflect the fact that there are variations of the yield strength throughout the cross section, as well as the presence of residual stresses, initial crookedness, and the non-linear behavior of materials as part of the shape.

The tangent modulus theory was introduced by Engesser and Considere. The modified Euler formula takes into account the inelastic behavior of materials as well as the magnitude and distribution of residual stresses, although the latter was not known by Engesser. It was suggested that the modulus of elasticity of the Euler approach should be replaced by the tangent modulus, E_t, which is equal to the slope of the stress-strain curve for the cross section beyond the proportional limit. This is illustrated in Fig. 4.2. The modified equation is:

$$P_t = \frac{\pi^2 E_t I}{\ell^2} \tag{4.8}$$

where

P_t = buckling load (= tangent modulus load)

E_t = tangent modulus obtained from the stress-strain relationship for the full cross-section, called a stub column curve

ℓ = length of the column

Since E_t is less than E, the load given by Eq. 4.8 is naturally less than that of Eq. 4.6.

Based on criticism that the tangent modulus theory neglected the fact that materials on the convex side would unload elastically while the materials on the concave side would continue loading, Engesser introduced his reduced modulus or double modulus theory. The tangent modulus was therefore replaced by E_r, which is a function of E, E_t, and cross-sectional shape. Consequently, the critical buckling load formula became

$$P_r = \frac{\pi^2 E_r I}{\ell^2} \tag{4.9}$$

where

P_r = buckling load (= reduced modulus load)

E_r = reduced modulus value

The stress distributions in the cross section according to the two theories are illustrated in Fig. 4.3.

For many years the reduced modulus theory was accepted as being the correct theory for column behavior in the inelastic range, although column tests that were carried out in the following years showed that the buckling usually occurred at loads just above the tangent modulus load.

This discrepancy was not resolved until Shanley [4, 7] drew attention to the basic assumption of the

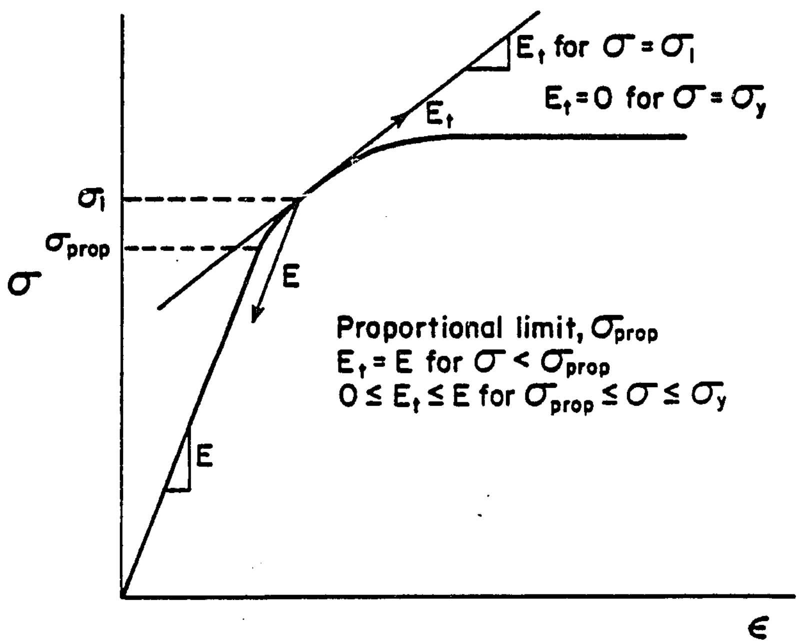

Fig. 4.2. Stub-column curve.

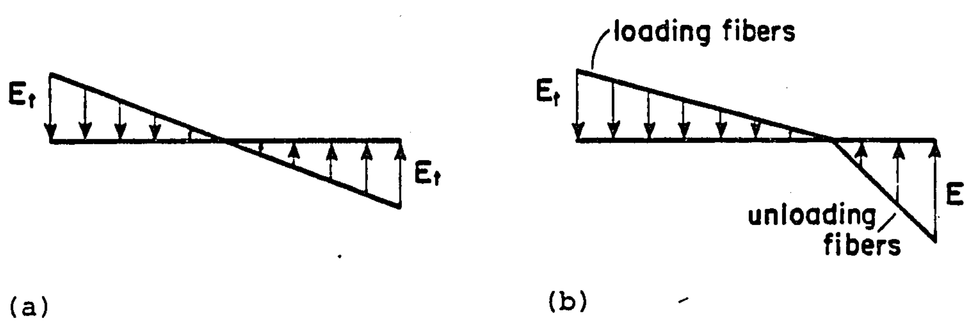

Fig. 4.3. Stress distribution of bent column due to applied load. -- (a) Tangent modulus theory; and (b) Reduced modulus theory.

reduced modulus approach, namely, that the initially perfect straight column remains straight until it reaches the reduced modulus load. He showed that the column will buckle at the tangent modulus load and then continue to deflect while the axial load increases. The tangent modulus load thus was correctly identified as the true buckling load of an inelastic, perfectly straight columns.

The principal defects of the tangent modulus theory are the requirements that the column is free from any initial curvature and that the load is applied concentrically [5]. Although it can deal with inelastic response characteristics, and therefore can account for the presence of residual stresses and non-linear material behavior, it cannot represent members which are initially curved. Actual columns exhibit geometric imperfections; these reduce the load-carrying capacity of the members.

The maximum strength theory was a new evolution in the development of column strength concepts [5]. This approach is based on realistic assumptions of the different parameters which contribute to the column strength and behavior. It takes into account the initial out-of-straightness, actual residual stresses, variation of the yield strength, and other column strength parameters. Since the column will start to bend as soon as the axial load is applied, the column strength and behavior are no longer representative of true buckling phenomenon. Rather, it is a load-deflection problem, and the maximum strength is reached at the point where any further deflection increases must be accompanied by a reduction of the axial load in order to maintain equilibrium. This point is at the peak of the load-deflection curve, as illustrated in Fig. 4.4.

For a given column, the maximum strength is lower than the tangent modulus load, due to the fact that the initial crookedness produces bending moments in the cross section as soon as the axial load is applied. These forces are indicated in Fig. 4.5. In other words, a portion of the axial load capacity is used to resist moment. However, since all structures members will be initially crooked to some extent, it is clear that the maximum strength approach is more correct.

Due to the complexity of the maximum strength approach, no simple formula can be devised along the lines of those for the Euler and the tangent modulus loads, for example. The maximum strength computation requires an incremental, iterative solution procedure that can only be achieved through a numerical approach using a computer. Details of this will be discussed later in this thesis.

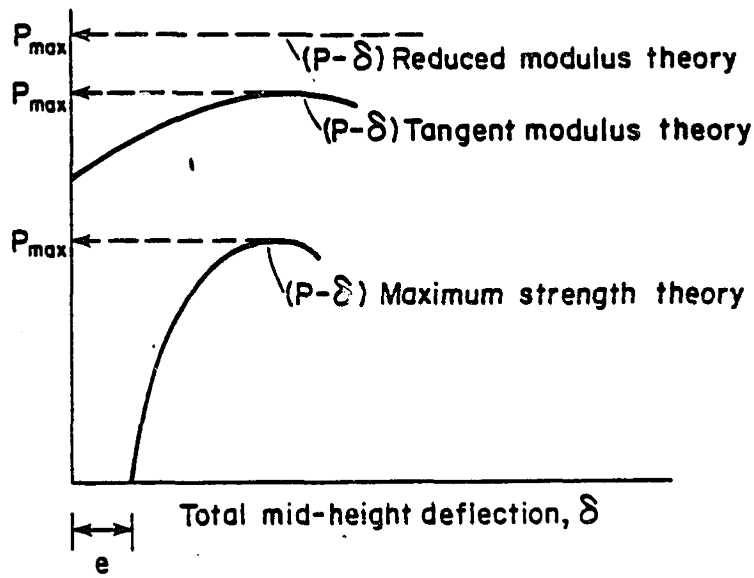

Fig. 4.4. Load-deflection curves for columns according to different buckling theory [5].

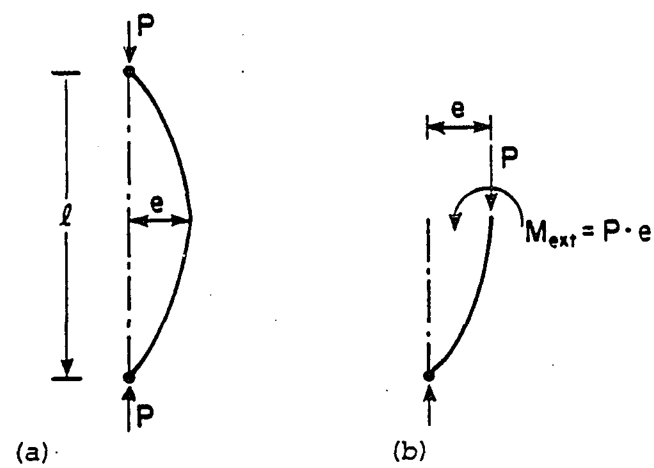

Fig. 4.5. Assumed configuration of initially curved member and the forces induced at mid-height section. -- (a) Initially curved column model; and (b) Column free-body diagram.

4.3. Residual Stress

4.3.1 Definition of Residual Stress

Residual stresses result from plastic deformations that take place in steel prior to the application of any external load [19]. The deformations occur as a result of the different cooling rates that prevail throughout the cross section after hot rolling or other forms of heat input. The portions that cool first will end up having compressive residual stresses, while those that cool the last will have tension [20].

Cold working is another source of residual stress formation. For example, steel members are commonly cold-straightened to reduce the initial crookedness. The stresses that are induced during this operation are known as cold-work residual stresses; they affect the final distribution and magnitude of the residual stresses in the shape, since they are imposed on a shape with other stresses already there due to other causes.

Welding operations are a major source of residual stresses. They play an appreciable role in their distribution and magnitude, particularly for small and medium sizes of plates and shapes, which are fabricated by welding together component plates [21]. The welding produces a localized heat input which causes differential cooling of the material in the weld and the adjacent areas. This leads to residual stresses that can be extremely high in a small region. The welding effect decreases on both sides of the weld, especially for heavy shapes, where there is little or no distortion of the original materials [13, 14].

Longitudinal stresses are taken into account in the theories dealing with column strength evaluation, because of their primary importance in determining the load-carrying capacity of a column. Since they are applied in the same direction as the externally applied stresses, they will act as a form of preloading of the shape, effectively reducing the ultimate strength of members that are loaded in compression.

4.3.2 Measurement of Residual Stress

It has already been indicated that the longitudinal residual stresses are a major factor for the behavior and strength of steel members. It is therefore important to be able to measure these stresses accurately. Much of the measurement work has been done in the United States, particularly at Lehigh University [5, 8, 9, 13, 14, 22, 23].

Many shapes of different geometry and fabrication methods have been examined to find the distribution and magnitude of the residual stresses. The complex nature of the formation of these stresses makes a theoretical analysis complicated. However, the work of Alpsten and others produced a numerical procedure which initially was applied only to hot-rolled members. Most of the available data have therefore been obtained through physical testing.

Different methods can be used to measure the residual stresses, and they are basically classified according to the following [19, 22].

1. Destructive testing,
2. Semi-destructive testing, and
3. Non-destructive testing.

As the name implies, destructive methods are based on the total destruction of the specimen. Sectioning [22] is probably the most commonly used technique. In thick members, sectioning may be followed by slicing to obtain the through thickness residual stress variation. The principles of sectioning and slicing are illustrated in Fig. 4.6.

Semi-destructive methods [19] require only local damage which cam be repaired by any number of methods. Two hold-drilling methods, namely, the Mathar's and Soete's methods, are examples of semi-destructive techniques, where holes of very small diameters are used to measure the residual stresses through local strain release. These methods have the advantage of removing only a small amount of the specimen material [22].

The above methods are sometimes known as "relaxation methods" [22] since the residual stresses are determined by measuring the elastic strain release that takes place when a section is cut into pieces or has a portion removed. The corresponding relaxed stress is obtained through Hooke's law. Although relaxation methods are easy to use and the equipment that is required is relatively simple, they are time- and money-consuming.

The disadvantages of the destructive methods have been one of the major incentives for developing non-destructive test methods. X-ray diffraction and ultrasonic testing [21] appear to be the most important since they can be used to measure the residual stresses in the material without damaging or destroying the test specimen. These techniques basically measure only the surface stresses, which can be detrimental in some cases [22] Ultrasonic measurements cannot determine the absolute magnitude of residual stresses but, rather, estimate the difference between principal stresses [22]. Much work appears to be needed before the X-ray and the ultrasonic processes can be used in practice.

A complete discussion of the different methods of residual stress measurement is considered beyond the scope of this investigation. More details of the various techniques and measurement are provided in references [21] and [22].

4.3.3 Effect of Residual Stress on Column Strength

Over the past 35 to 40 years, a number of investigations has shown that one of the main factors influencing the strength and behavior of centrally loaded steel columns is the magnitude and distribution of residual stresses in the column cross section. This has been verified experimentally [12, 13, 14] as well as theoretically [5, 8, 9].

The parts of the cross section that contain compressive residual stresses will yield before others when the column is loaded in compression. The combination of compressive residual and applied stresses therefore will prompt plastic behavior of portions of the section. These portions consequently lose their stiffness once they yield, and therefore can no longer contribute to the stiffness of the member. Tests [13,14] and theoretical investigations [5] have shown that the welded built-up shapes which are formed from oxygen-cut component plates display a higher strength than the similar columns from universal mill plates with as hot-rolled tips. This is because of the more desirable residual stress distribution of such shapes, since the flame-cut plates exhibit high tensile residual stresses at the flange tips.

Since yielded fibers have no stiffness (assuming a linear elastic-perfectly plastic stress-strain relationship for the steel), it is essential that the still elastic portion of the cross section can be determine, since this determines the buckling resistance of the column. The idealized stress-strain relationship is given in Fig. 4.7.

The stub column stress-strain relationship, Fig. 4.2, reflects the presence of residual stresses, since yielding will start in a fiber when the sum of applied and residual stresses in that fiber become equal to the yield stress. Thus, the beginning of yielding implies that the stress-strain relationship for the complete cross section is no longer linear. The latter would apply to a tension test coupon, for example, where no internal stresses exist. Therefore, as the compressive stresses increase, additional fibers in the cross section will yield. The plateau in the curve is reached when all fibers have yielded. This occurs for a load equal to the yield stress times the cross-sectional areas; this is commonly known as the yield load.

4.3.3 Distribution of Residual Stresses

The distribution and magnitude of the residual stress are greatly affected by the geometry, size, and manufacturing operations for the steel members.

Hot-rolled and welded built-up shapes display different distributions, according to the fabrication methods. Thus, hot-rolled sections exhibit compressive

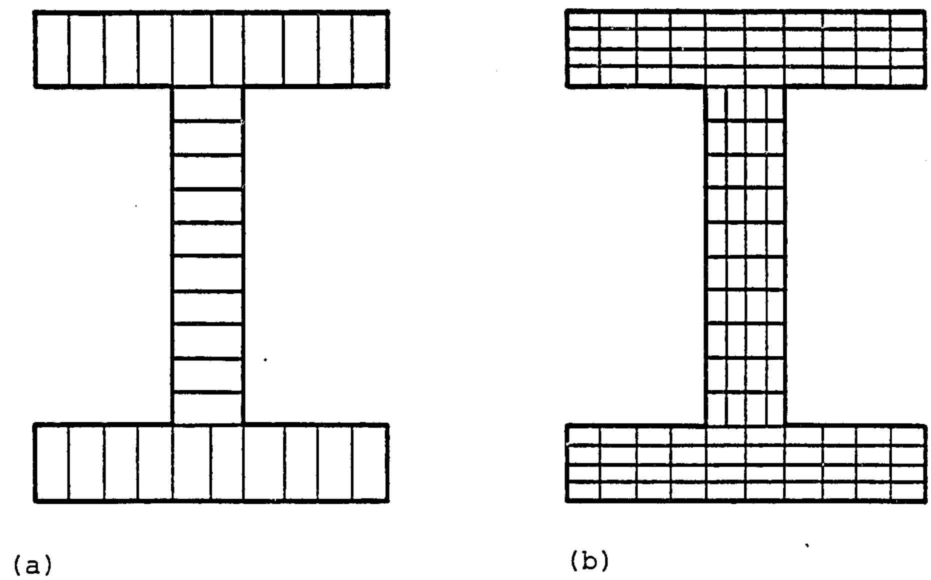

Fig. 4.6. Sectioning and slicing of a wide-flange shape to measure residual stresses. -- (a) Sectioning; and (b) Slicing.

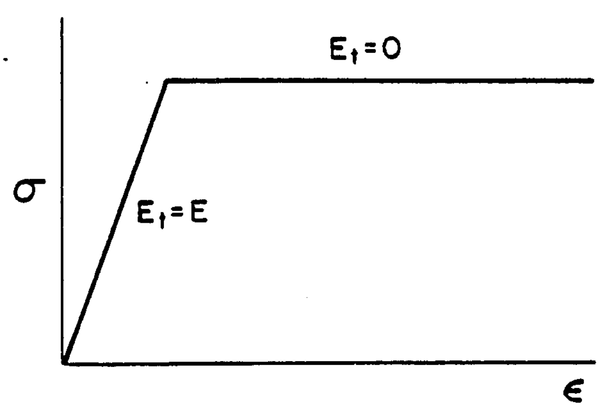

Fig. 4.7. Idealized stress-strain curve.

residual stresses at the flange tips and tension at the web-flange juncture [12]. Welded built-up members with flame-cut flange plates have high tensile residual stresses at the flange edges and flange-to-web juncture, due to the heat induced by the welding of the shapes. Welded built-up shapes with universal mill plates as flanges contain compressive residual stress at the flange tips. This distribution is similar to that of hot-rolled sections. The welding also produces high tensile stresses at the flange-to-web juncture. Typical residual stress distribution in different rolled and welded shapes are shown in Fig. 4.8.

It was found [12] that the stresses do not vary significantly through the thickness of the component plates for small and medium size shapes and plates, while this variation is pronounced for heavy steel shapes [12, 13, 14]. Although the variation through the thickness should be incorporated in the most accurate column strength analysis, the differences in column strength are normally less than 5 percent from that obtained on the basis of surface measurement only [5, 8, 13, 14].

Studies [13] have shown that the yield stress level does not influence the magnitude and distribution of the residual stresses. It was concluded [14] that welding contributes an important share of the final distribution for small and medium size welded built-up shapes. it was also

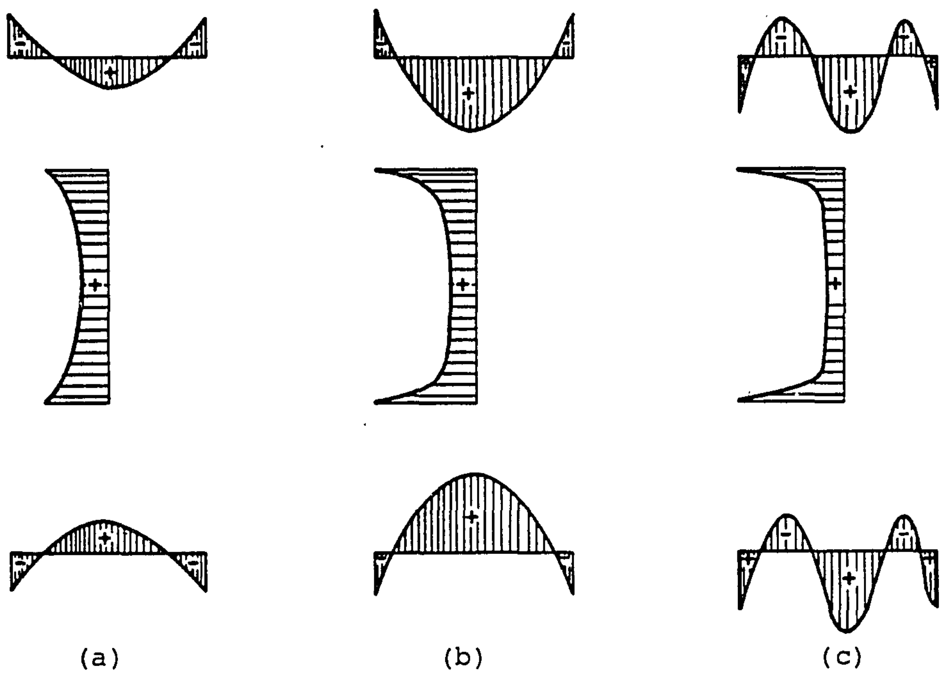

Fig. 4.8. Typical residual stress distributions in hot-rolled and welded built-up wide-flange shapes. -- (a) Hot-rolled shapes; (b) Universal Mill (UM) welded built-up shapes; and (c) Flame-cut (FC) welded built-up shapes.

shown [14] that the residual stresses caused by the welding in the areas of cross section away from the weld area far smaller for heavy shapes, because the input heat is relatively small for heavy members as compared to light and medium sizes [14]. Therefore, the final distribution in heavy shapes is more affected by the stresses due to causes other than welding [13, 14].

4.4 Initial Crookedness

Initial out-of-straightness is a geometric imperfection that results from manufacturing and fabrication processes. It is generally referred to as sweep or camber, and the materials delivery standards [24] strict limits on the magnitudes that are acceptable.

Initial curvature was long considered one of the primary causes of the divergence between experimental and theoretical evaluations of the strength of columns.

The initial crookedness can assume any number of configurations. Fig. 4.9 illustrates several cases [5].

Since the initial out-of-straightness plays a significant role for the column strength and behavior, any rational design approach should take into account its presence and magnitude in the estimation of column strength.

The complex nature of the initial curvature makes it convenient to use a simple form for the crooked member. As a slightly conservative approach, it was assumed [5, 6] that the actual initial crookedness can be approximated by one half of a sine wave. This gives a symmetric shape of the curved column, with the maximum amplitude at mid-height. Dealing with the actual configuration is complicated, although it is possible to use a finite element formulation to determine the maximum load. The difference between this load and the one determined on the basis of the member with half sine wave will be small.

As a result of the crookedness, every section along the column length is subjected to a moment as well as axial load. This is illustrated in Fig. 4.10. For this reason, the maximum column strength will be reduced. Thus, as the curvature increases, the column strength decreases. This is shown in Fig. 4.11.

The specification straightness requirement [24] limits the initial curvature to approximately $\ell/1000$, where ℓ is the column length. This value was the basis for the maximum strength curves that now are part of the Canadian limit states design standard for structural steel buildings [5, 17]. It was specifically chosen because it represents an extreme in the sense that no larger values are acceptable in actual steel members as they are delivered from the steel mills.

A value of $e = \ell/1500$ was found to be the approximate average value of the out-of-straightness in hot-rolled

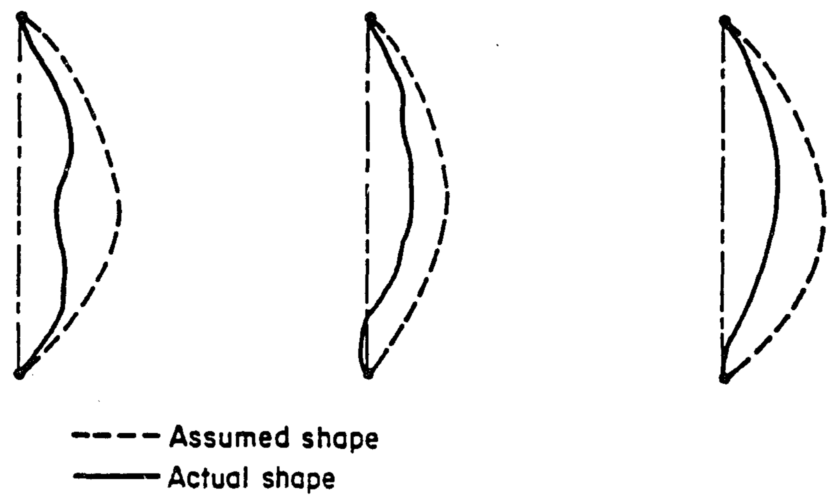

Fig. 4.9. Actual and assumed shapes of some steel columns [5].

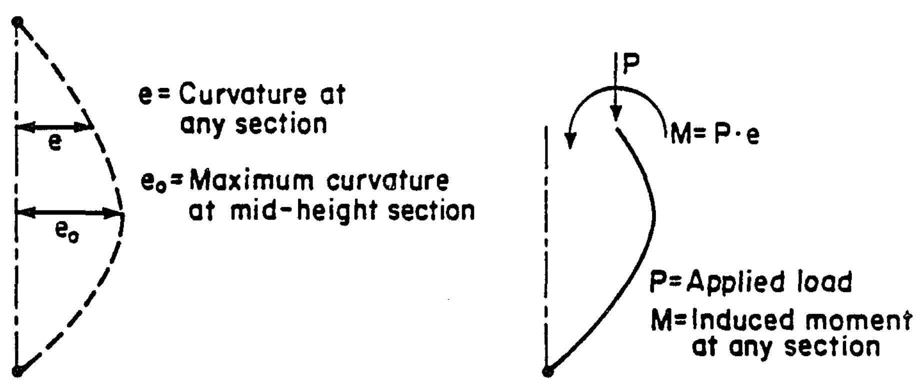

Fig. 4.10. Assumed initially crooked column configuration and free-body forces.

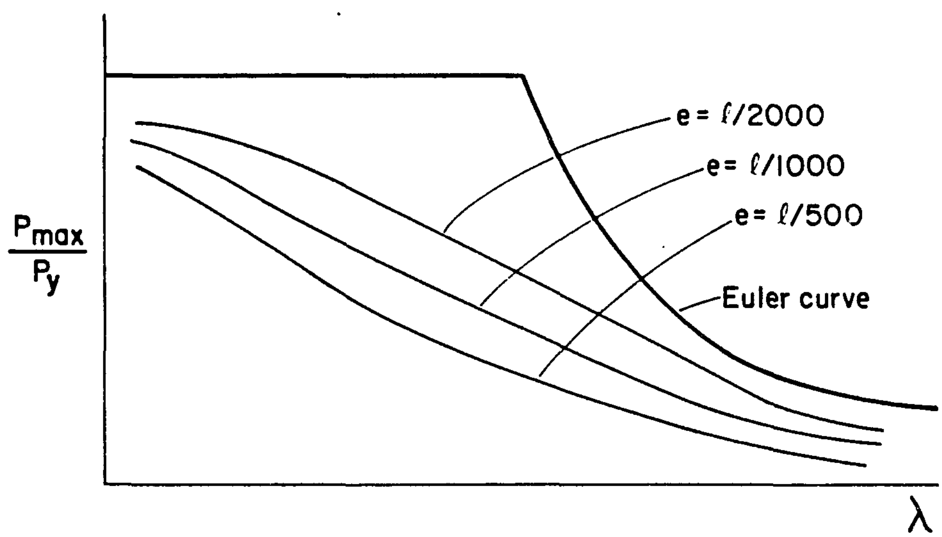

Fig. 4.11. Influence of initial curvature on column strength. -- Note the use of the non-dimensional slenderness λ, given by $\lambda = \frac{1}{\pi}\sqrt{\frac{\sigma_y}{E}}\ \frac{L}{r}$

wide-flange shapes [5]. As a result, it was used in the development of probabilistically based column strength curves [5]; these are now the foundation for the LRFD specification of AISC [18].

The maximum strength theory gives the best estimate of column strength and the correlation between tests and theory is good.

CHAPTER 5

MAXIMUM STRENGTH OF HEAVY STEEL COLUMNS

5.1. Introduction

The objective of this chapter is to describe the method that is used to find the maximum strength of steel columns. Particular emphasis will be placed on the treatment of heavy steel shapes; both hot-rolled and welded built-up members will be considered. Actual residual stresses are taken into account, along with the variation of the yield stress throughout the cross section, and the initial out-of-straightness.

5.2. Maximum Strength Model

Maximum column strength cannot be found from a single closed-form solution, such as the tangent modulus load, for example. Rather, a numerical solution must be used to predict the maximum load which satisfies equilibrium between internal and external forces, taking into account the residual stresses and other parameters. The development of this model was based on the following assumptions [5].

1. The material behavior can be represented by an elastic-perfectly plastic stress-strain relationship.

2. The initial crookedness and all successive deflections due to the applied load can be described by a half sine wave.
3. The distribution of residual stresses along the length of column is constant, and there is no variation through the thickness.
4. Plane sections remain plane for the full range of response.
5. Yielded fibers will unload elastically.
6. The yield strength may vary throughout the cross section, but it is assumed constant through the thickness and along the length of the member for a given point in the cross section.
7. Stresses and strains are only computed at mid-height of the column.

A complete discussion of the effects of these assumptions on the maximum column strength is found in reference [19].

It has been shown [5] that the maximum strength model that is used here gives buckling loads that are slightly conservative, as compared to a model that does not assume the configuration of the half sine wave of the buckled column [5, 15].

The computer program that has been used in this study is essentially based on the concept that equilibrium between the internal and the external forces must be maintained at all levels. Referring to Fig. 5.1, the two equilibrium equations are:

$$P = P_{int} \tag{5.1}$$

$$P \cdot \delta = M_{int} \tag{5.2}$$

where P_{int} and M_{int} are the internal axial force and moment, respectively. Consequently:

$$P_{int} = \frac{M_{int}}{\delta} \tag{5.3}$$

where δ is the sum of the value of the initial curvature and the lateral displacement, V_p, due to the applied load, P. Thus:

$$\delta = e + V_p \tag{5.4}$$

A numerical integration is required to solve Eq. (5.3).

The cross section is idealized into individual segments where the yield strength and the residual stresses are considered constant. This is illustrated in Fig. 5.2. Also, tensile forces, stresses, and strains are considered positive in the following formulation.

The stress in an element due to the applied load can be expressed in the following non-dimensional form [5].

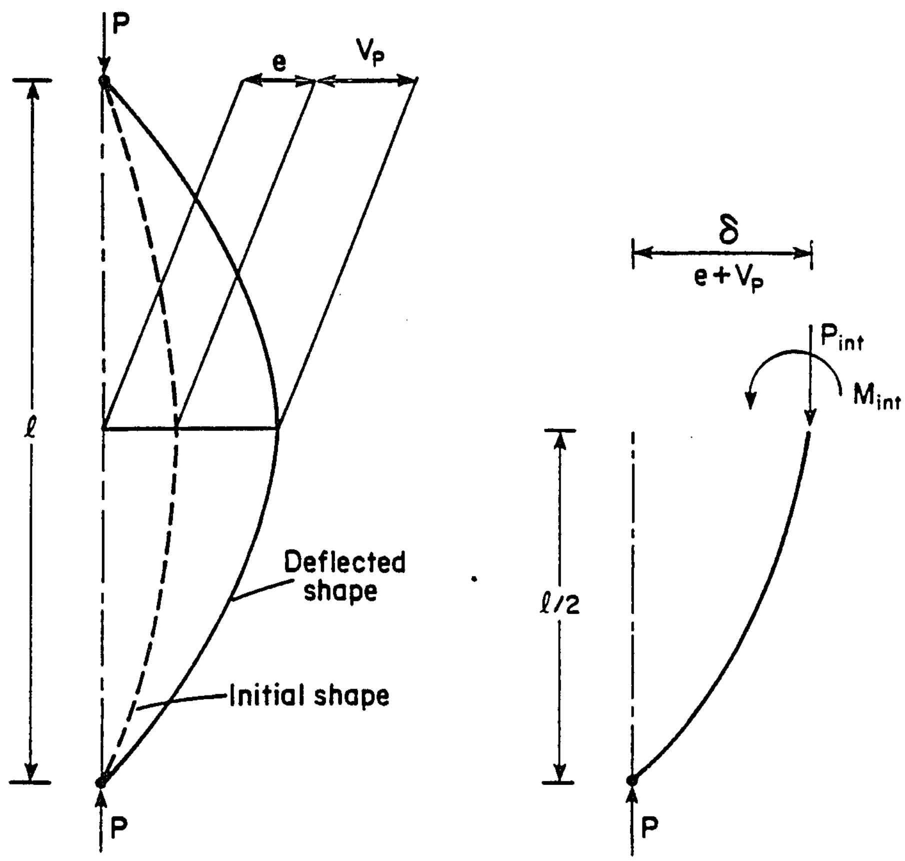

(a) (b)

Fig. 5.1. Column model for maximum strength computations. -- (a) Deflected column shape; and (b) Forces at mid-height section.

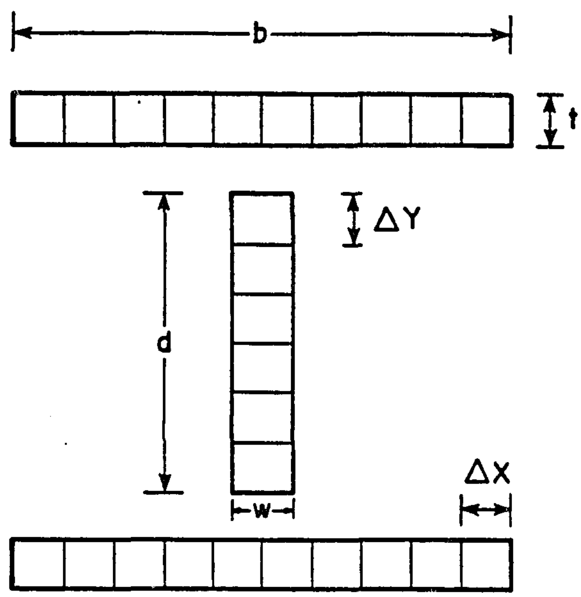

Fig. 5.2. Discretized cross section for column strength computation.

$$\frac{\sigma_i}{\sigma_y} = \frac{\varepsilon_i}{\varepsilon_y} = \frac{\varepsilon_{ri}}{\varepsilon_y} + \frac{\varepsilon_p}{\varepsilon_y} + \theta\frac{\xi_i}{\varepsilon_y} \tag{5.5}$$

where

σ_i, ε_i = stresses and strains in element i

σ_y, ε_y = the overall average yield stress and strain of the cross section

ε_{ri} = residual strain in element i, given by Hooke's law

ε_p = axial load strain in element i

θ = curvature of the column due to deflection V_p

ξ_i = distance from the element centroid to the bending axis considered (major, minor)

Equation 5.5 is valid only for the elastic range, i.e., when the total stress is less than the yield stress. If the total stress is higher than the yield stress, then Equation 5.5 is replaced by:

$$\frac{\sigma_i}{\sigma_y} = \frac{\sigma_{yi}}{\sigma_y} \quad \text{if} \quad \sigma_i \geq \sigma_{yi} \tag{5.6}$$

and

$$\frac{\sigma_i}{\sigma_y} = -\frac{\sigma_{yi}}{\sigma_y} \quad \text{if} \quad \sigma_i \leq -\sigma_{yi} \tag{5.7}$$

The above two equations indicate yielding in tension and compression of element i, respectively.

For a specific value of lateral displacement, V_p, at the mid-height cross section, the only unknown in the above equations is the axial load strain, ε_p. Since the curvature may be computed from the assumption that the deflected shape is described by a half sine wave that has the maximum amplitude at mid-height, the deflection equation is

$$V = \delta \sin \frac{\pi x}{\ell} \tag{5.8}$$

For small deflection, the curvature at $x = \ell/2$ is found from

$$\theta = \frac{d^2 v}{dx^2} \tag{5.9}$$

and differentiating Equation 5.8 twice results in

$$\theta = \frac{\pi^2}{\ell^2} V_p \tag{5.10}$$

By assuming an initial value of the applied axial strain, ε_p, the iteration procedure is started and the following quantities are numerically evaluated:

$$\text{Axial load:} \quad \frac{P_{int}}{P_y} = \frac{1}{\sigma_y \cdot A} \sum_{i=1}^{N} \sigma_i A_i \tag{5.11}$$

$$\text{Moment:} \quad \frac{M_{int}}{P_y} = \frac{1}{\sigma_y \cdot A} \sum_{i=1}^{N} \sigma_i A_i \varepsilon_i \tag{5.12}$$

where

P_y = yield of the cross section = $\sigma_y . A$

A_i = area of element i

The accuracy of the numerical iteration for equilibrium can be checked against a tolerance or error requirement:

$$\frac{\Delta P}{P_y} = \frac{P_{int}}{P_y} - \frac{M_{int}}{P_y \cdot \delta} \leq \Delta_{min} \tag{5.13}$$

If Δ_{min} exceeds the assigned value of Δ_{min}, a new value of $\frac{\Delta P}{Py}$ is computed. Eventually, a sufficiently accurate solution will be found. In this study a tolerance level corresponding to at Δ_{min} value of 0.2% has been used.

Residual stresses are checked for equilibrium and adjusted when necessary before the iteration procedure starts. A complete listing of the maximum load program MAXLD [5] is found in Appendix A, along with the appropriate documentation.

5.3. Residual Stress Data

The residual stress that has been used in this study are all data determined in laboratory measurements. This information was generated from tests in North America [12, 14, 27] and elsewhere [26]. The average values of residual stresses (i.e., average of the inside and outside surface measurements) were calculated from the available data, and it was then assumed that the residual stress was constant through the plate thickness. For use with the discretized cross section, the residual stress was therefore assumed to be constant within each cross-sectional segment.

Residual stresses exist in the shape before any external loads are applied. However, it may be found that the cross section is not in equilibrium for zero axial load, since the residual stress measurements and the discretization of the cross section may have been too coarse to allow computational equilibrium. The residual stresses therefore must be adjusted before any calculations are made. In other words, for zero applied axial load, it is required that

$$\int_A \sigma_r dA = 0 \tag{5.14}$$

or for a numerical integration

$$\sum_{i=1}^{N} \sigma_{ri} A_i = 0 \tag{5.15}$$

The MAXLD computer program has the capability to adjust and redistribute the residual stresses to ensure that this basic requirement is met. The redistribution is done according to Eqs. (5.14) and (5.15) to assure equilibrium of the residual stress distribution for zero load.

It is noted that it is not necessary to use only measured residual stresses in the computations with MAXLD. Instead, theoretical residual stress values may be adopted, as long as values are specified for each of the cross-sectional segments. This was done in the case of the European column strength study of Beer and Schultz, for example [16].

5.4. Choice of Initial Out-of-Straightness

Initial curvature of steel members cannot be avoided because of manufacturing and related processes. Therefore, any rational design approach should take this into account in order to estimate the capacity of structural steel members more precisely. For simplicity, it was assumed that the initial crookedness configuration can be represented by a half sine wave which has the maximum amplitude at mid-height of column [5].

The column strength curves for each shape used in this study were constructed using different magnitudes of the initial crookedness. The MAXLD computer program incorporates this parameters in the calculation process for the maximum column strength.

Four different values were chosen for this investigation, reflecting a broad range of practical out-of-straightness. Thus, the strength was computed for e-values of $\ell/500$, $\ell/1000$, $\ell/1500$, and $\ell/2000$. The value of $\ell/1000$ represents the maximum allowable out-of-straightness of the specification [25], and $\ell/1500$ is the average value [5].

5.5. Material Strength Data

The strength of the material plays a significant role in the load-carrying capacity of steel members. Since the residual stresses are independent of the material yield strength, as discussed earlier, the selected steel shapes were analyzed using different common steel grades, but with the same levels and distribution of residual stresses. In consequence, if residual stresses are available only for a steel shape in one steel grade, the same values were used for the shape in other grades as well.

The cross section which is to be analyzed is divided into discrete segments, as discussed previously. Each element is assumed to have a constant yield stress level, but it may vary from one element to another. This depends on manufacturing and fabrication methods; for example, flame-cutting and welding will produce local areas of increased material strength. For the hot-rolled shapes, it was assumed that the cross section has a constant yield stress equal to the stub-column yield stress (if available) or the tensile test specimen value.

The column curves were generated using mild and high strength steel with yield stresses of 36 and 50 ksi, respectively. These steel grades are used extensively for construction purposes in the United States and Canada today.

Two European heavy steel shapes were incorporated in this investigation. These were designated HD 400X685 and HD 260X274, using European standards [26], and had been produced by the steel company Arbed of Luxembourg. The shapes had yield stresses of 25 and 28 ksi, as determined from simple tension tests. These two shapes were analyzed using the above yield stress values, as well as 36 and 50 ksi.

The welded built-up shapes that were analyzed had either universal mill (UM) or flame-cut (FC) flange plates. The former leave the built-up shapes with a compressive residual stress at the flange tips, and distribution is not unlike that of hot-rolled shapes. In particular, the welding causes higher tensile stresses at the flange-to-web juncture, as well as higher compressive residual stresses at the flange tips. The welding also affects the material properties in localized areas, to the effect that the yield stress of the weld region and adjacent areas will be the same as that of the weld electrode. This is normally higher than that of the base metal. Consequently, for the universal mill built-up shapes the weld region strength was increased to the weld strength for both flange and web components. The other parts of the cross section were assigned a yield stress equal to that of the base metal.

Welded built-up shapes using plates with flame-cut edges have different distributions of the residual stresses and the yield stress. Due to the heat input of the welding and flame-cutting, high tensile residual stresses will develop in these areas of the shape. The heating and rapid cooling of the areas produce finer-grained crystalline structures of the steel, which thus ends up having a significantly higher strength than the rest of the shape. As a result, in the maximum column strength analysis of these shapes, the weld and edge regions have been assigned yield stress values equal to that of the weld electrode strength. This approach has been confirmed through numerous studies of column strength [5].

All of the shapes dealt with in this study were homogeneous, i.e., the flanges and web always were made from the same material. The modulus of elasticity was assumed to be constant for all shapes ($E = 29 \times 10^3$ ksi).

CHAPTER 6

DISCUSSION OF RESULTS

6.1. Introduction

The purpose of this chapter is to discuss the overall computational results. In particular, the discussion will examine the effects of the various imperfection parameters on the strength and behavior of heavy steel columns.

The discussion will focus on the influence of the variation of parameters such as the column flange thickness and its relationship to the overall shape geometry. In view of the limited data that are currently available regarding the strength and behavior of heavy columns, it is deemed of special importance to quantify all of the terms that govern this. Finally, the results must be compared and evaluated in light of what is known and used for lighter shapes.

The column curves are illustrated using the values of P_{max}/P_y as the ordinate, and the non-dimensionalized slenderness parameter, lambda (λ), as the abscissa, with a range of initial out-of-straightness. Lambda (λ) is given by the expression

$$\lambda = \frac{1}{\pi}\sqrt{\frac{\sigma_y}{E}}\;\frac{\ell}{r} \qquad (6.1)$$

where all quantities have been defined previously. The comparison between strong and weak axis of bending is included in this investigation, and will be discussed in detail.

6.2 Hot-Rolled Shapes

Residual stresses and other data for five heavy hot-rolled wide-flange shapes were obtained for this investigation, with flange thicknesses ranging from 1.105 to 5.0 inches. The data for the shapes are given in Table 6.1 and the computational results are shown in Figs. 6.1 through 6.57. These figures were constructed using different combinations of residual stresses, yield stress, initial curvature, and bending axis.

All shapes show the same tendency of decreasing strength as a function of the imperfection parameters. Figure 6.2 gives an example of this. The effects are especially pronounced for slenderness in the intermediate range of 0.8 to 1.2. It is further confirmed that the imperfections are less important as the column gets very long. Consequently, the behavior approaches that of the elastic column in this case, as indicated in Fig. 6.15, for example. Similarly, the strength of short columns approaches the yield load, i.e., the strength is not affected by overall buckling. This is indicated in all of the column curves that are shown, especially for λ-values less than about 0.3.

Table 6.1. Data for hot-rolled shapes.

Column Sections	t (in)	d (in)	w (in)	b (in)	A_2 (in^2)	bt/dw	α (1/in)	β ($1/in^2$)	bt_2 (in^2)
W 12 x 120	1.11	13.12	.71	12.32	36.5	1.46	1.97	.16	13.61
HD 260 x 274 (European)	1.97	12.83	1.35	10.87	54.83	1.24	1.20	.11	21.41
W 12 x 426	3.035	18.67	1.875	16.695	124.96	1.45	.78	.05	50.67
HD 400 x 685 (European)	3.15	18.94	2.27	16.97	135.6	1.24	.75	.044	53.40
W 14 x 730	5.0	21.75	3.0	18.0	215.25	1.38	.51	.028	90.0

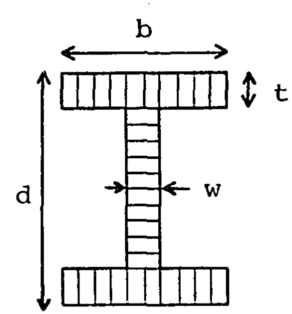

It may be seen from the figures that the initial out-of-straightness has a significant effect on the column strength and behavior. It is found that as the initial curvature decreases, the relative strength increases, as illustrated by Fig. 6.21, for example. As was found in earlier studies, there appears to be a more significant increase in the strength as the e-value goes from $\ell/500$ to $\ell/1000$ than when it goes from $\ell/1000$ to $\ell/2000$, for example. This confirms the results of Bjorhovde [5].

To expand on these findings, the results were compared in detail at the specific λ-value of 0.8, to study the effects in the most critical slenderness ratio range. It was found that the relative strength was increased by an average of 10% for all shapes as e was reduced from $\ell/500$ to $\ell/1000$. It was further increased by 4% when e decreased from $\ell/1000$ to $\ell/1500$, and another 2% as e decreased to $\ell/2000$. Considering other slenderness ratios, it was found that the variation in the initial out-of-straightness had virtually no effect for the very short and the very long columns, as would be expected.

The yield stress plays an important role in the strength and behavior of steel columns, to the effect that their strength is proportional to F_y to a certain degree. The results show that the increase of the relative strength is much greater for columns of intermediate length than for long and short columns. For example, at the λ-values of 0.2, 1.0, and 1.8, the strength gain was on the order of 0.4%, 6.6%, and 1.7%, respectively. This confirms that for short columns the imperfections do not affect the column strength very much.

The strength of long columns is mostly controlled by elastic behavior. The strength gained by increasing the yield strength of the material will therefore be much smaller than that of intermediate columns. Hence, it is concluded that increasing the yield strength will only significantly increase the relative strength of intermediate columns; the absolute strength (in terms of kips, e.g.) is increased in direct proportion to F_y the shorter the column becomes.

The axis of bending is one of the primary factors for column strength; examples are shown in Figs. 6.29 and 6.30. it is observed from these figures that the strength for x-axis bending is higher than that of y-axis bending, due to the geometry of the cross section for the wide-flange shapes. The lower capacity for the weak axis case is very pronounced for intermediate columns. The axis of bending is not important for short columns, since they will actually fail by squashing (not flexural buckling). The percentages of reduction of the relative weak axis versus strong axis strength for λ-values of 0.2, 1.0, and 1.8 were found to be on the order of 0.3%, 15%, and 6%, respectively, for 36 ksi steel and an initial curvature of $e = \ell/1000$. As the column length increases, the effect of the bending axis decreases.

It was observed that the maximum column strength curves occasionally crossed each other when bending about the weak and strong axis were compared, as illustrated in Fig. 6.37. This may be due to the fact that early elastic unloading of certain fibers occurs when bending takes place about the weak axis. As a result, this case will show higher strength than the strong axis, although the difference is not large. Also, this usually occurred only for longer columns.

The results for all hot-rolled heavy shapes were compared to each other, using different geometric parameter combinations as shown in Figs. 6.53 through 6.57. The parameters that were used were the flange thickness, t; t/b, the ratio of the flange thickness to the flange width; bt, the flange area; bt/dw, the ratio of the flange area to the web area; b^2t, the flange thickness times the flange width squared; α, defined as the plate-factor, which is a measure of the rate of cooling after rolling, given by $\alpha = \frac{2(b + t)}{bt}$ [14]; and β, defined as the width-factor, which is also a measure of the rate of cooling after rolling, given by $\beta = \frac{\alpha}{b}$ [14]. The purpose of these choices was to determine whether the column strength was especially influenced by any of the geometric parameters, attempting to resolve the questions that had been raised in the past regarding heavy versus light columns, for example. Thus, previous studies indicated that shapes with larger flange thicknesses might have lower relative strengths.

It was found that the flange thickness, t, is the geometric factor which most clearly reflects the relative strength of heavy hot-rolled shapes. The average relative strength values for 36 and 50 ksi steel are shown in Figs. 6.53 and 6.54 when bending takes place about x- and y-axis, respectively. The influence of other parameters is illustrated in Figs. 6.55 through 6.57; it is seen that they are not as clearly indicative of the effects as the flange thickness alone. In addition, using t as a parameter makes comparison much easier to perform.

Figure 6.53 indicates that the relative strength decreases as the thickness increases, until t equals approximately 3 inches. With some minor variations, the strength then increases along with t. The inconsistent variation of the relative strength for thicknesses between 3.0 and 3.5 inches for $\lambda = 0.4$ is attributed to the residual stress distribution and magnitude for the shapes that are included. As t increases from 1.1 to 1.97 inches, the corresponding relative strength drops by an average of 3%

for $\lambda = 0.4$. As it increases further from 2 to 3 inches, the variation of the relative strength is small.

As the slenderness ratio goes up, the corresponding reduction or increase of the relative strength will be different for 36 and 50 ksi yield stress. For example, for $\lambda = 0.8$, as t increases from 1.10 to 1.97 inches, the relative column strength drops by 10% for 36 ksi steel and by 8% for 50 ksi steel. The same tendency is observed as t increases to 3 inches, where 36 ksi steel column strength decreases by 4% and 50 ksi steel column strength by 3%. At this slenderness ratio ($\lambda = 0.8$), it is observed that when t increases beyond 3 inches, a consistent increase in the column relative strength results. This amounts to 7% and 5% for 36 and 50 ksi steel, respectively.

For long columns, as exemplified by a slenderness of 1.2, the column strength varies in the same fashion as explained above. That is, the relative strength drops until t equals approximately 3 inches, and the increases. The relative strength changes that occur as the yield stres goes up from 36 to 50 ksi are small.

Figure 6.54 gives the weak axis column strength data. It is seen that as t increases, the relative strength decreases until the flange thickness reaches a value of approximately 3 inches. Subsequently, the relative strength increases. Although the degree of increase or decrease may be different for each column, the trends are the same. For a slenderness of $\lambda = 0.4$, the maximum reduction occurs when t goes from 1.10 to 1.97 inches, it equals about 4% as an average value for both steel grades. The strength appears to be constant between t = 3 and t = 3.5 inches, after which an increase is found.

A great reduction in the strength is observed when λ increases to 0.8 and t goes from 1.10 to 1.97 inches. This reduction is on the order of 18% for 36 ksi steel and 13% for 50 ksi steel. The relative strength drops further as t increases to 3 inches, with decreases of 5% and 4% for mild and high strength steel, respectively.

As λ is increased to 1.2, the same tendencies are observed, although with different rates of decrease or increase. As t increases from 1.10 to 1.97 inches, the relative strength decreases by 12% for 36 ksi steel and 6% for 50 ksi steel. This decreases further as t goes to 3 inches, and then increases as the thickness increases to 5 inches.

It is concluded from the preceding discussion that the strength of heavy hot-rolled wide-flange columns is significantly affected by the flange thickness. As the latter increases, the corresponding relative strength decreases until the flange thickness reaches a value of approximately 3 inches. As the yield stress of the material increases, the relative strength differences become slightly less affected by t.

The heavy wide-flange shape W 12 x 120 represents an unusual case. It was originally (mid-1960s) produced in A 514 steel, but rolled shapes are no longer supplied in this steel grade. The residual stresses that were obtained for the shape in the 99 ksi steel strength (100 ksi nominal) were also used for analysis of the shape in 36 and 50 ksi steel, since the residual stress is not a function of F_y. Numerical convergence difficulties developed in the analysis of this shape; these could not be resolved, as illustrated in Figs. 6.41 and 6.43, where it is seen that as yield stress increased, longer columns permitted a converging solution to be obtained.

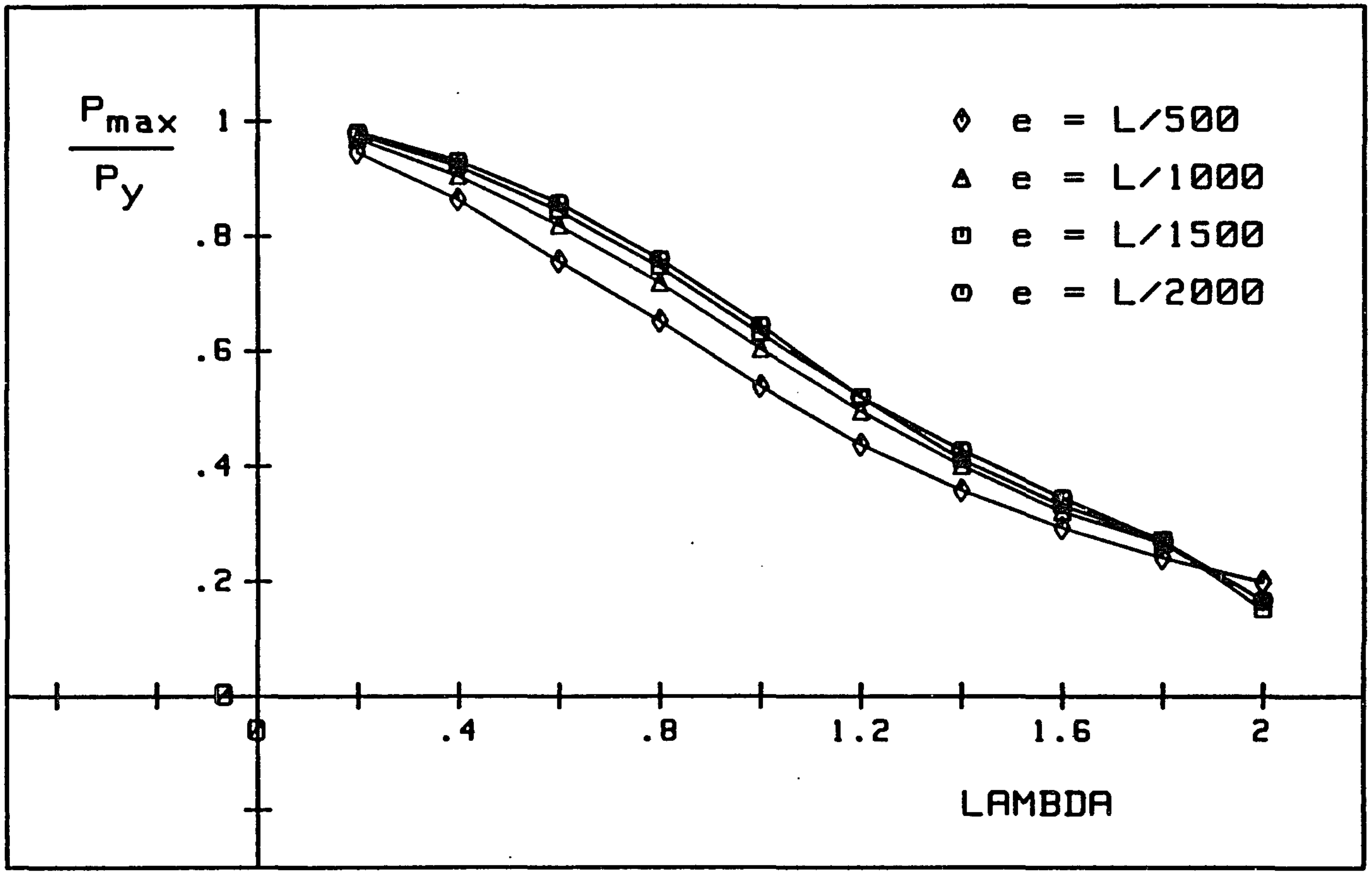

Fig. 6.1. Maximum strength column curves for shape HD 260 x 274 (European) with yield stress of 28 ksi and x-axis bending.

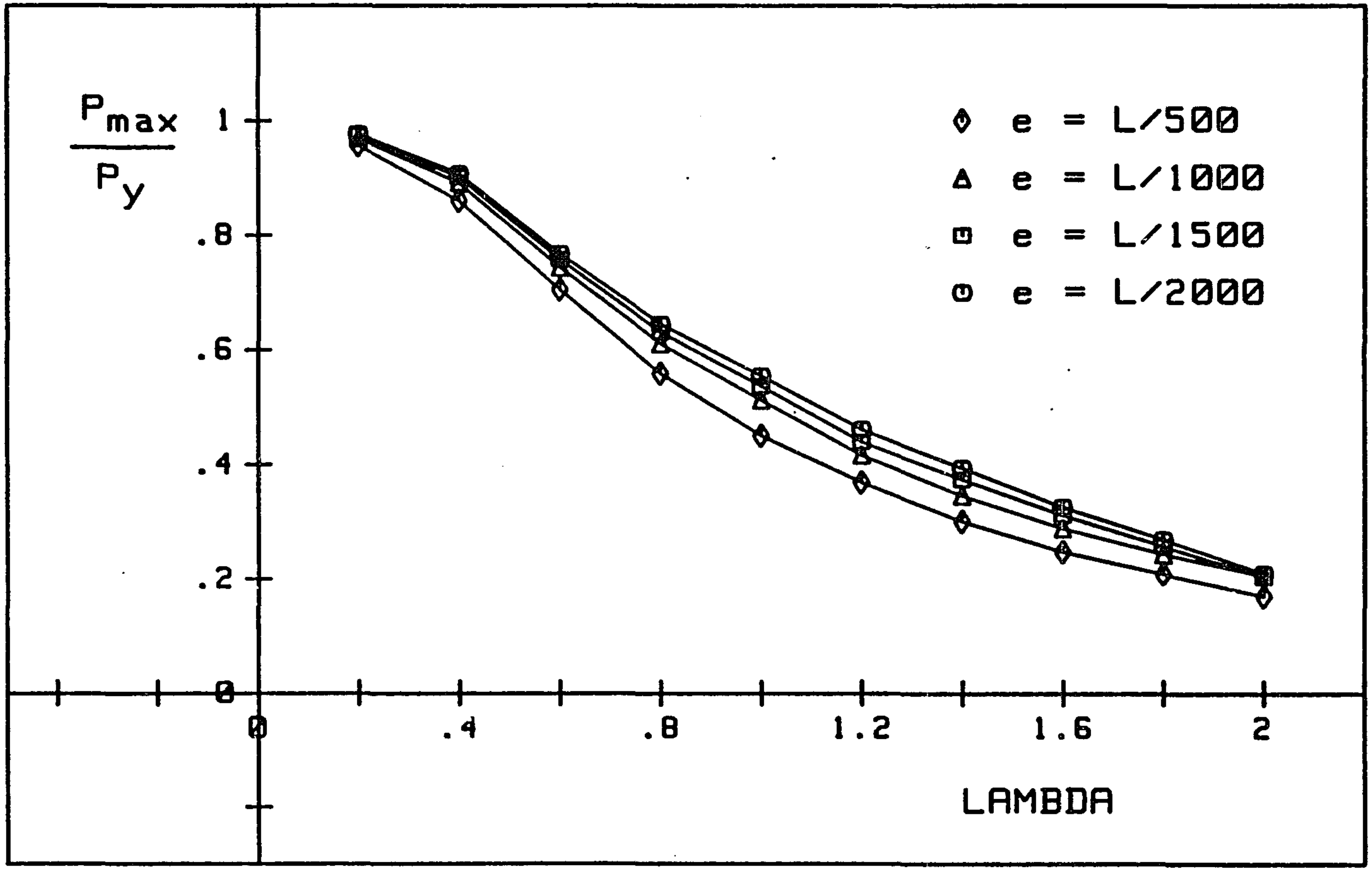

Fig. 6.2. Maximum strength column curves for shape HD 260 x 274 (European) with yield stress of 28 ksi and y-axis bending.

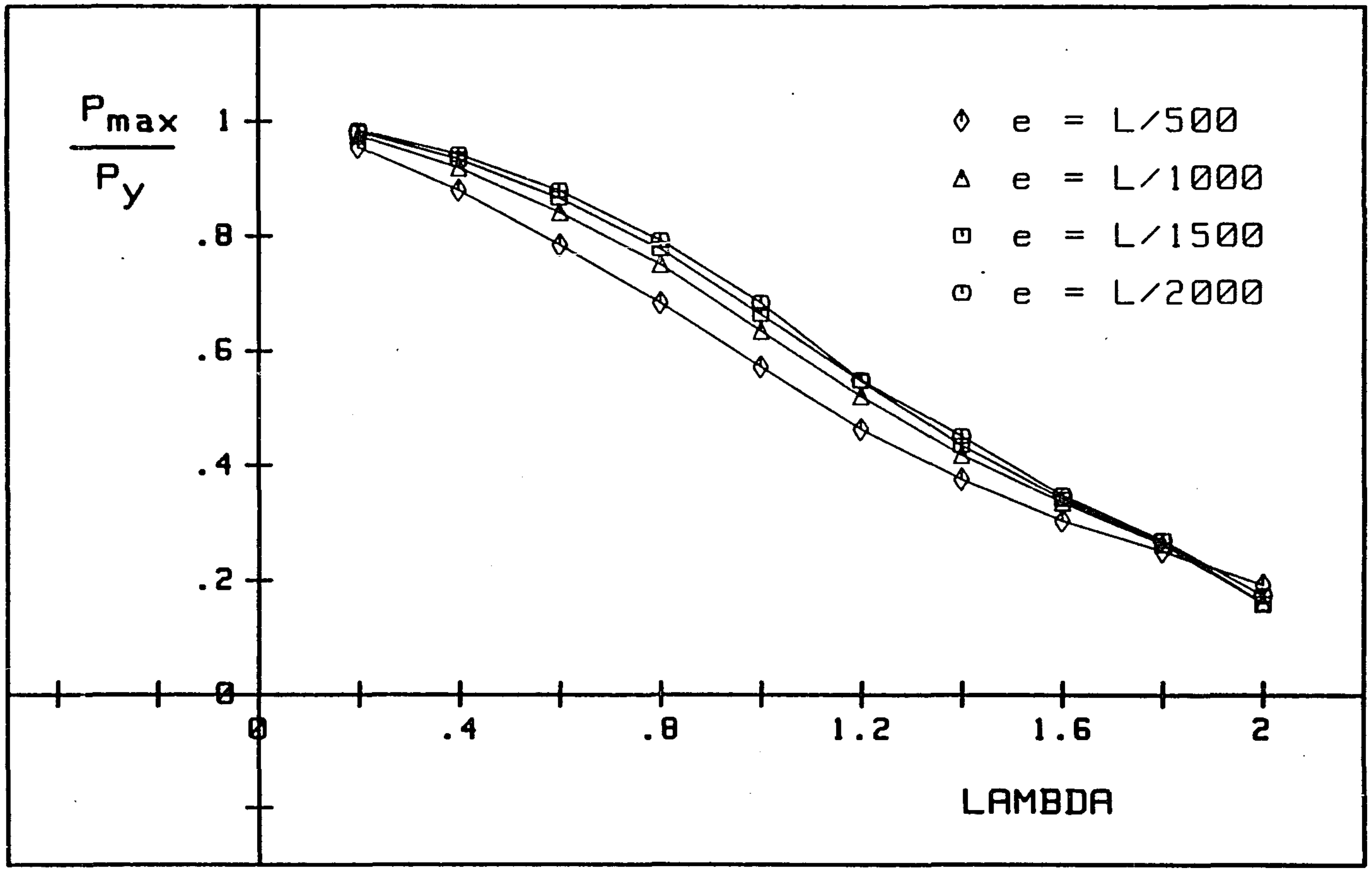

Fig. 6.3. Maximum strength column curves for shape HD 260 x 274 (European) with yield stress of 36 ksi and x-axis bending.

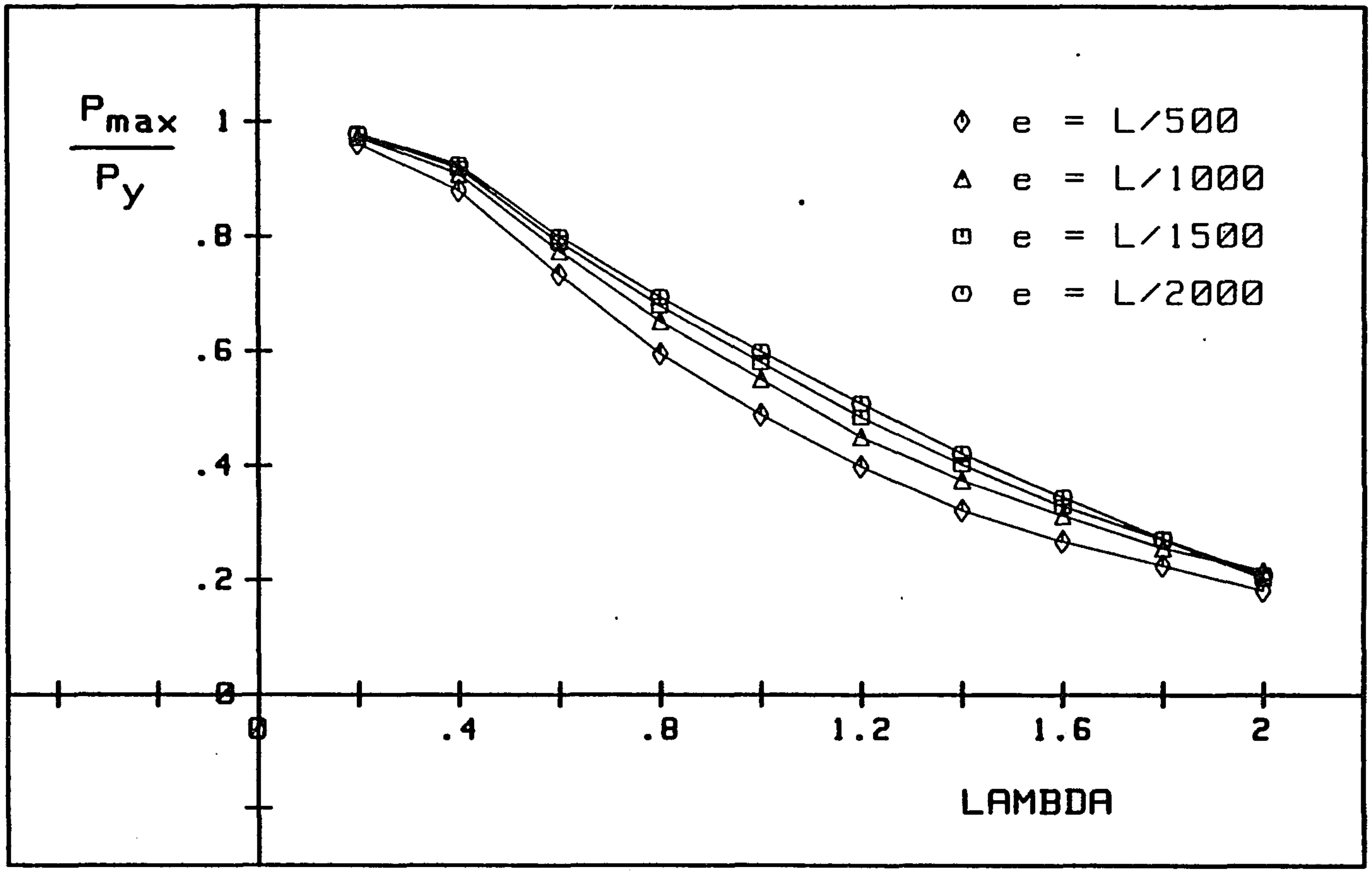

Fig. 6.4. Maximum strength column curves for shape HD 260 x 274 (European) with yield stress of 36 ksi and y-axis bending.

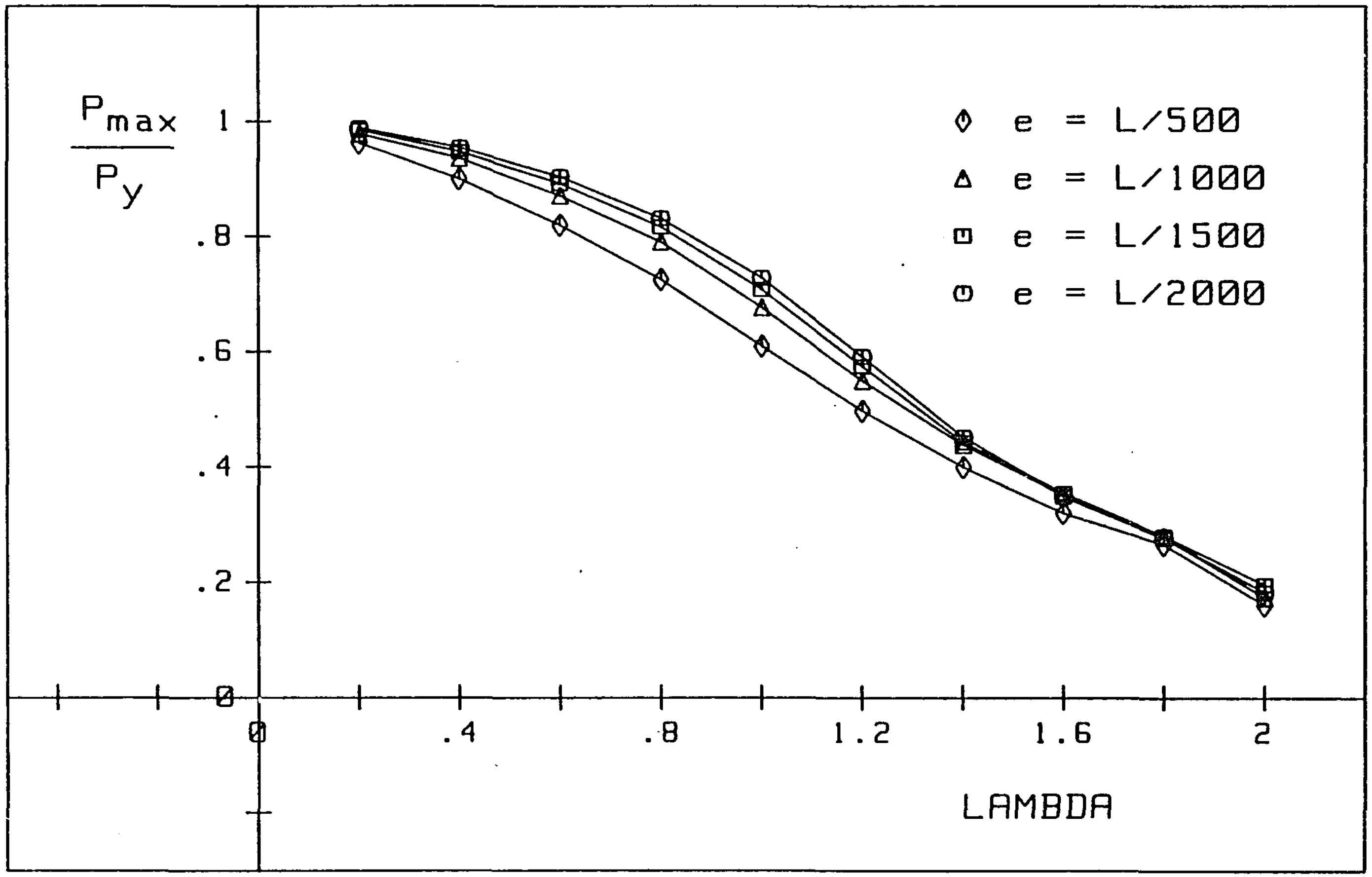

Fig. 6.5. Maximum strength column curves for shape HD 260 x 274 (European) with yield stress of 50 ksi and x-axis bending.

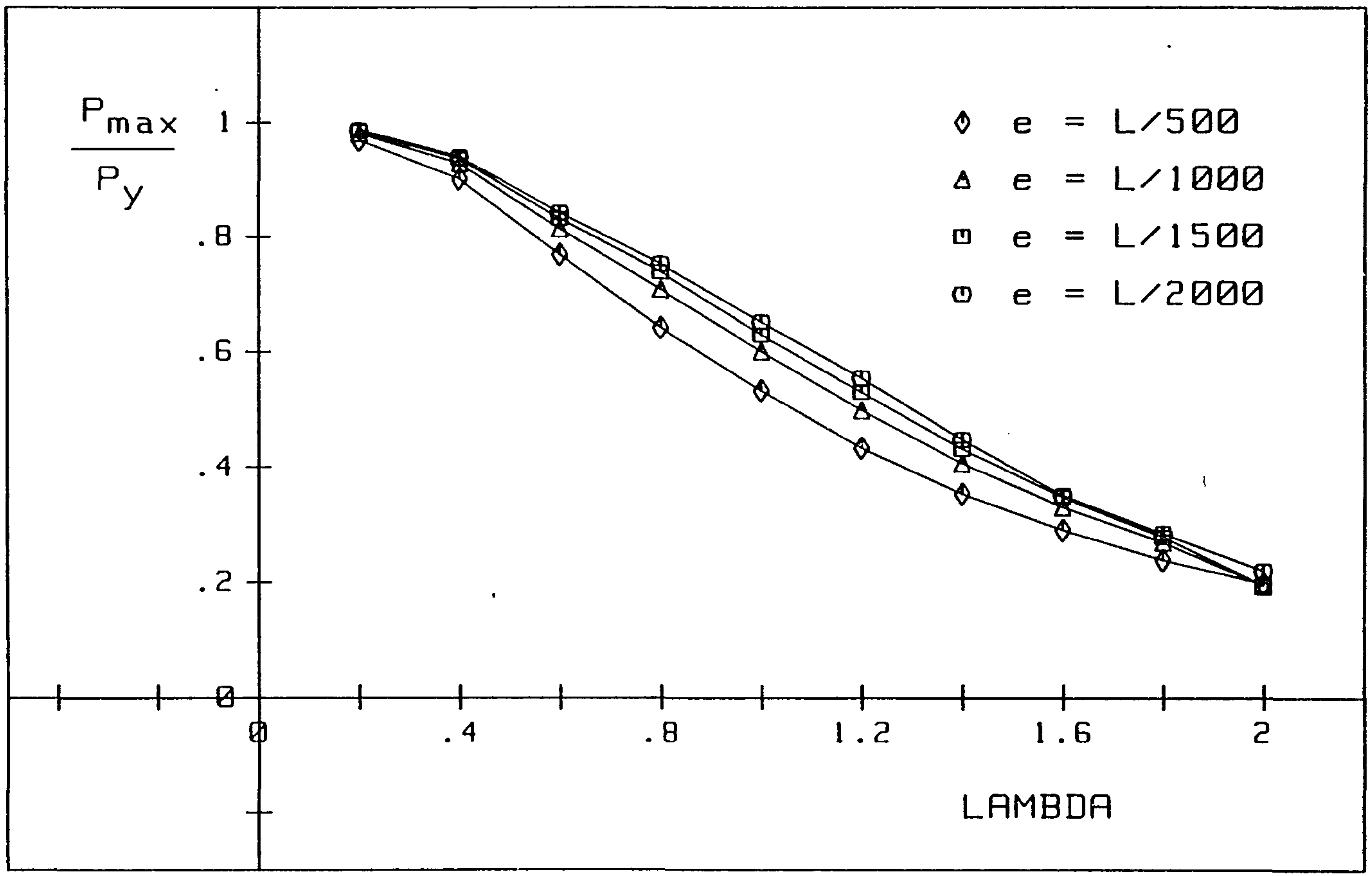

Fig. 6.6. Maximum strength column curves for shape HD 260 x 274 (European) with yield stress of 50 ksi and y-axis bending.

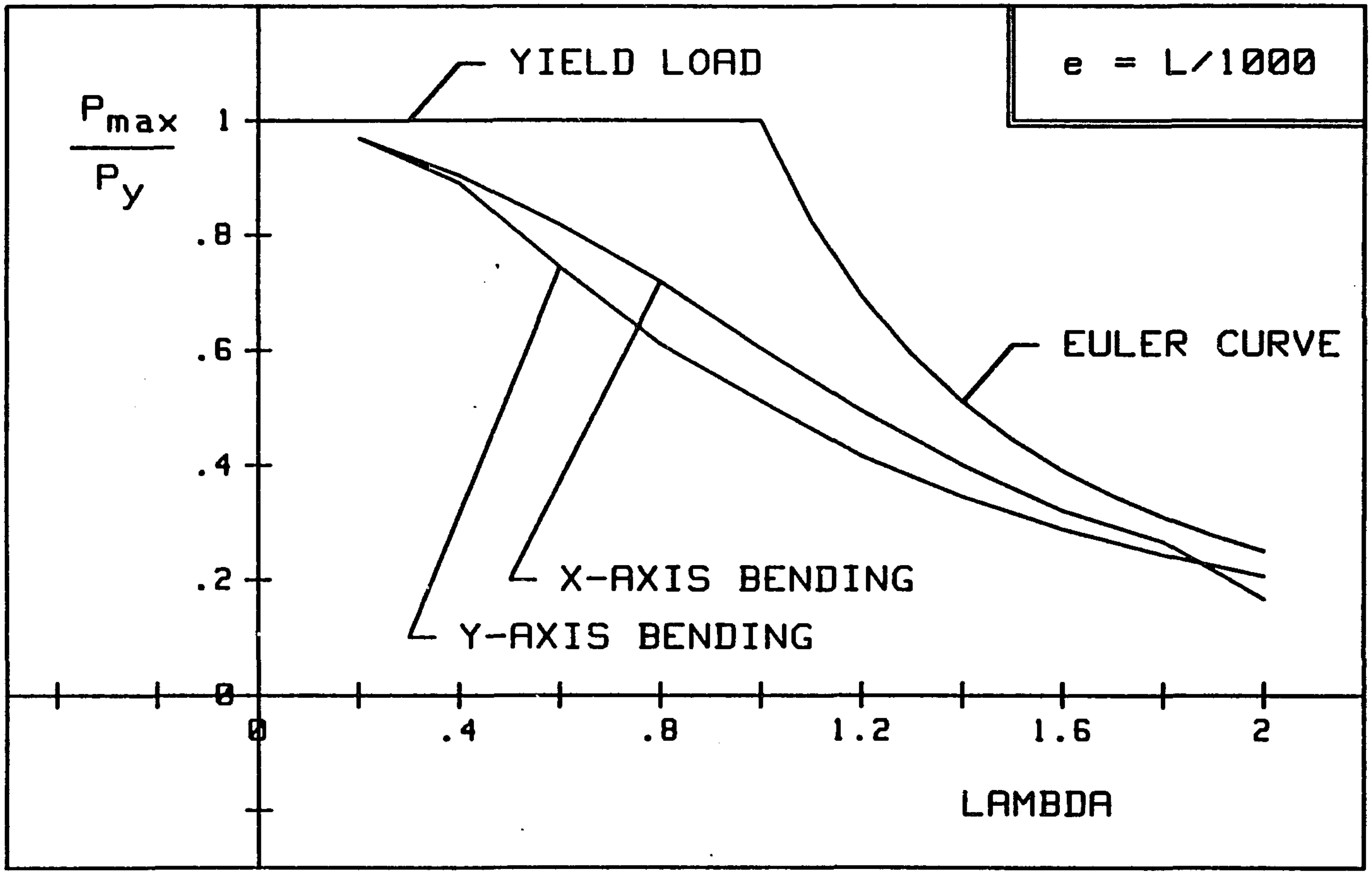

Fig. 6.7. x- and y-axis maximum strength column curves for shape HD 260 x 274 (European) with yield stress of 28 ksi.

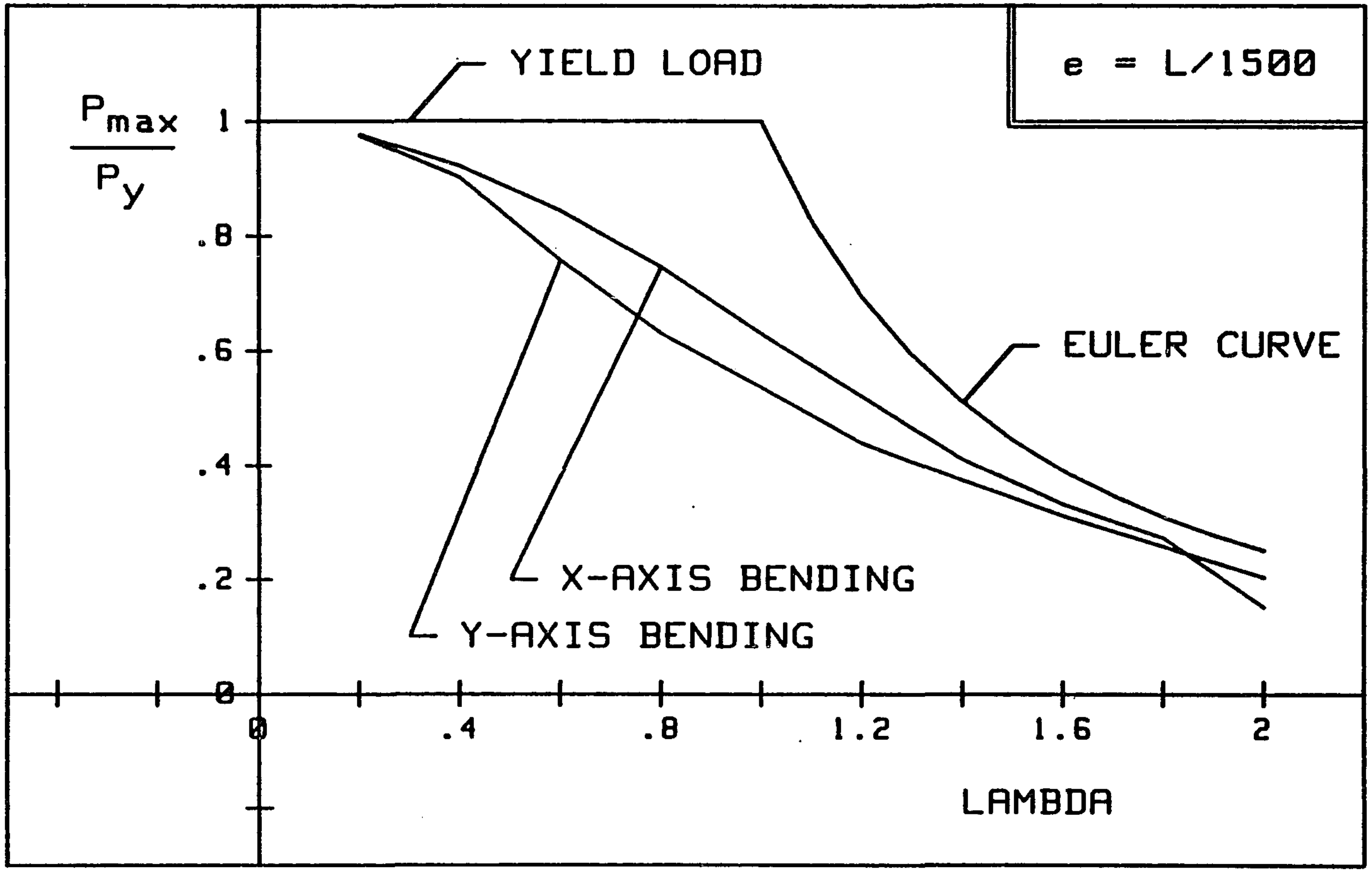

Fig. 6.8. x- and y-axis maximum strength column curves for shape HD 260 x 274 (European) with yield stress of 28 ksi.

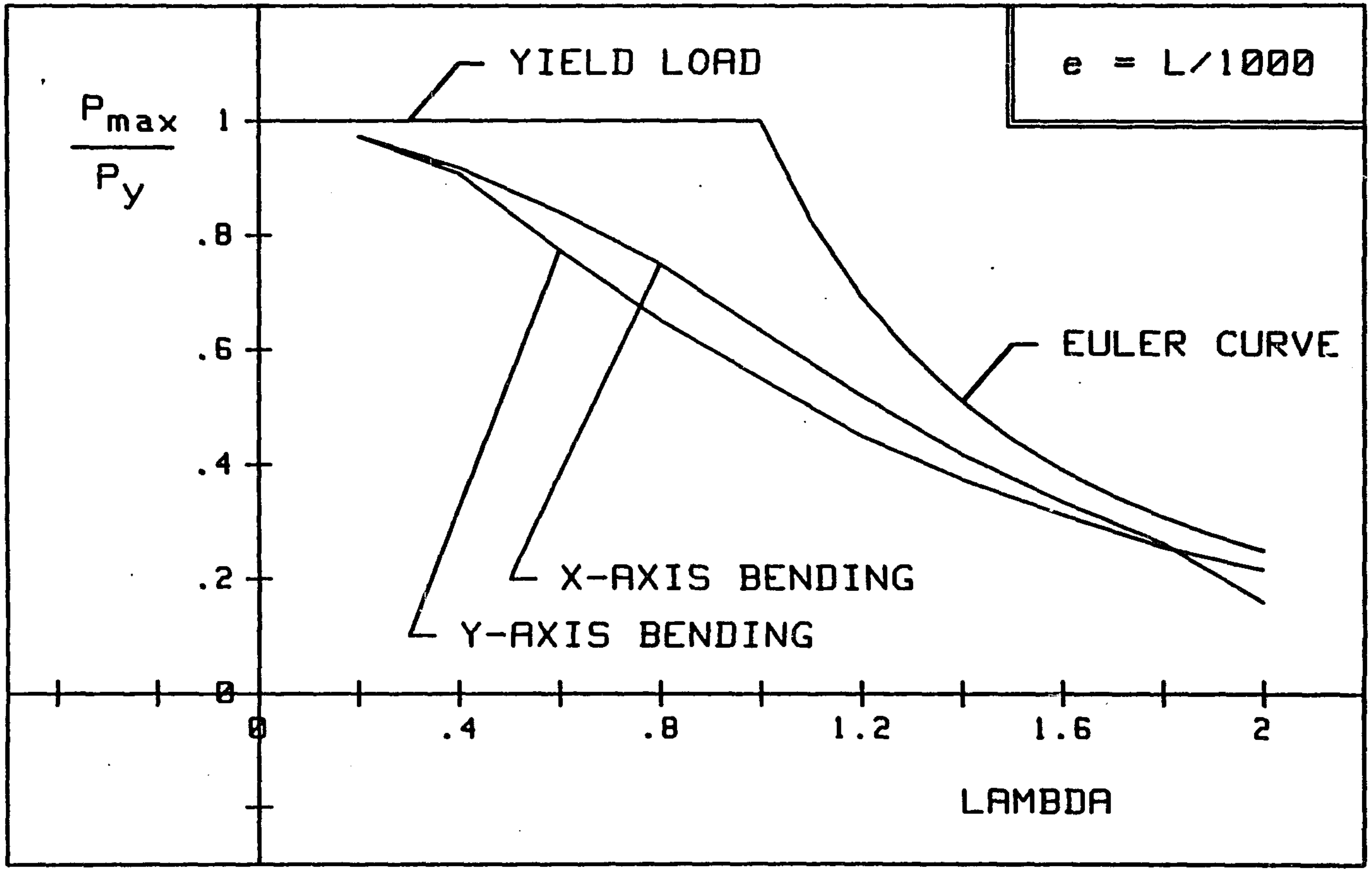

Fig. 6.9. x- and y-axis maximum strength column curves for shape HD 260 x 274 (European) with yield stress of 36 ksi.

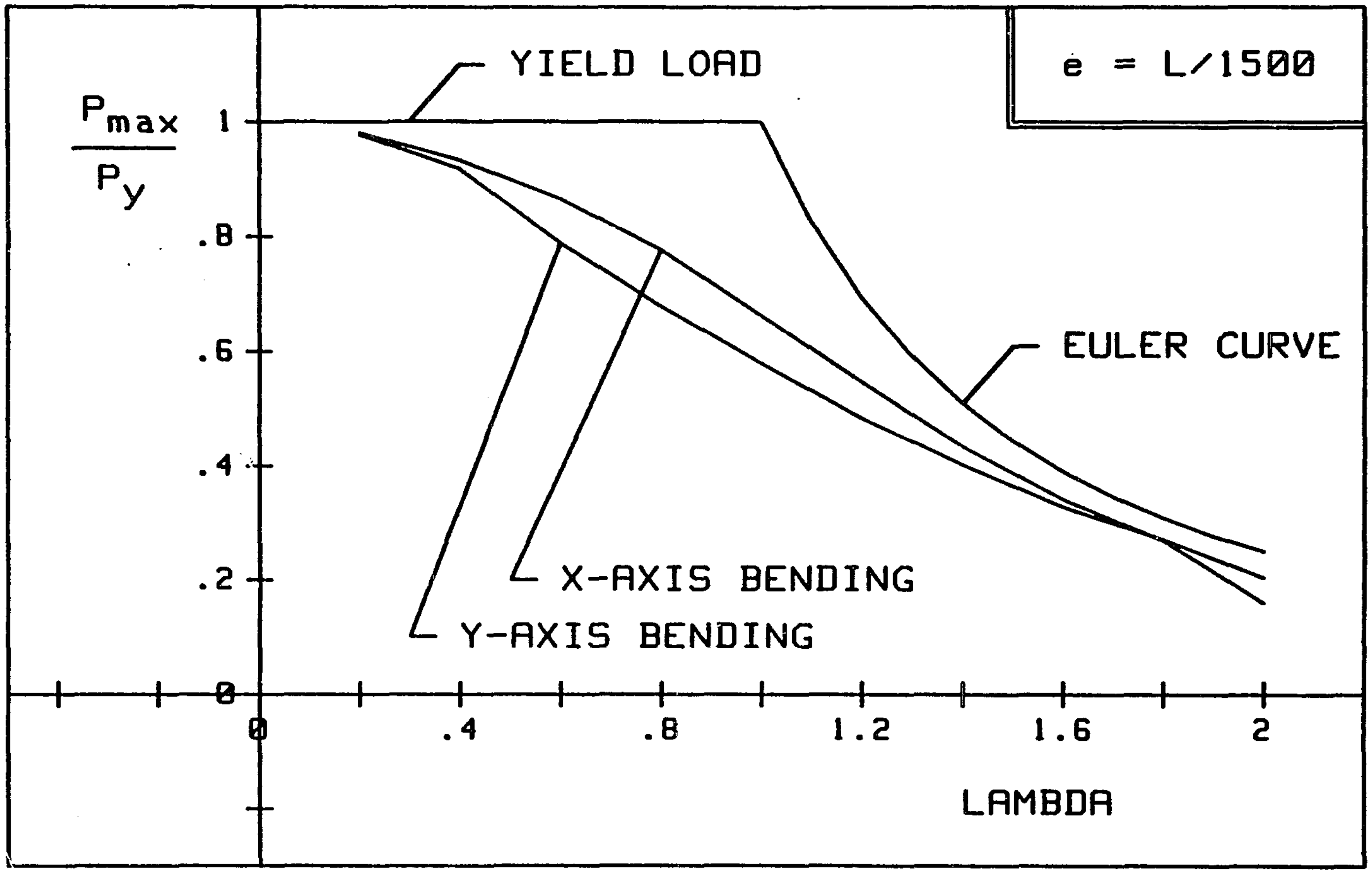

Fig. 6.10. x- and y-axis maximum strength column curves for shape HD 260 x 274 (European) with yield stress of 36 ksi.

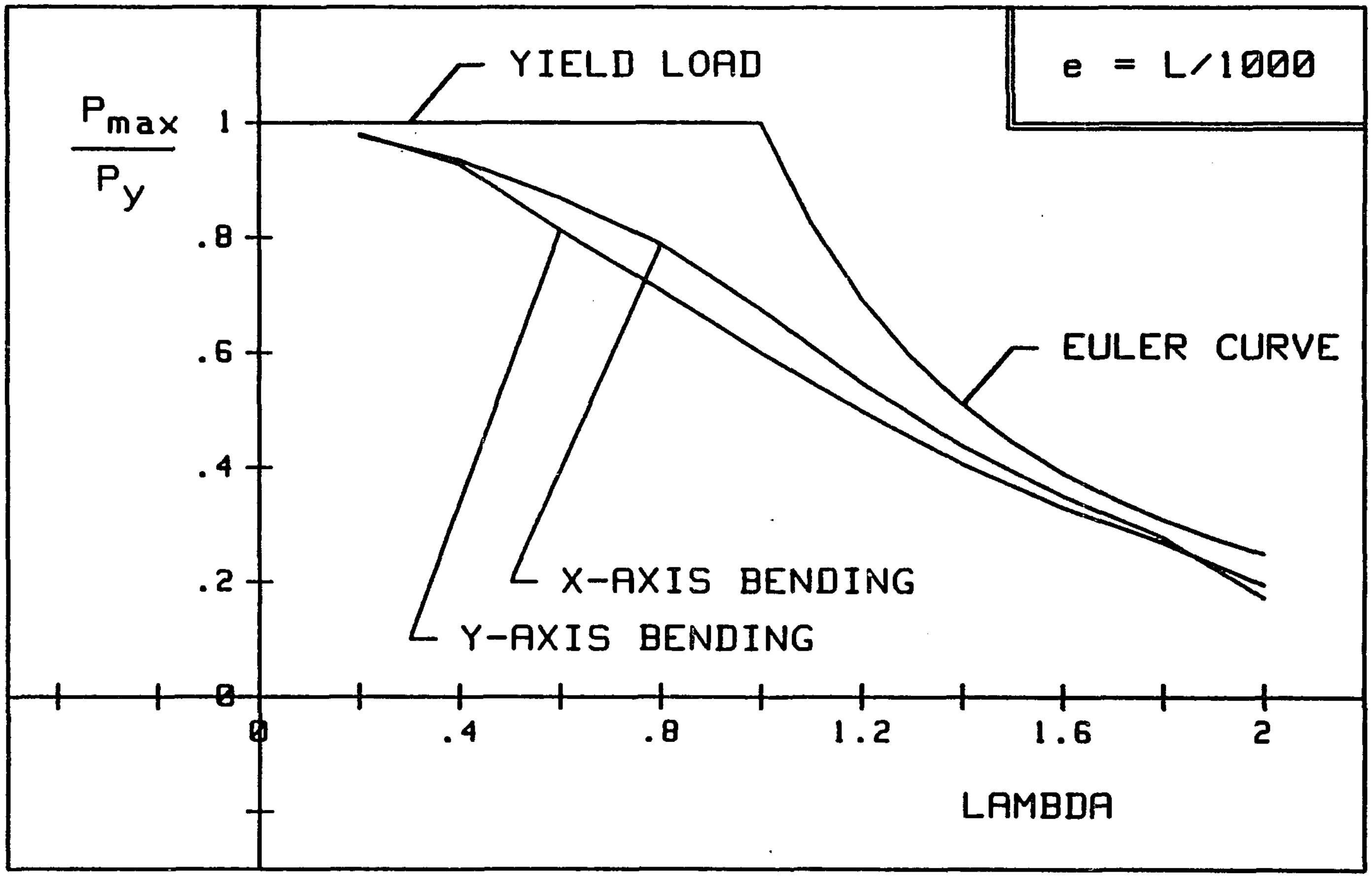

Fig. 6.11. x- and y-axis maximum strength column curves for shape HD 260 x 274 (European) with yield stress of 50 ksi.

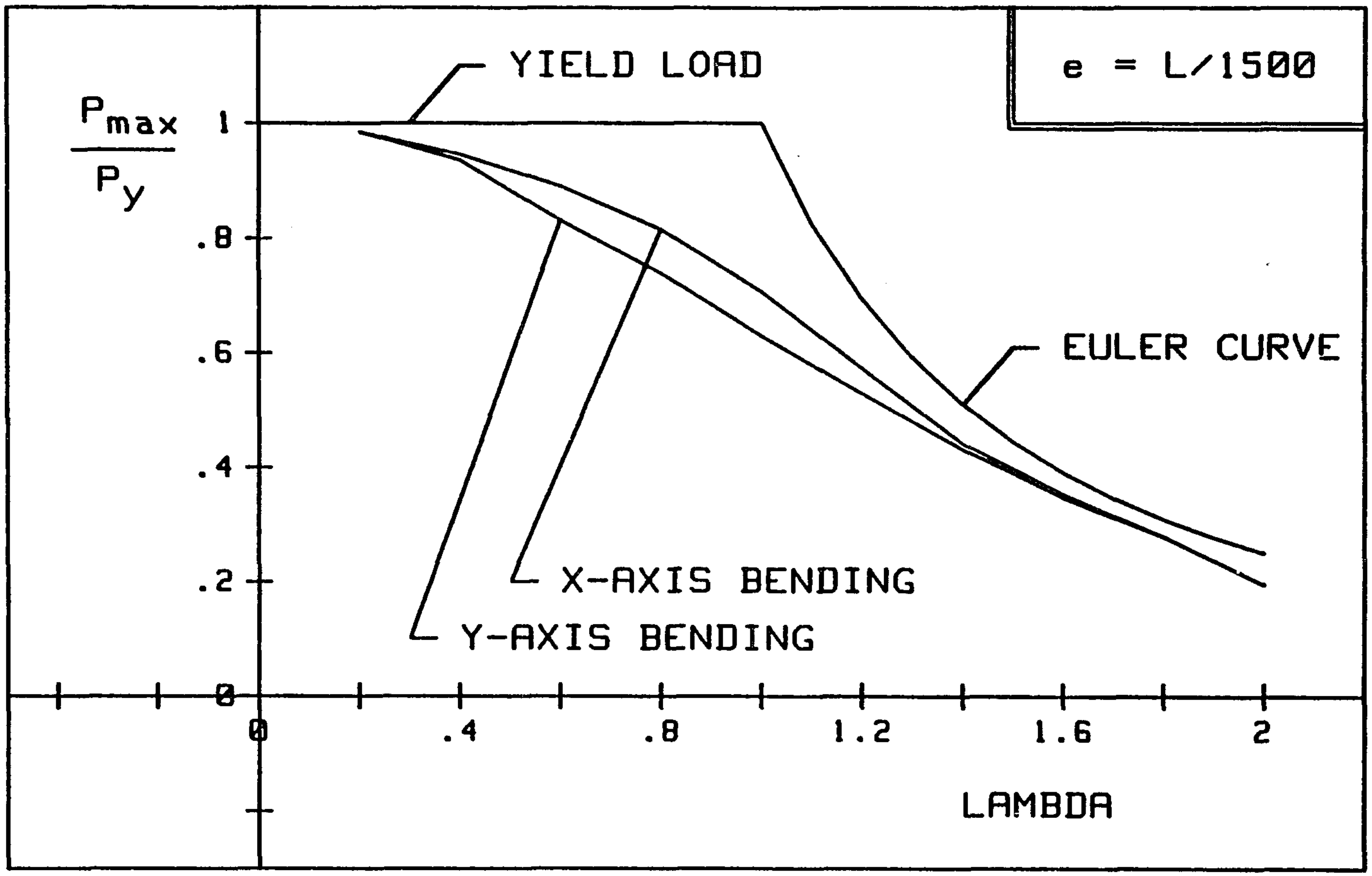

Fig. 6.12. x- and y-axis maximum strength column curves for shape HD 260 x 274 (European) with yield stress of 50 ksi.

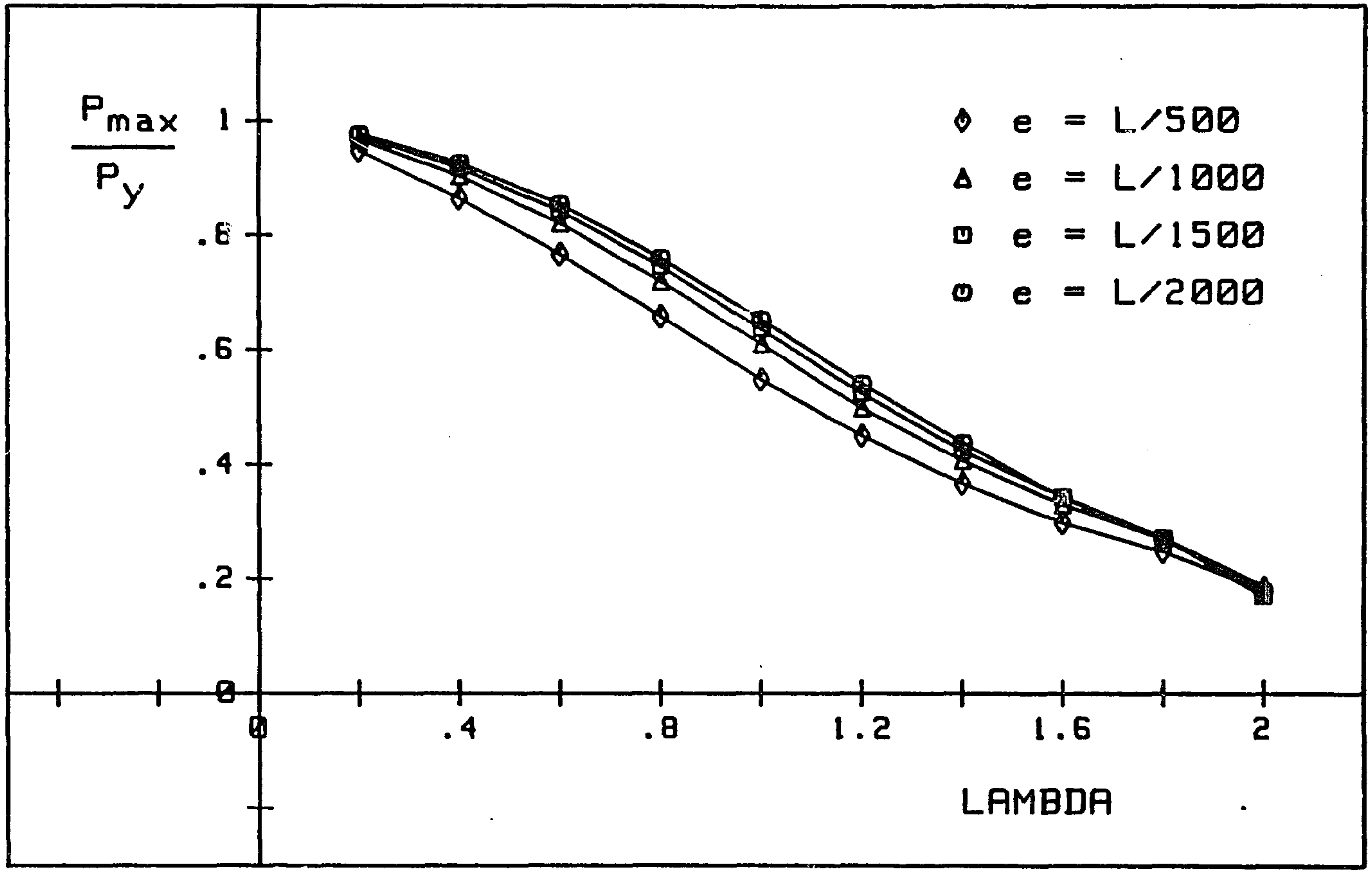

Fig. 6.13. Maximum strength column curves for shape W 14 x 426 with yield stress of 36 ksi and x-axis bending.

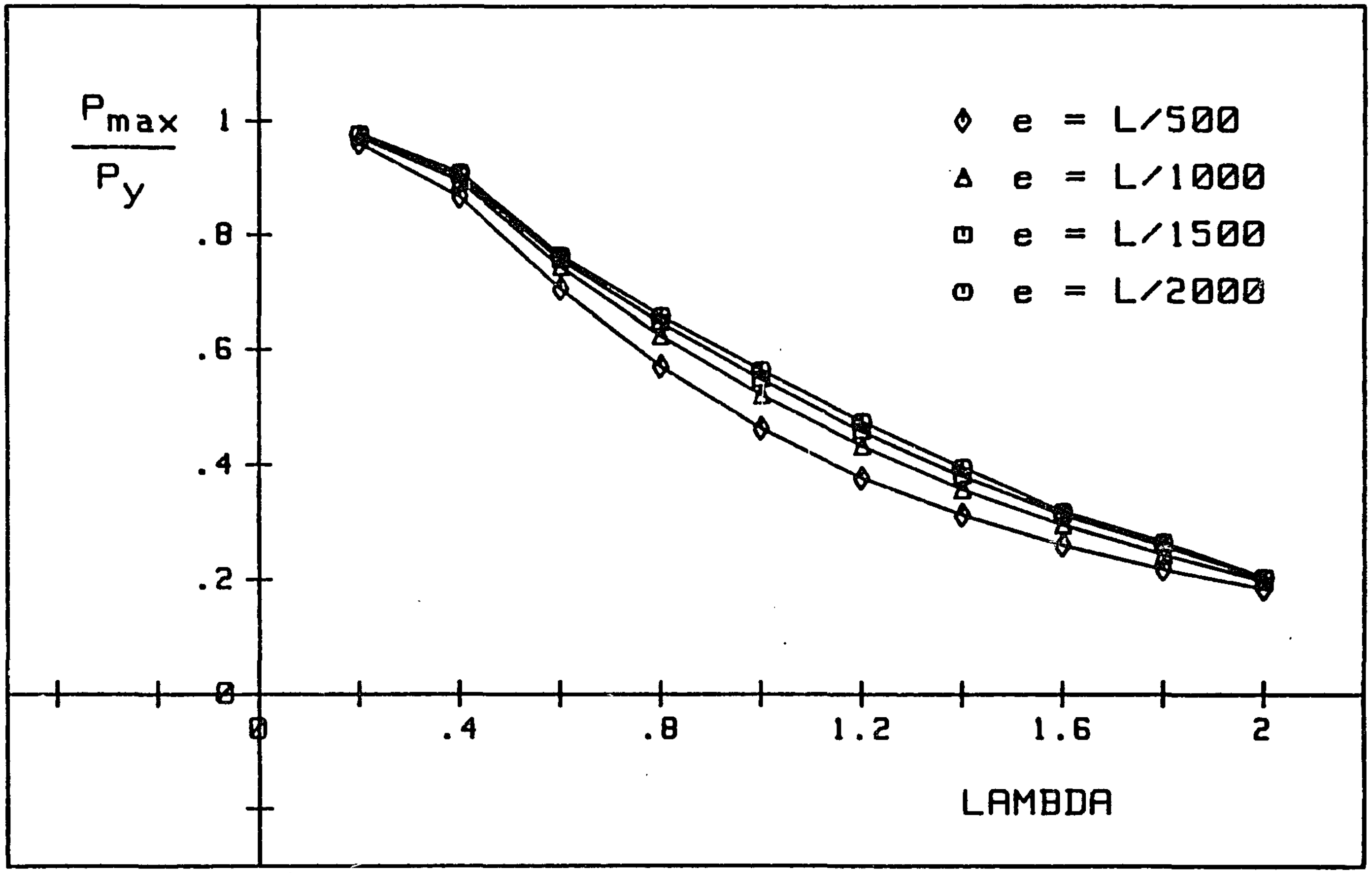

Fig. 6.14. Maximum strength column curves for shape W 14 x 426 with yield stress of 36 ksi and y-axis bending.

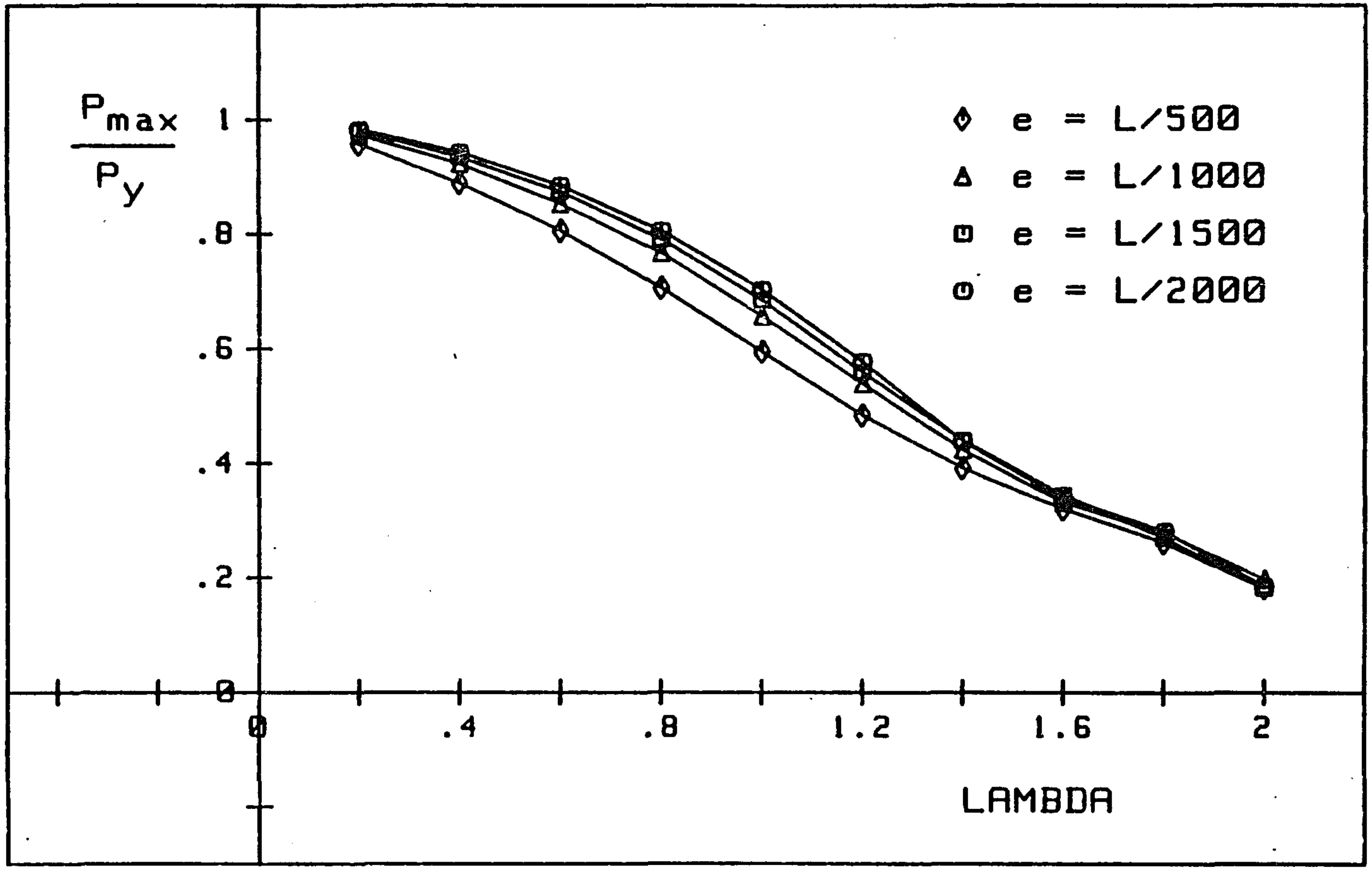

Fig. 6.15. Maximum strength column curves for shape W 14 x 426 with yield stress of 50 ksi and x-axis bending.

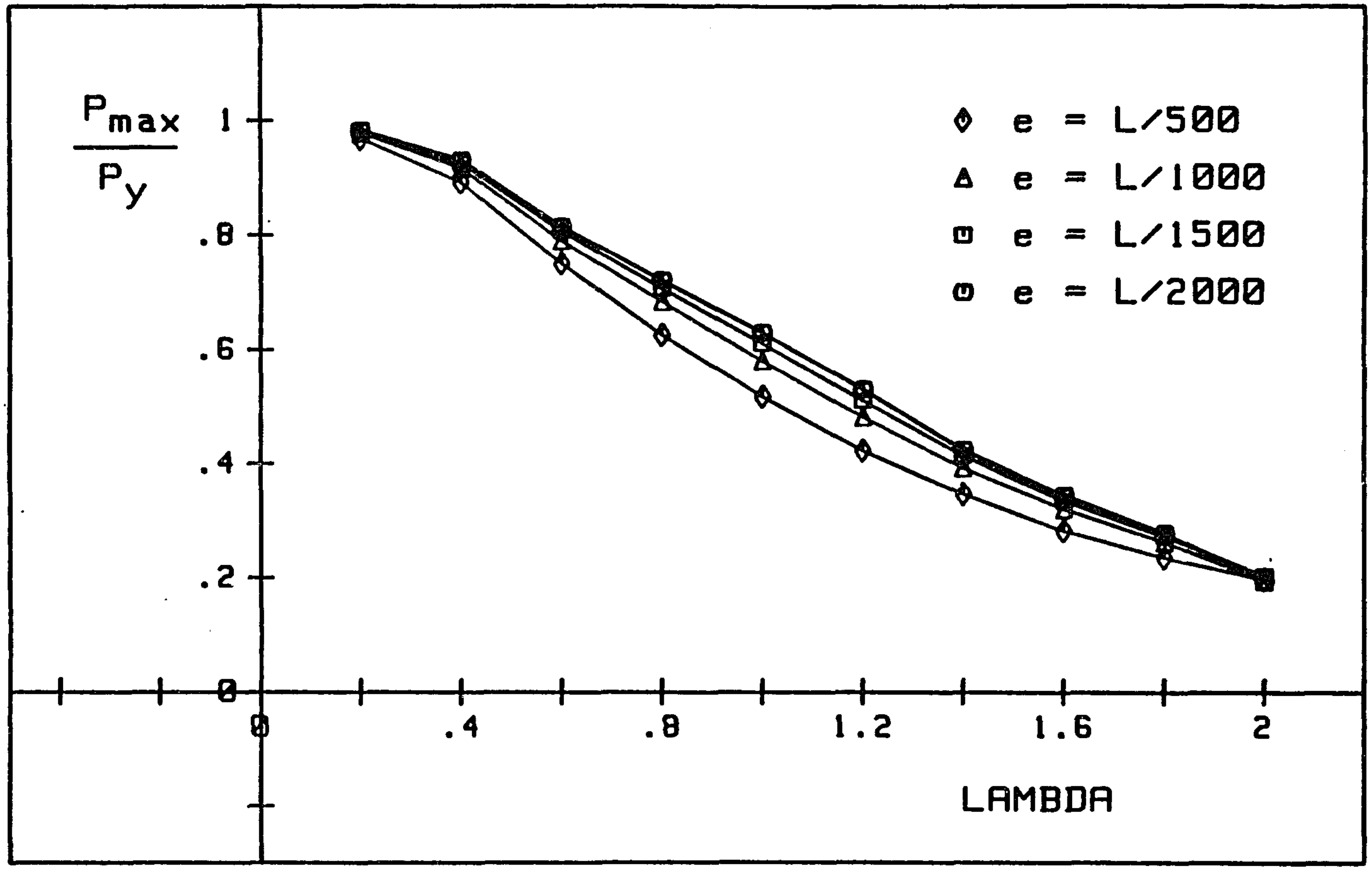

Fig. 6.16. Maximum strength column curves for shape W 14 x 426 with yield stress of 50 ksi and y-axis bending.

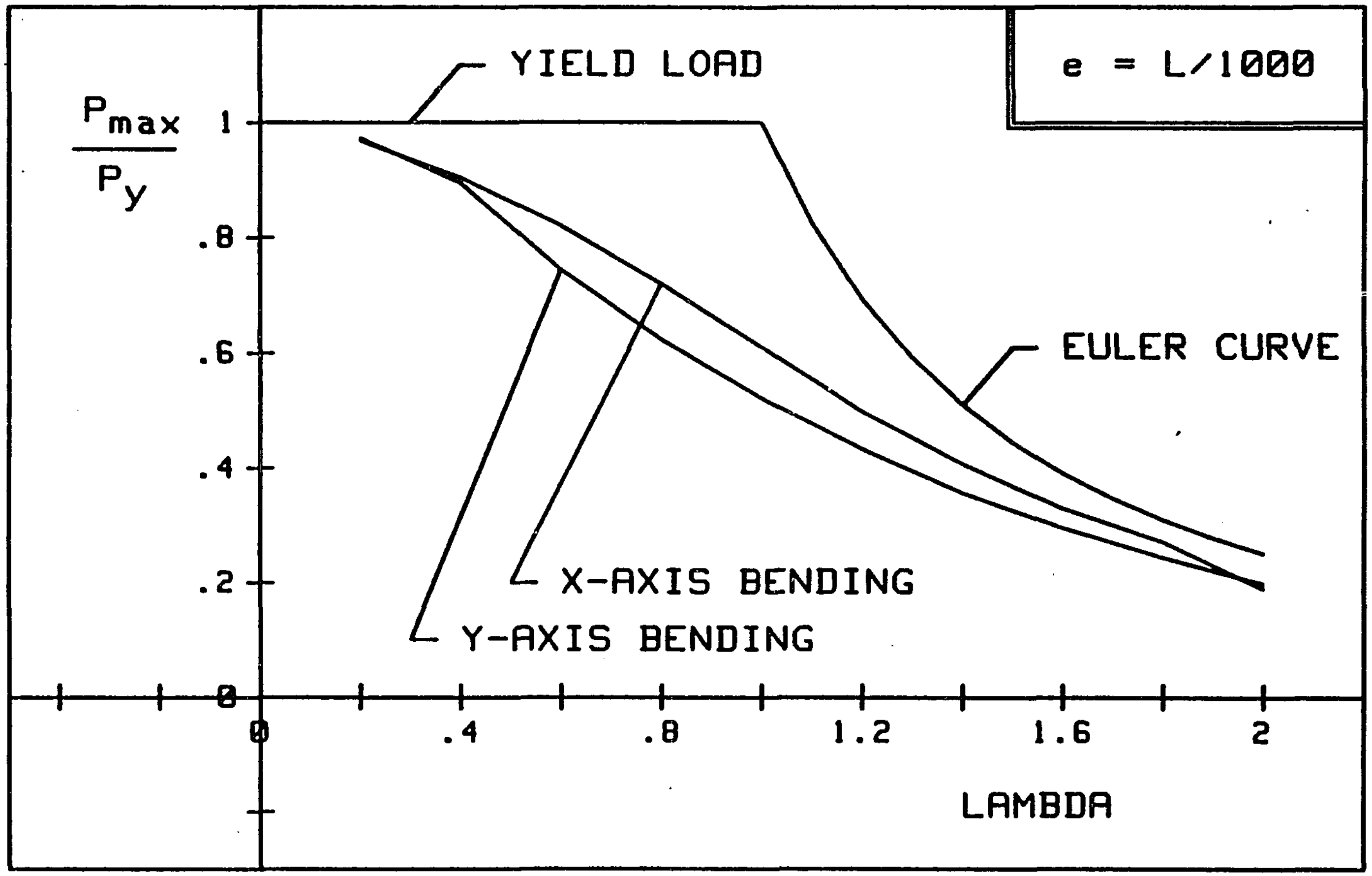

Fig. 6.17. x- and y-axis maximum strength column curves for shape W 14 x 426 with yield stress of 36 ksi.

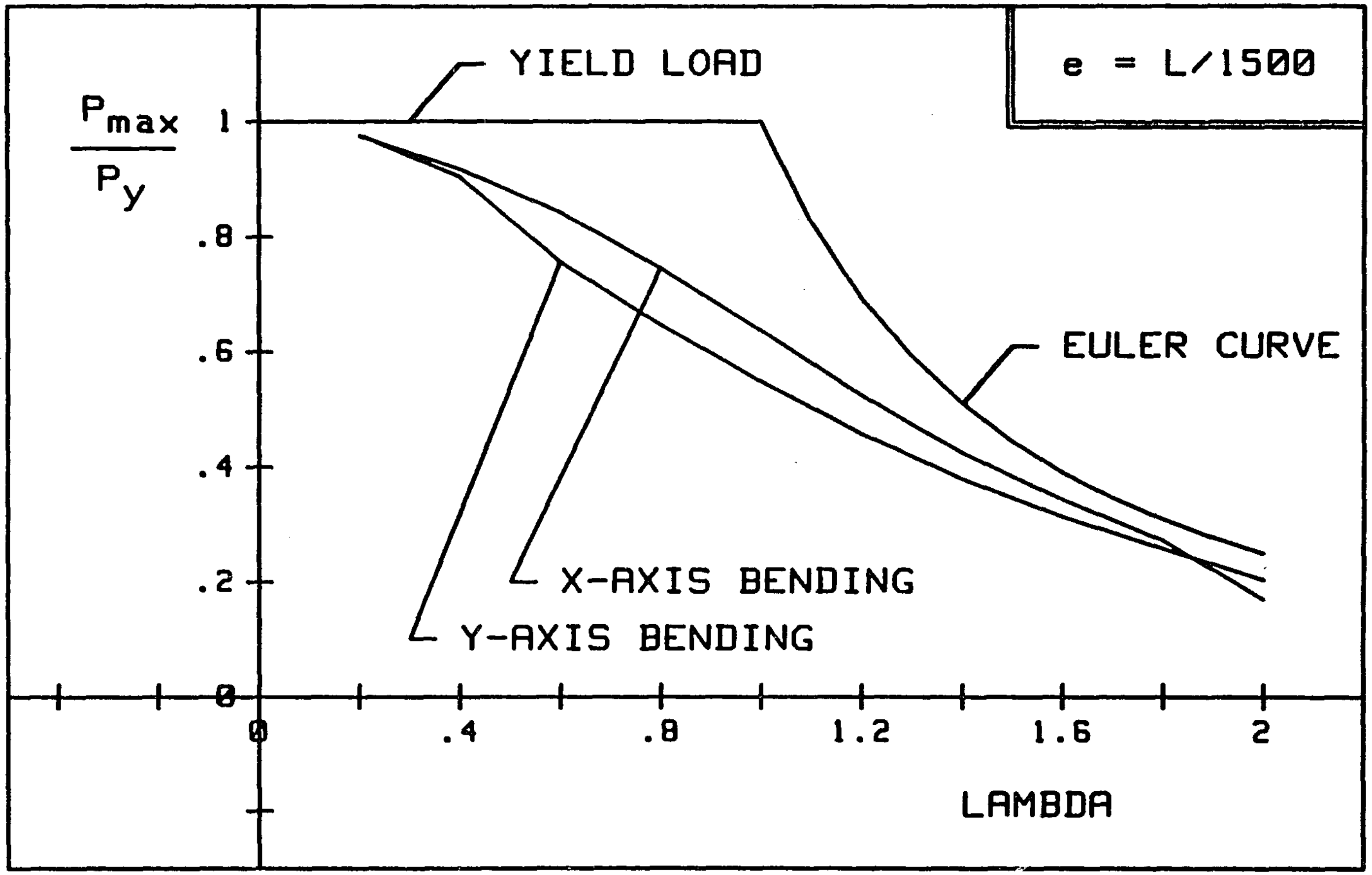

Fig. 6.18. x- and y-axis maximum strength column curves for shape W 14 x 426 with yield stress of 36 ksi.

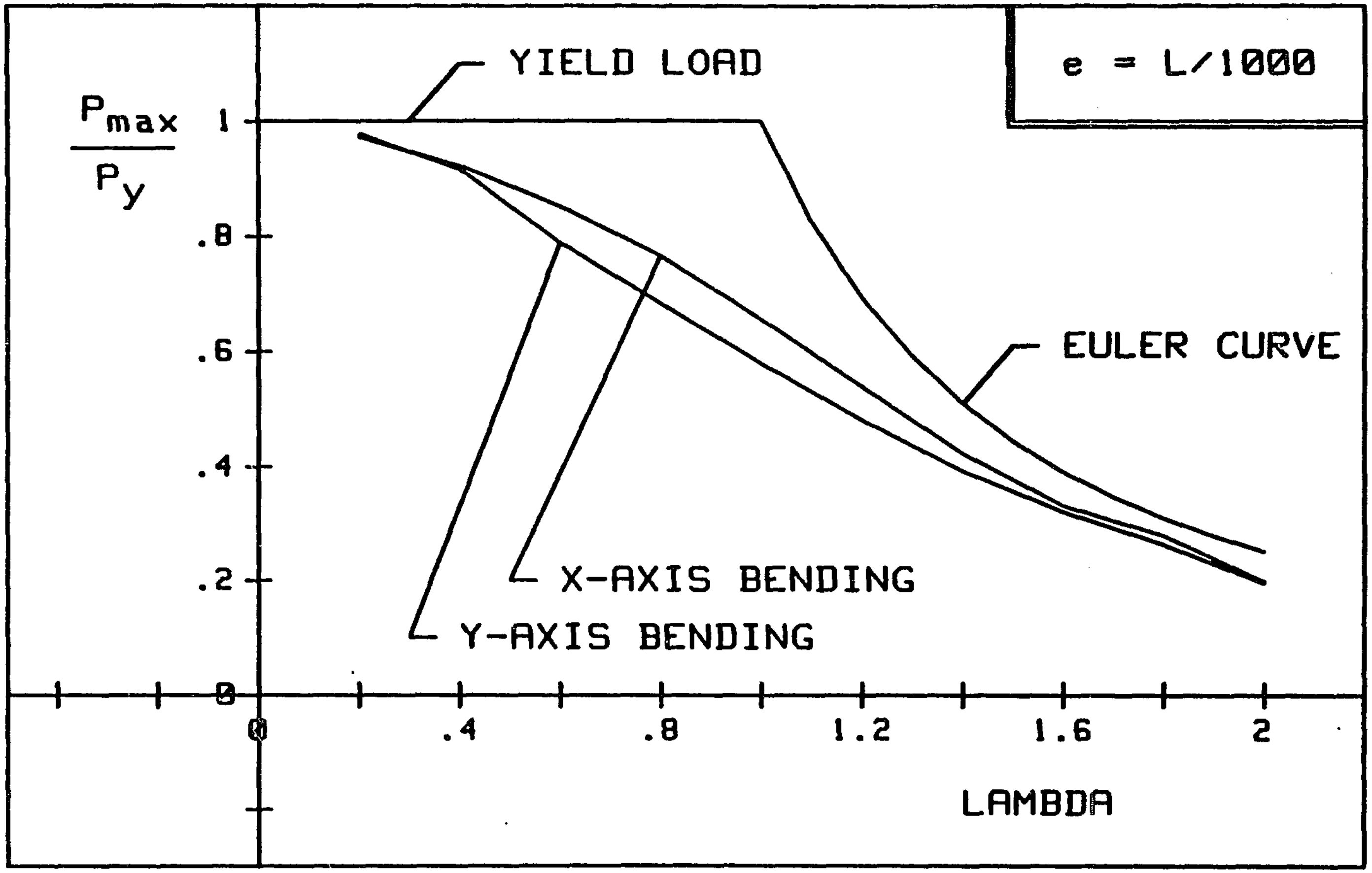

Fig. 6.19. x- and y-axis maximum strength column curves for shape W 14 x 426 with yield stress of 50 ksi.

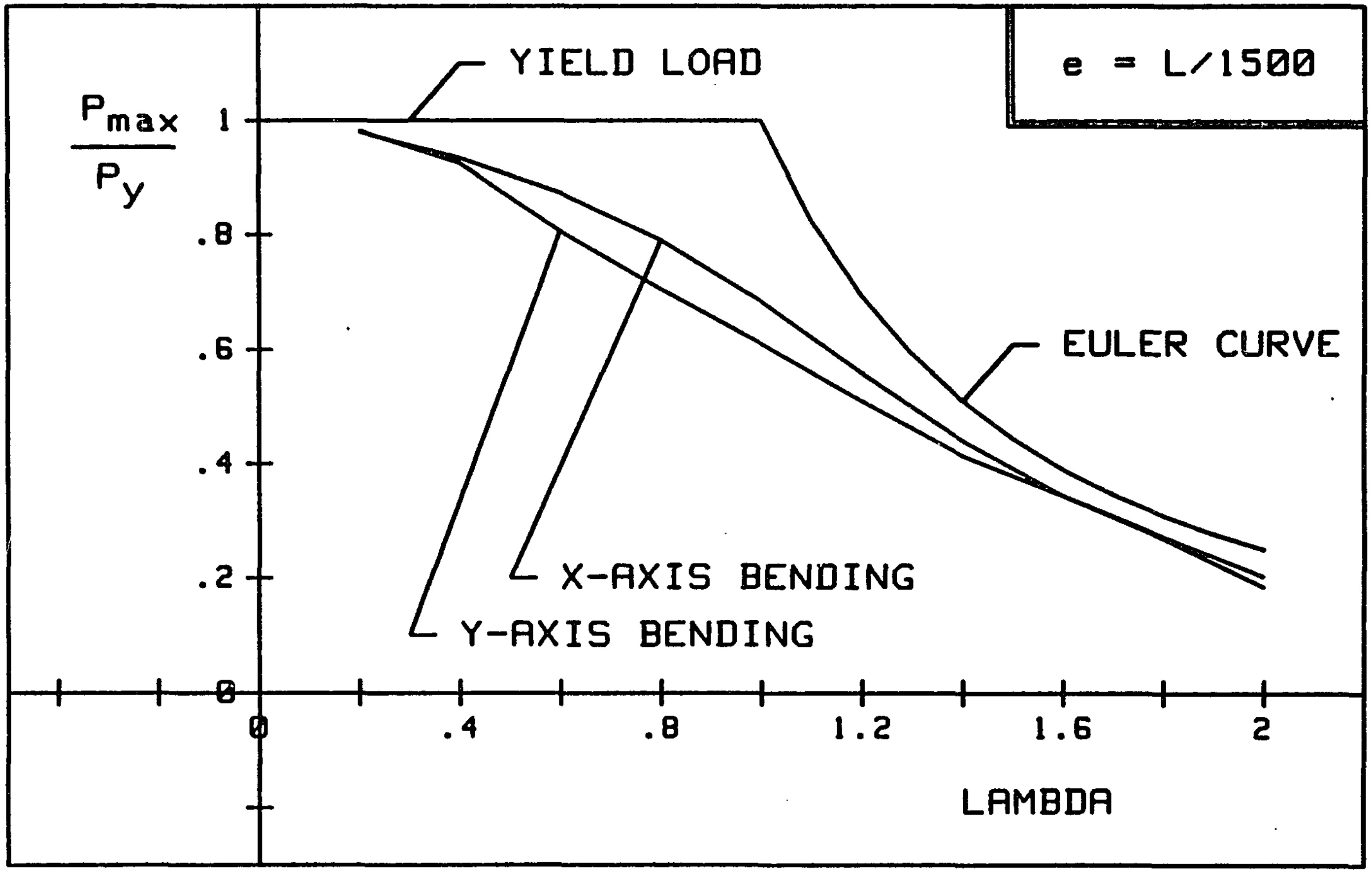

Fig. 6.20. x- and y-axis maximum strength column curves for shape W 14 x 426 with yield stress of 50 ksi.

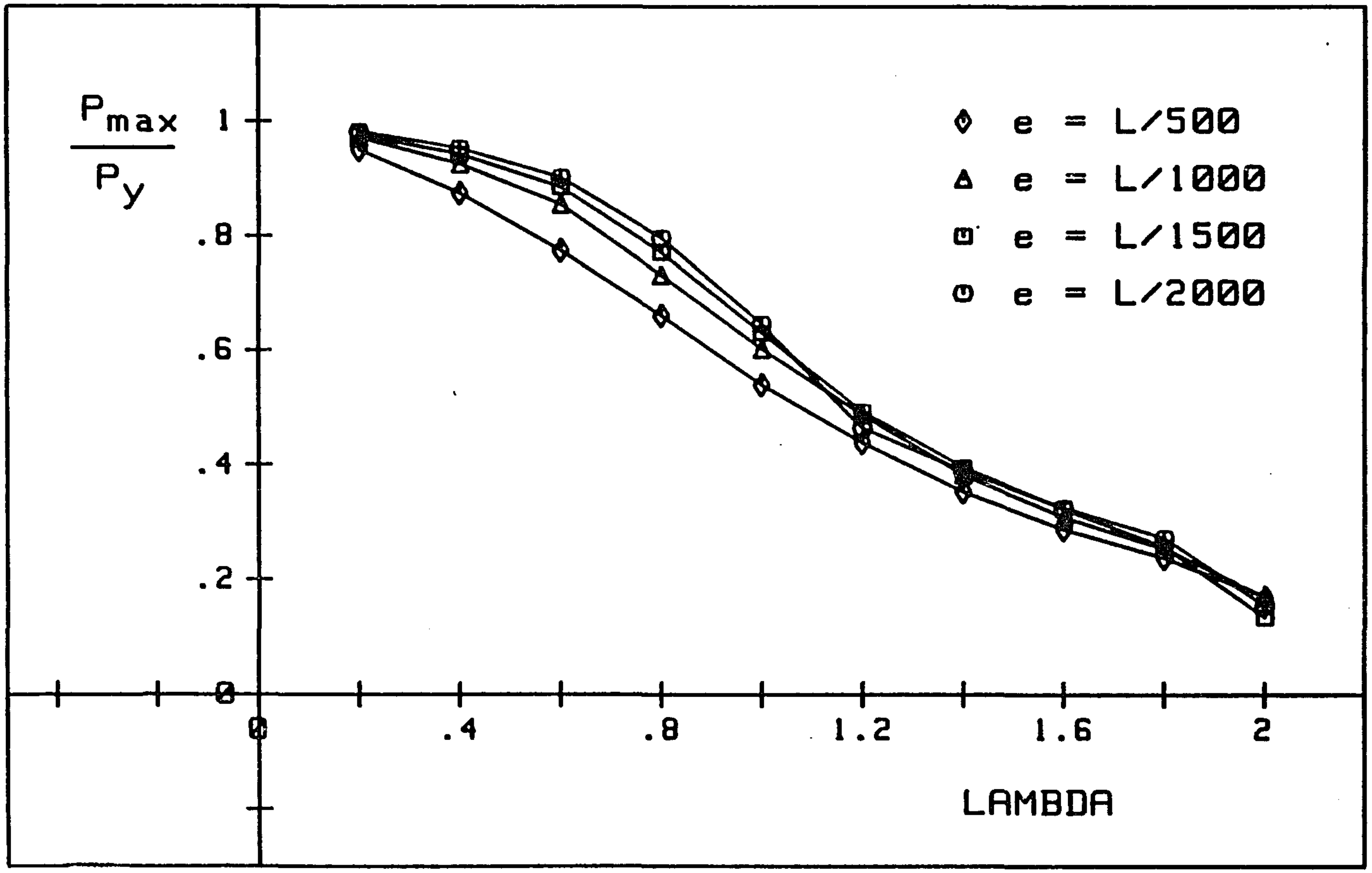

Fig. 6.21. Maximum strength column curves for shape HD 400 x 685 (European) with yield stress of 25 ksi and x-axis bending.

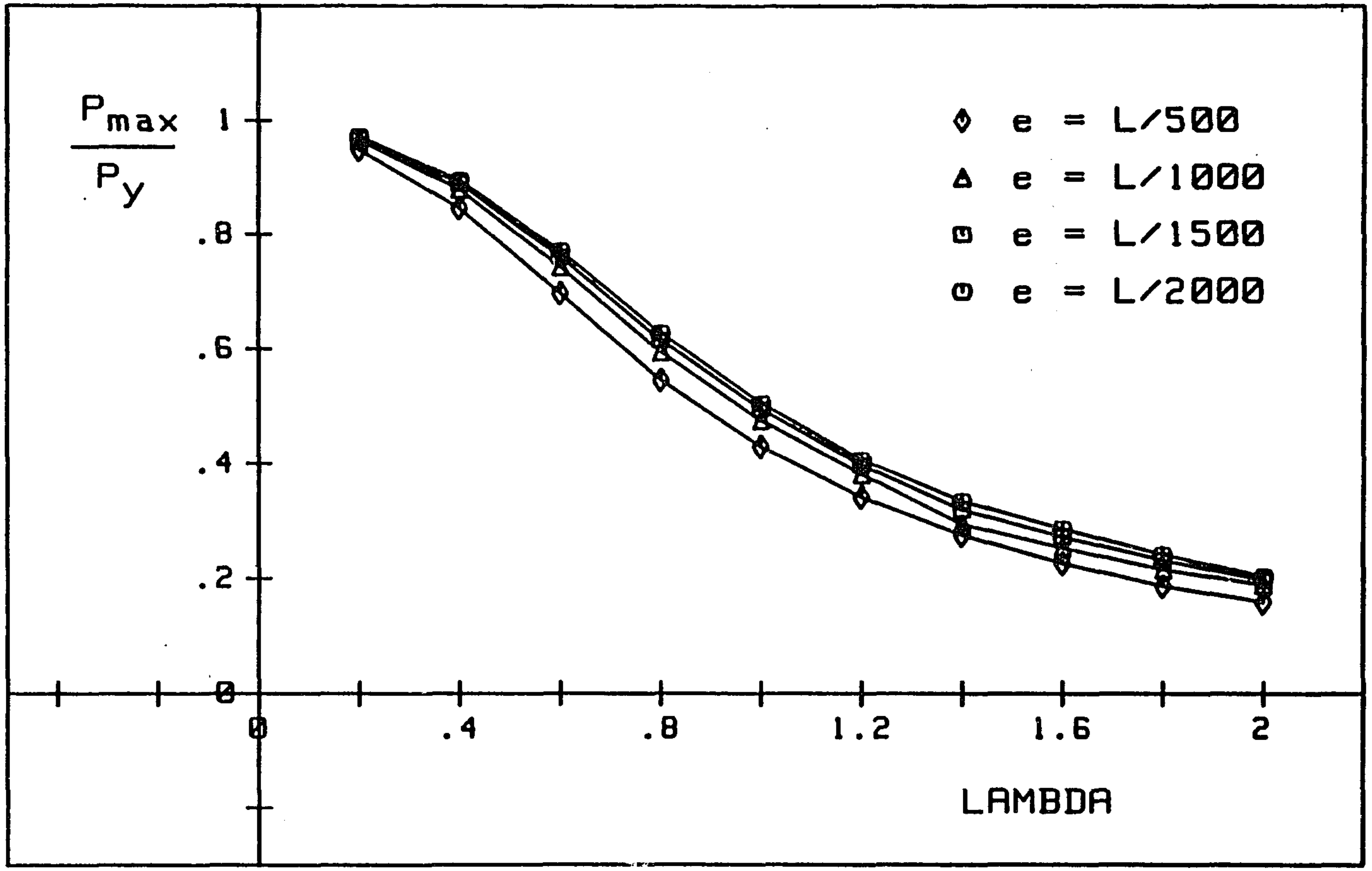

Fig. 6.22. Maximum strength column curves for shape HD 400 x 685 (European) with yield stress of 25 ksi and y-axis bending.

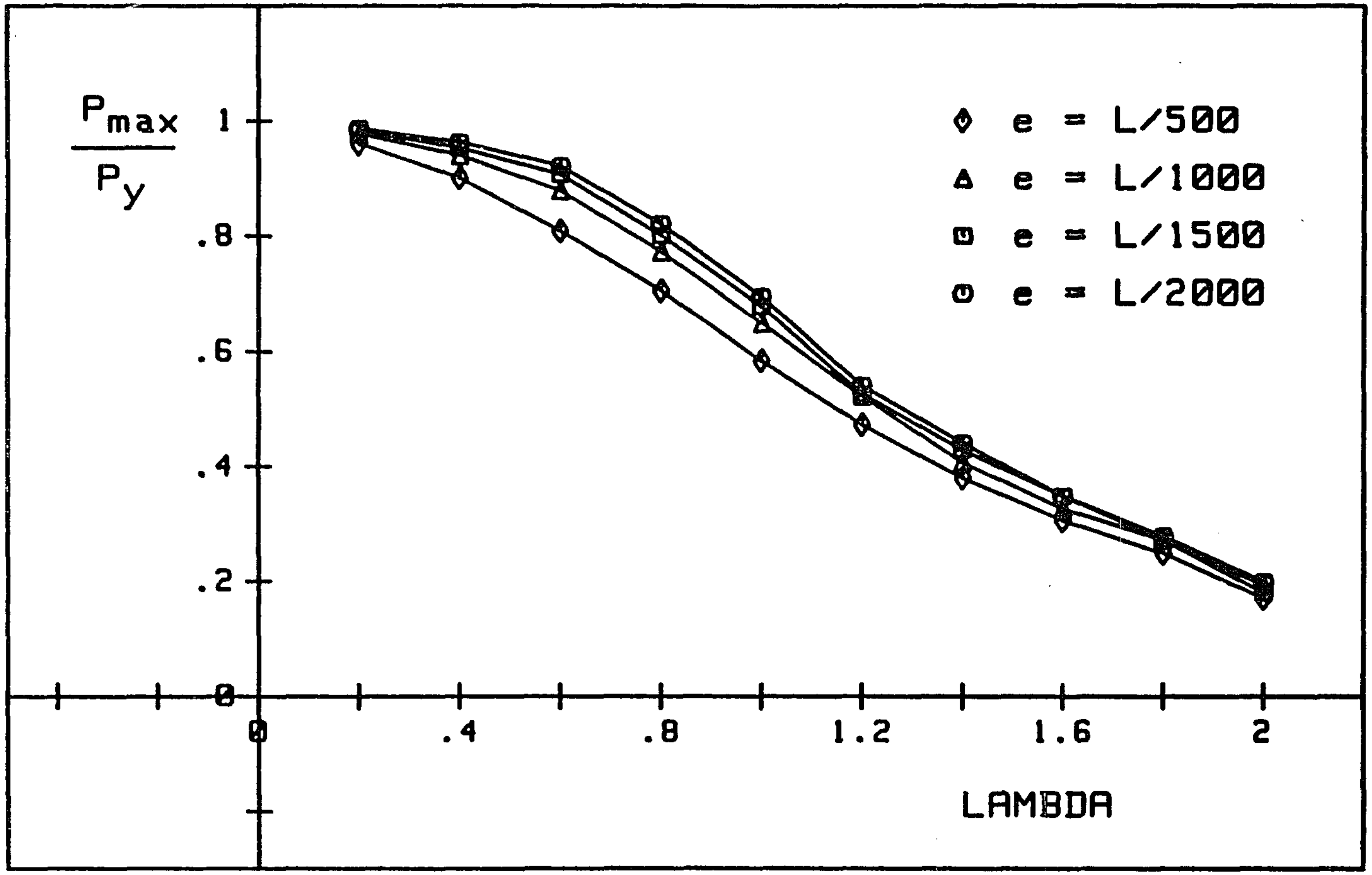

Fig. 6.23. Maximum strength column curves for shape HD 400 x 685 (European) with yield stress of 36 ksi and x-axis bending.

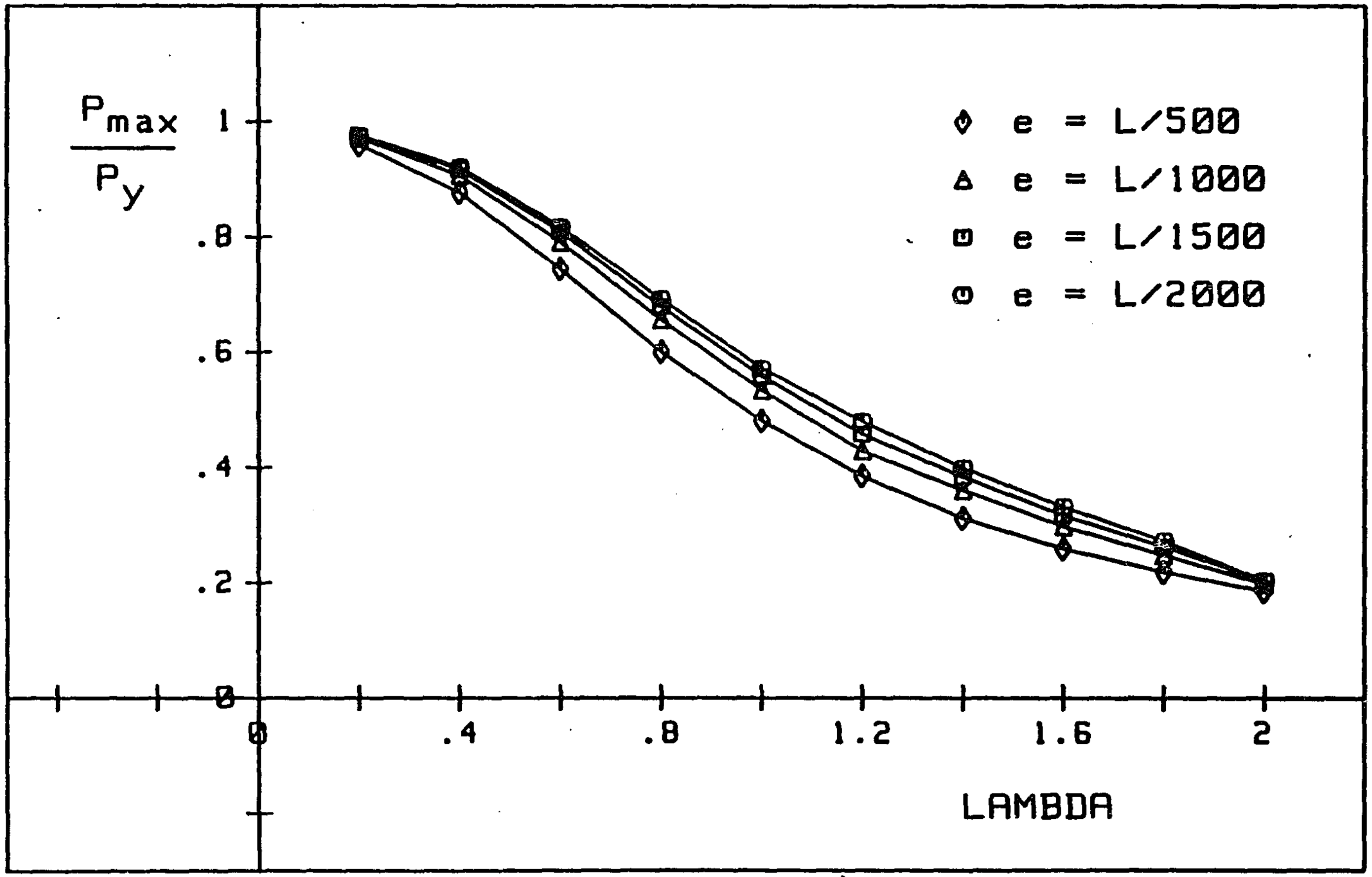

Fig. 6.24. Maximum strength column curves for shape HD 400 x 685 (European) with yield stress of 36 ksi and y-axis bending.

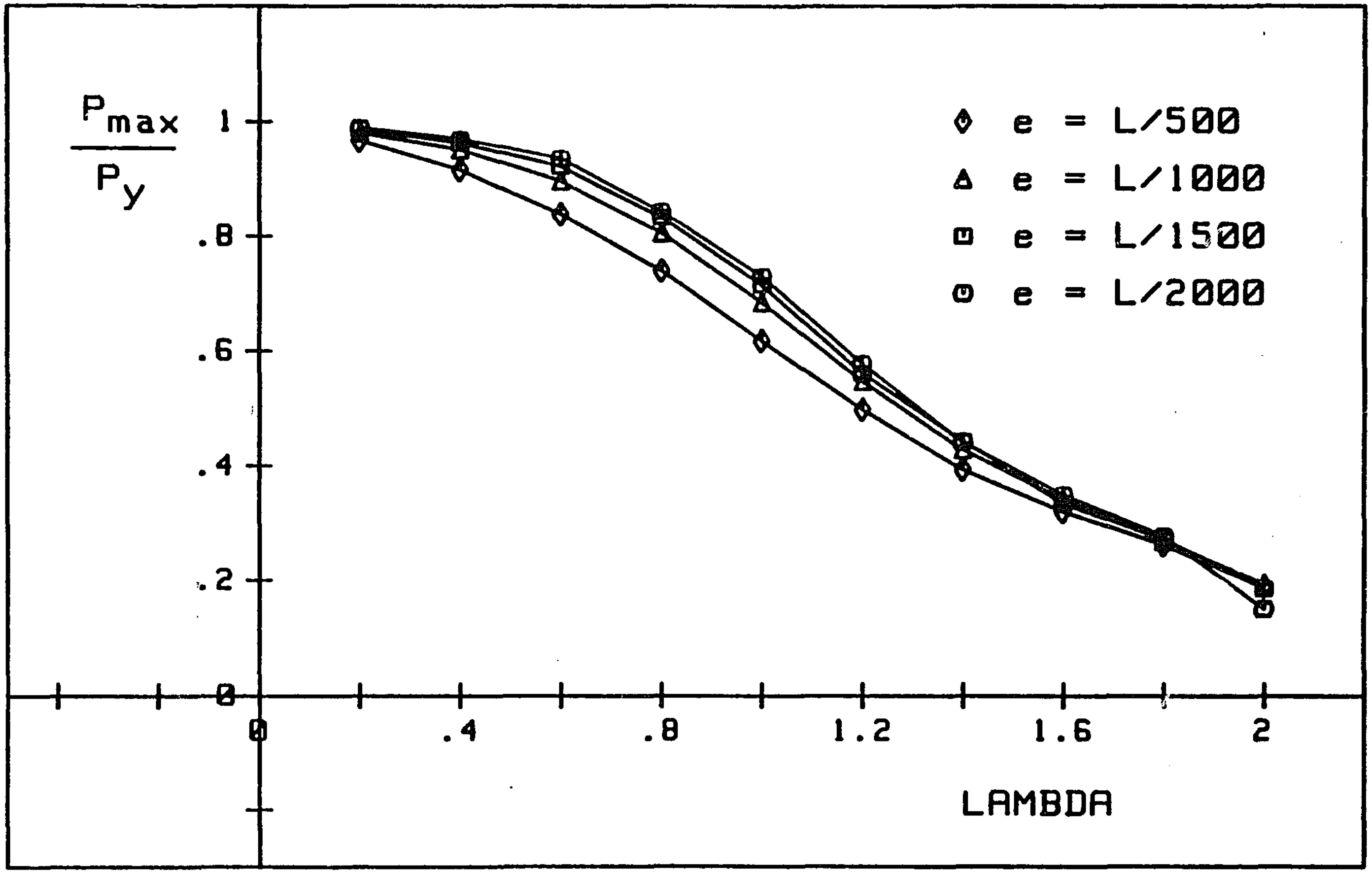

Fig. 6.25. Maximum strength column curves for shape HD 400 x 685 (European) with yield stress of 50 ksi and x-axis bending.

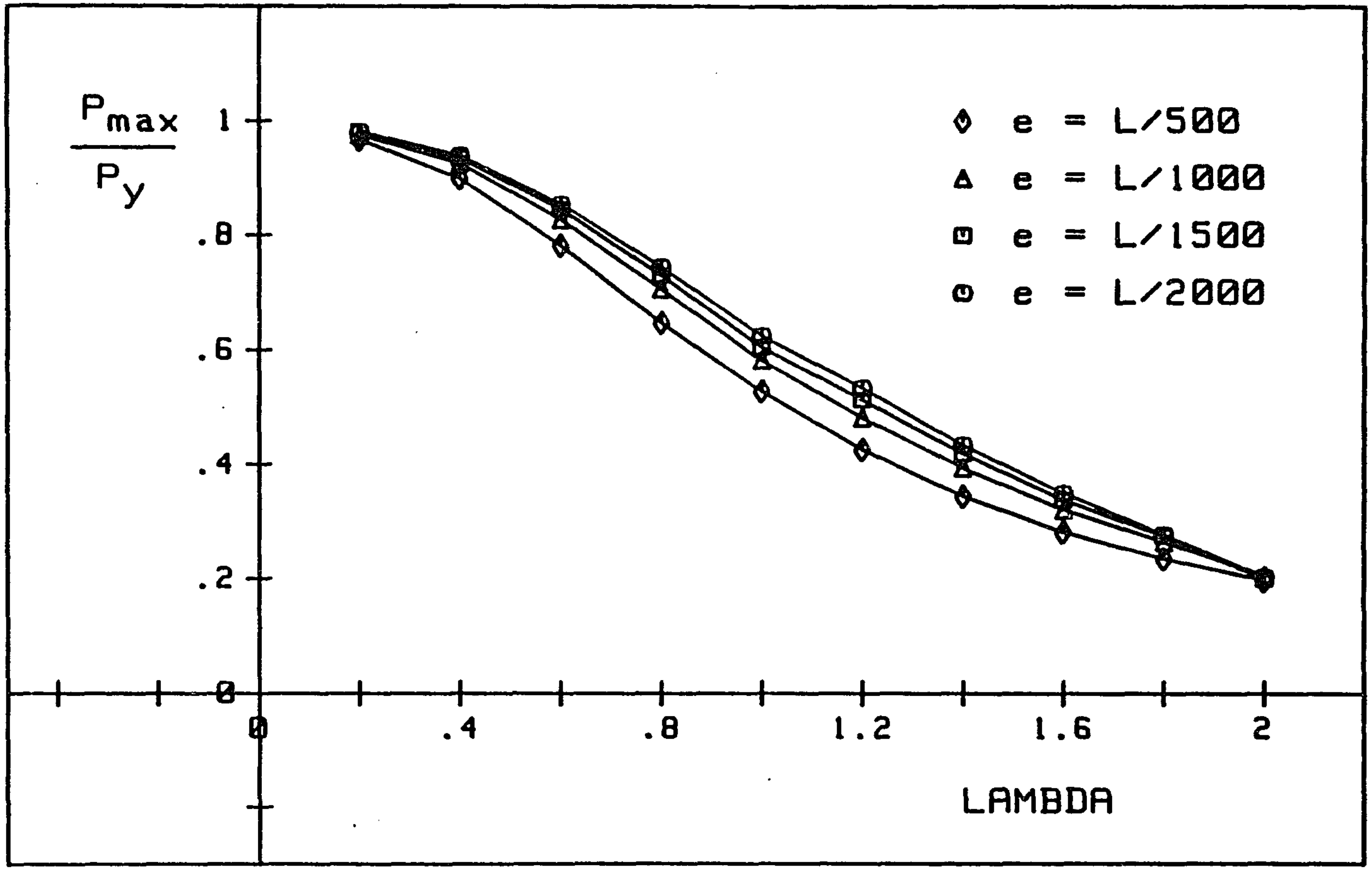

Fig. 6.26. Maximum strength column curves for shape HD 400 x 685 (European) with yield stress of 50 ksi and y-axis bending.

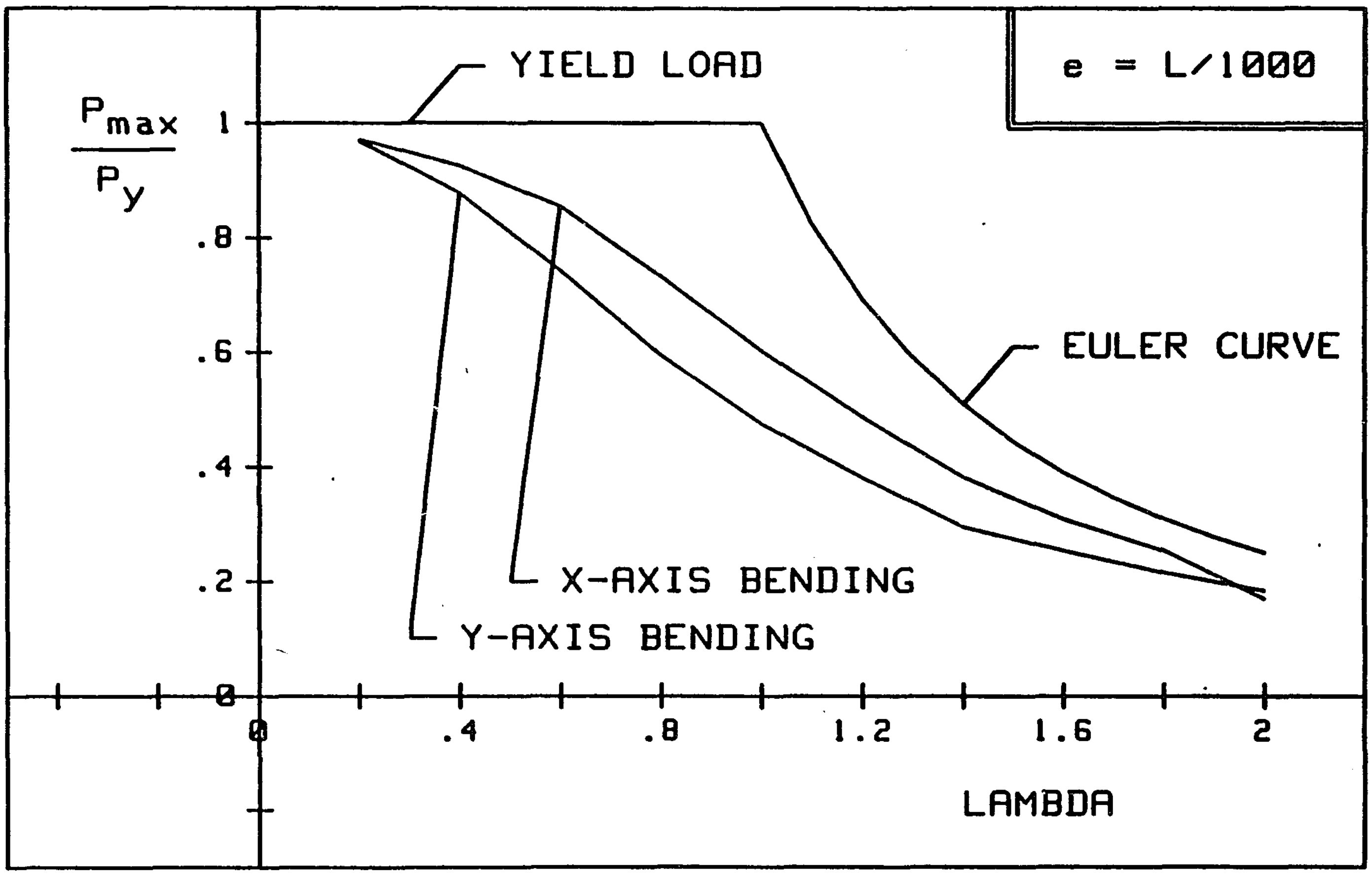

Fig. 6.27. x- and y-axis maximum strength column curves for shape HD 400 x 685 (European) with yield stress of 25 ksi.

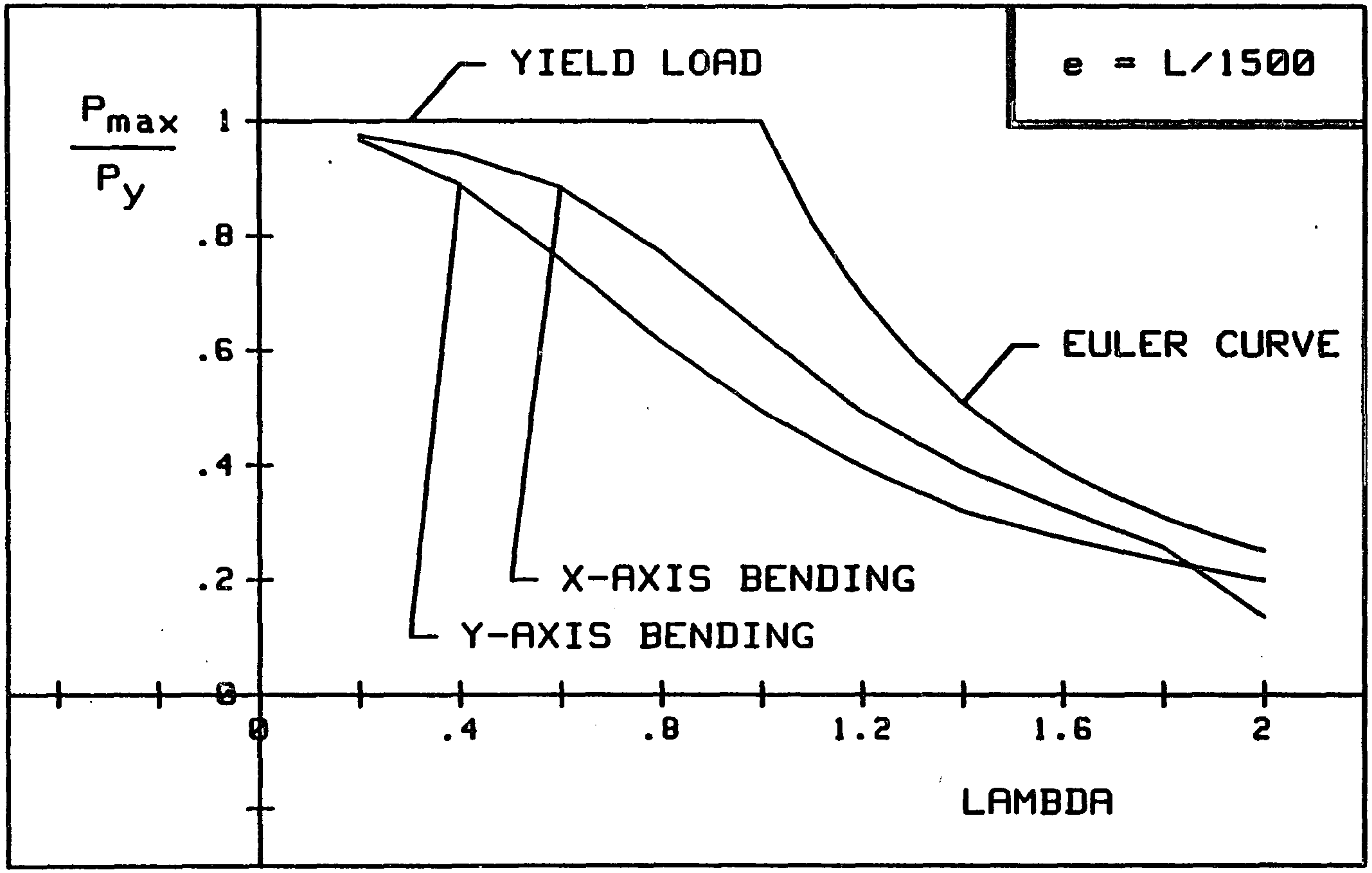

Fig. 6.28. x- and y-axis maximum strength column curves for shape HD 400 x 685 (European) with yield stress of 25 ksi.

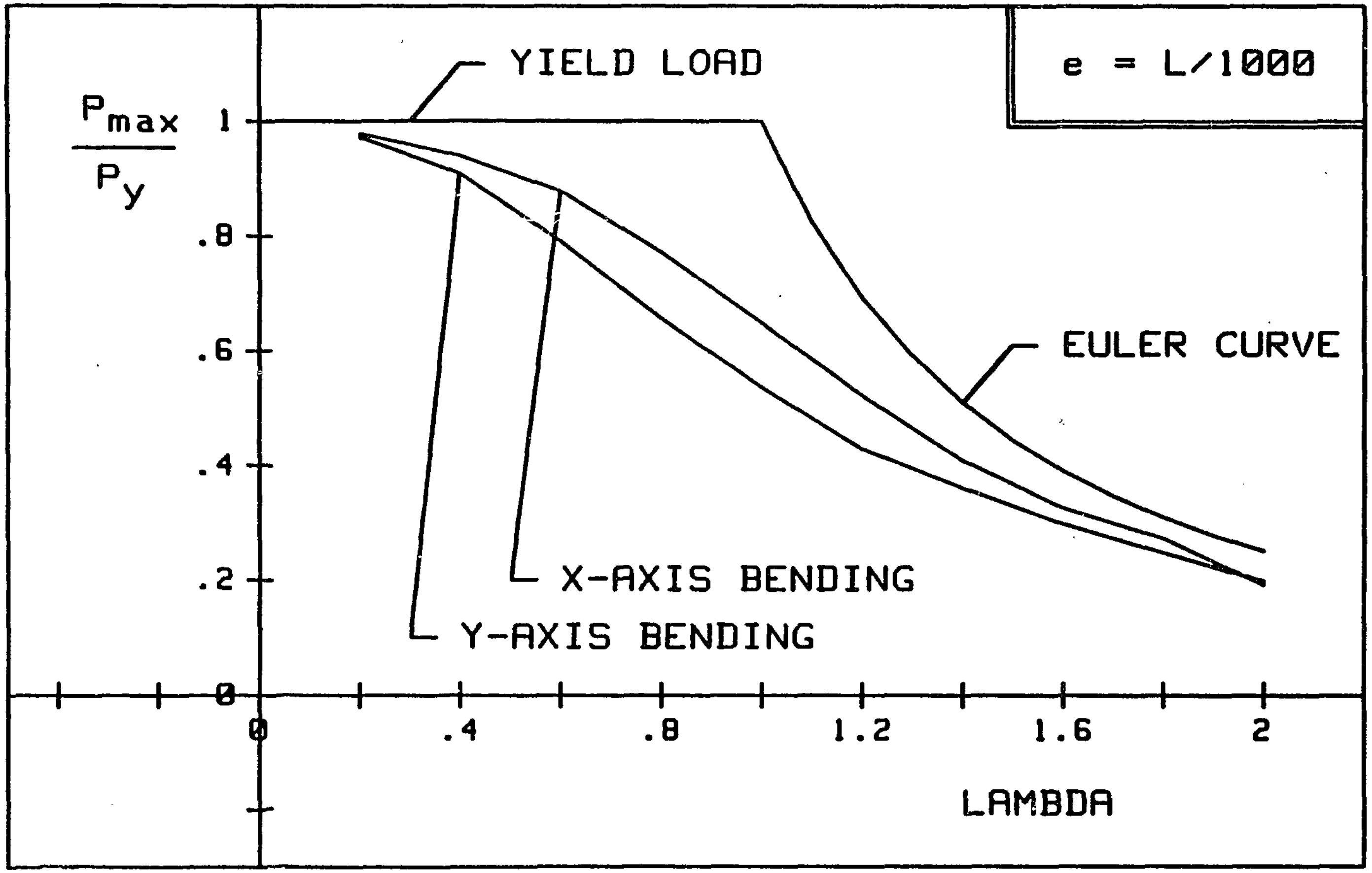

Fig. 6.29. x- and y-axis maximum strength column curves for shape HD 400 x 685 (European) with yield stress of 36 ksi.

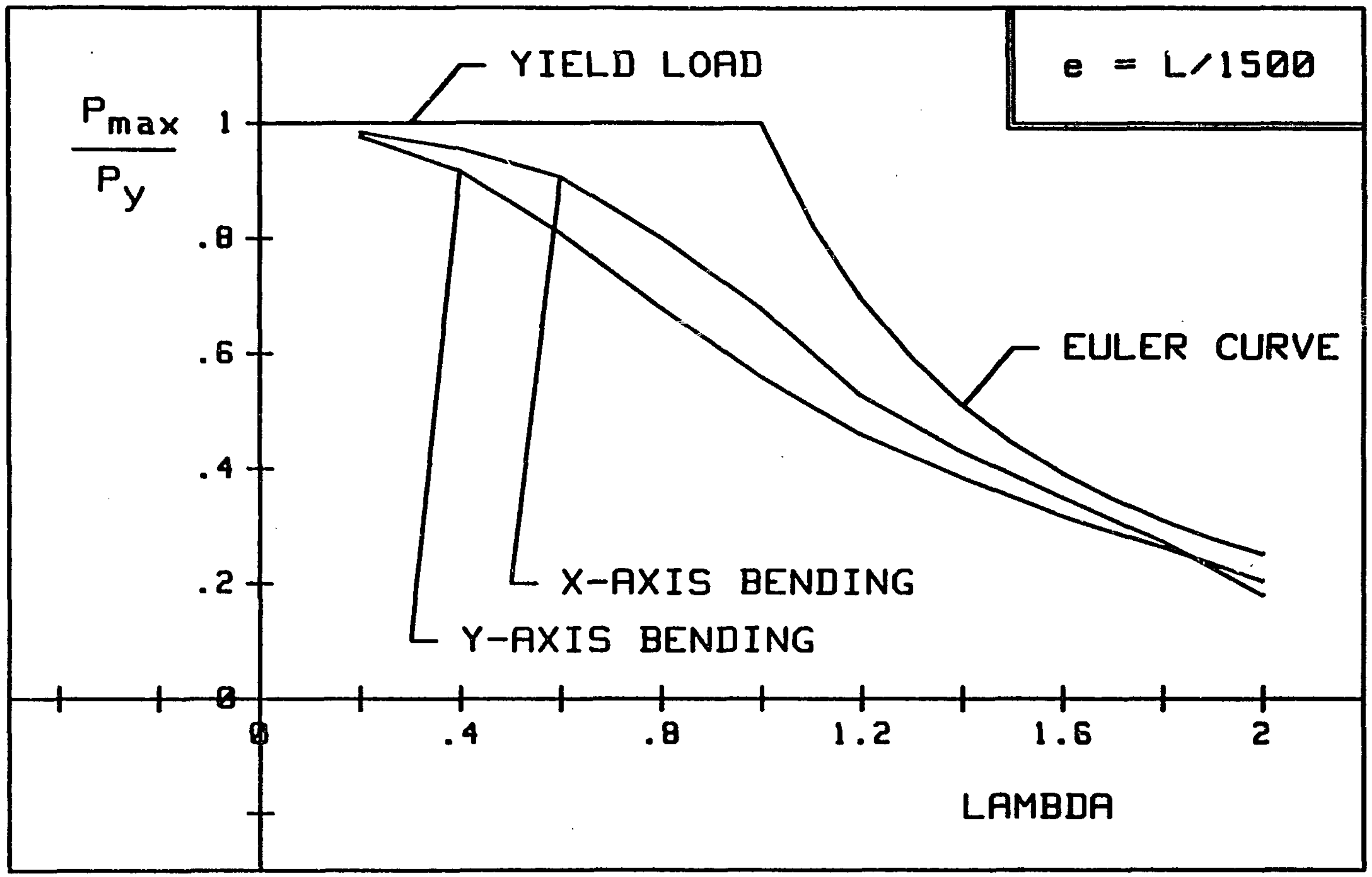

Fig. 6.30. x- and y-axis maximum strength column curves for shape HD 400 x 685 (European) with yield stress of 36 ksi.

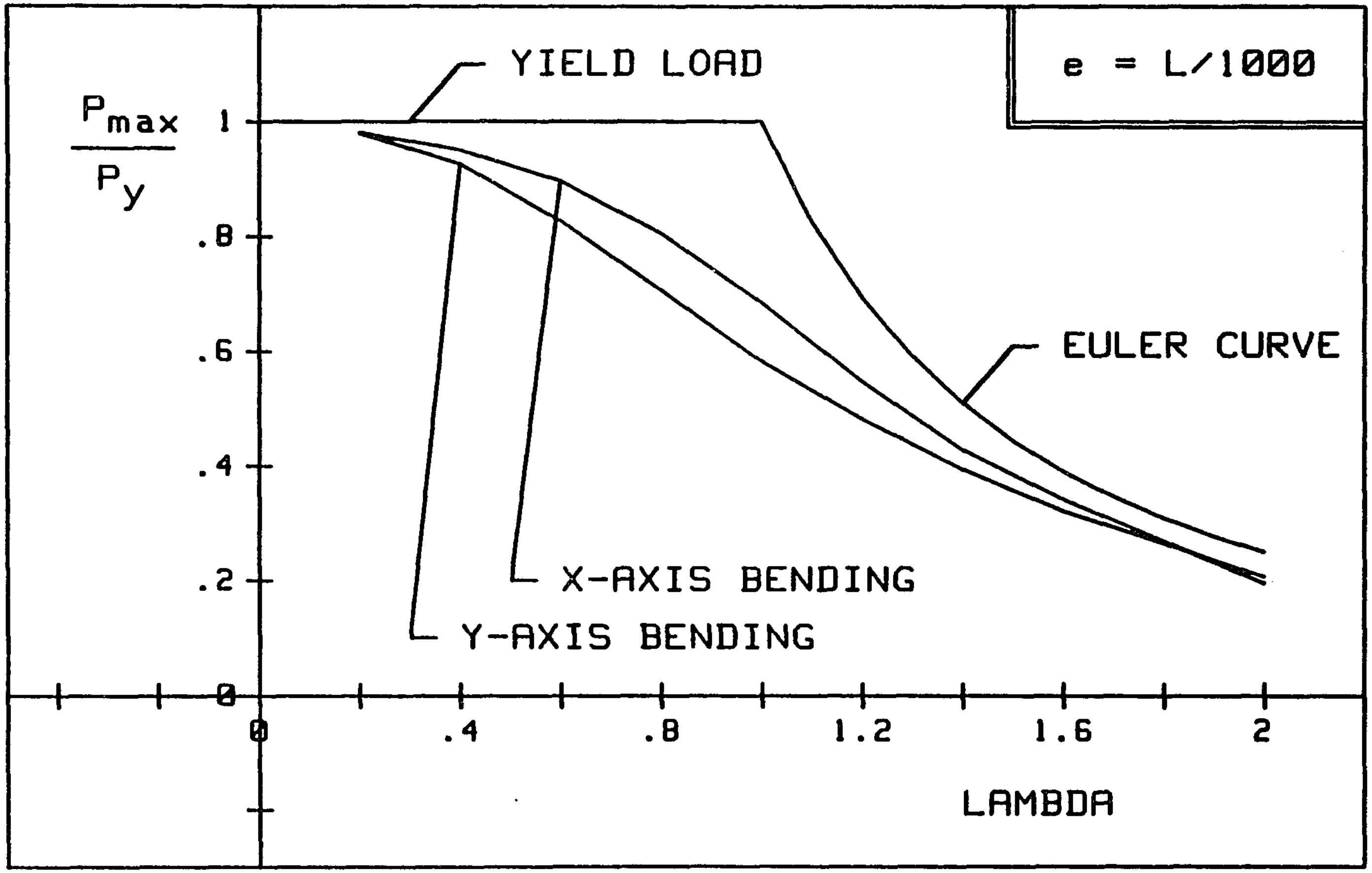

Fig. 6.31. x- and y-axis maximum strength column curves for shape HD 400 x 685 (European) with yield stress of 50 ksi.

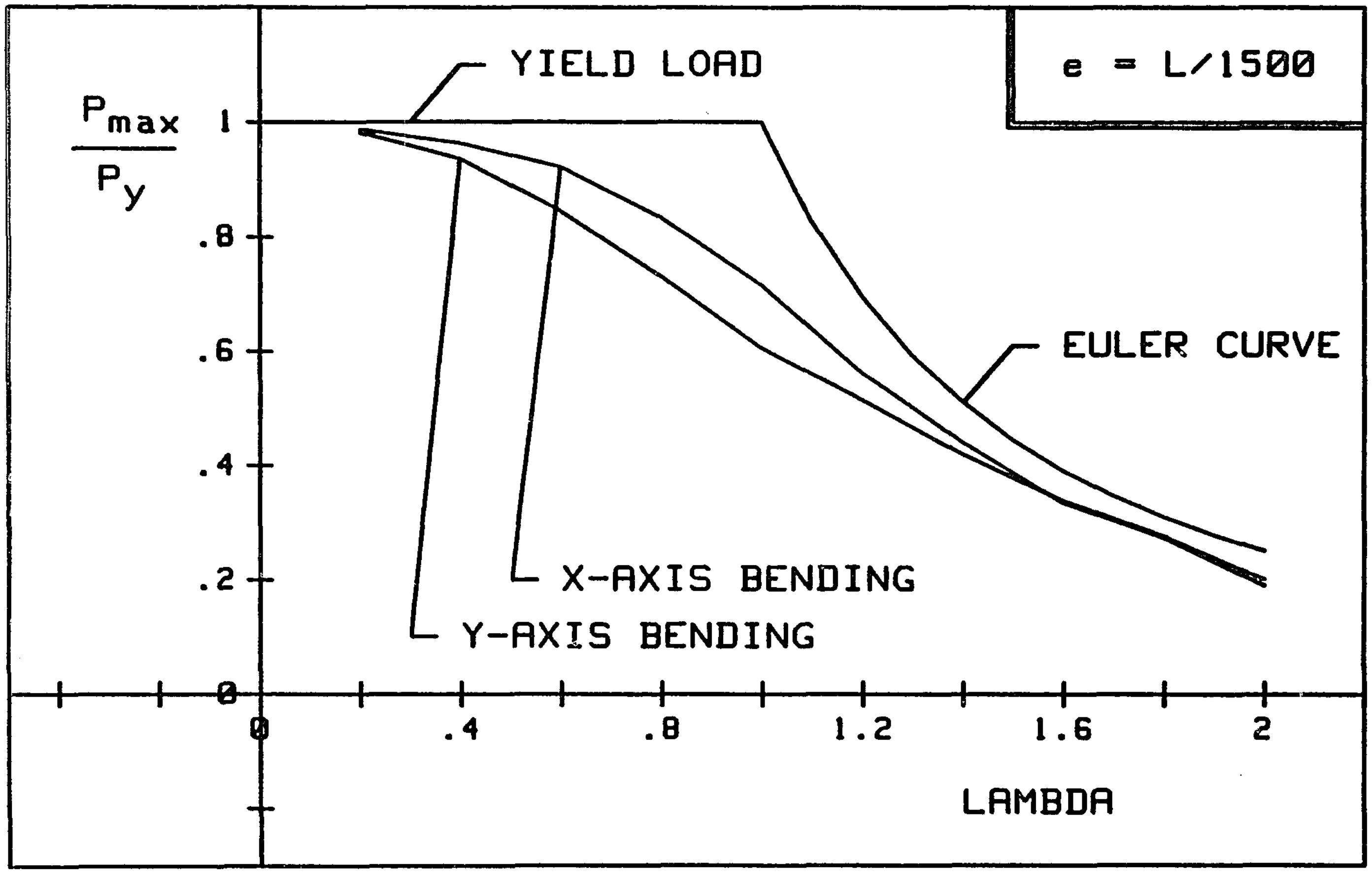

Fig. 6.32. x- and y-axis maximum strength column curves for shape HD 400 x 685 (European) with yield stress of 50 ksi.

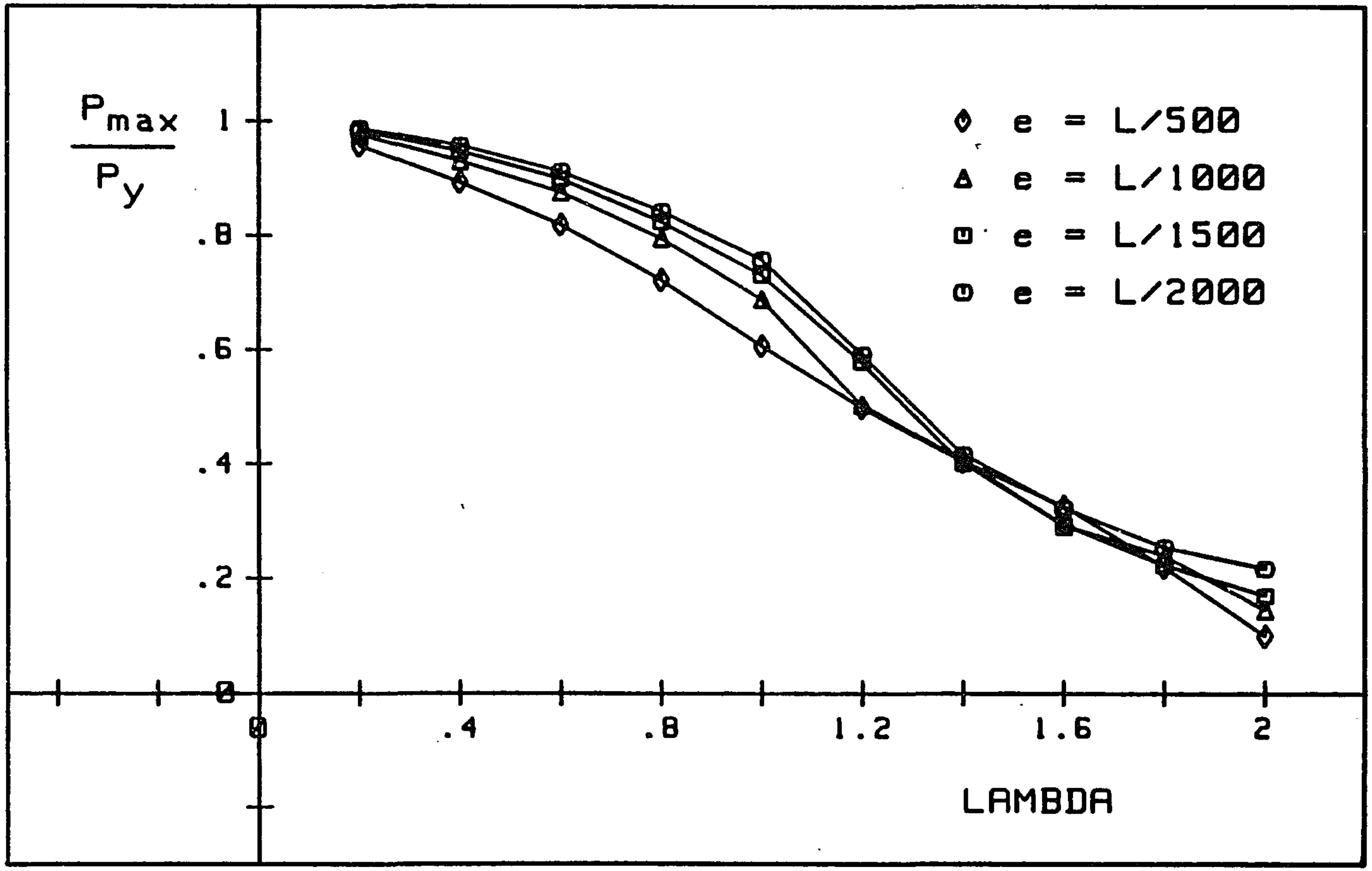

Fig. 6.33. Maximum strength column curves for shape W 14 x 730 with yield stress of 36 ksi and x-axis bending.

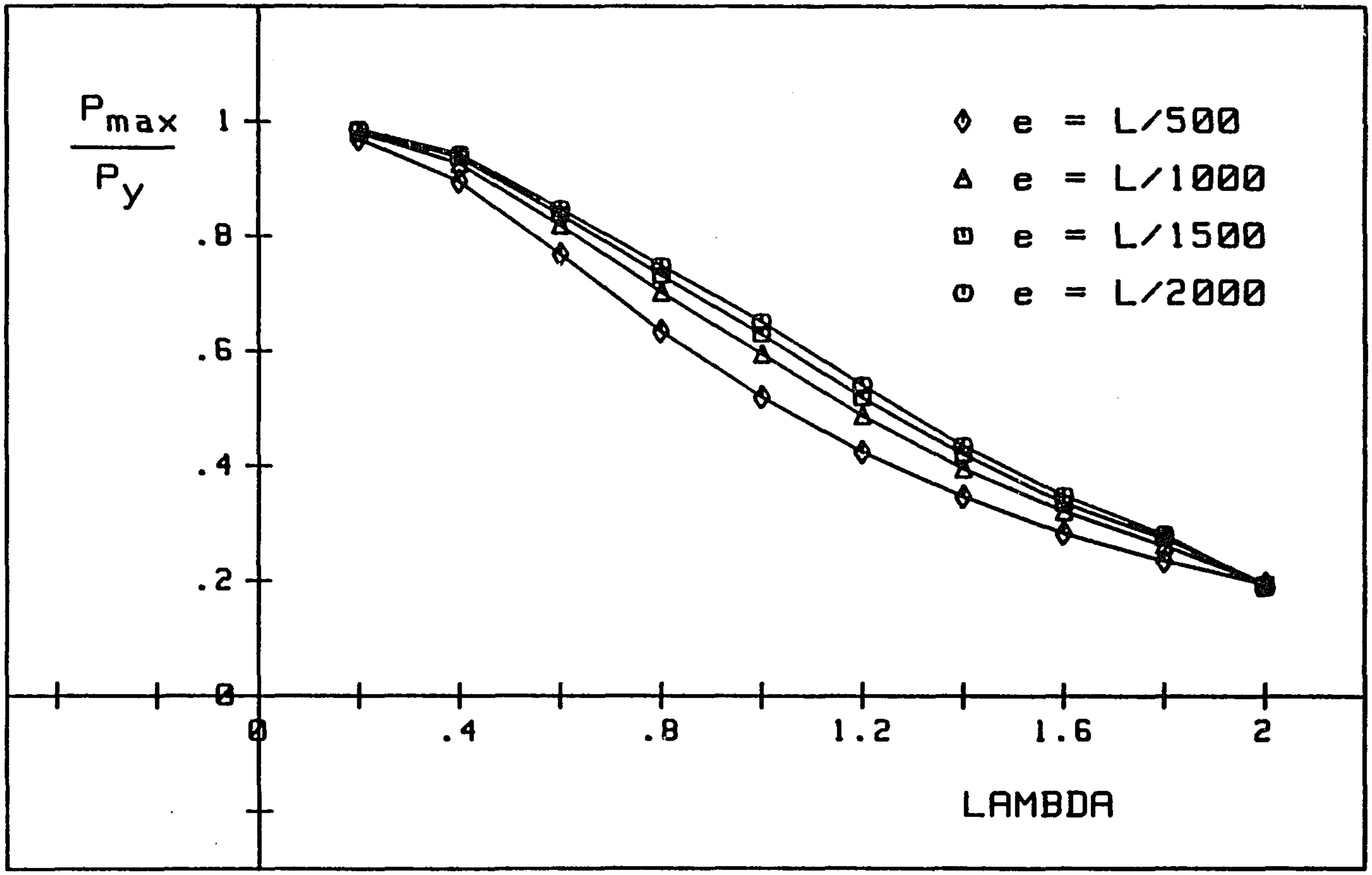

Fig. 6.34. Maximum strength column curves for shape W 14 x 730 with yield stress of 36 ksi and y-axis bending.

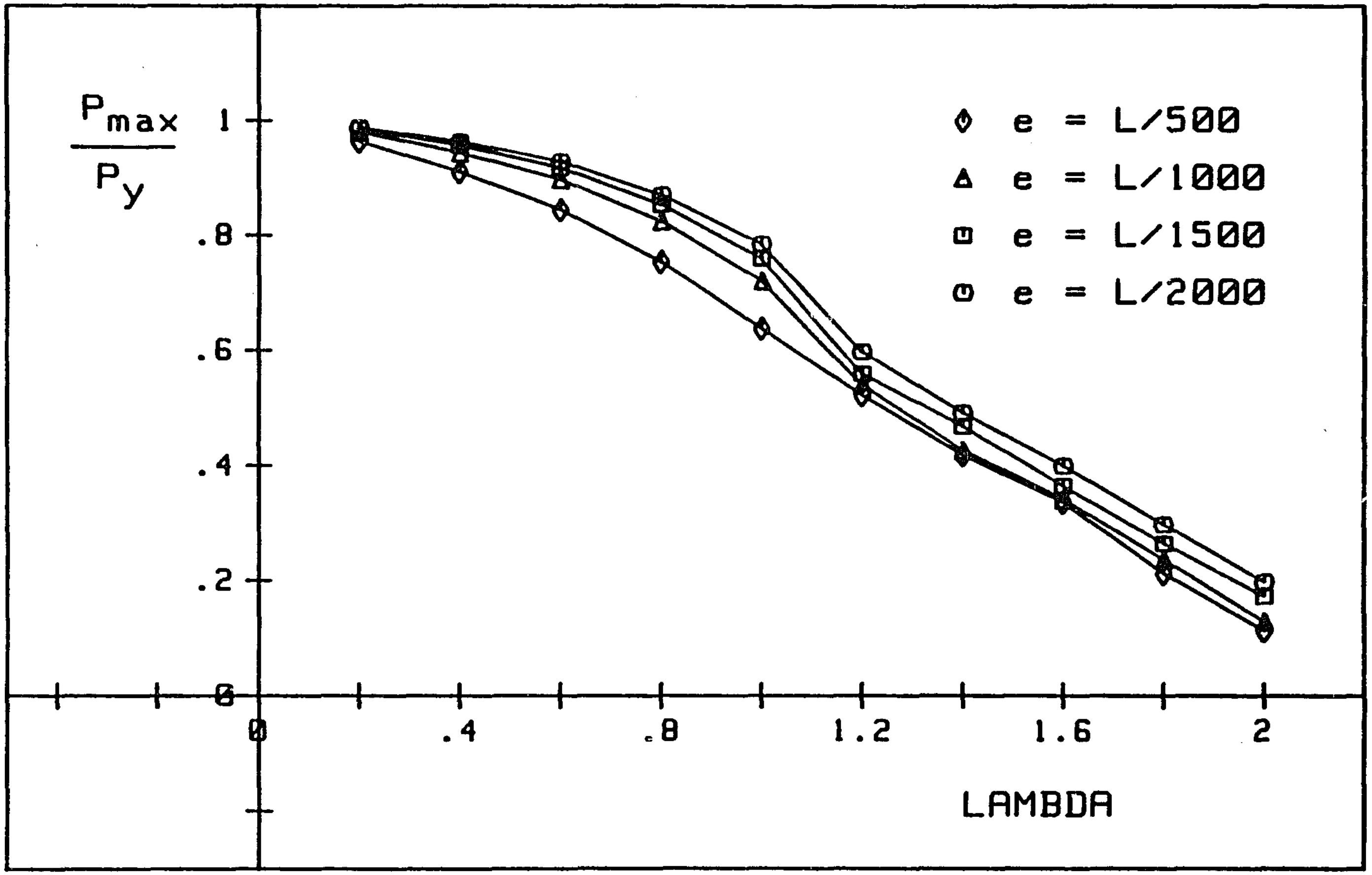

Fig. 6.35. Maximum strength column curves for shape W 14 x 730 with yield stress of 50 ksi and x-axis bending.

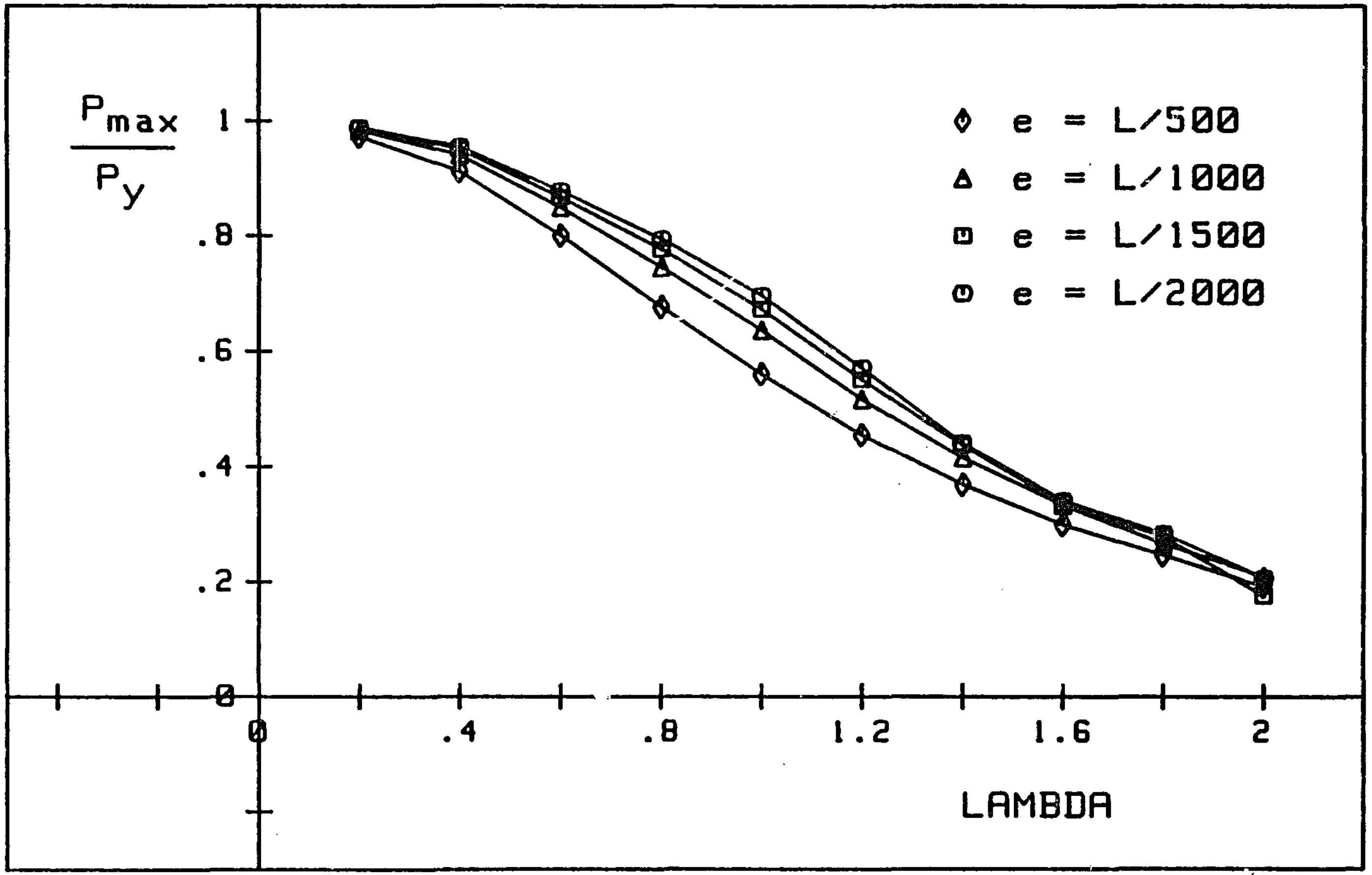

Fig. 6.36. Maximum strength column curves for shape W 14 x 730 with yield stress of 50 ksi and y-axis bending.

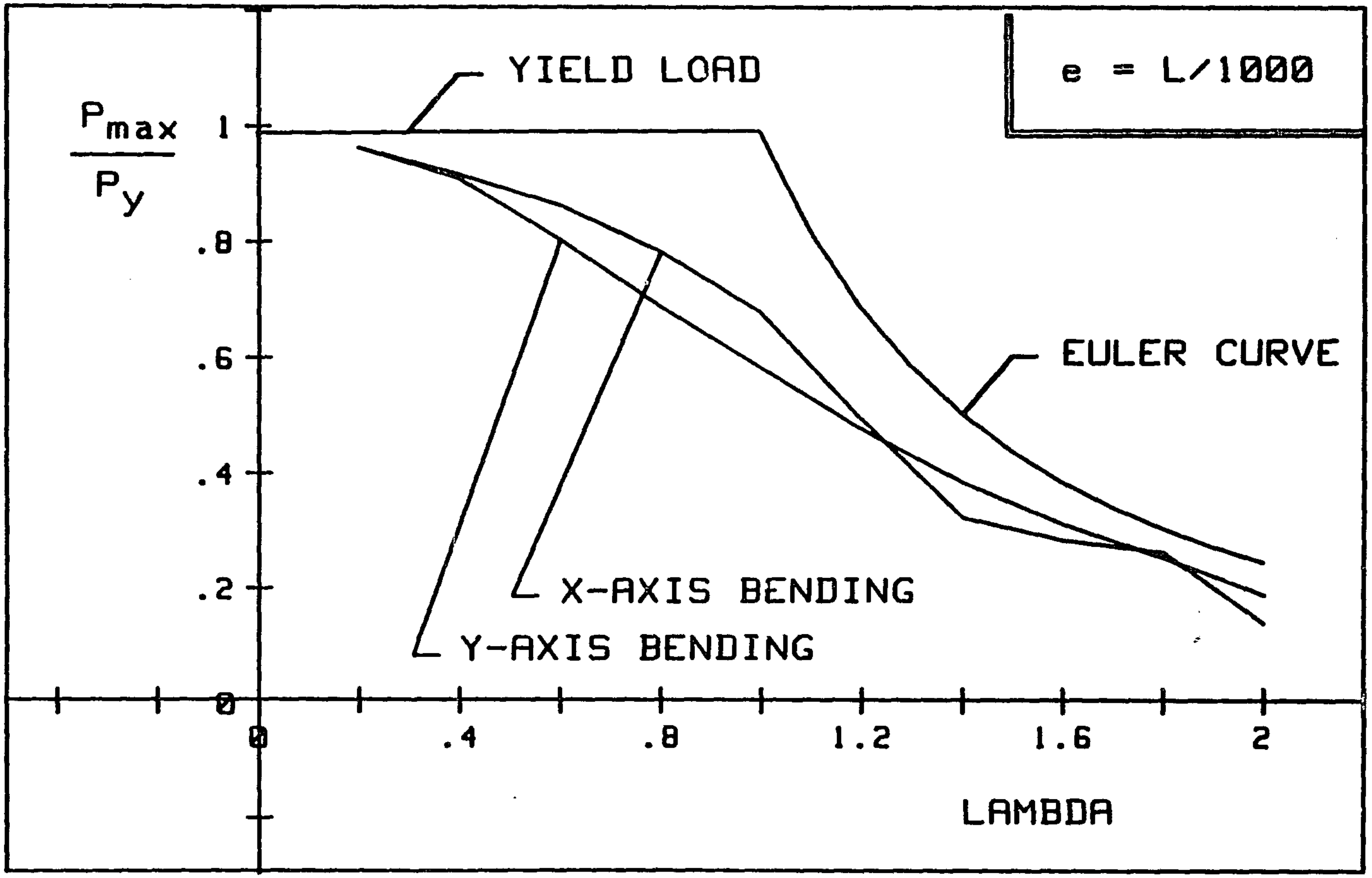

Fig. 6.37. x- and y-axis maximum strength column curves for shape W 14 x 730 with yield stress of 36 ksi.

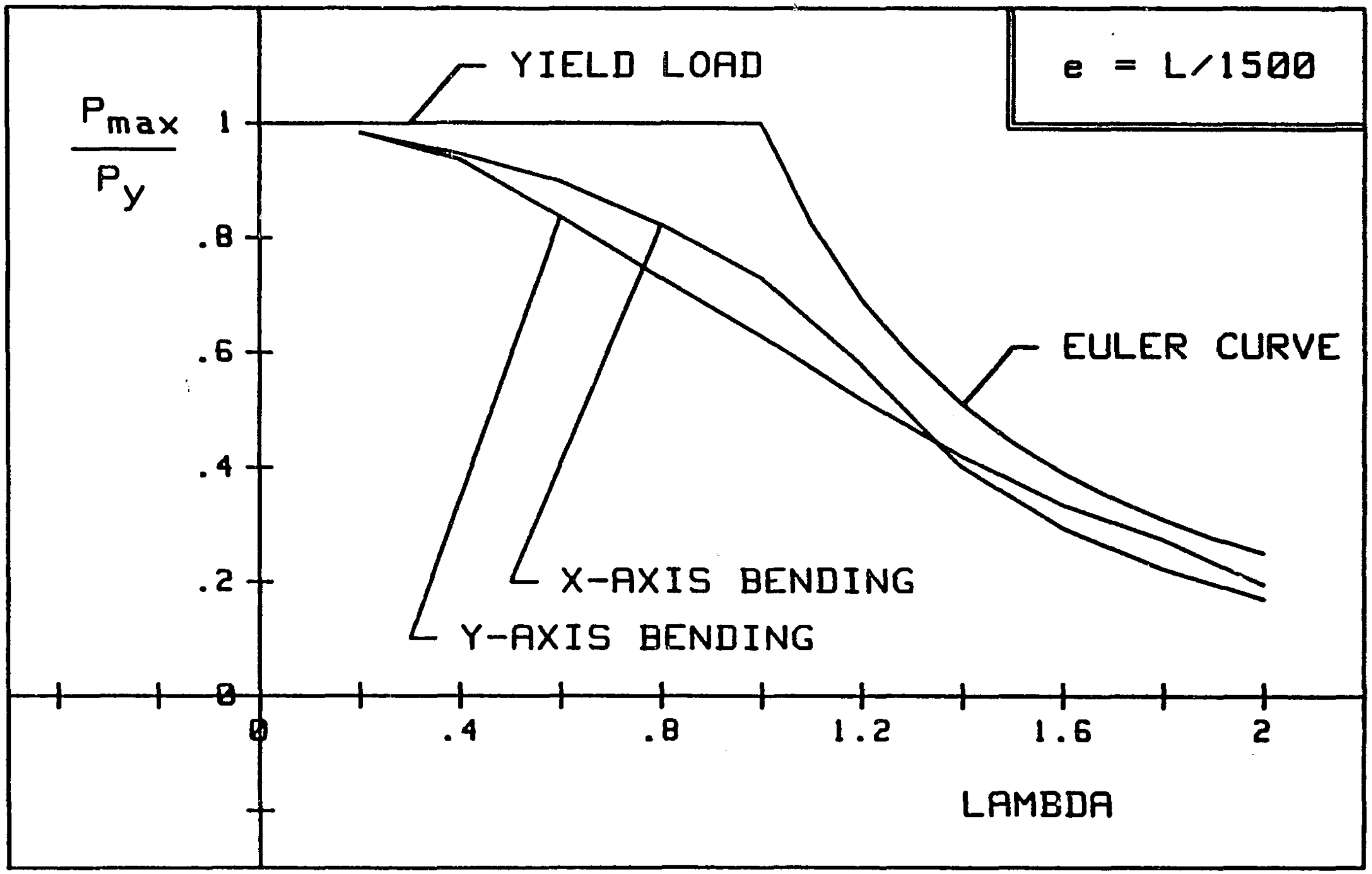

Fig. 6.38. x- and y-axis maximum strength column curves for shape W 14 x 730 with yield stress of 36 ksi.

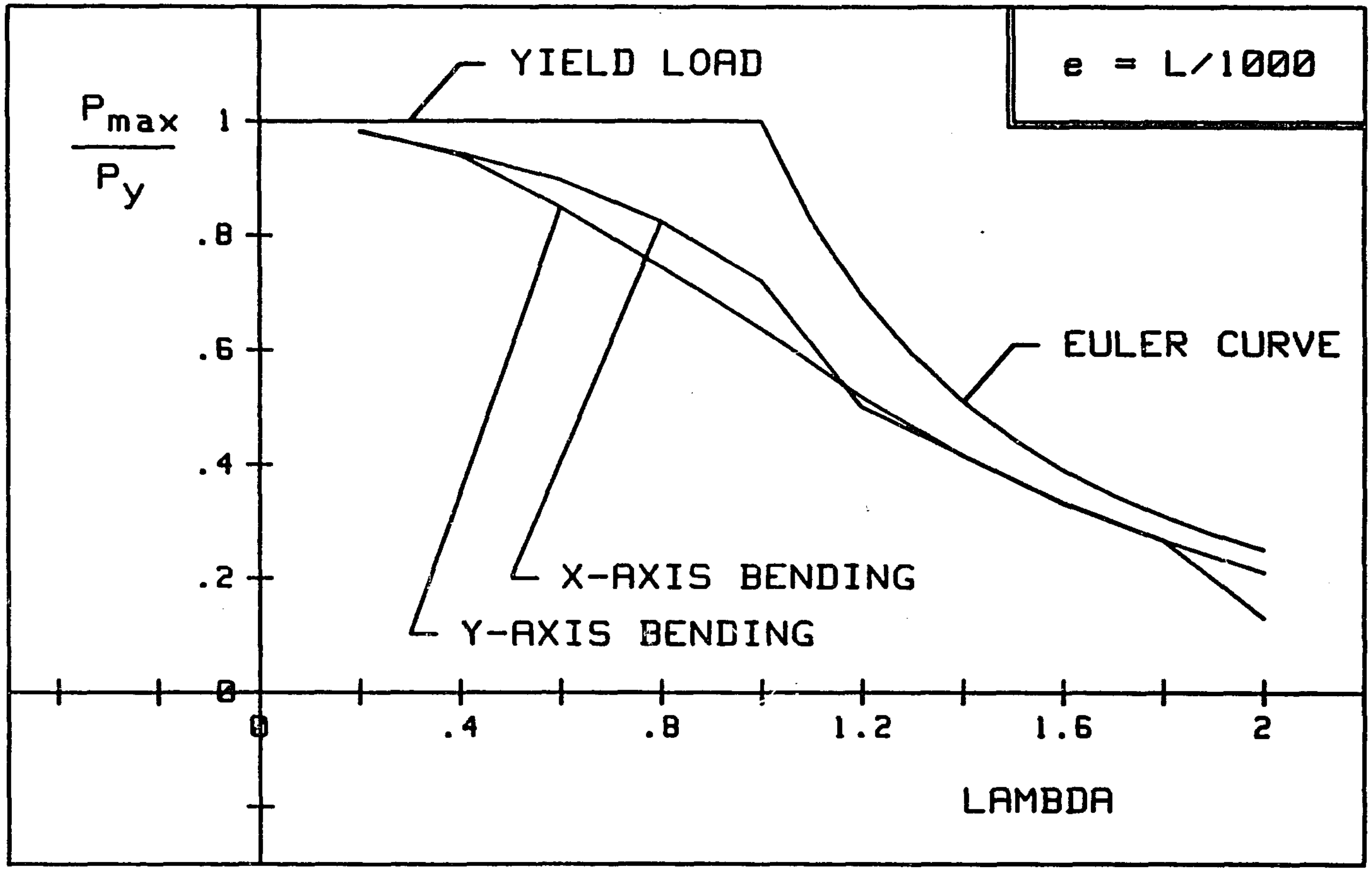

Fig. 6.39. x- and y-axis maximum strength column curves for shape W 14 x 730 with yield stress of 50 ksi.

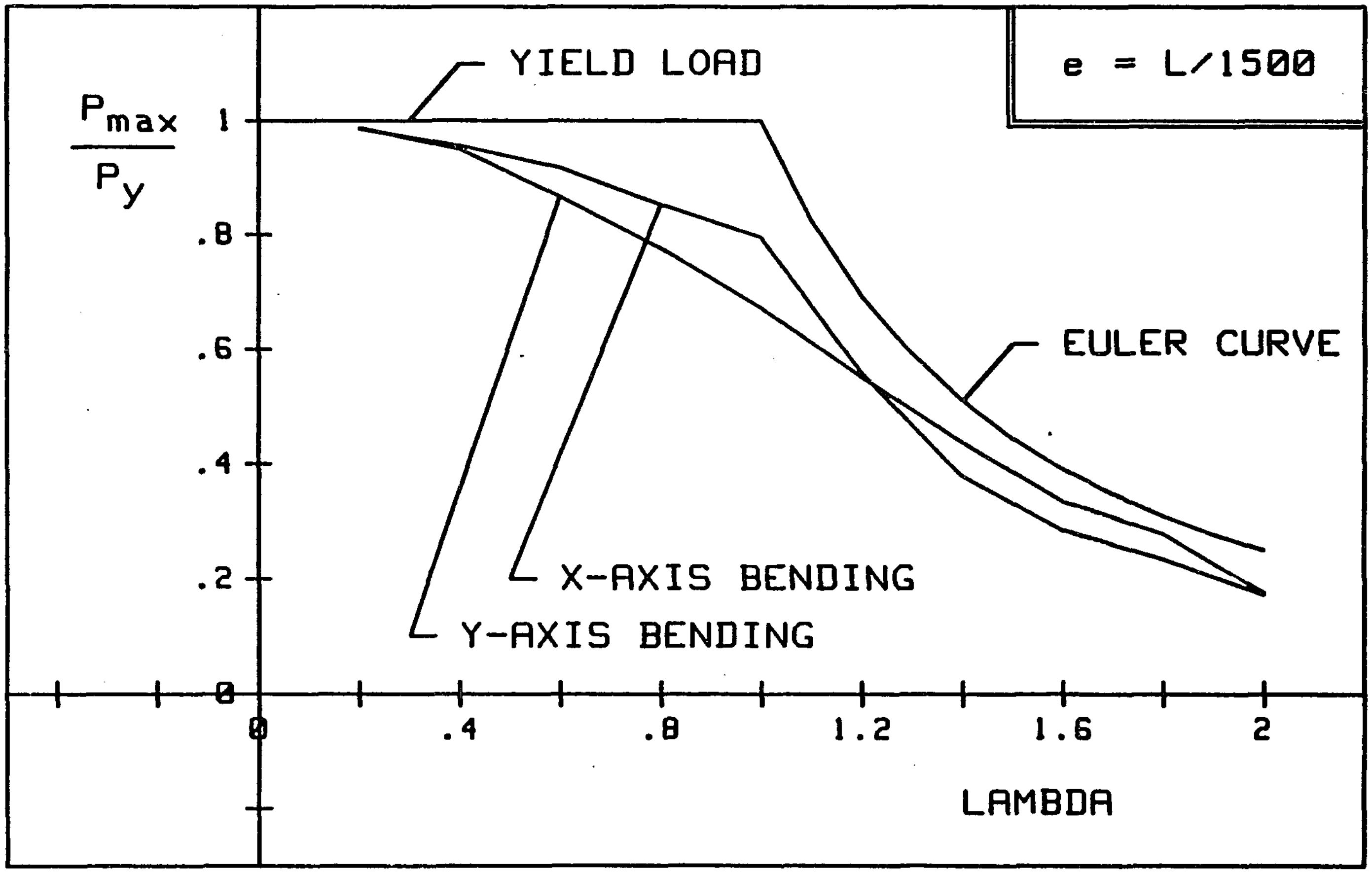

Fig. 6.40. x- and y-axis maximum strength column curves for shape W 14 x 730 with yield stress of 50 ksi.

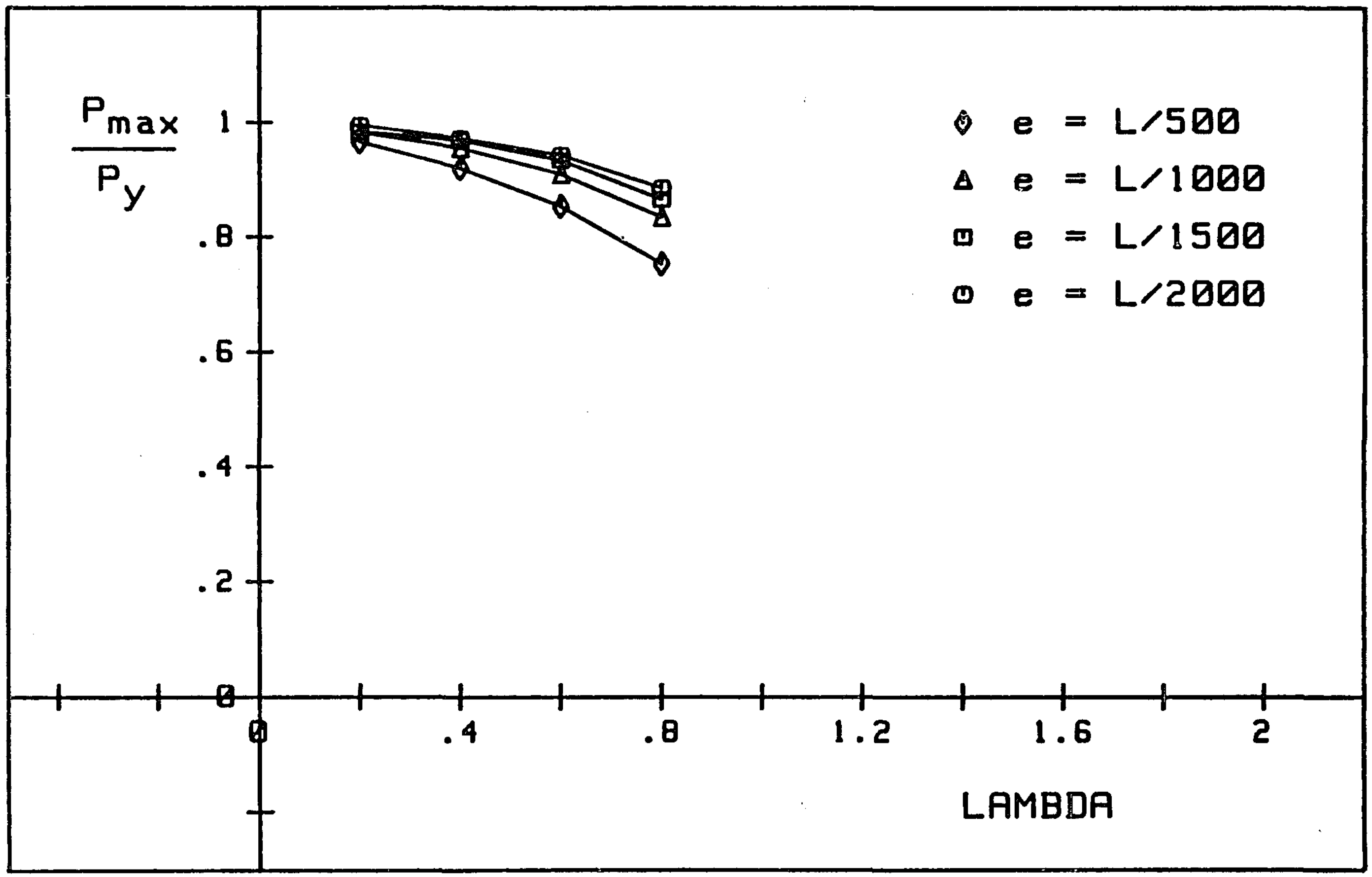

Fig. 6.41. Maximum strength column curves for shape W 12 x 120 with yield stress of 36 ksi and x-axis bending.

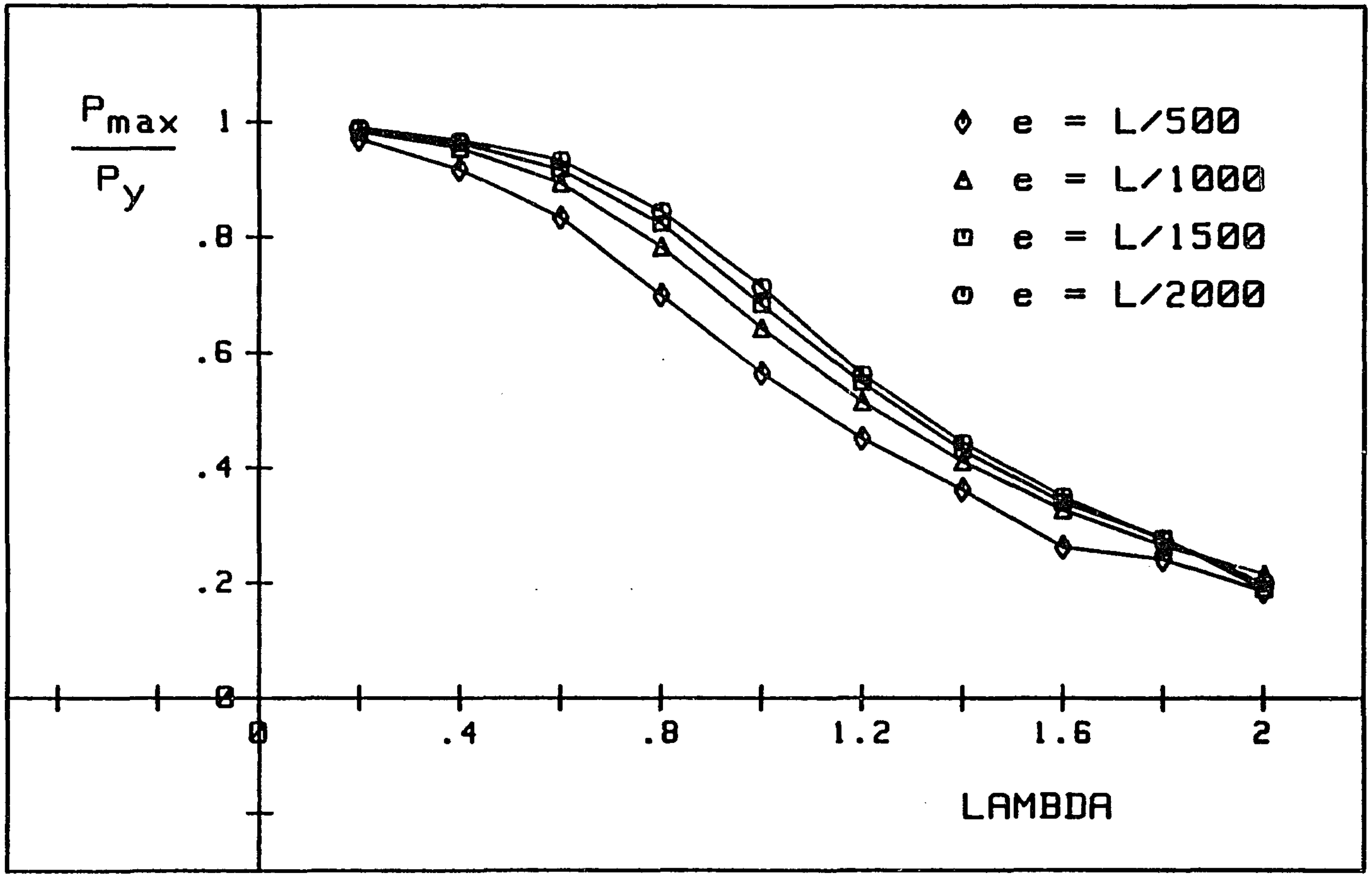

Fig. 6.42. Maximum strength column curves for shape W 12 x 120 with yield stress of 36 ksi and y-axis bending.

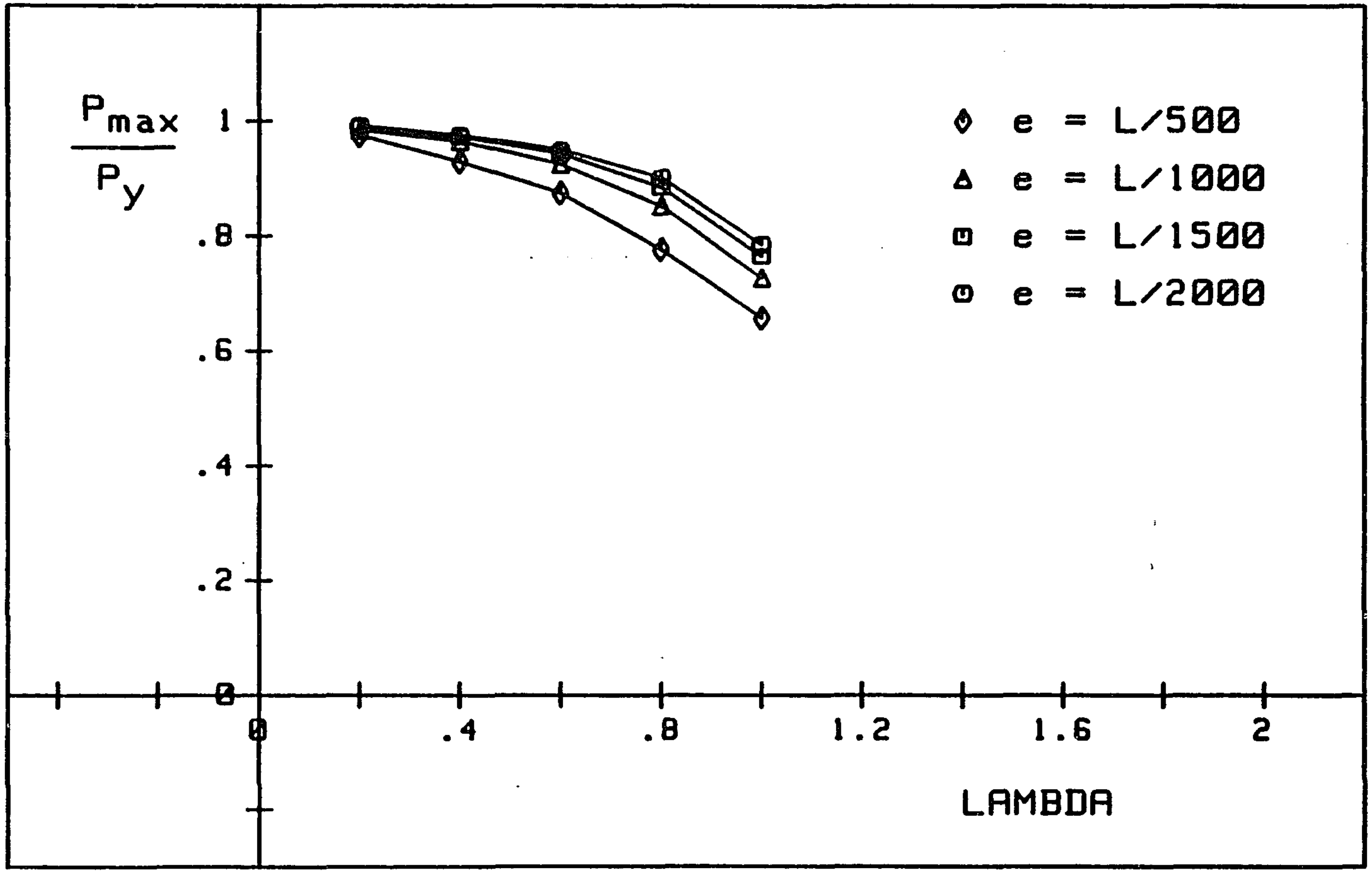

Fig. 6.43. Maximum strength column curves for shape W 12 x 120 with yield stress of 50 ksi and x-axis bending.

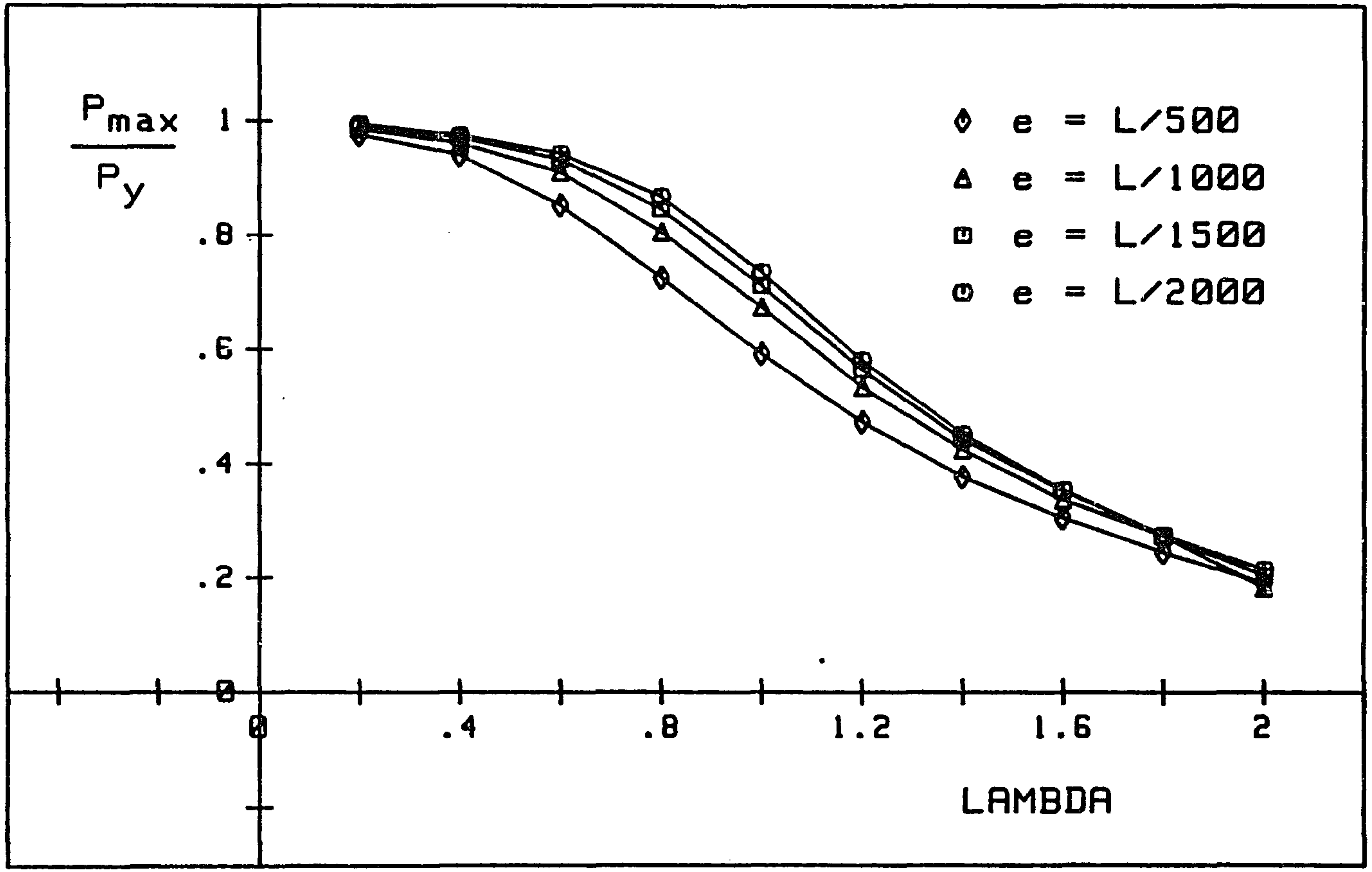

Fig. 6.44. Maximum strength column curves for shape W 12 x 120 with yield stress of 50 ksi and y-axis bending.

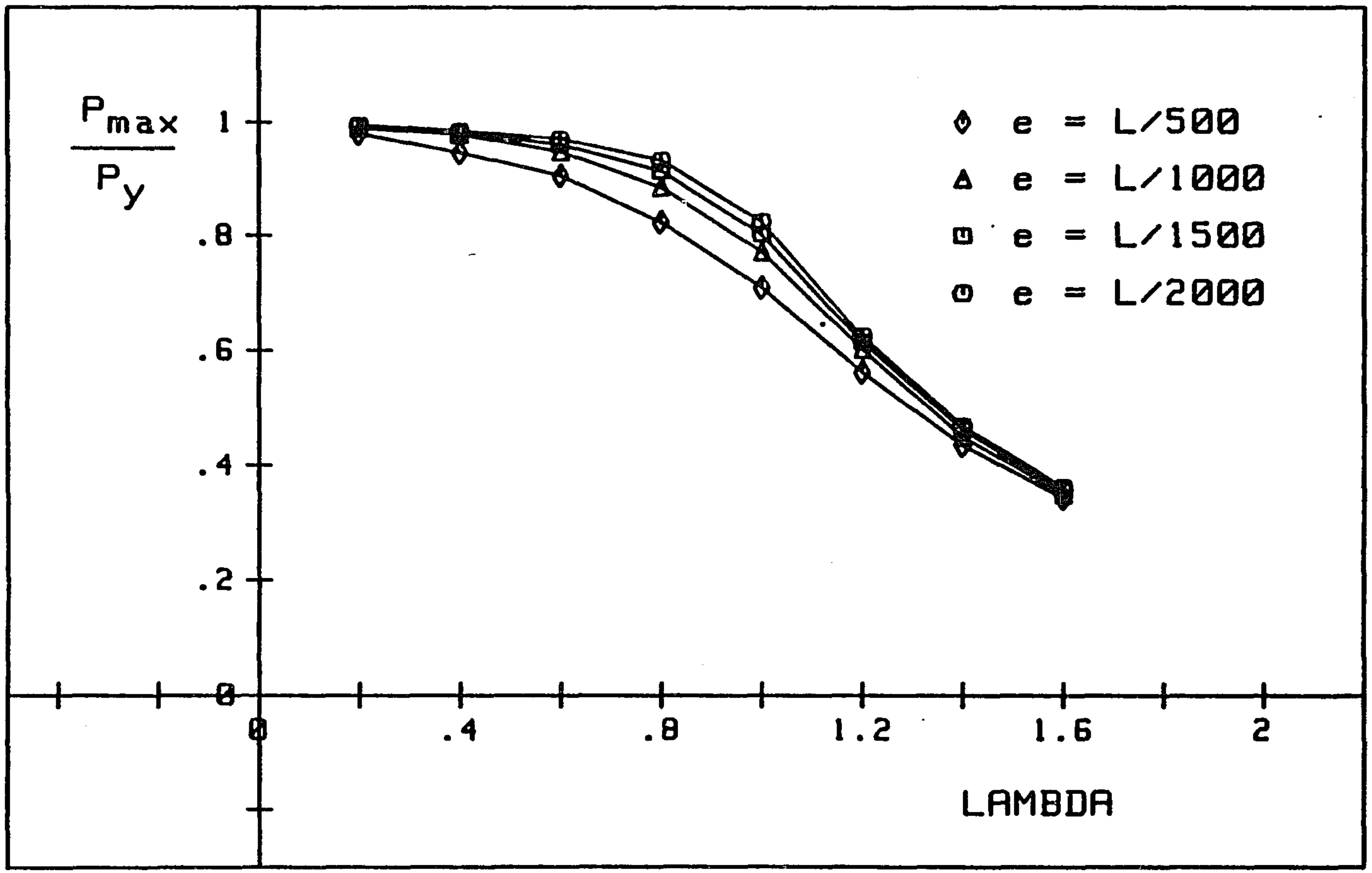

Fig. 6.45. Maximum strength column curves for shape W 12 x 120 with yield stress of 99 ksi and x-axis bending.

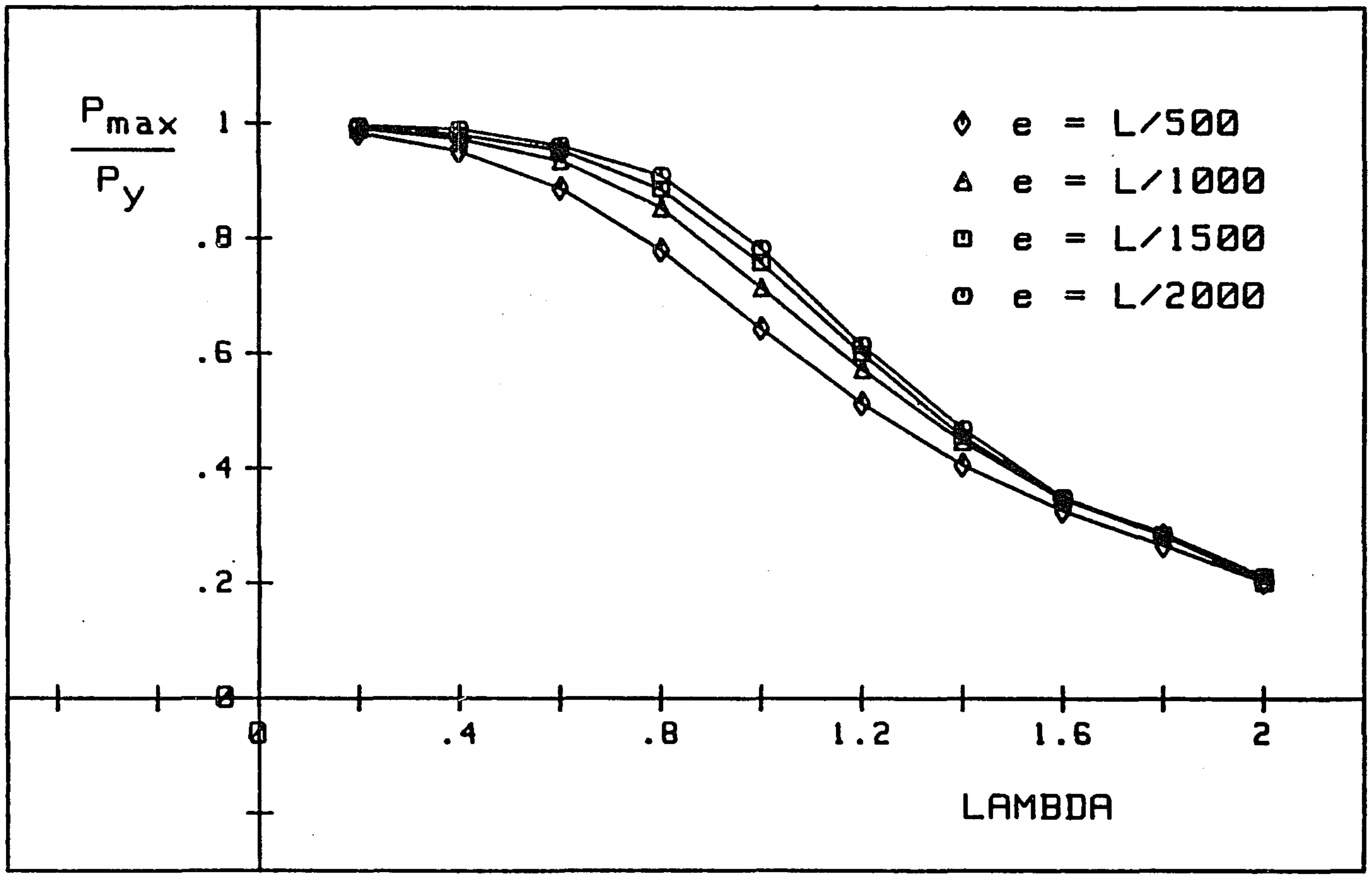

Fig. 6.46. Maximum strength column curves for shape W 12 x 120 with yield stress of 99 ksi and y-axis bending.

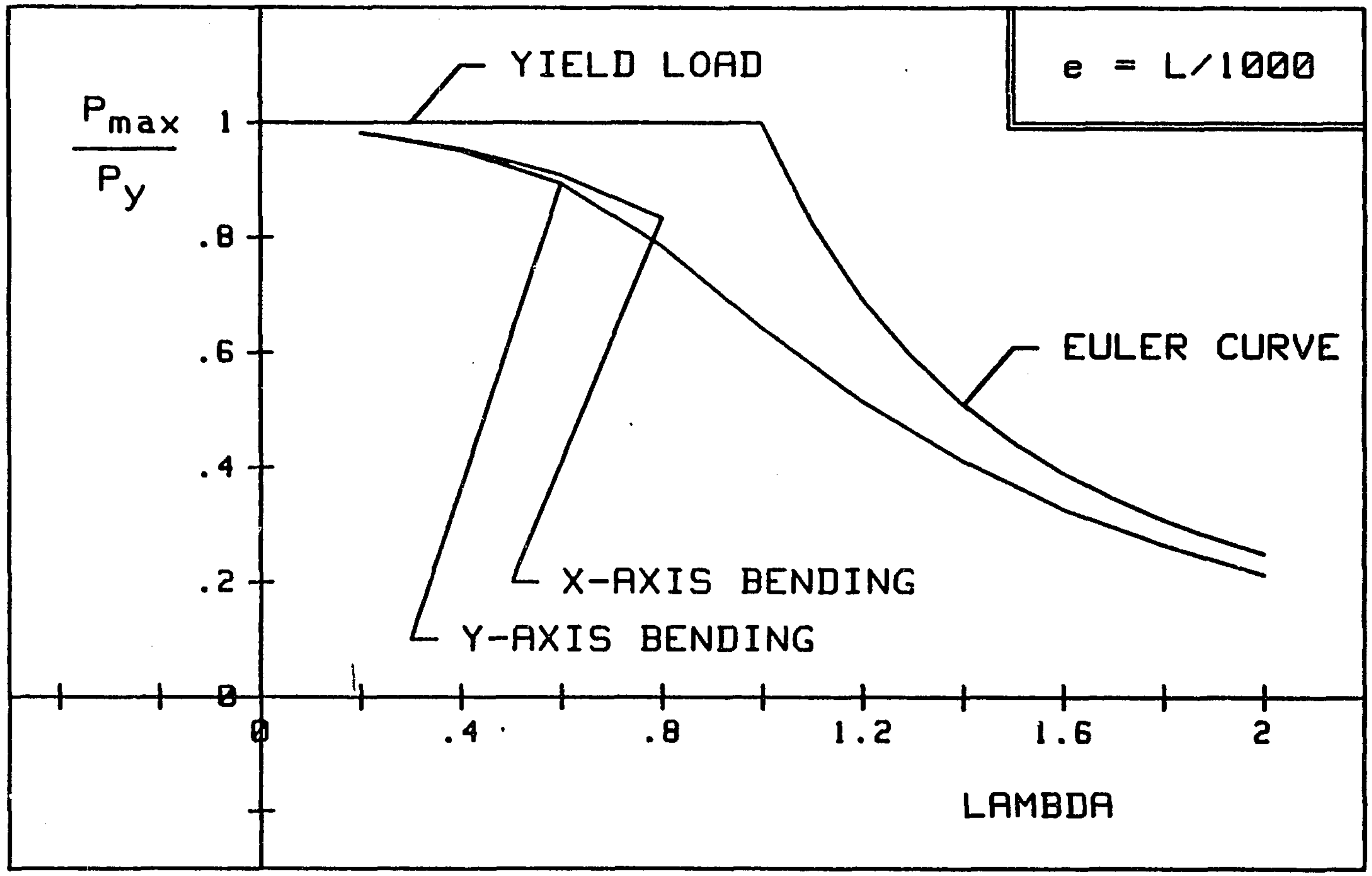

Fig. 6.47. x- and y-axis maximum strength column curves for shape W 12 x 120 with yield stress of 36 ksi.

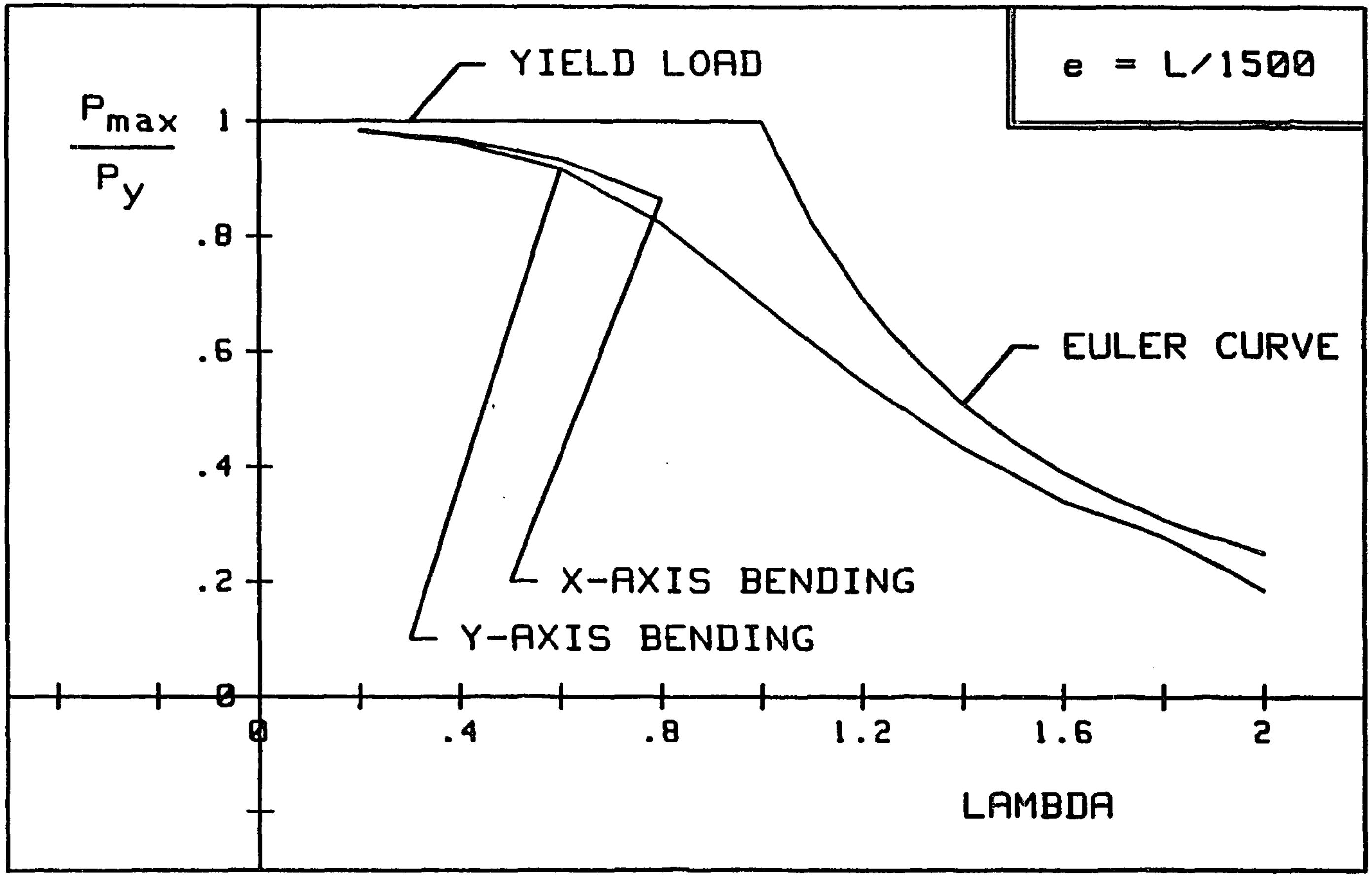

Fig. 6.48. x- and y-axis maximum strength column curves for shape W 12 x 120 with yield stress of 36 ksi.

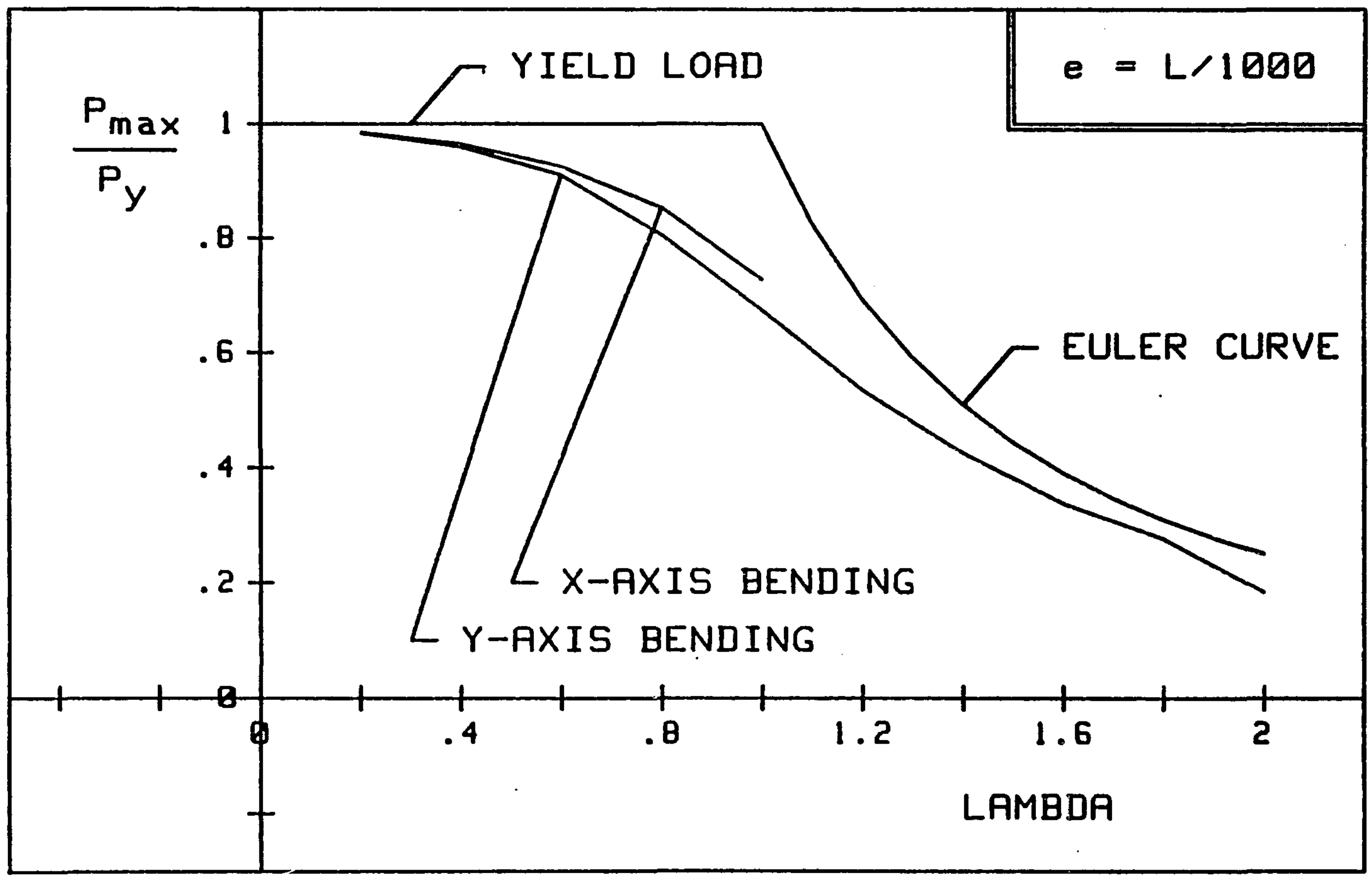

Fig. 6.49. x- and y-axis maximum strength column curves for shape W 12 x 120 with yield stress of 50 ksi.

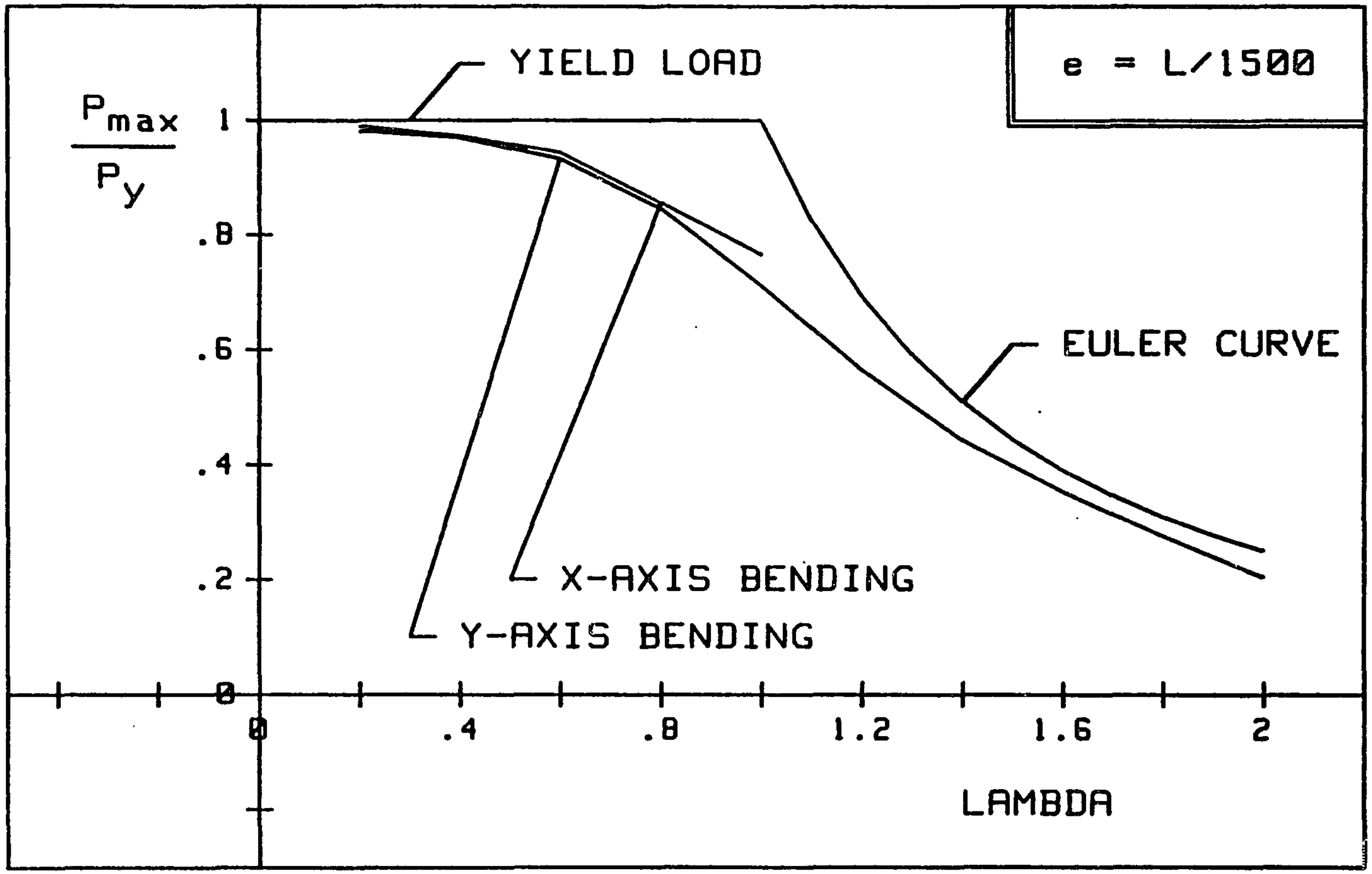

Fig. 6.50. x- and y-axis maximum strength column curves for shape W 12 x 120 with yield stress of 50 ksi.

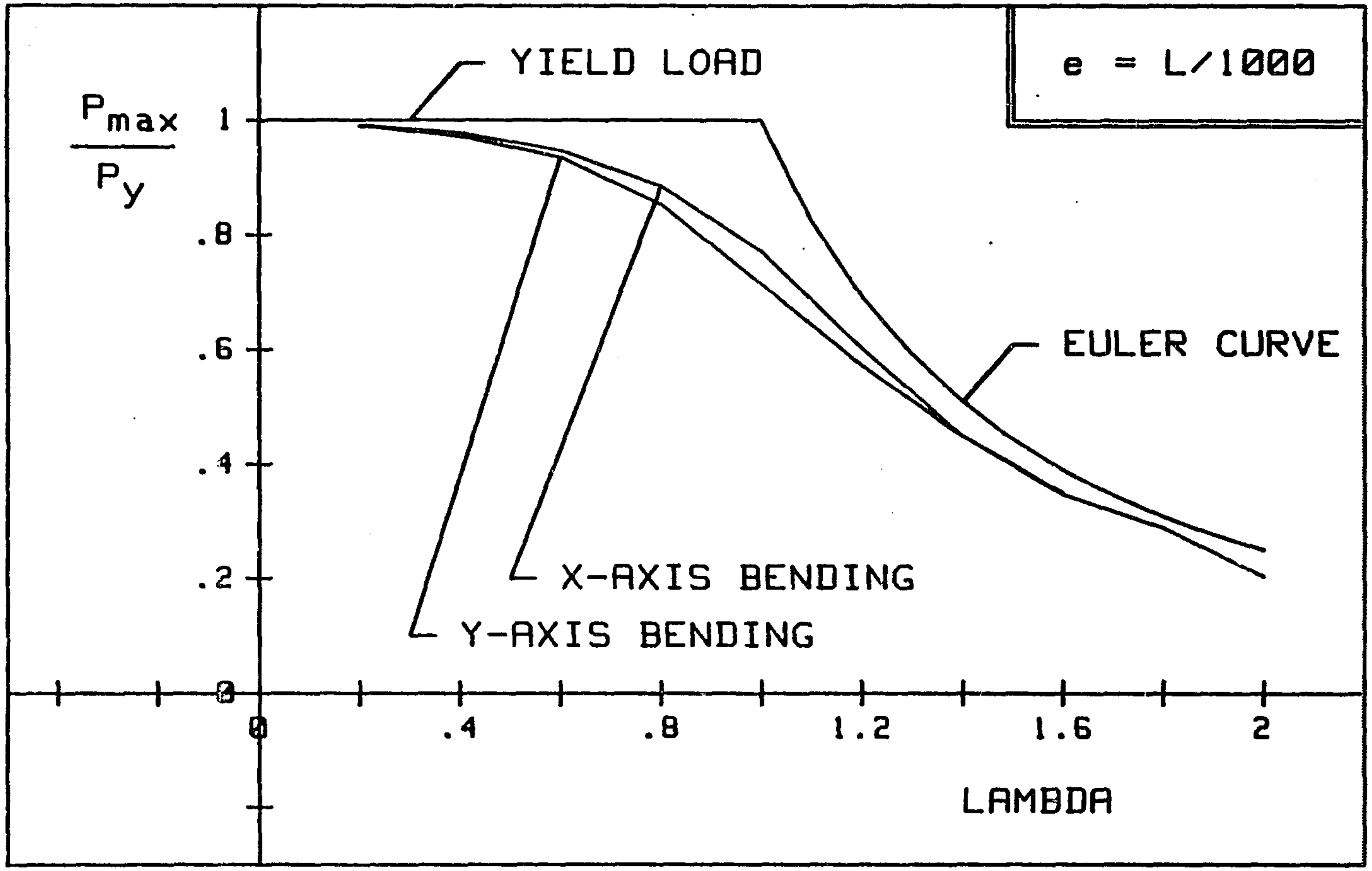

Fig. 6.51. x- and y-axis maximum strength column curves for shape W 12 x 120 with yield stress of 99 ksi.

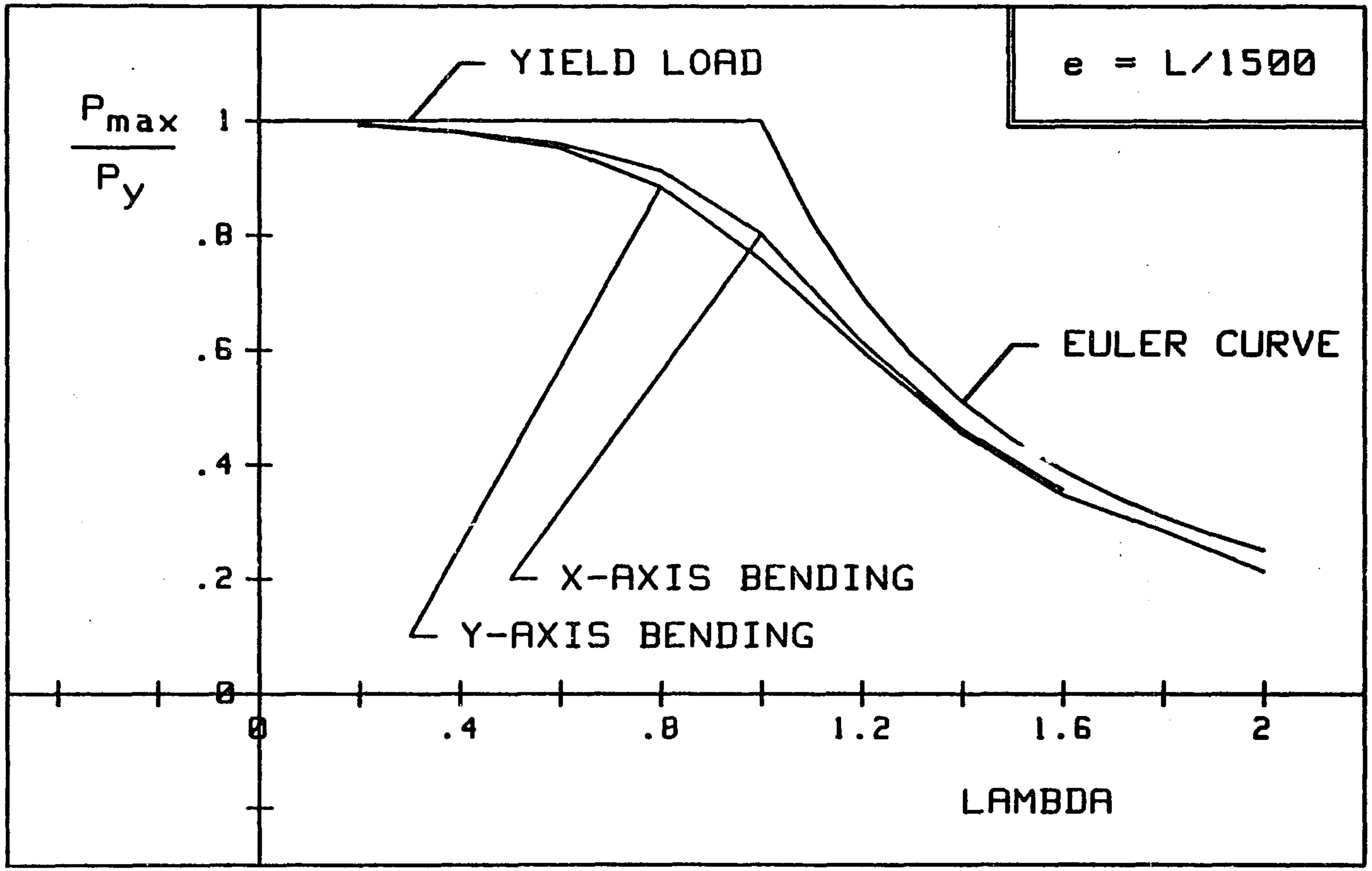

Fig. 6.52. x- and y-axis maximum strength column curves for shape W 12 x 120 with yield stress of 99 ksi.

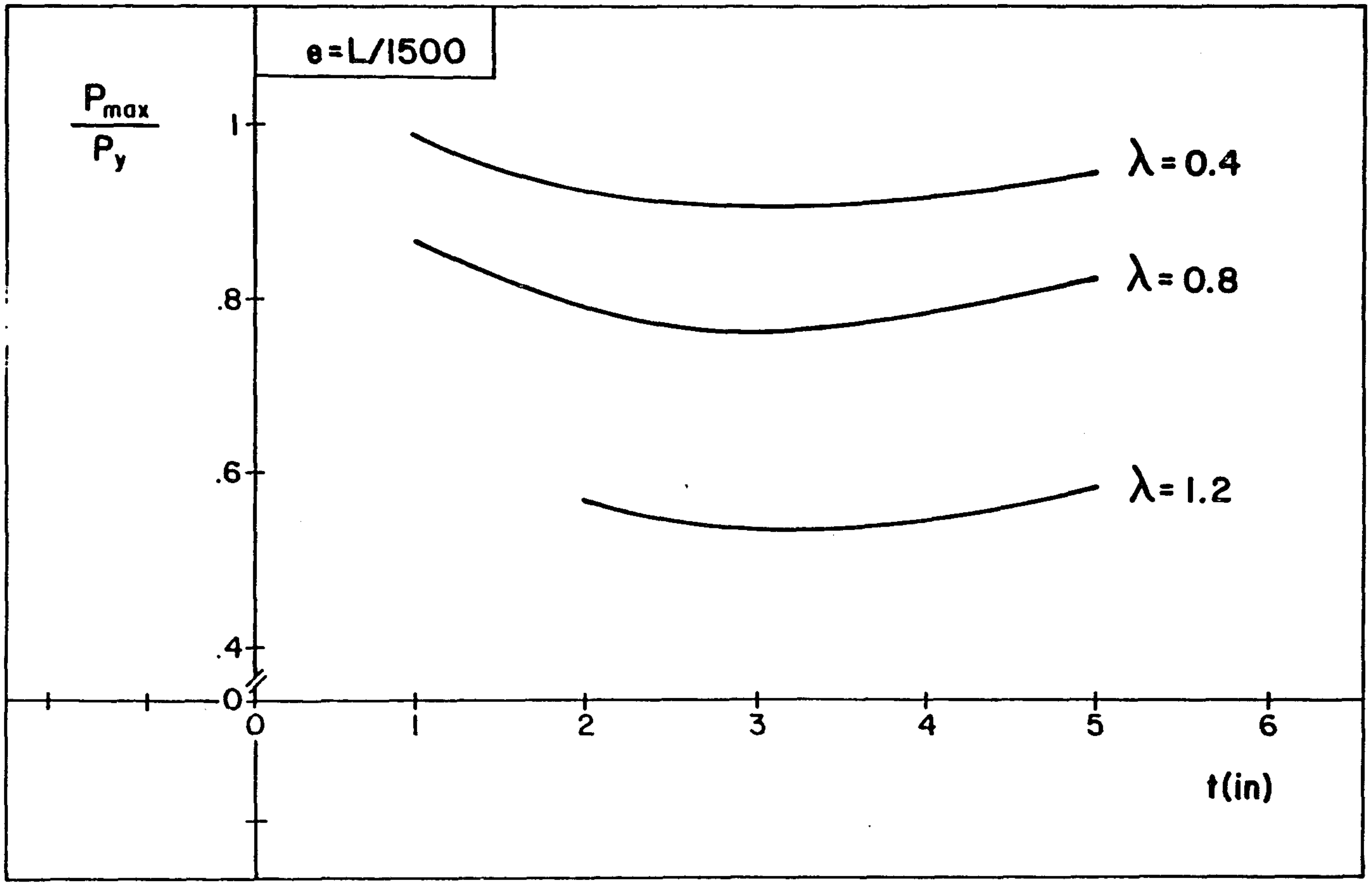

Fig. 6.53. Relationship between maximum column strength and flange thickness for hot-rolled wide-flange shapes (x-axis bending).

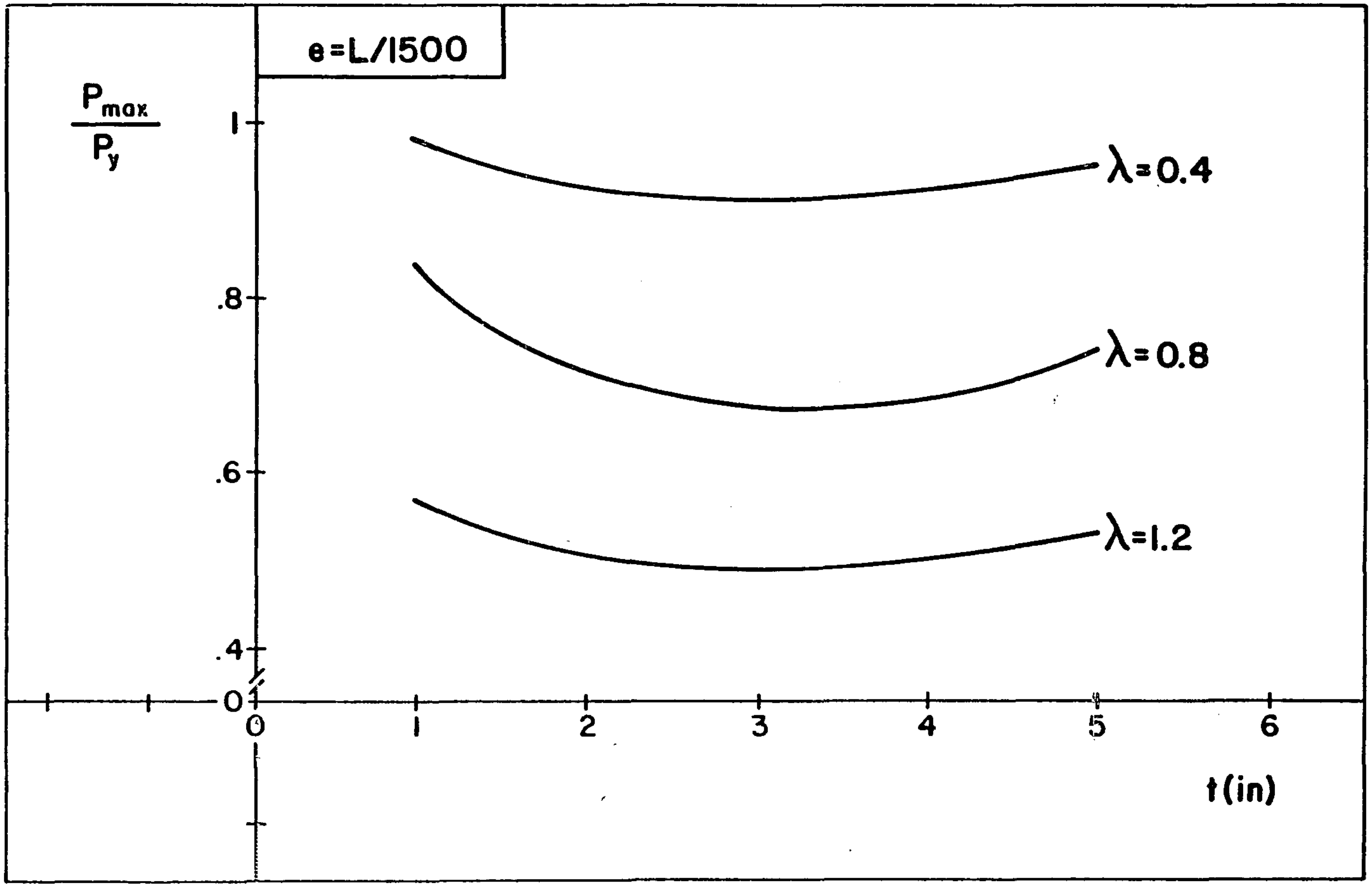

Fig. 6.54. Relationship between maximum column strength and flange thickness for hot-rolled wide-flange shapes (y-axis bending).

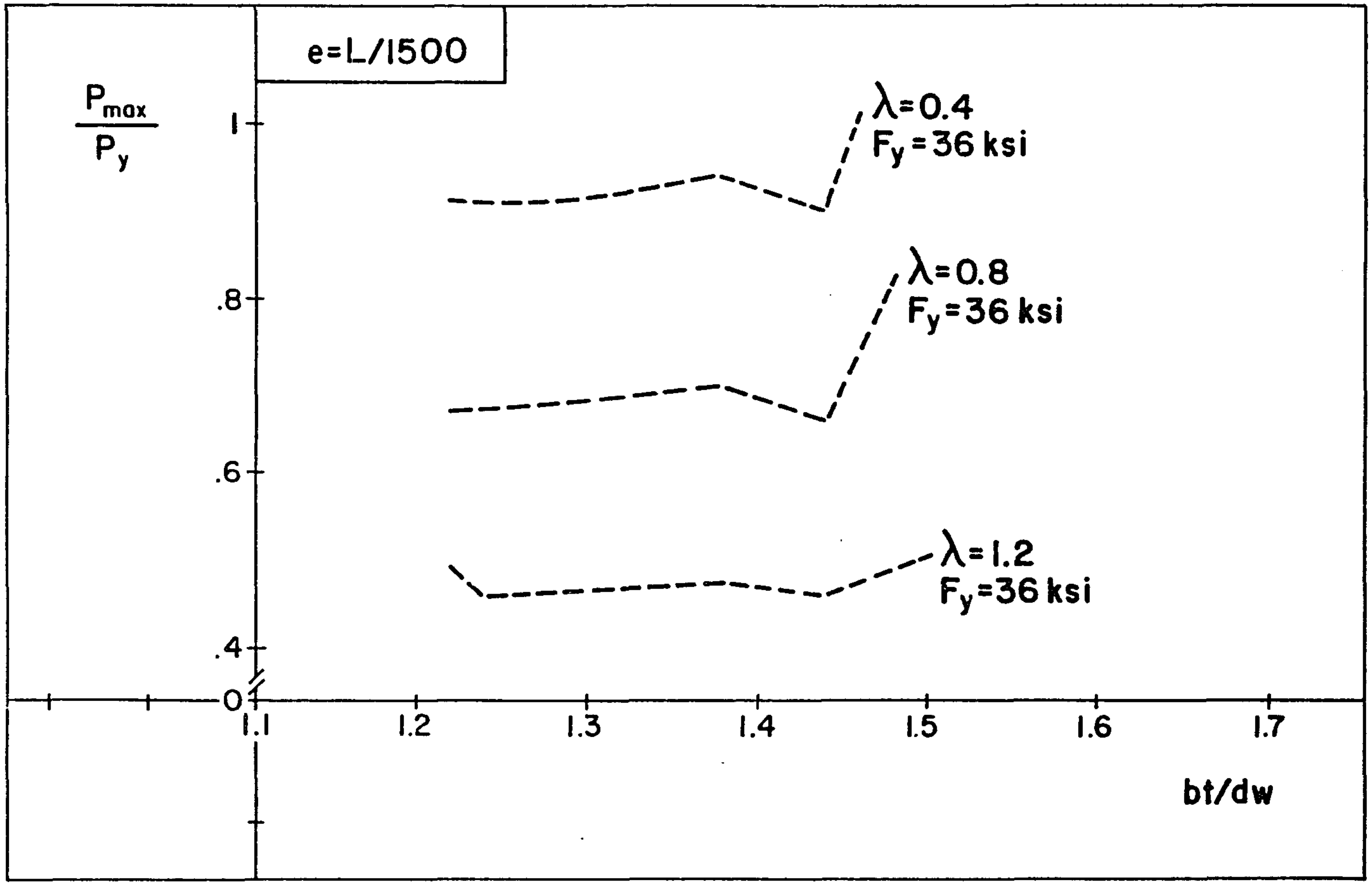

Fig. 6.55. Relationship between maximum column strength and the parameter bt/dw for hot-rolled wide flange shapes (y-axis bending).

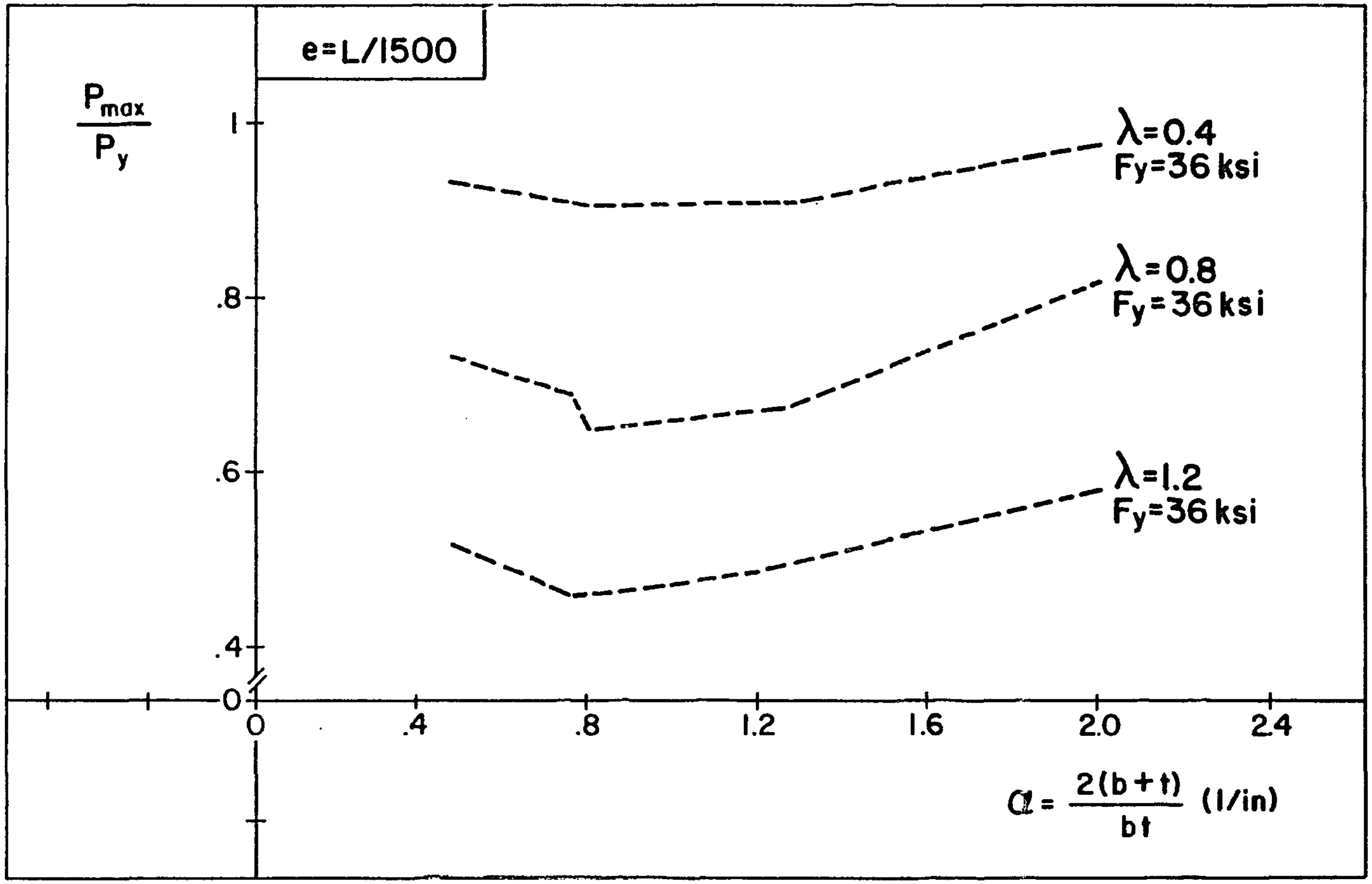

Fig. 6.56. Relationship between maximum column strength and the parameter α for hot-rolled wide-flange shapes (y-axis bending).

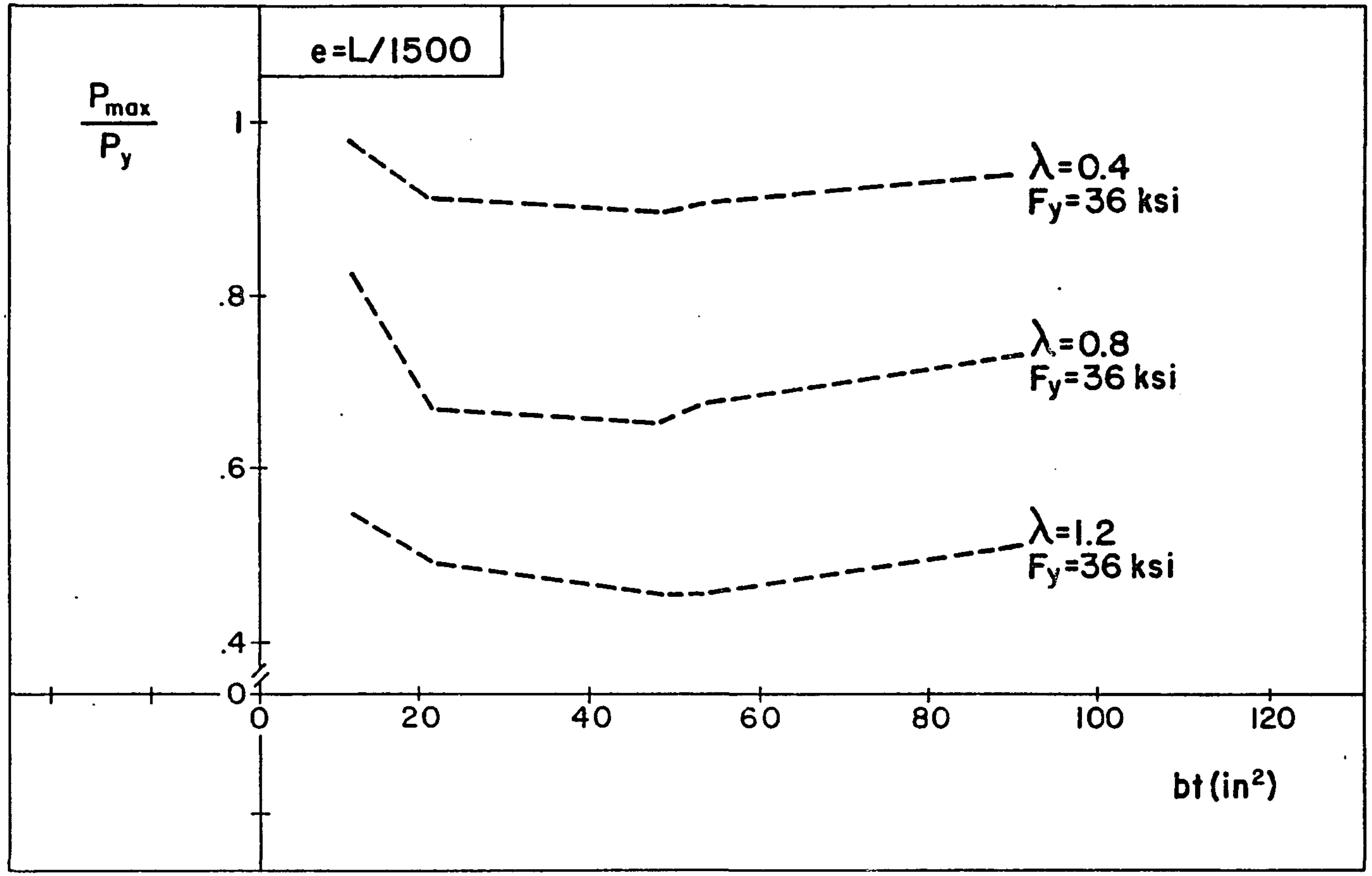

Fig. 6.57. Relationship between maximum column strength and the flange area, bt, for hot-rolled wide-flange shapes (y-axis bending).

6.3 Welded Built-up Shapes

The preceding section dealt with the results obtained for hot-rolled shapes using the MAXLD computer program. The following gives the data that were found for welded built-up wide-flange shapes, five of which were used for this study. Dimensions and other data for the shapes are given in Table 6.2.

The results of the computations are shown in Figs. 6.58 through 6.141. These curves were generated for the same column strength parameter combinations as for hot-rolled shapes.

It was observed that for all relative strength is affected by the initial out-of-straightness, the residual stress, the variation of the yield stress, and the welding that was performed to produce the shape. Due to the localized heating, welding operations change the residual stress pattern in a region whose extent is a function of the amount of heat as well as the location of the welds and the size of the component plates. For this reason, the yield stress is not constant throughout the cross section.

As was found for hot-rolled shapes, the effects of the various column strength parameters are most significant in the intermediate slenderness ratio range, i.e., for λ-values between 0.8 to 1.2. Short and long columns are much less influenced by the various parameters. Thus, short

Table 6.2. Data for welded built-up shapes.

Column Sections	t (in)	d (in)	w (in)	b (in)	A_2 (in^2)	bt/dw	α (1/in)	β (1/in^2)	bt_2 (in^2)
H 12 x 210 (FC)	2.0	13.0	1.5	12.0	61.5	1.23	1.17	.097	24.0
H 14 x 15 (UM)	2.36	14.55	1.45	13.8	79.39	1.54	.99	.07	32.57
H 20 x 354 (FC)	2.0	24.0	1.5	20.0	110.0	1.11	1.10	.06	40.0
H 24 x 428 (FC)	2.0	24.0	1.50	24.0	126.0	1.33	1.08	.05	48.0
H 24 x 1122 (FC)	6.0	24.0	3.5	24.0	33.0	1.714	.42	.02	144.0

columns will reach the full yield load, since the load buckling is not a factor for the behavior of stocky cross sections such as those that are used in this study. An example is shown in Fig. 6.62.

As the column becomes longer (say, for $\lambda > 1.2$), the imperfections effects are also less, and the column curve will approach (but never coincide with, due to the out-of-straightness) the Euler (elastic) curve. All of the curves in the various figures show this effect. Initial crookedness has the same kind of influence regarding the maximum column strength, as was found for hot-rolled shapes.

Further comparisons were made between shapes as regards the effects of changing the magnitude of the yield stress, specifically, considering 36 and 50 ksi steel. It was observed that the strength increases by an amount corresponding to the increase in F_y for short columns, since these are failing by full cross section yielding. For long columns the effect was negligible, since their behavior is essentially governed by elastic buckling. The strength increases due to going from $F_y = 36$ ksi to $F_y = 50$ ksi are about 16% for a λ-value of 1.0, and then taper off for higher values.

Buckling about the principal axes is also considered for those shapes. It is observed that for welded built-up shapes with flame-cut edges, the weak axis curves in some cases will cross the strong axis curves, as illustrated in Figs. 6.98 and 6.105 (36 ksi steel and 70 ksi electrodes). It is judged that in general, this phenomenon may happen because the flange tips have high tensile residual stresses combined with high strength steel (due to the local effects of flame cutting, as explained previously).

Shapes using universal mill flange plates display strong and weak axis buckling characteristics that are similar to those of hot-rolled shapes, i.e., bending about the x-axis gives higher relative strength than the y-axis, but the differences can be small. The latter is due to the fact that the web-to-flange juncture contains high strength welding electrode steel, with high tensile residual stresses. Figures 6.82 through 6.89 illustrate these findings.

All of the results for the welded built-up wide-flange shapes are shown in Figs. 6.138 through 6.141 representing major and minor axis bending for combinations of 36 and 50 ksi steel; 70 ksi electrodes, 36 and 50 ksi steel; 100 ksi electrodes, respectively. The strength characteristics are evaluated in the following, using the same three λ-values that were used for the hot-rolled shapes, namely, $\lambda = 0.4$, 0.8, and 1.2. Since there are three shapes that have the same flange thickness (2 inches), the average value for these shapes is utilized, assuming that this is representative.

It is clear that the relative strength of long columns (λ = 1.2) is basically not affected by the magnitude of the flange thickness. This applies to x-axis as well as y-axis bending. For example, the relative strength variation for columns with 50 ksi steel and 70 ksi weld electrodes is less than 1% as the thickness goes from 2 to 6 inches.

Short columns show basically the same tendency, especially for higher grade steel. There is a reduction of about 7% in the column strength as t increases from 2 to 2.4 inches, for the combination of 36 ksi steel and 70 ksi weld metal. Following that, the strength is virtually unchanged as t increases to 6 inches. Also, higher grade steel is influenced less by variations in the flange thickness. For example, when 50 ksi steel and 70 ksi electrodes material are used, the reduction in relative strength is less than 2% as t goes from 2 to 6 inches.

The buckling strength as influenced by the axis of bending displays the same properties as the hot-rolled shapes. That is, a reduction of about 9% is found when t goes from 2 to 2.4 inches for y-axis failure; this loss is only about 3% for the x-axis case. A further loss of approximately 4% is found for the y-axis as t increases to 6 inches. Therefore, the drop in relative strength is greater for weak axis than strong axis buckling.

The relative strength of intermediate length columns in x-axis bending is found to exhibit a tendency to increase along with t only up to 2.4 inches, and then remains virtually constant as t goes to 6 inches. This can be seen in Fig. 6.138. Thus, for the 36 ksi-70 ksi base metal-weld metal combination, the strength is increased by about 8% as t goes from 2 to 2.4 inches and then a slight drop occurs .9% as t increases further to 6 inches. The 36-100 material combination shows an increase of about 7% as t increases from 2 to 2.4 inches, although the strength continues to increase as t goes to 6 inches. This is illustrated in Fig. 140. These effects are less pronounced for the 50-70 and 50-100 combinations. Although the 36-100 and 50-100 material combinations are not used in practice, it is adopted in this study to investigate the effects on the strength and behavior of welded shapes.

In consequence of the above discussion, it appears that the strength of intermediate length columns will increase as the flange thickness goes to 2.5 inches; thereafter, it is basically a constant value. This conclusion also applies to the weak axis bending case.

Therefore, in general, the relative strength of long and short welded built-up wide-flange columns is not affected by the variation of the flange thickness. Columns of intermediate length display a strength increase as t goes to about 2.5 inches; it is then essentially a constant as t increases to 6 inches.

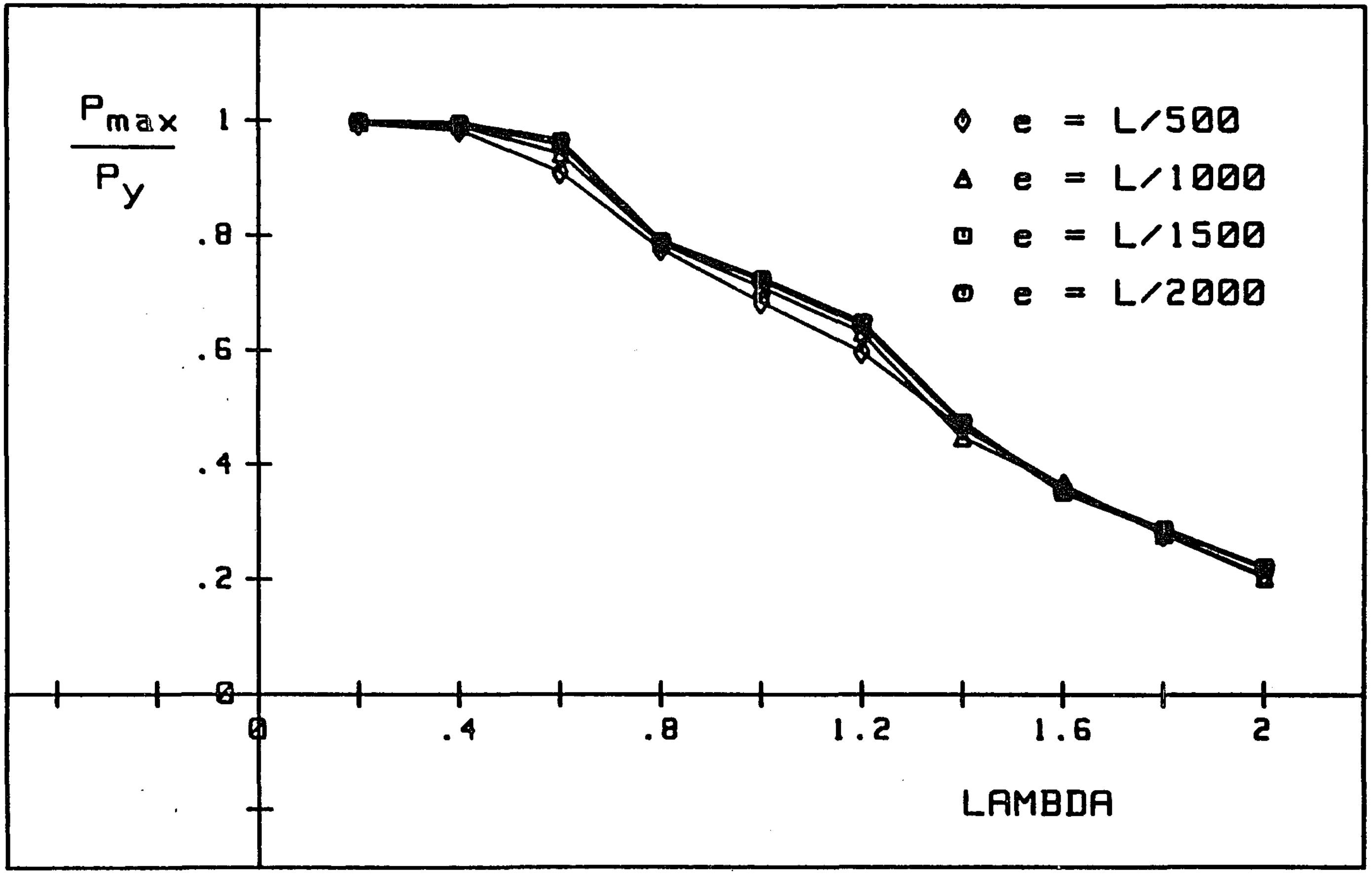

Fig. 6.58. Maximum strength column curves for shape H 12 x 210 (36 ksi steel, 70 ksi electrodes) and x-axis bending.

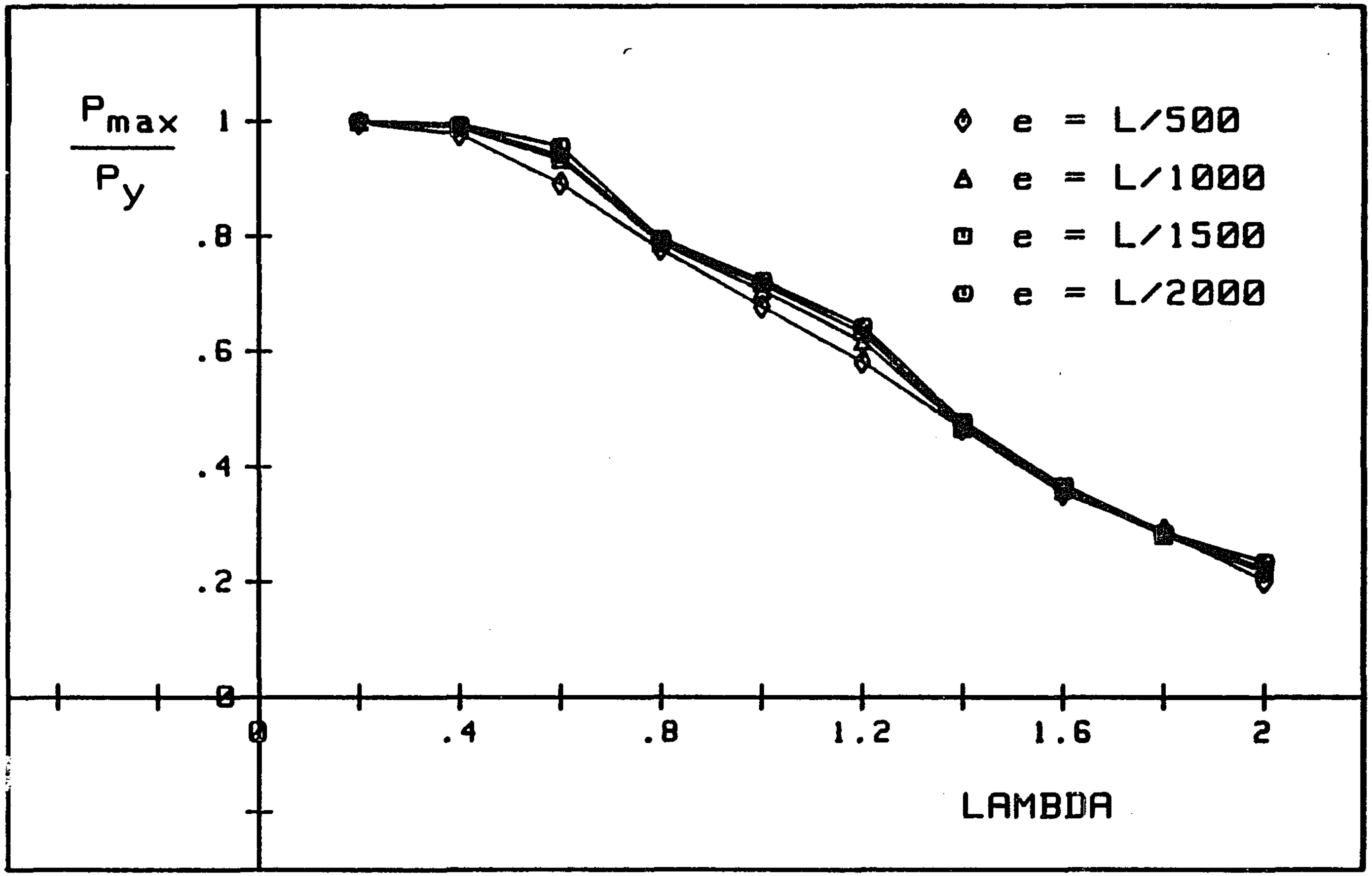

Fig. 6.59. Maximum strength column curves for shape H 12 x 210 (36 ksi steel, 70 ksi electrodes) and y-axis bending.

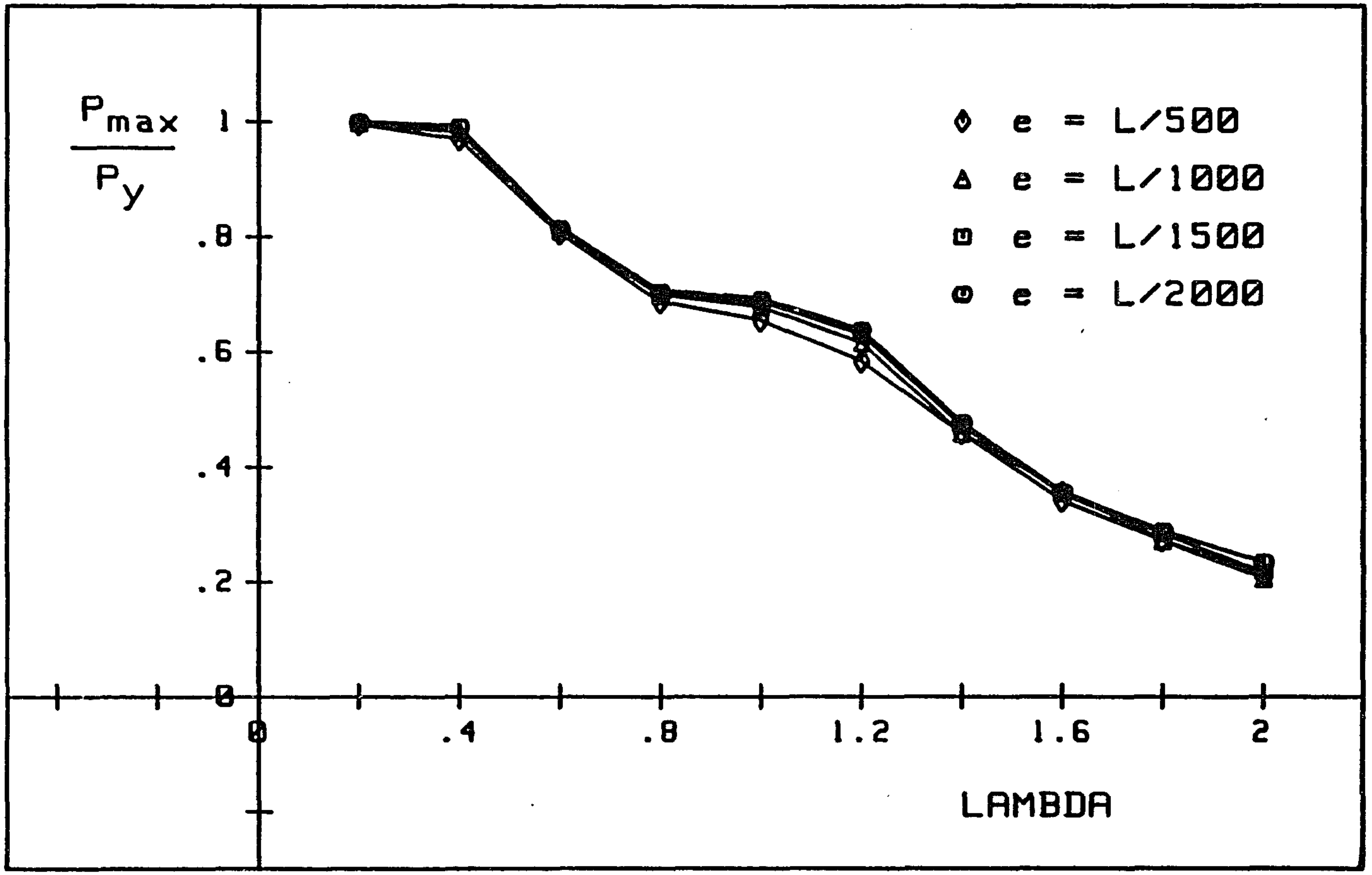

Fig. 6.60. Maximum strength column curves for shape H 12 x 210 (36 ksi steel, 100 ksi electrodes) and x-axis bending.

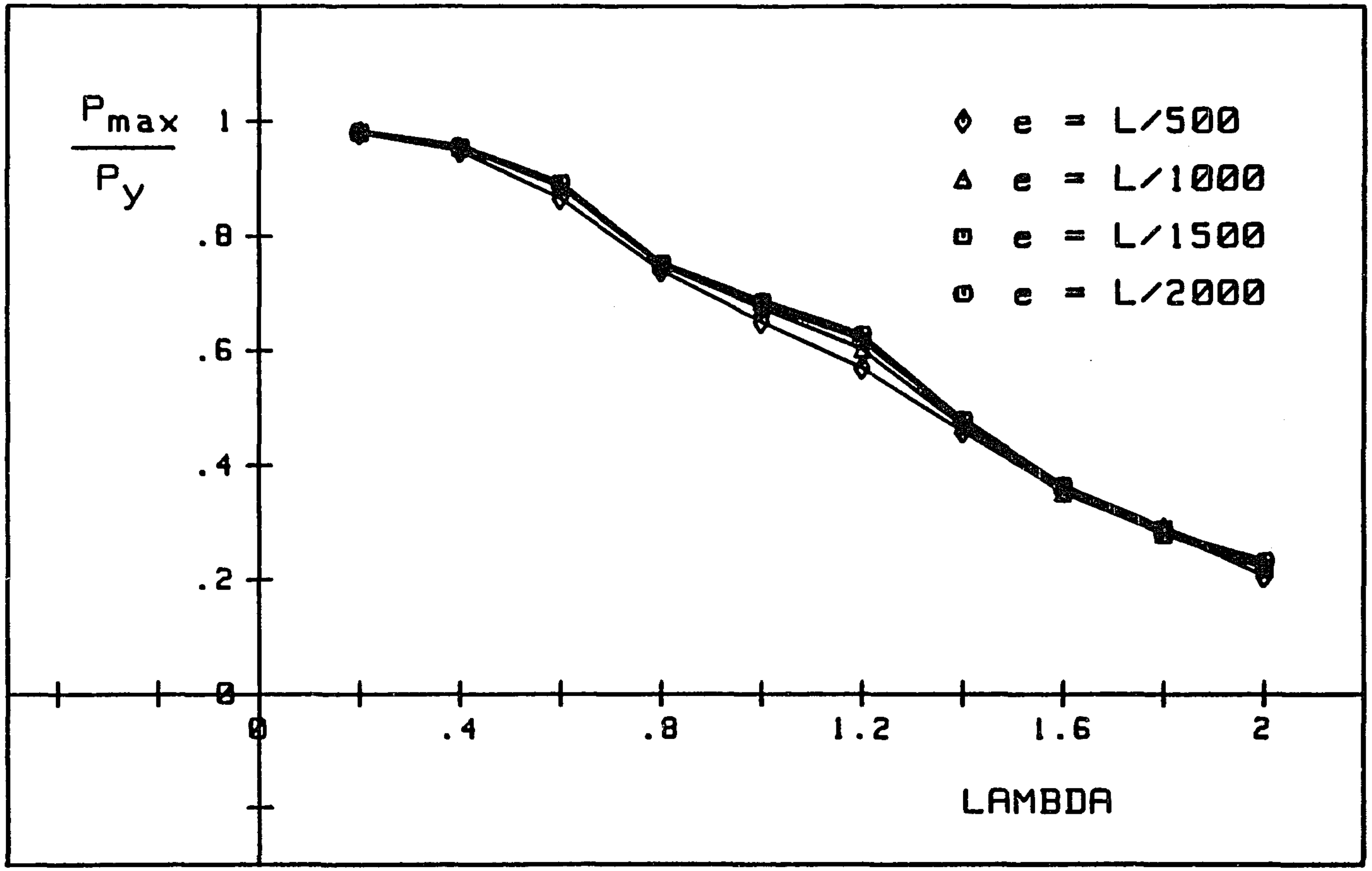

Fig. 6.61. Maximum strength column curves for shape H 12 x 210 (36 ksi steel, 100 ksi electrodes) and y-axis bending.

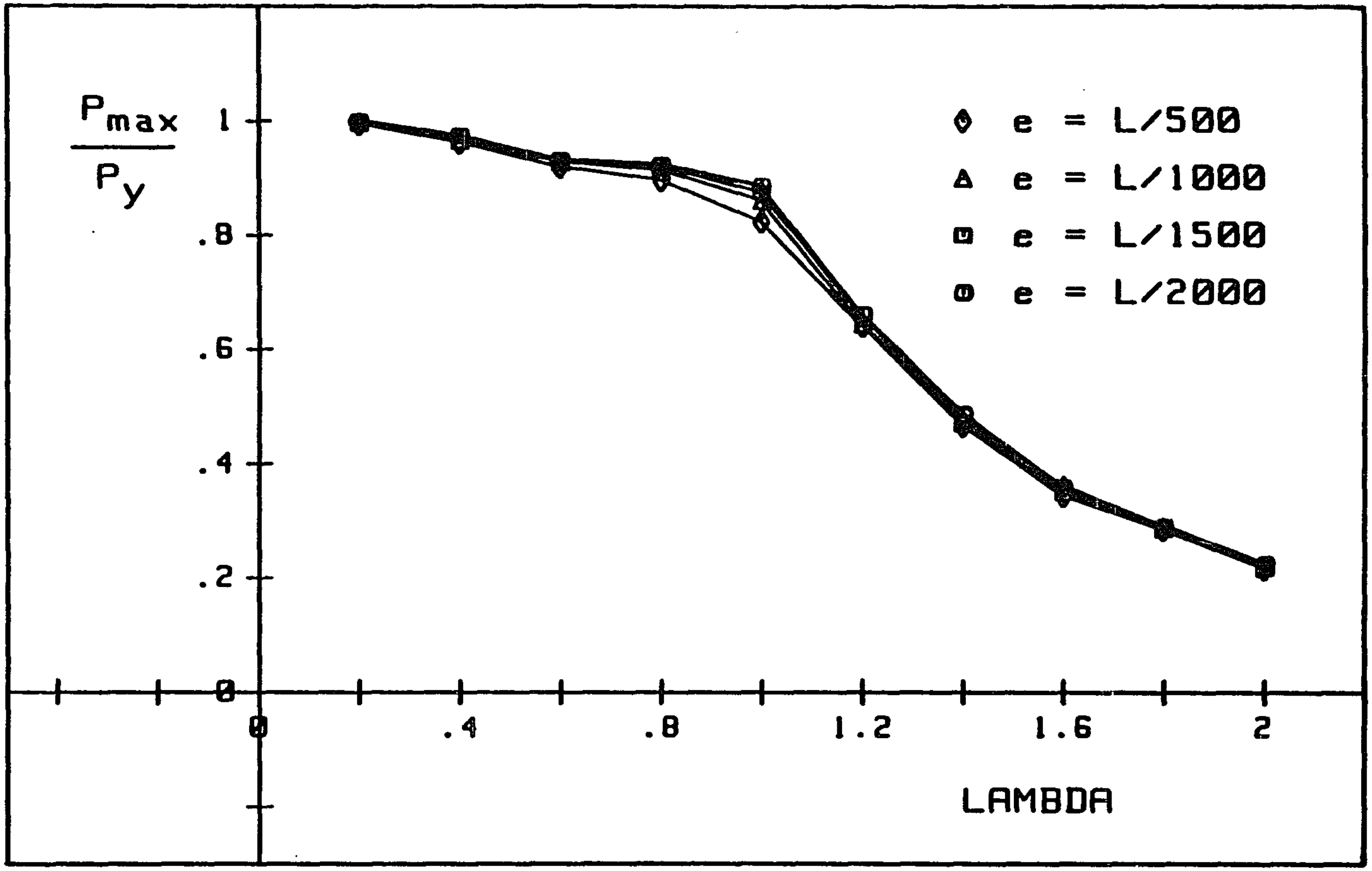

Fig. 6.62. Maximum strength column curves for shape H 12 x 210 (50 ksi steel, 70 ksi electrodes) and x-axis bending.

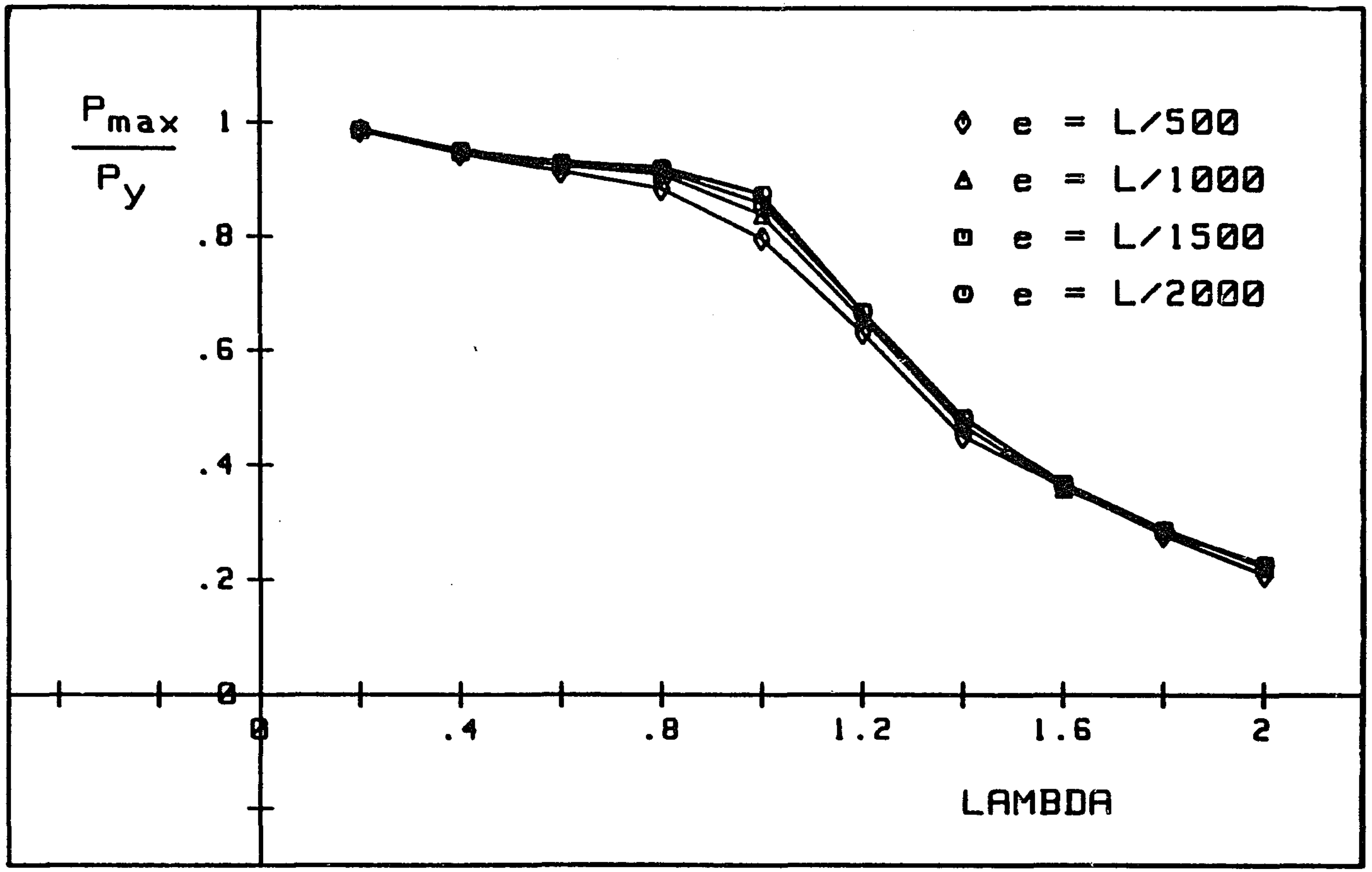

Fig. 6.63. Maximum strength column curves for shape H 12 x 210 (50 ksi steel, 70 ksi electrodes) and y-axis bending.

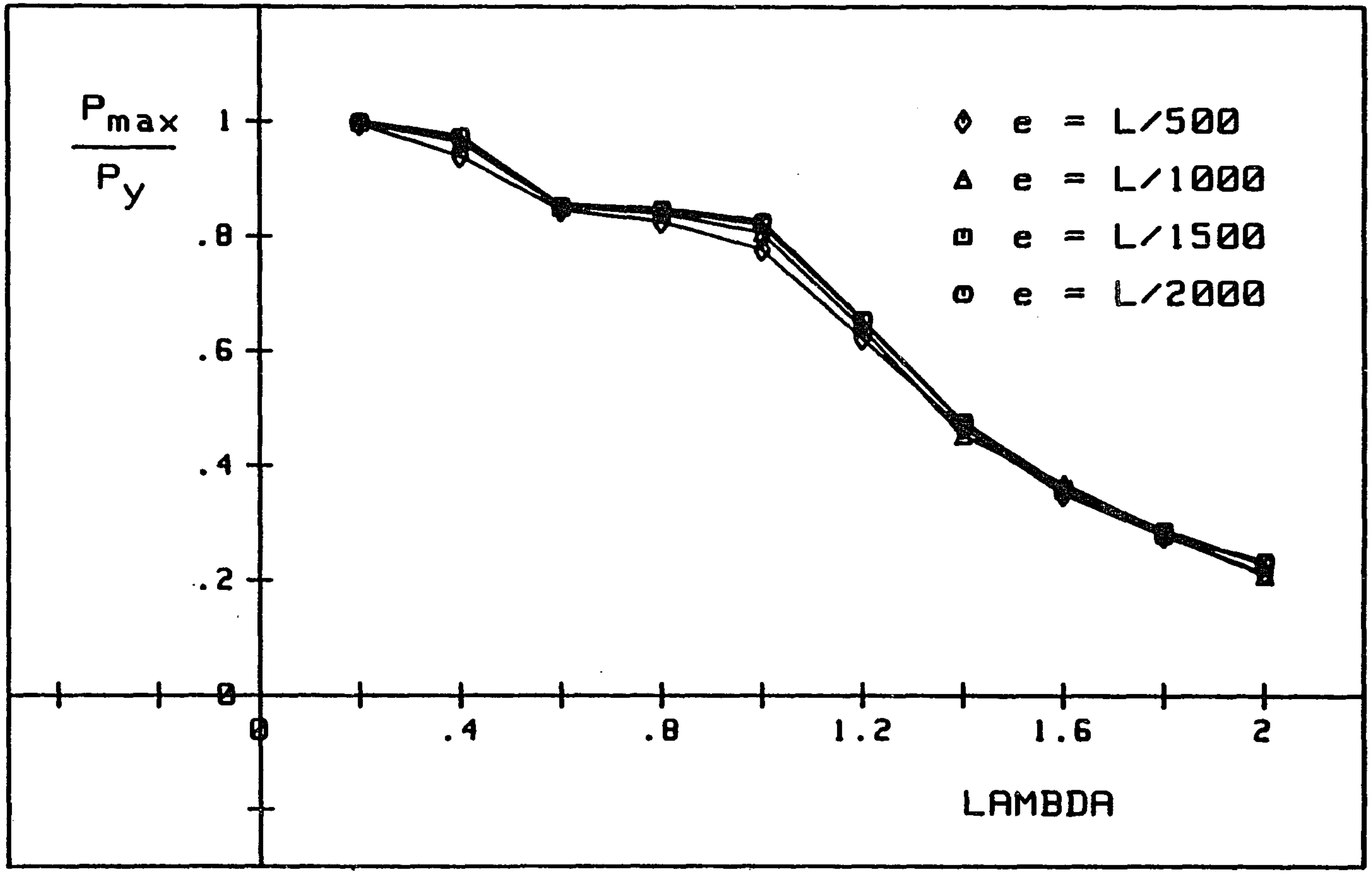

Fig. 6.64. Maximum strength column curves for shape H 12 x 210 (50 ksi steel, 100 ksi electrodes) and x-axis bending.

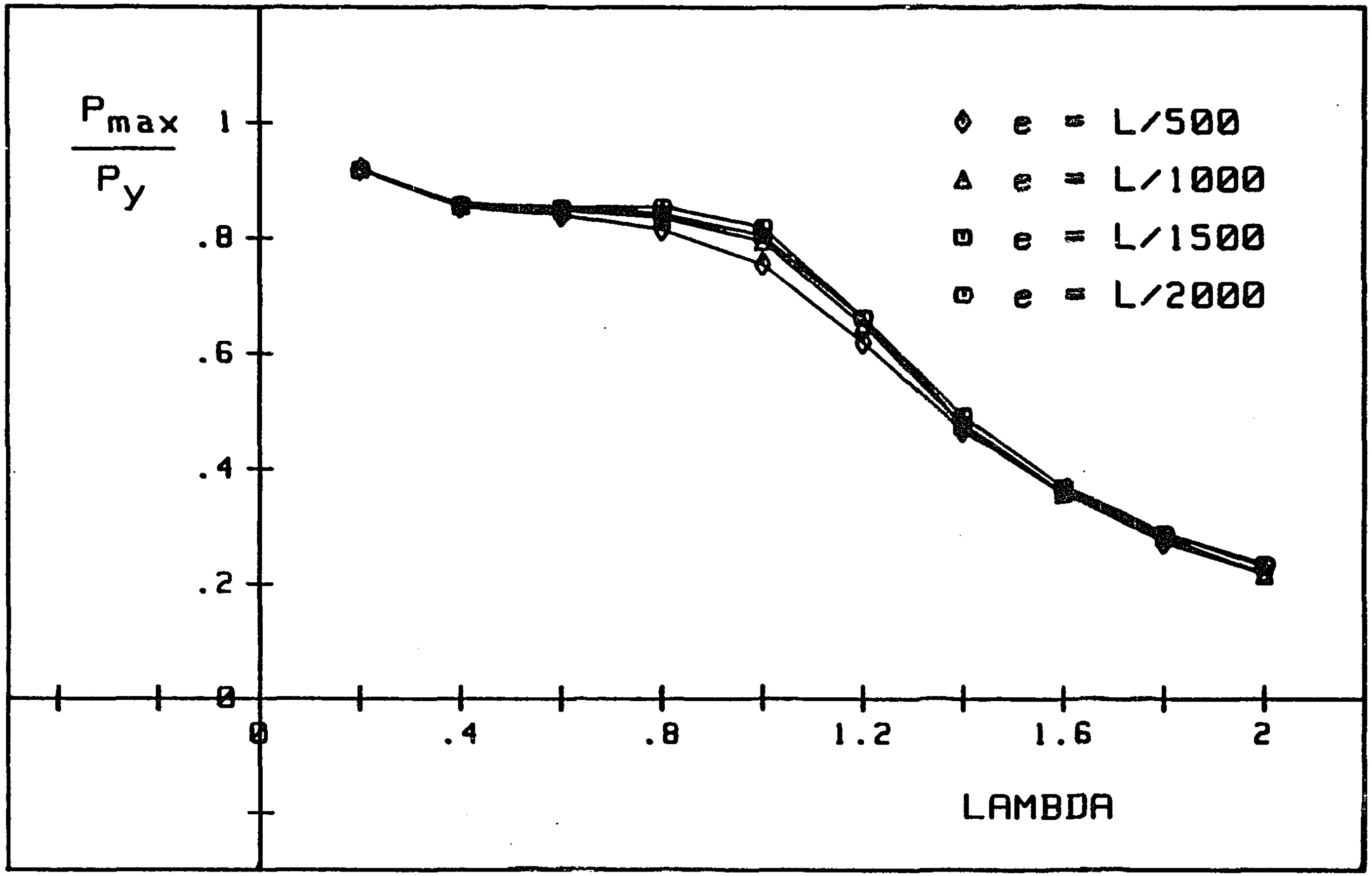

Fig. 6.65. Maximum strength column curves for shape H 12 x 210 (50 ksi steel, 100 ksi electrodes) and y-axis bending.

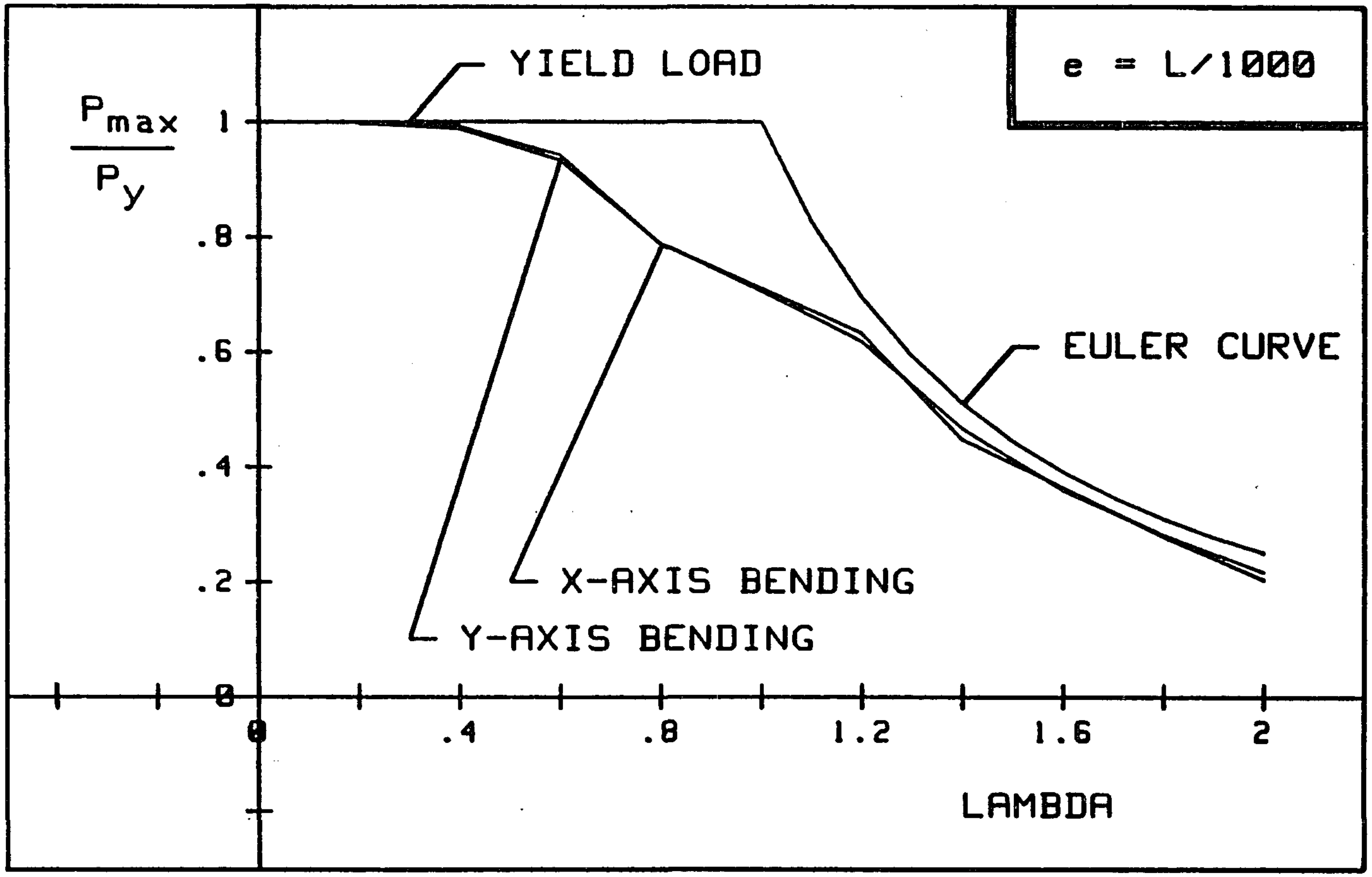

Fig. 6.66. x- and y-axis maximum strength column curves for shape H 12 x 210 (36 ksi steel, 70 ksi electrodes).

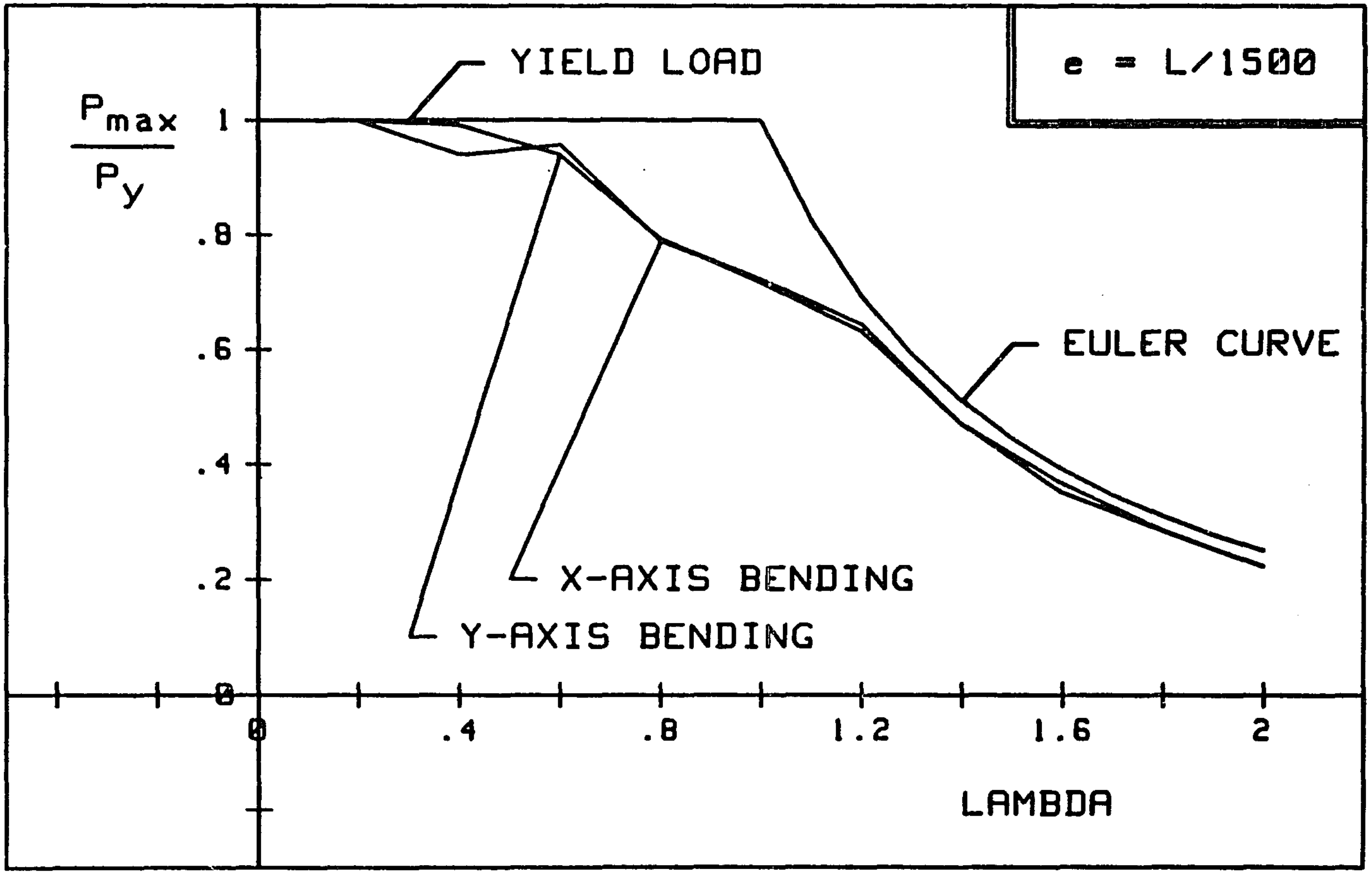

Fig. 6.67. x- and y-axis maximum strength column curves for shape H 12 x 210 (36 ksi steel, 70 ksi electrodes).

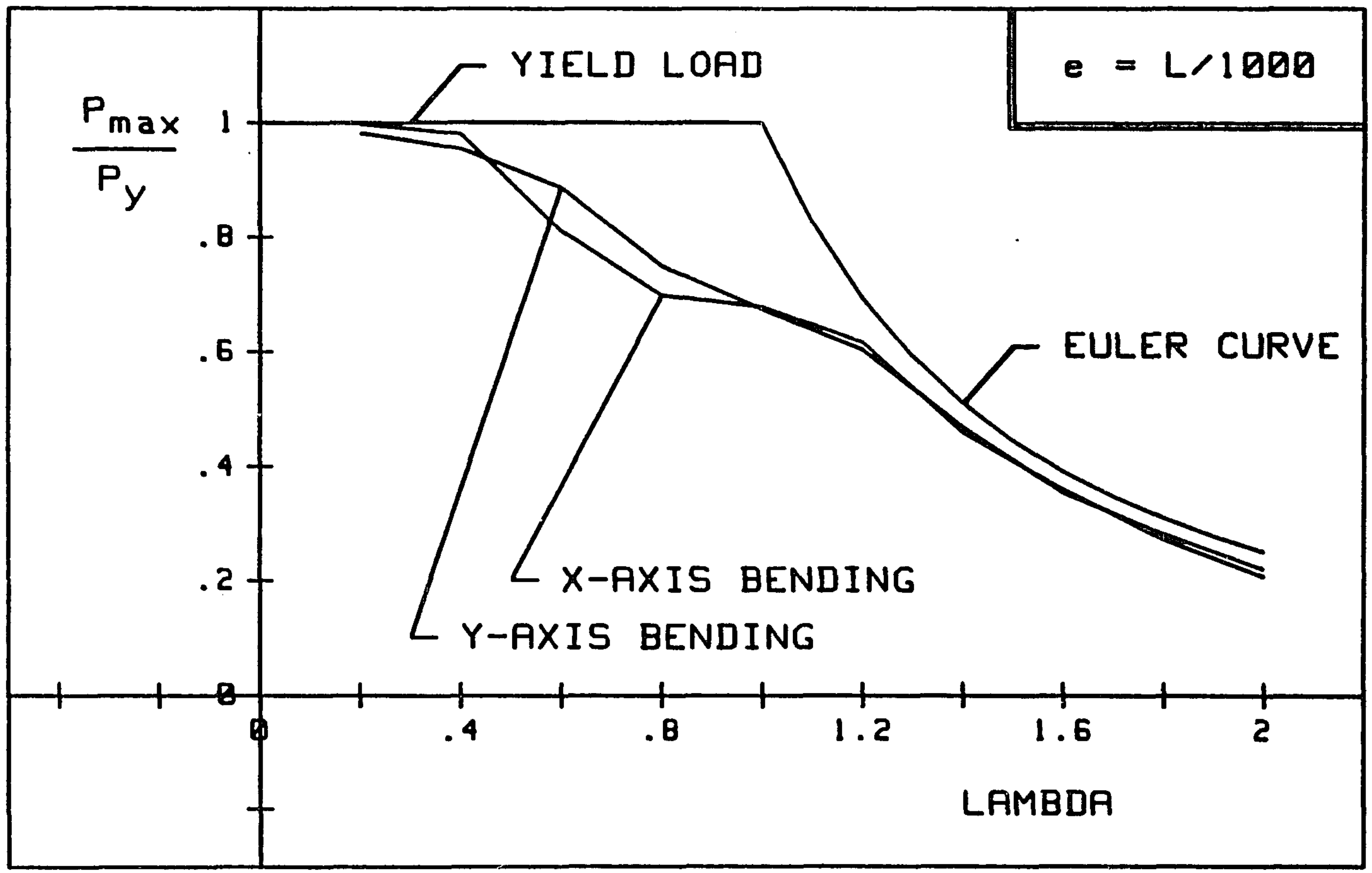

Fig. 6.68. x- and y-axis maximum strength column curves for shape H 12 x 210 (36 ksi steel, 100 ksi electrodes).

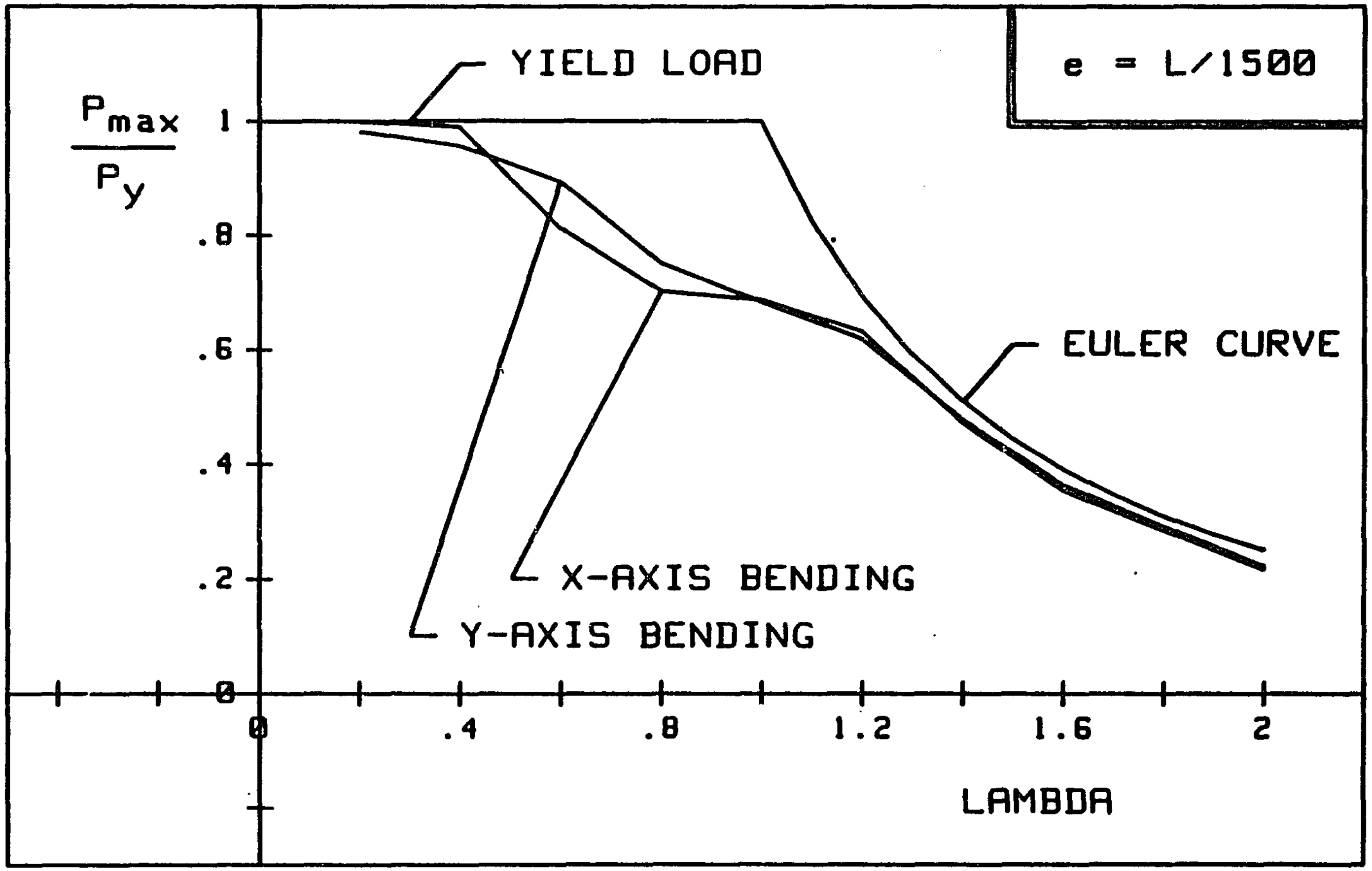

Fig. 6.69. x- and y-axis maximum strength column curves for shape H 12 x 210 (36 ksi steel, 100 ksi electrodes).

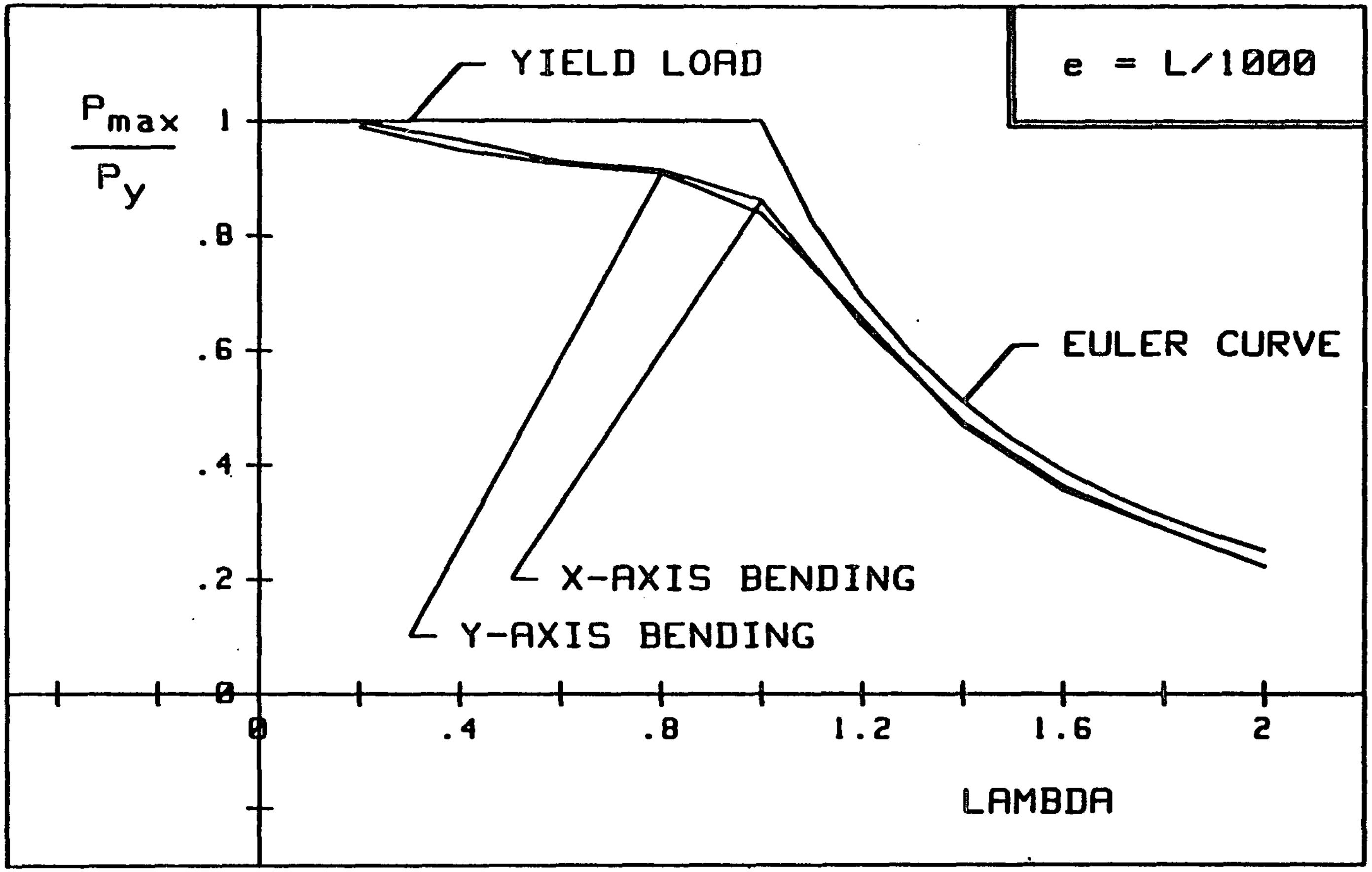

Fig. 6.70. x- and y-axis maximum strength column curves for shape H 12 x 210 (50 ksi steel, 70 ksi electrodes).

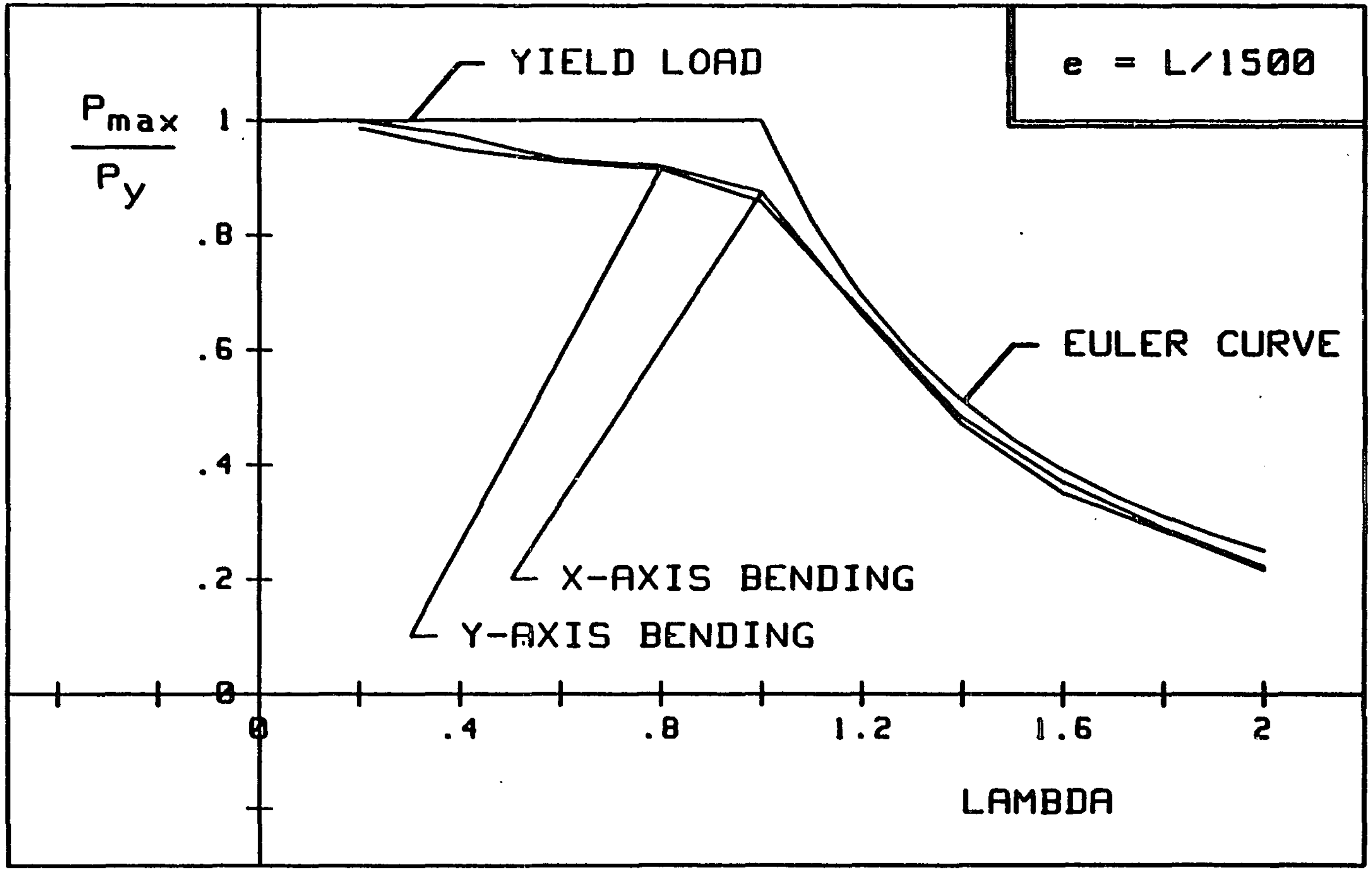

Fig. 6.71. x- and y-axis maximum strength column curves for shape H 12 x 210 (50 ksi steel, 70 ksi electrodes).

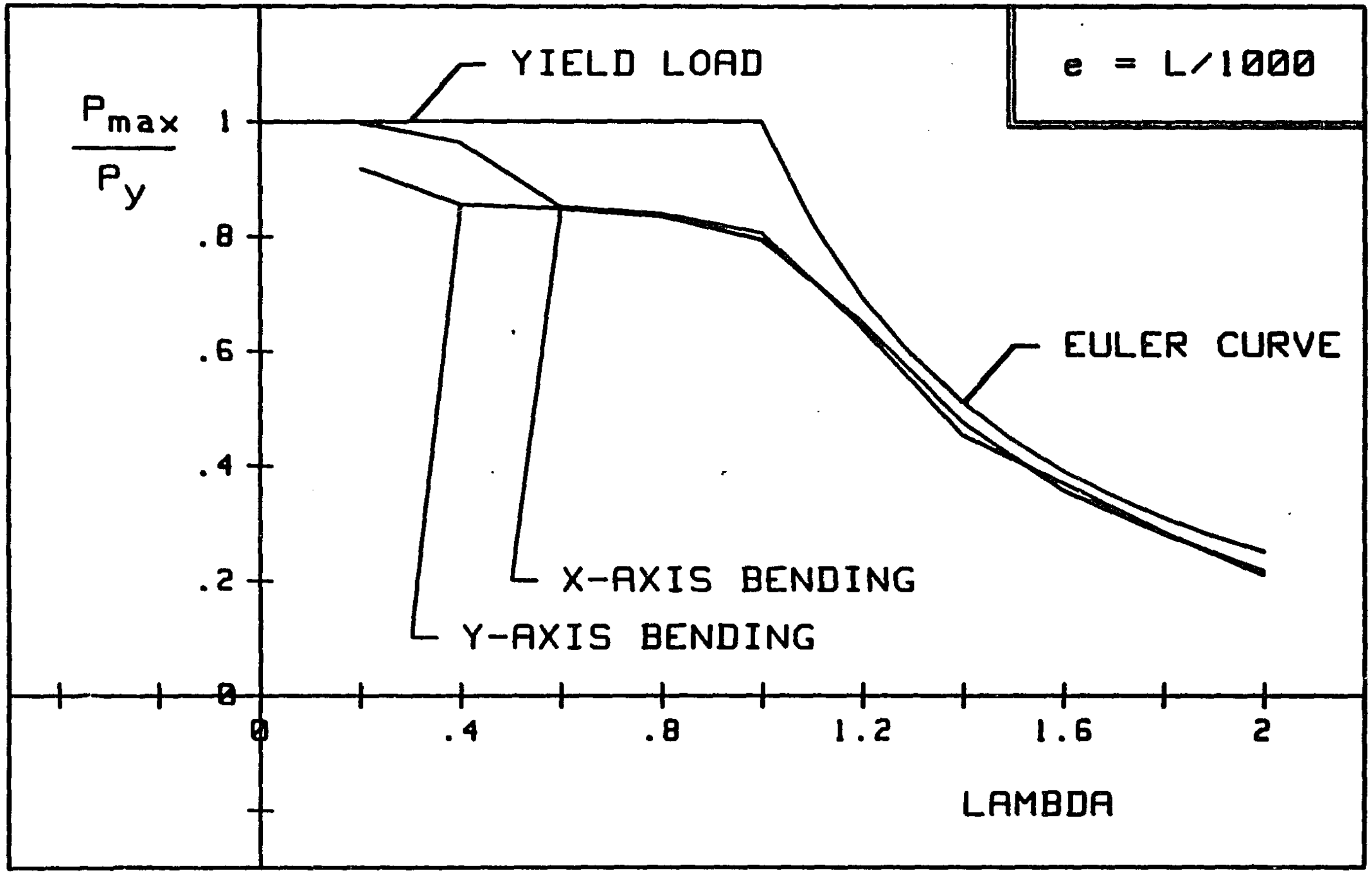

Fig. 6.72. x- and y-axis maximum strength column curves for shape H 12 x 210 (50 ksi steel, 100 ksi electrodes).

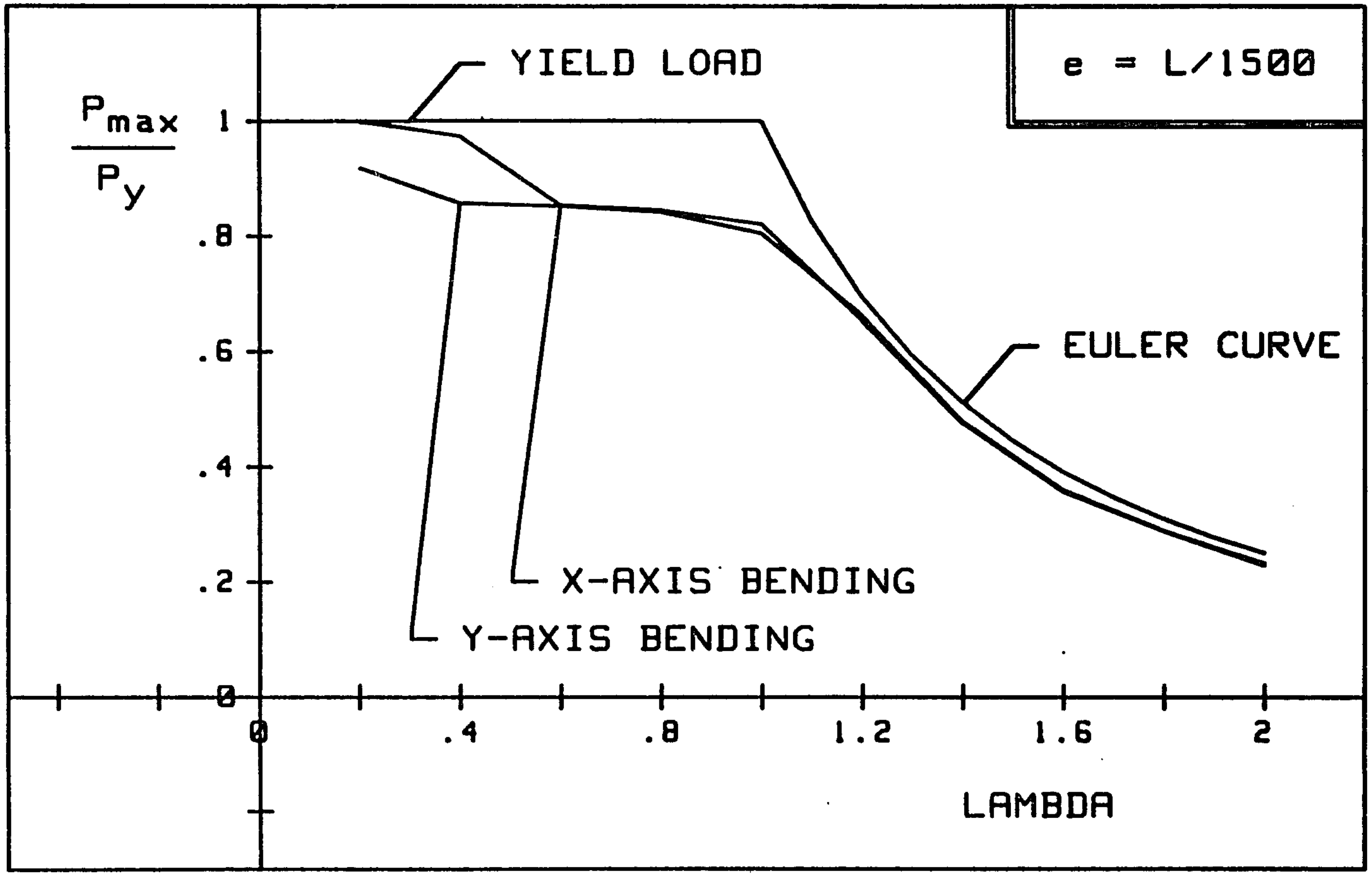

Fig. 6.73. x- and y-axis maximum strength column curves for shape H 12 x 210 (50 ksi steel, 100 ksi electrodes).

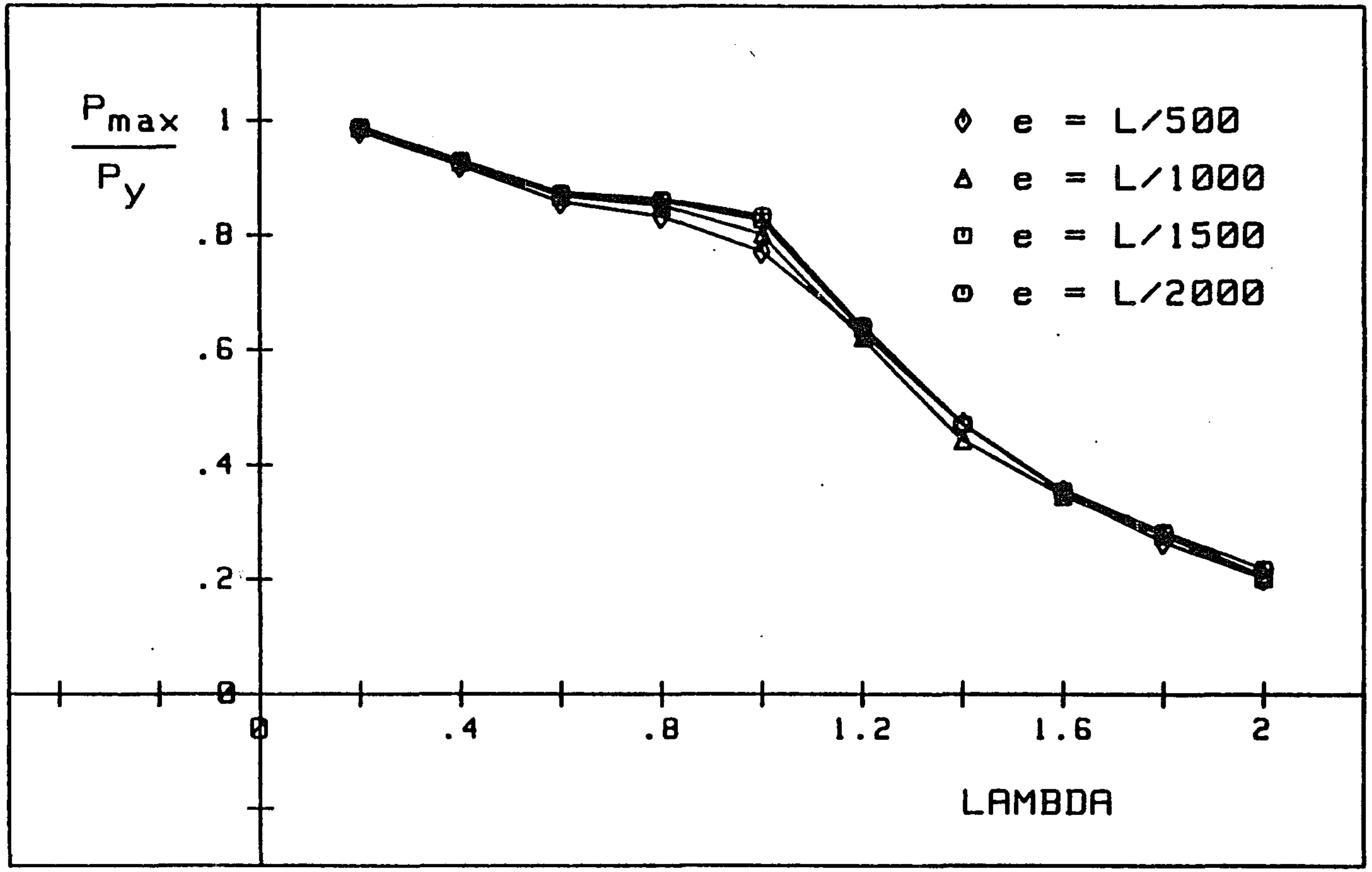

Fig. 6.74. Maximum strength column curves for shape H 14 x 15 (36 ksi steel, 70 ksi electrodes) and x-axis bending.

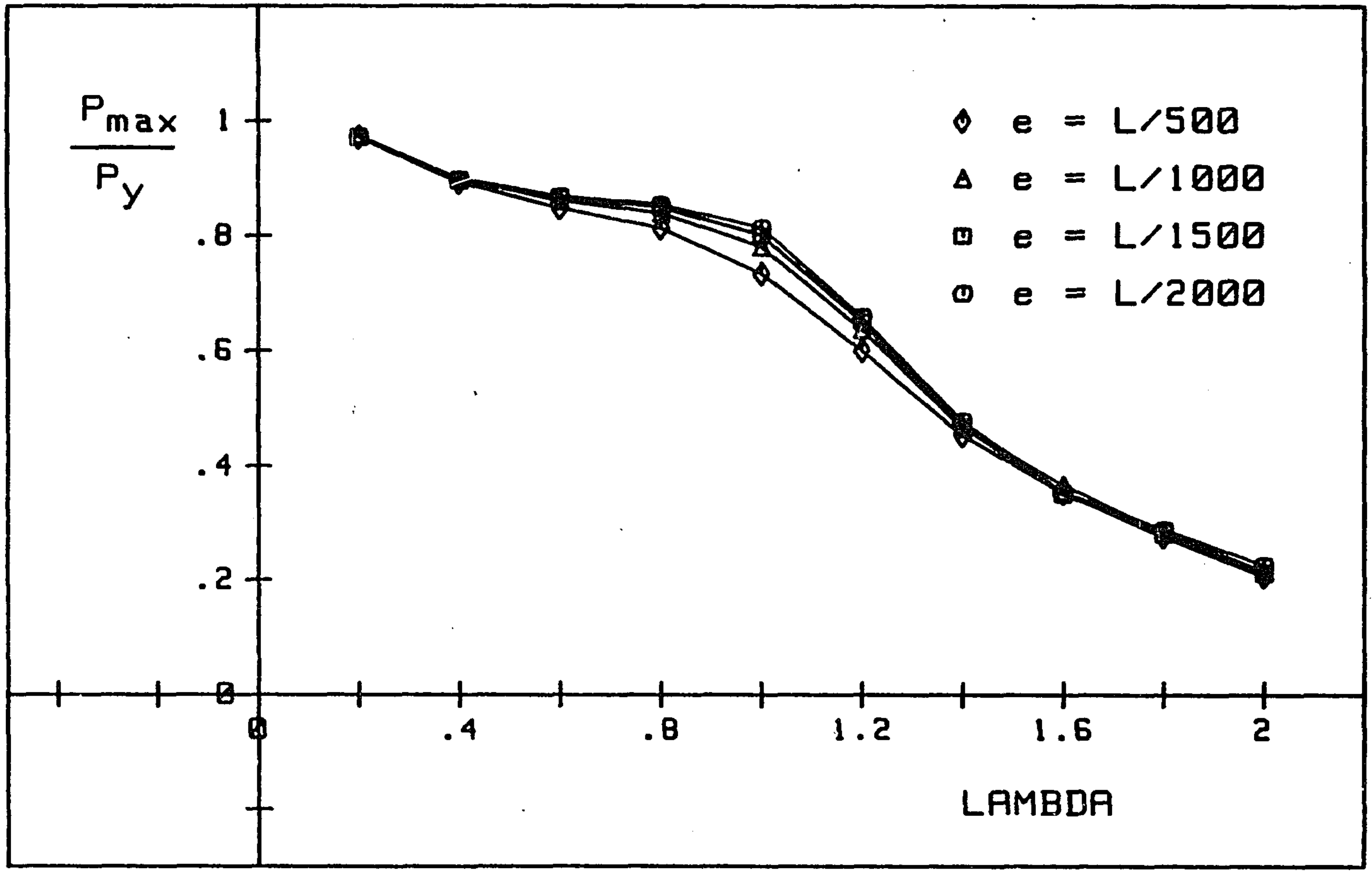

Fig. 6.75. Maximum strength column curves for shape H 14 x 15 (36 ksi steel, 70 ksi electrodes) and y-axis bending.

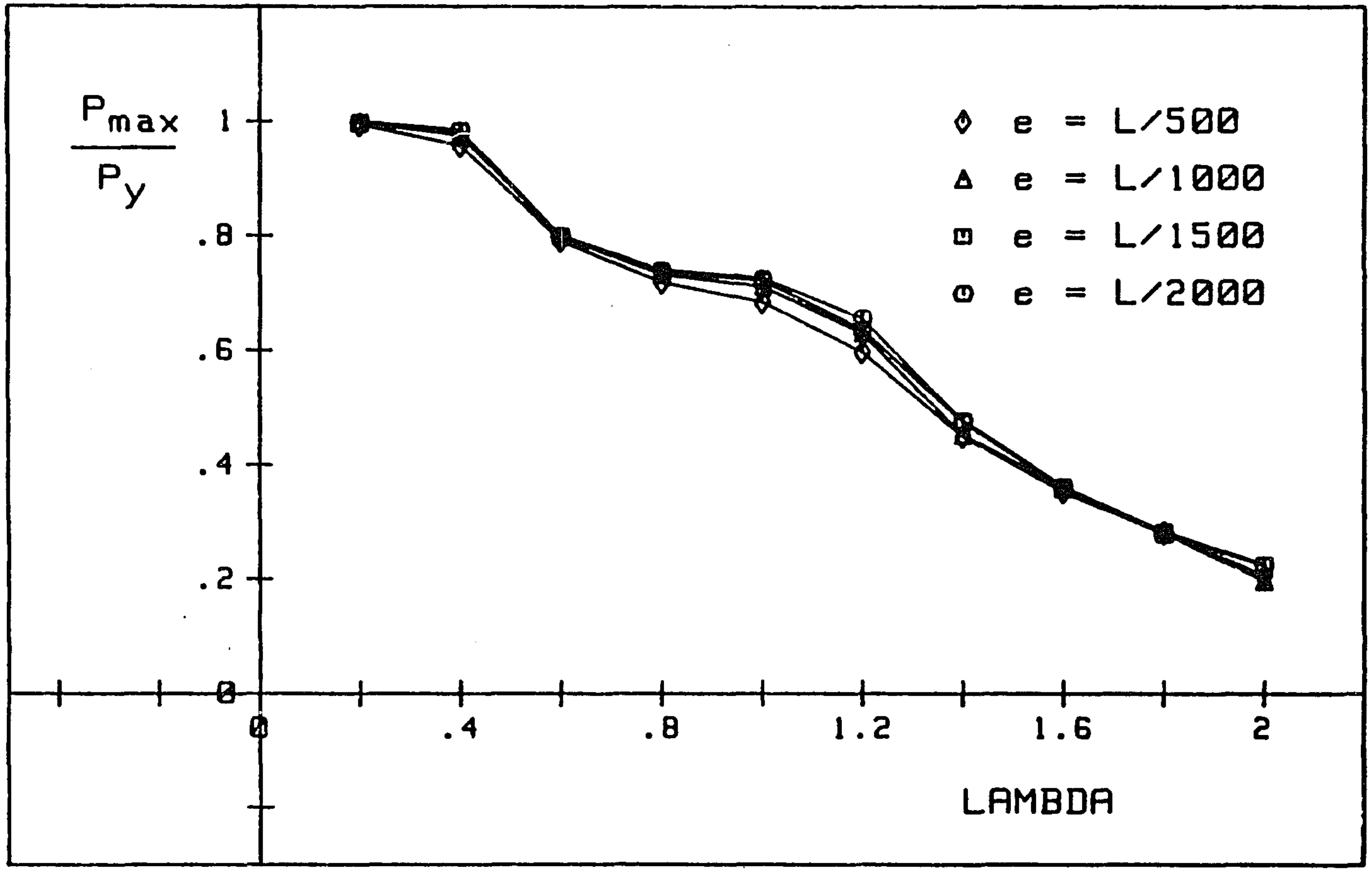

Fig. 6.76. Maximum strength column curves for shape H 14 x 15 (36 ksi steel, 100 ksi electrodes) and x-axis bending.

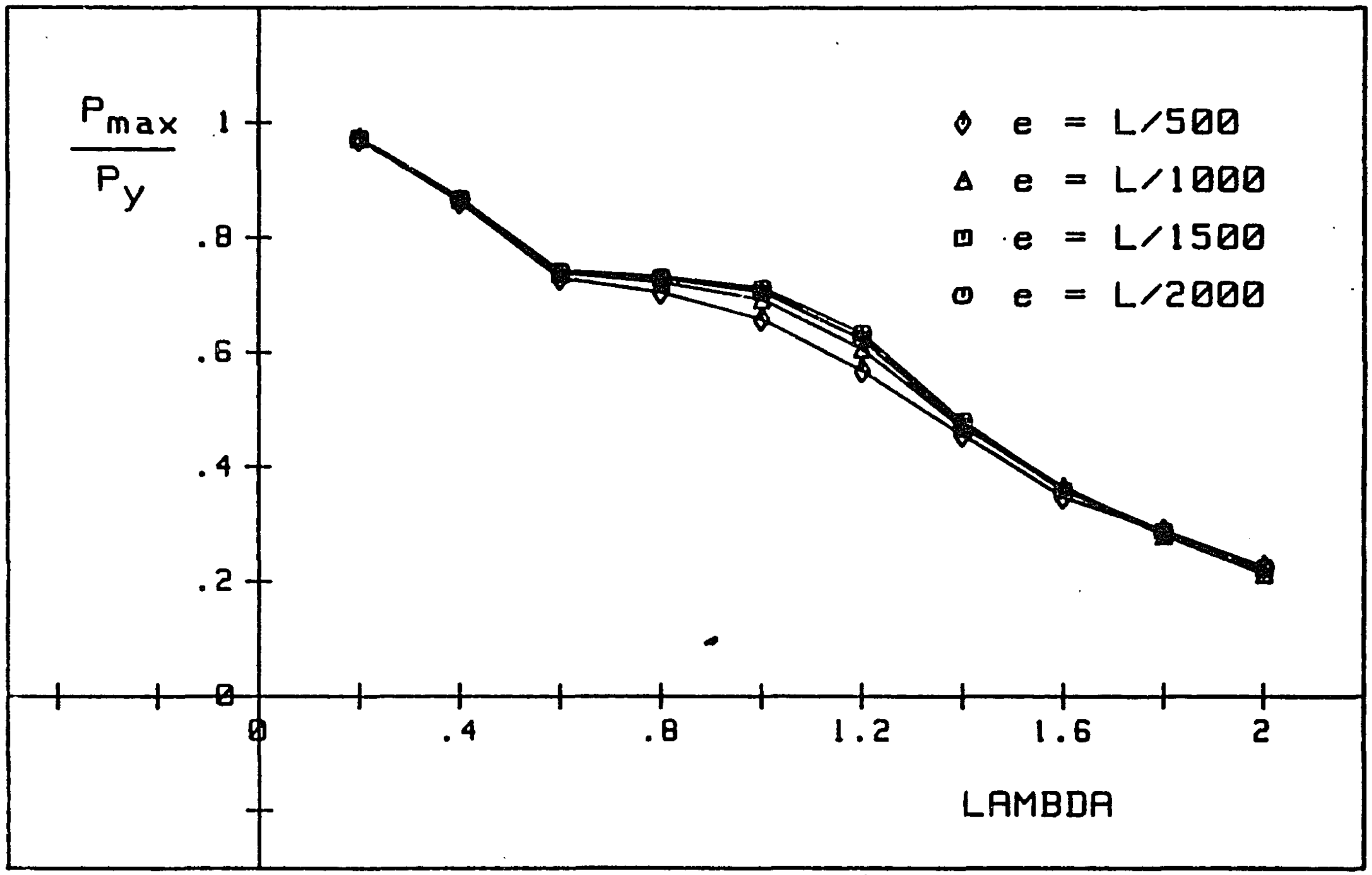

Fig. 6.77. Maximum strength column curves for shape H 14 x 15 (36 ksi steel, 100 ksi electrodes) and y-axis bending.

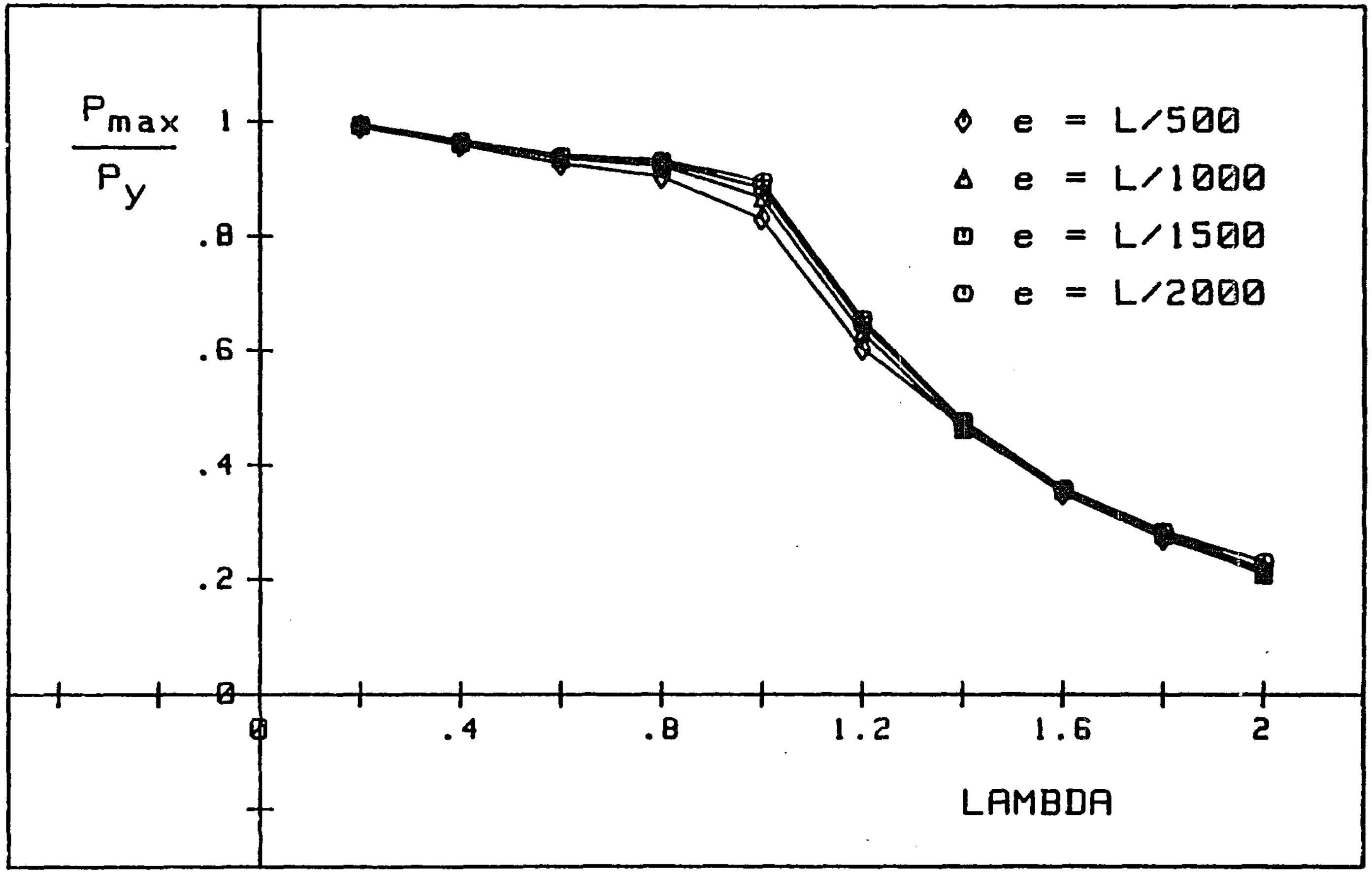

Fig. 6.78. Maximum strength column curves for shape H 14 x 15 (50 ksi steel, 70 ksi electrodes) and x-axis bending.

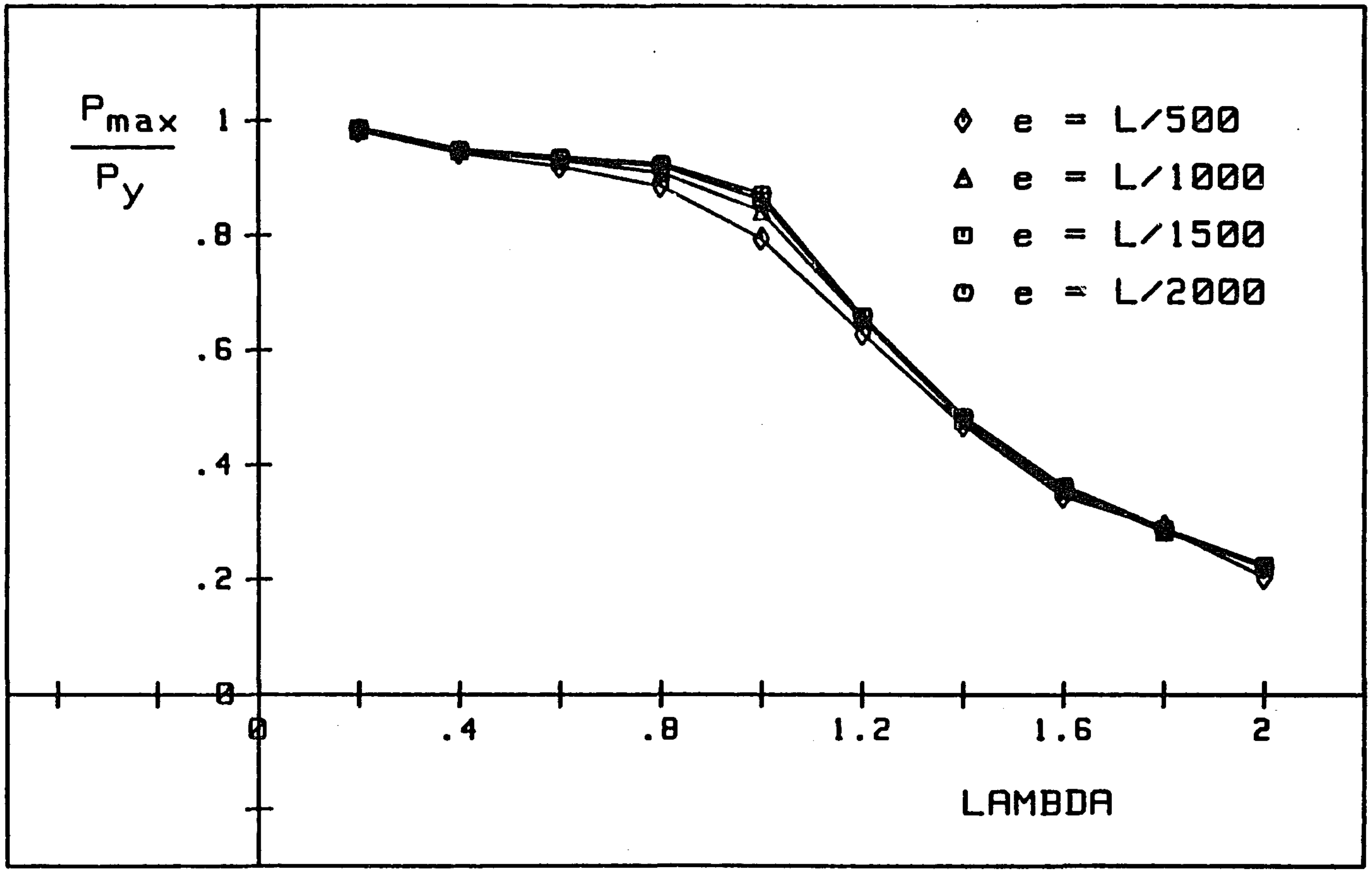

Fig. 6.79. Maximum strength column curves for shape H 14 x 15 (50 ksi steel, 70 ksi electrodes) and y-axis bending.

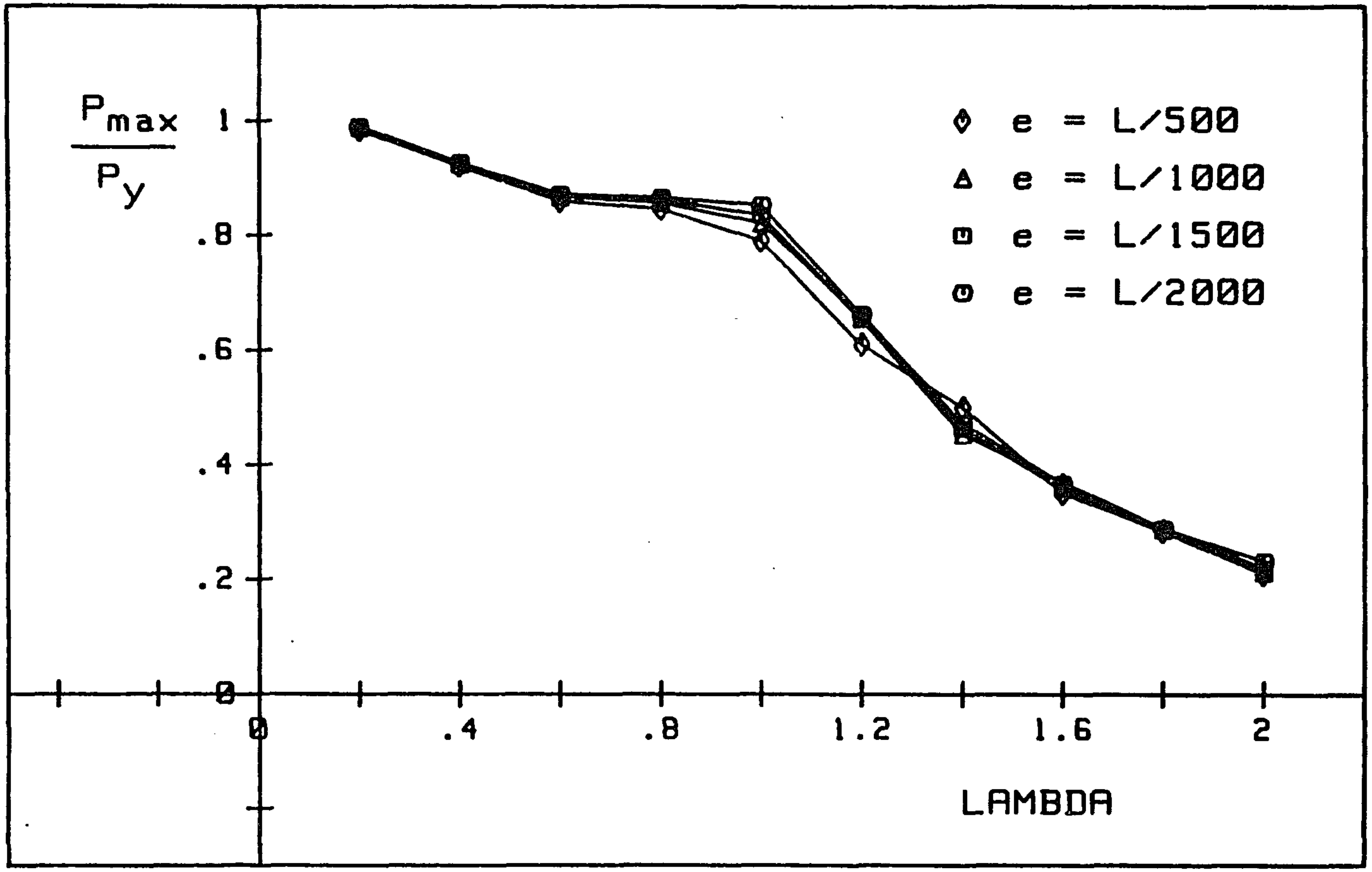

Fig. 6.80. Maximum strength column curves for shape H 14 x 15 (50 ksi steel, 100 ksi electrodes) and x-axis bending.

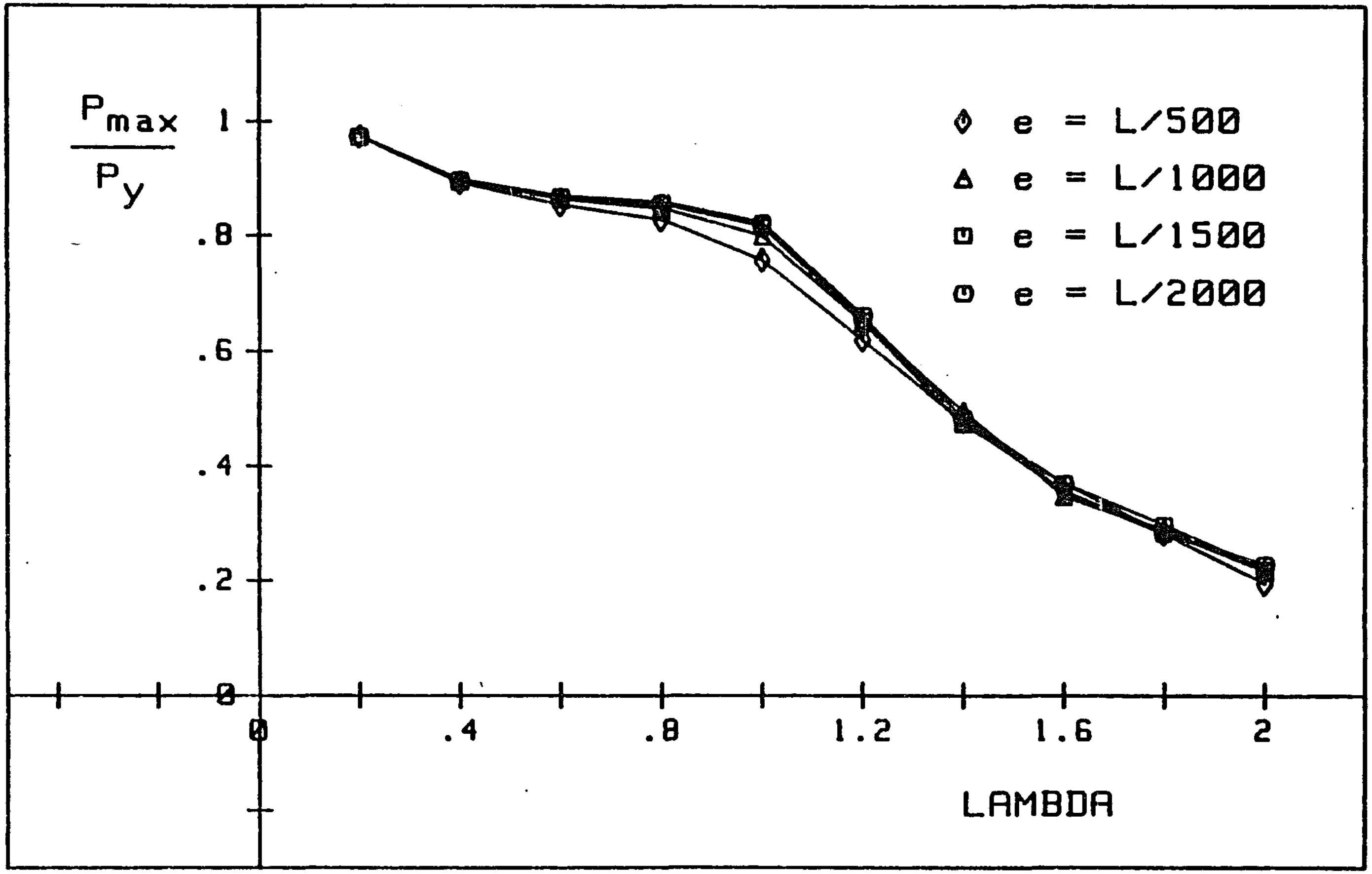

Fig. 6.81. Maximum strength column curves for shape H 14 x 15 (50 ksi steel, 100 ksi electrodes) and y-axis bending.

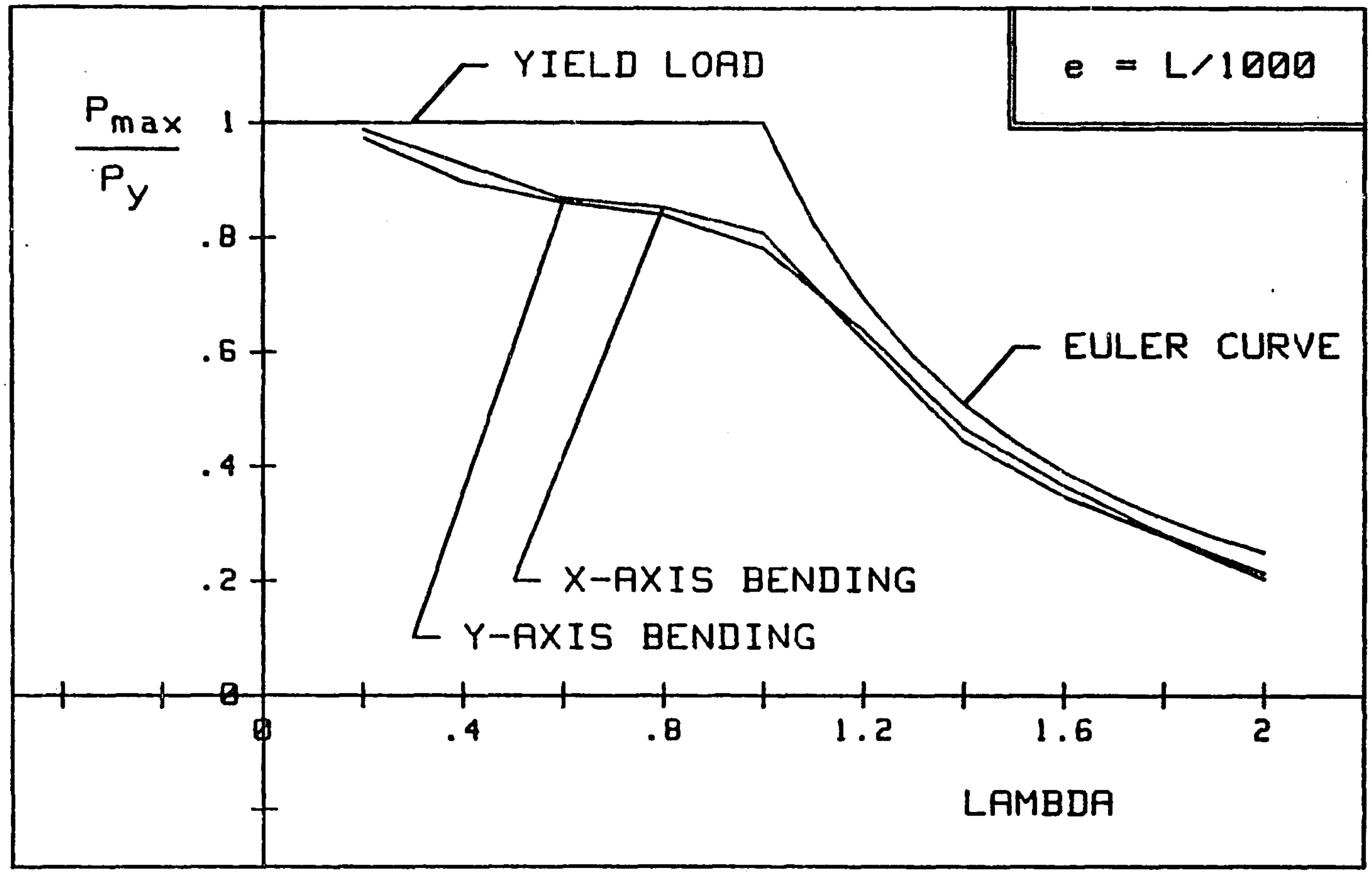

Fig. 6.82. x- and y-axis maximum strength column curves for shape H 14 x 15 (36 ksi steel, 70 ksi electrodes).

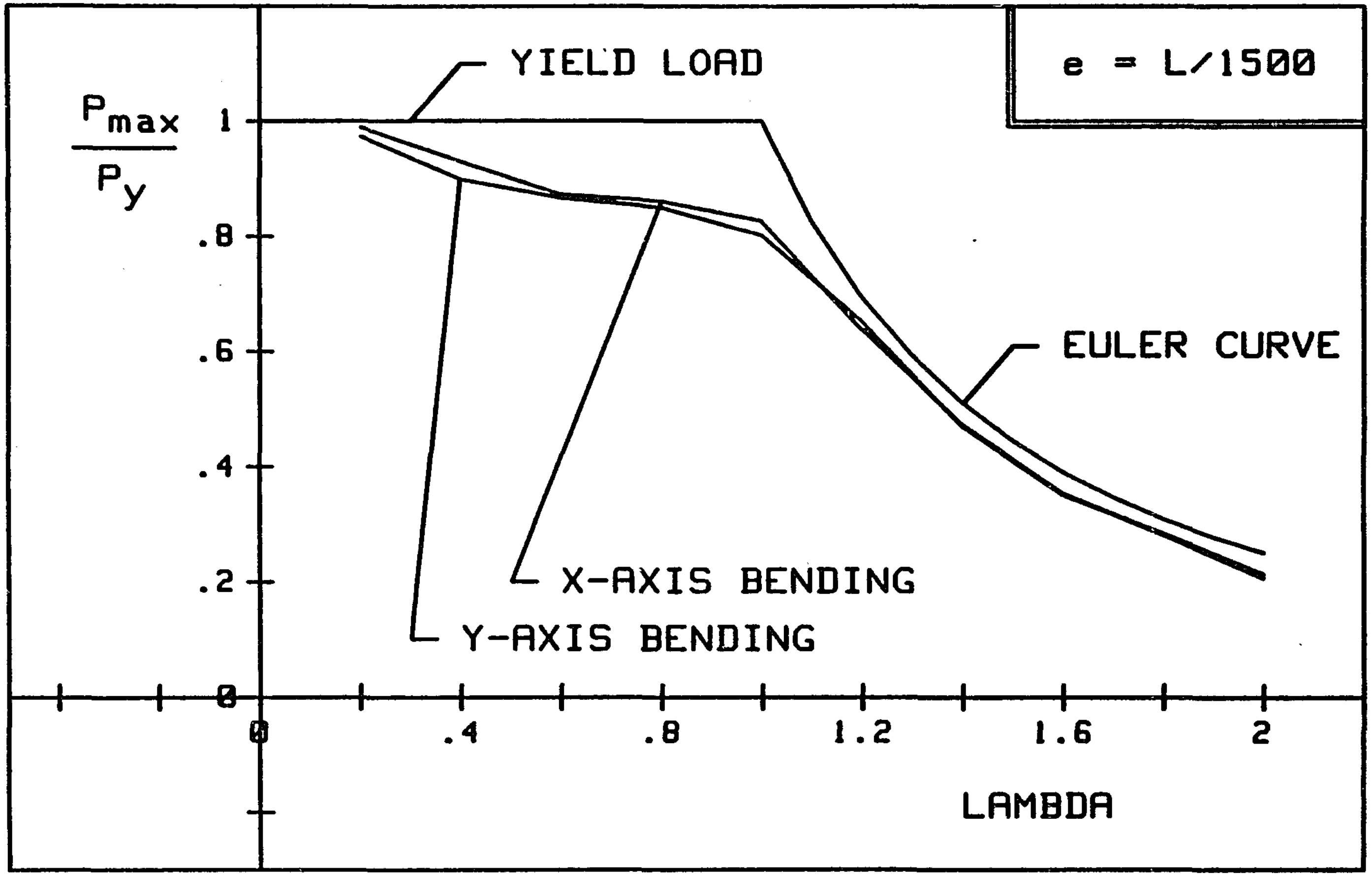

Fig. 6.83. x- and y-axis maximum strength column curves for shape H 14 x 15 (36 ksi steel, 70 ksi electrodes).

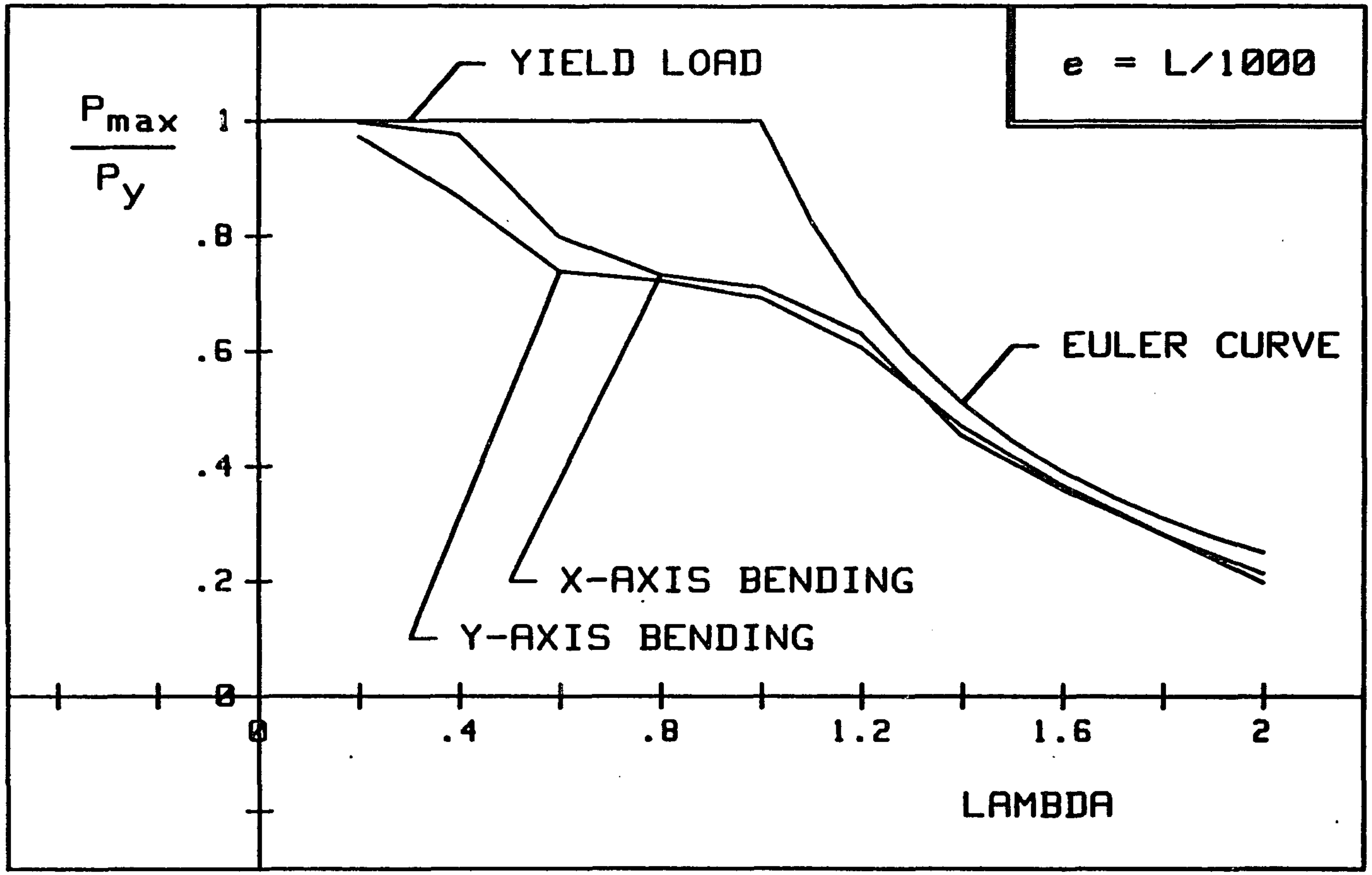

Fig. 6.84. x- and y-axis maximum strength column curves for shape H 14 x 15 (36 ksi steel, 100 ksi electrodes).

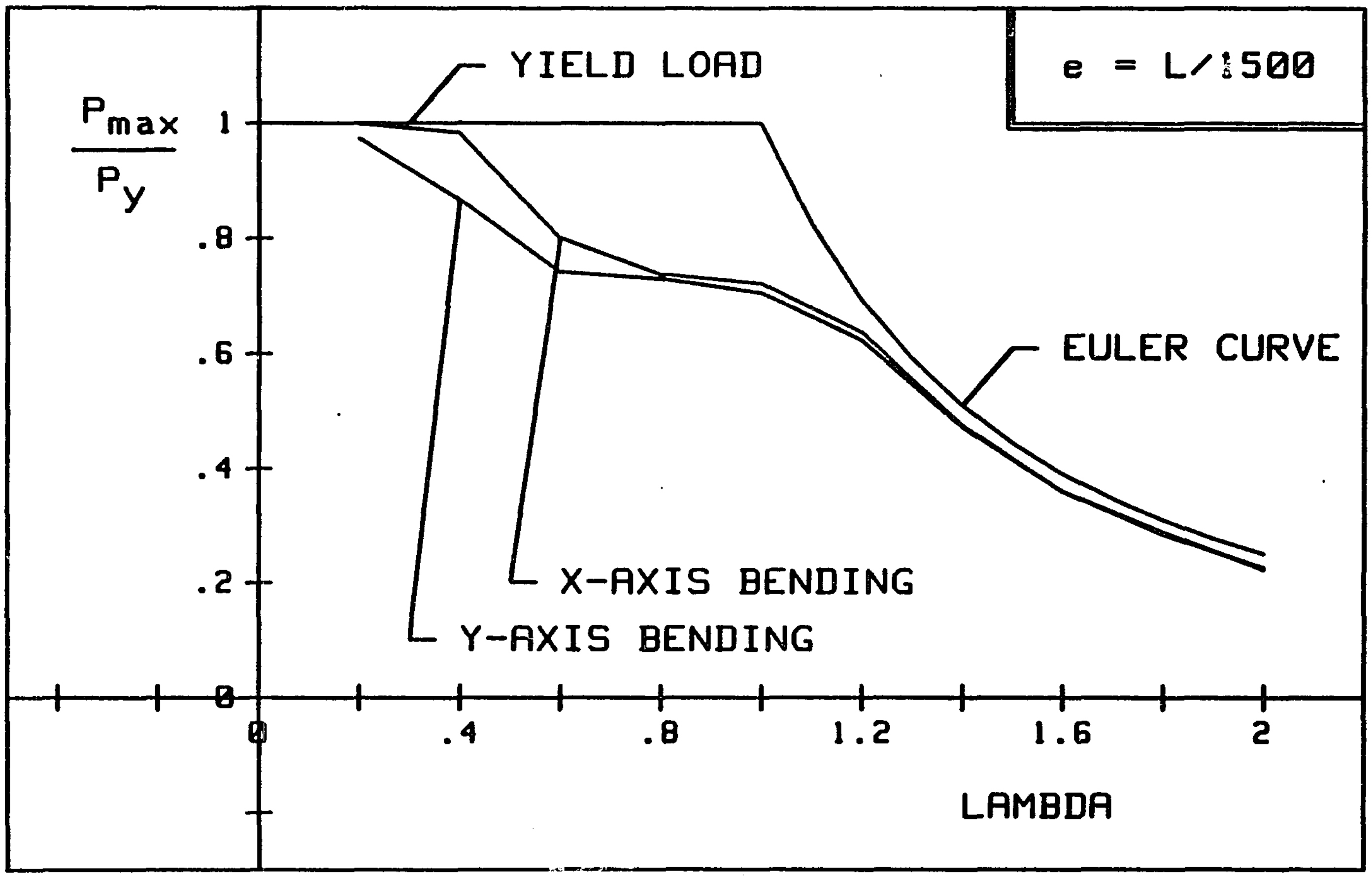

Fig. 6.85. x- and y-axis maximum strength column curves for shape H 14 x 15 (36 ksi steel, 100 ksi electrodes).

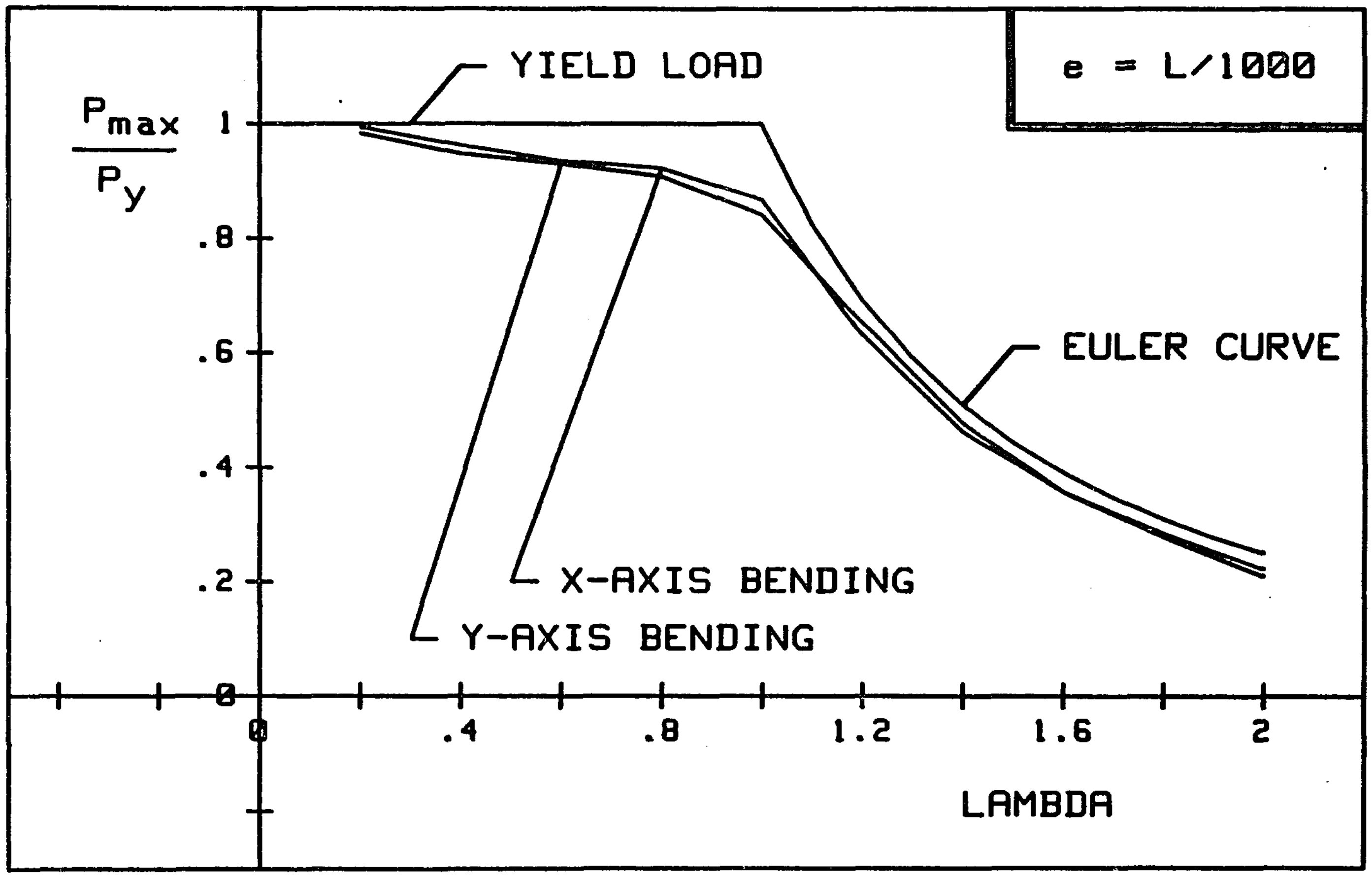

Fig. 6.86. x- and y-axis maximum strength column curves for shape H 14 x 15 (50 ksi steel, 70 ksi electrodes).

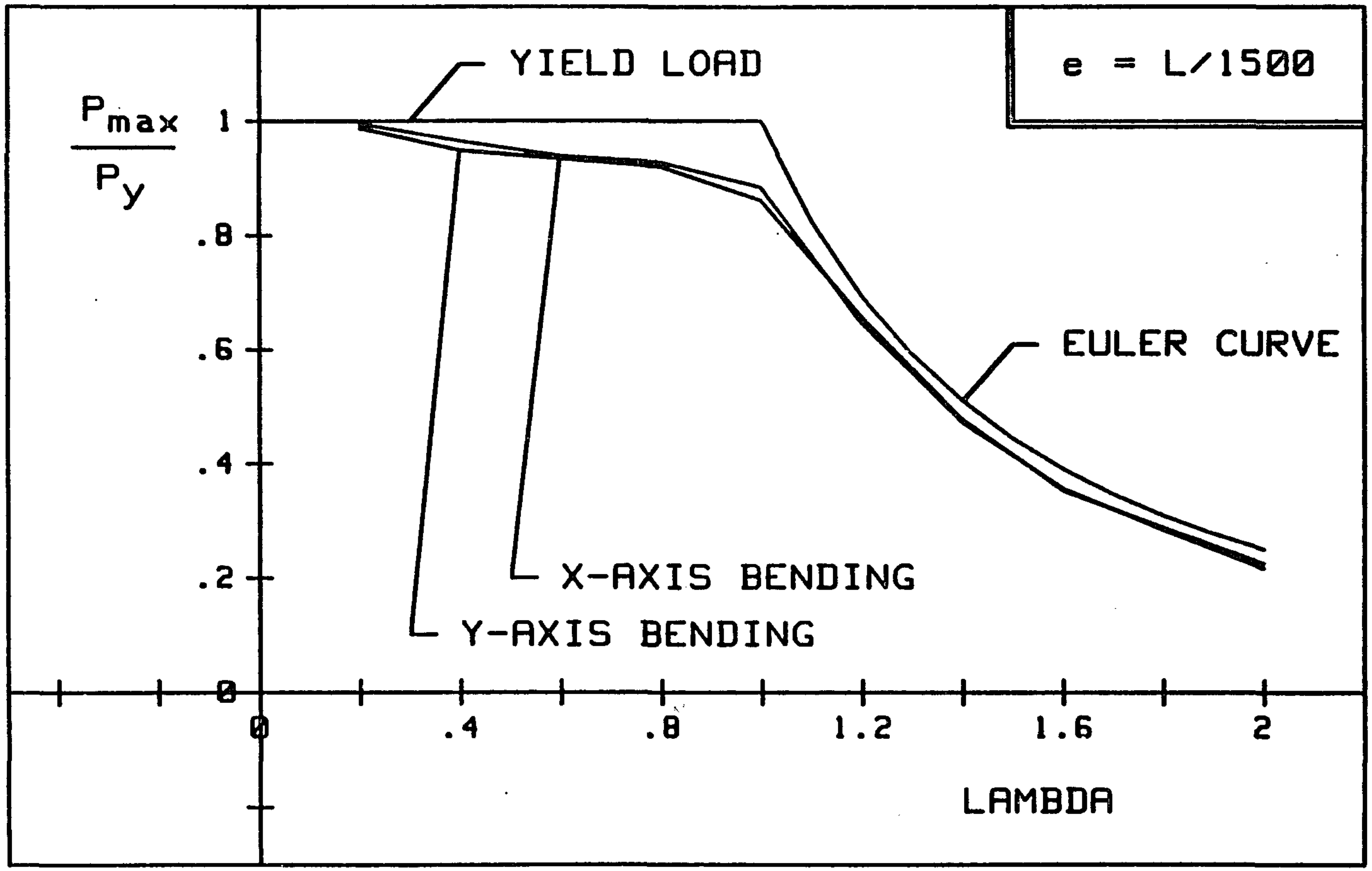

Fig. 6.87. x- and y-axis maximum strength column curves for shape H 14 x 15 (50 ksi steel, 70 ksi electrodes).

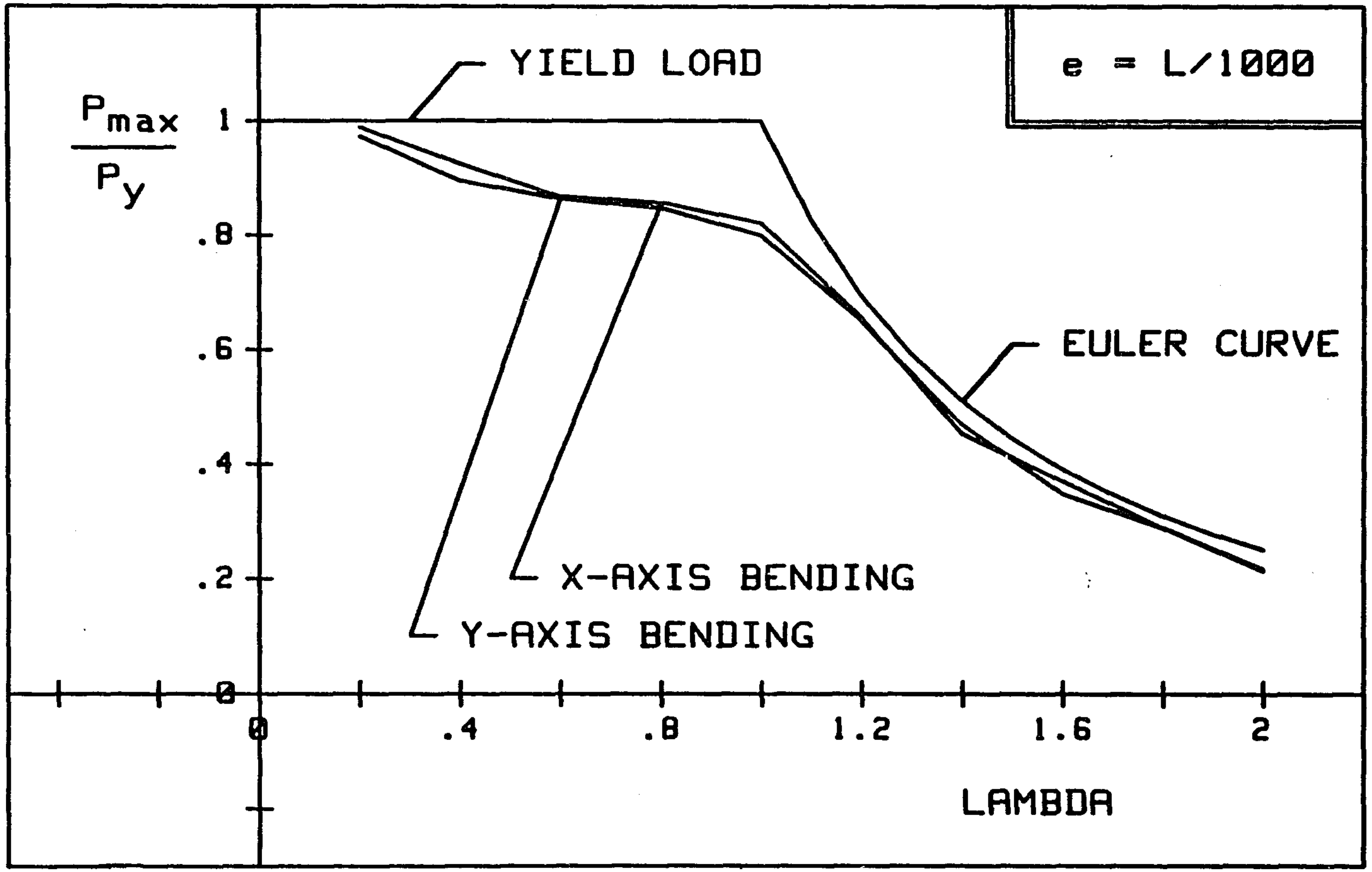

Fig. 6.88. x- and y-axis maximum strength column curves for shape H 14 x 15 (50 ksi steel, 100 ksi electrodes).

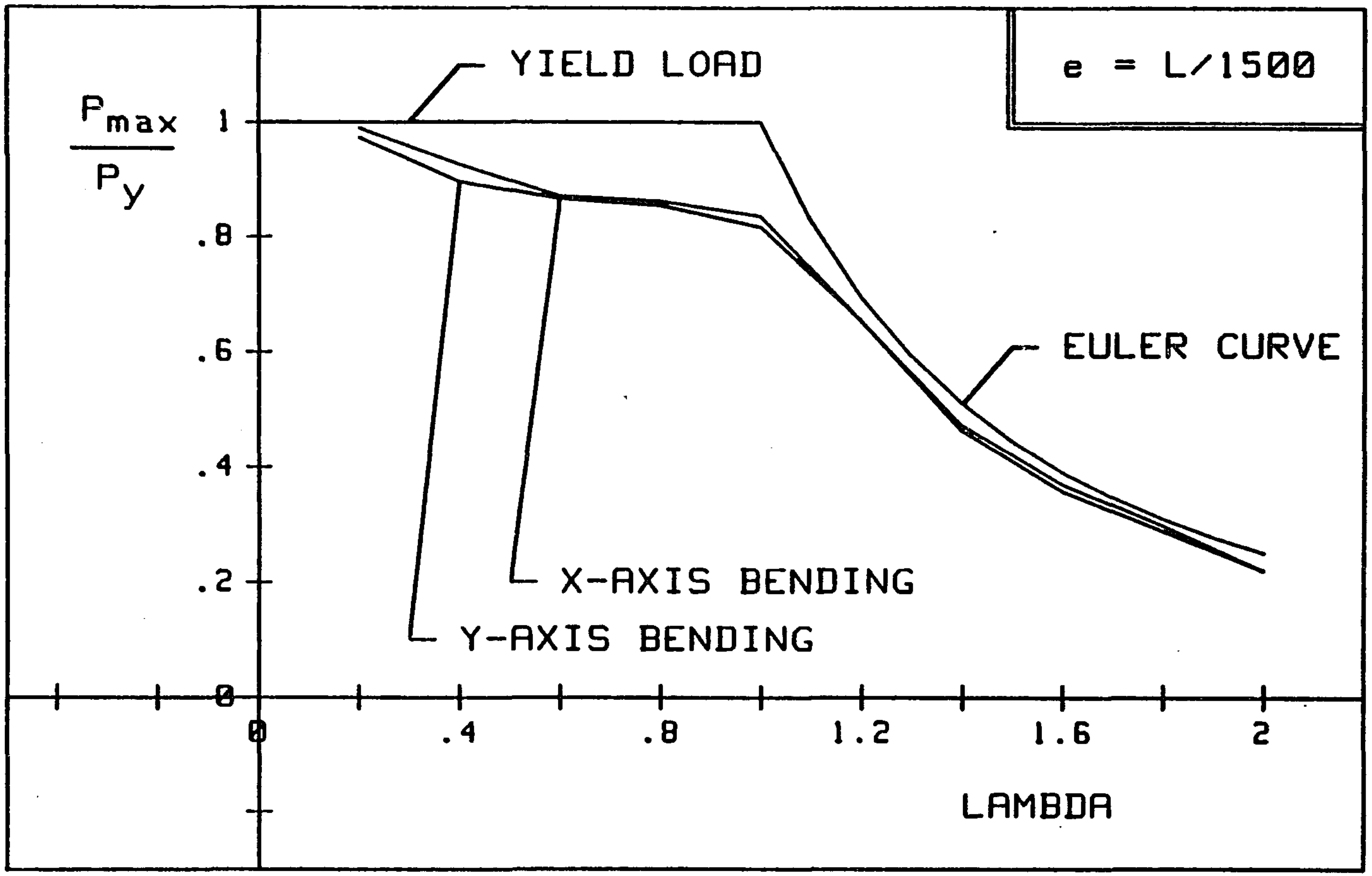

Fig. 6.89. x- and y-axis maximum strength column curves for shape H 14 x 15 (50 ksi steel, 100 ksi electrodes).

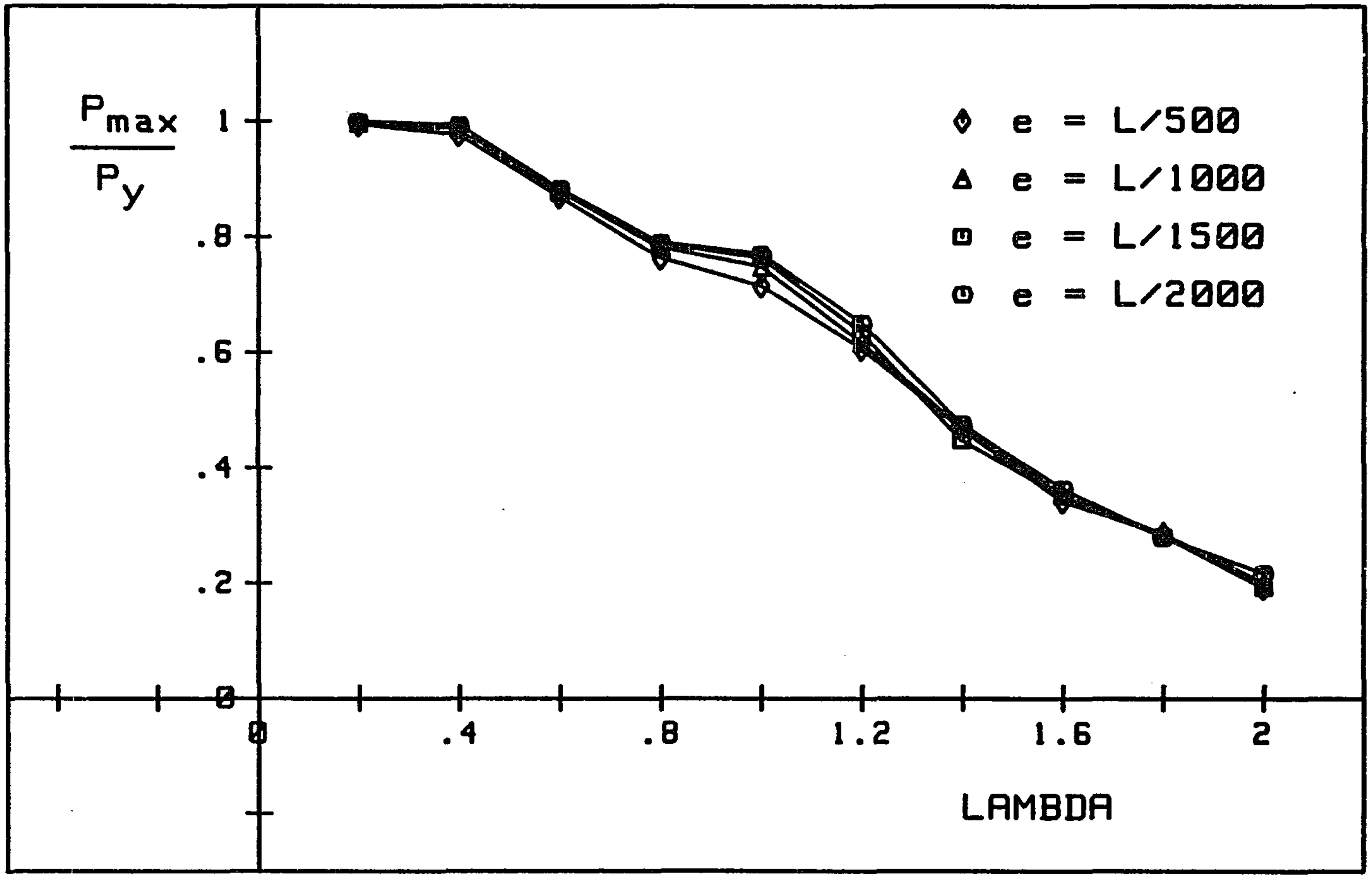

Fig. 6.90. Maximum strength column curves for shape H 20 x 354 (36 ksi steel, 70 ksi electrodes) and x-axis bending.

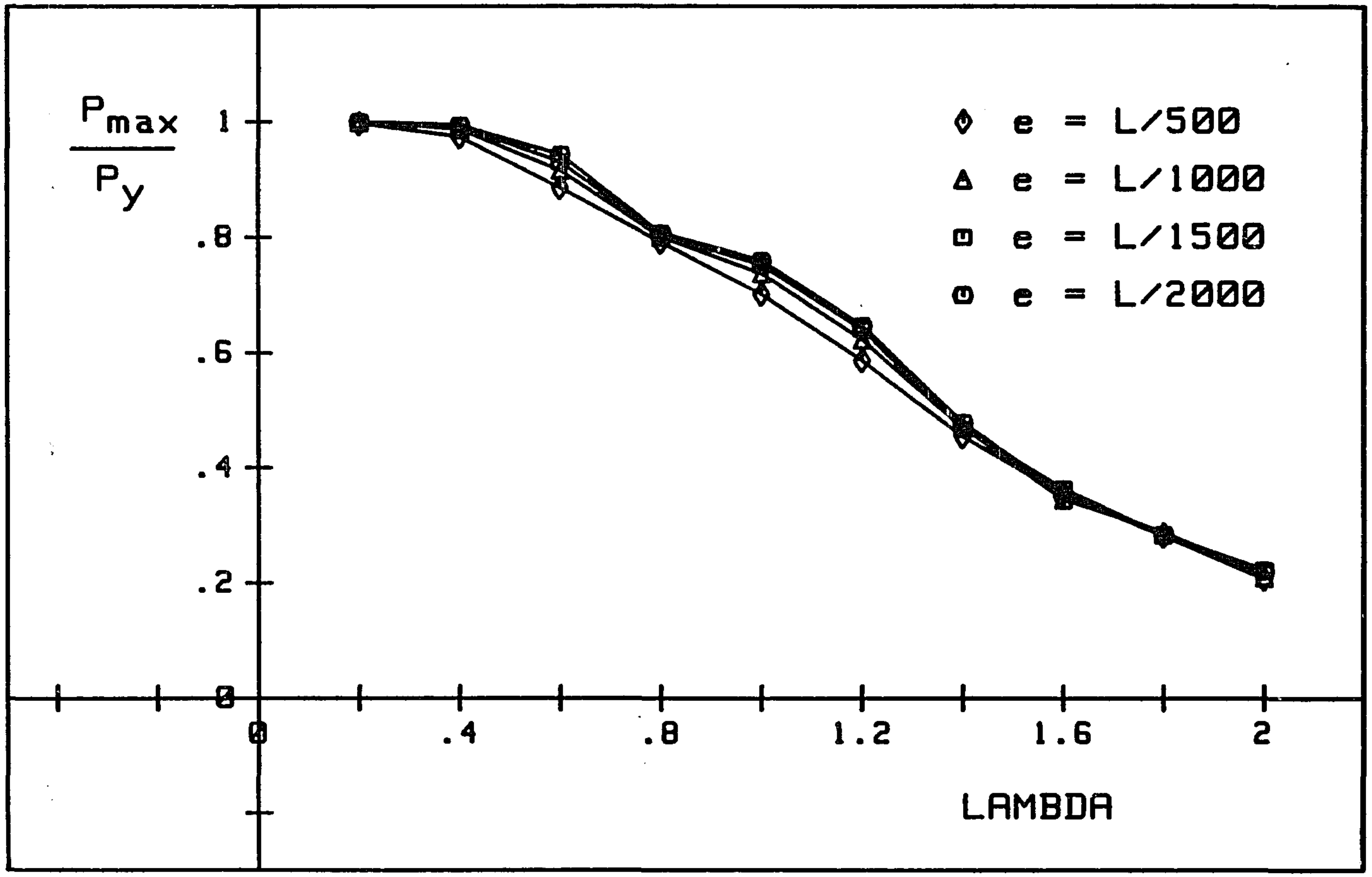

Fig. 6.91. Maximum strength column curves for shape H 20 x 354 (36 ksi steel, 70ksi electrodes) and y-axis bending.

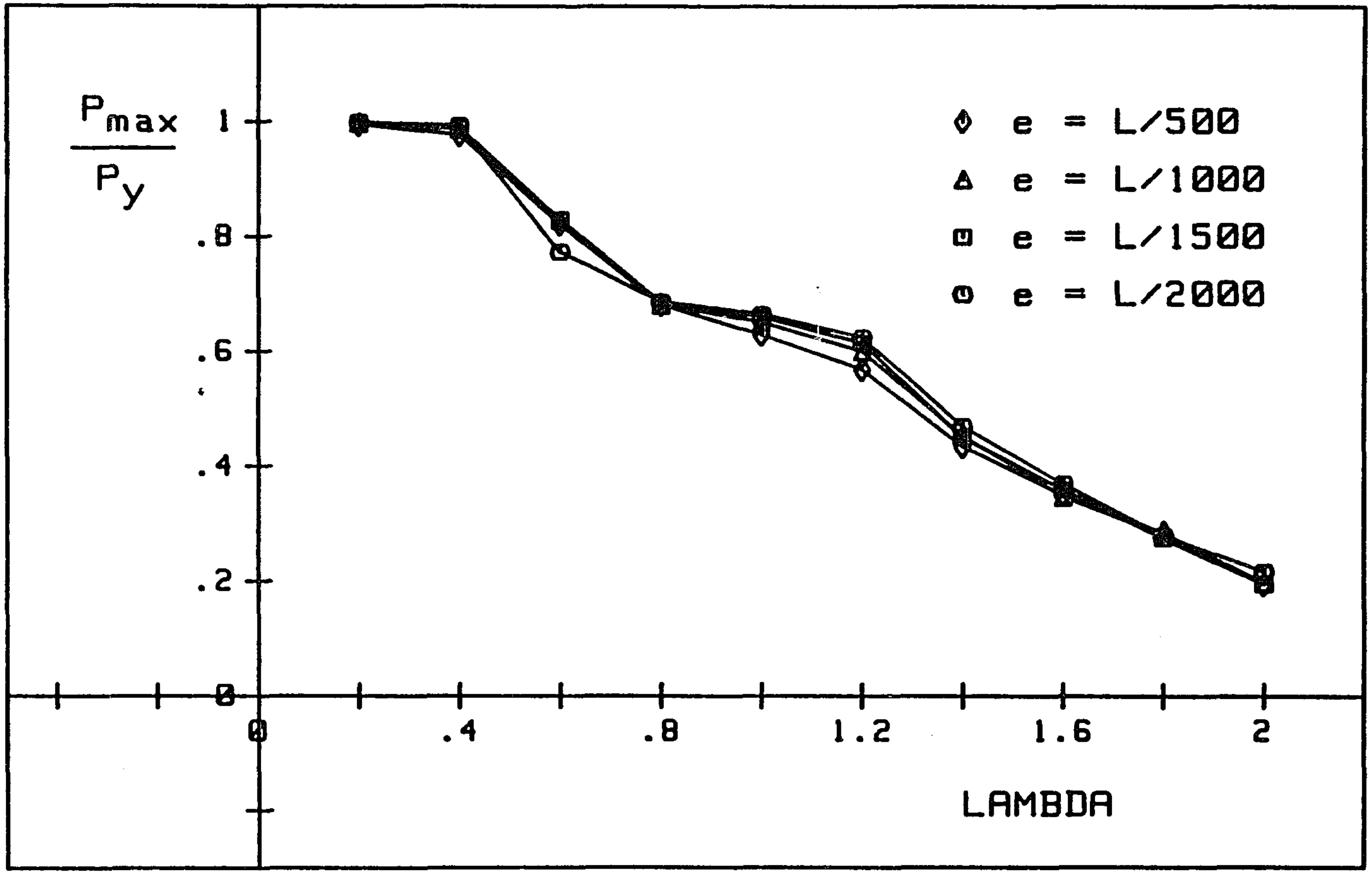

Fig. 6.92. Maximum strength column curves for shape H 20 x 354 (36 ksi steel, 100 ksi electrodes) and x-axis bending.

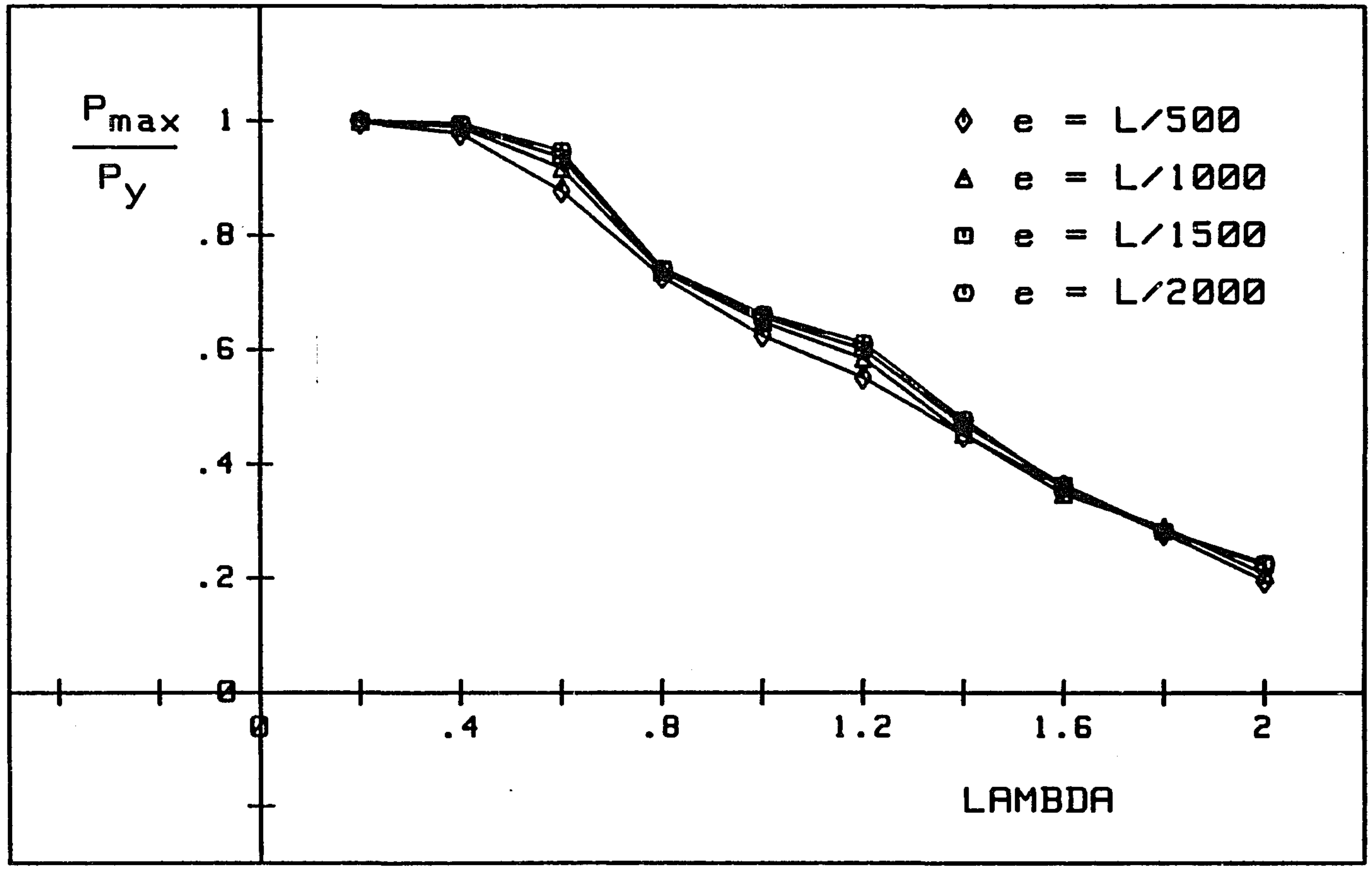

Fig. 6.93. Maximum strength column curves for shape H 20 x 354 (36 ksi steel, 100 ksi electrodes) and y-axis bending.

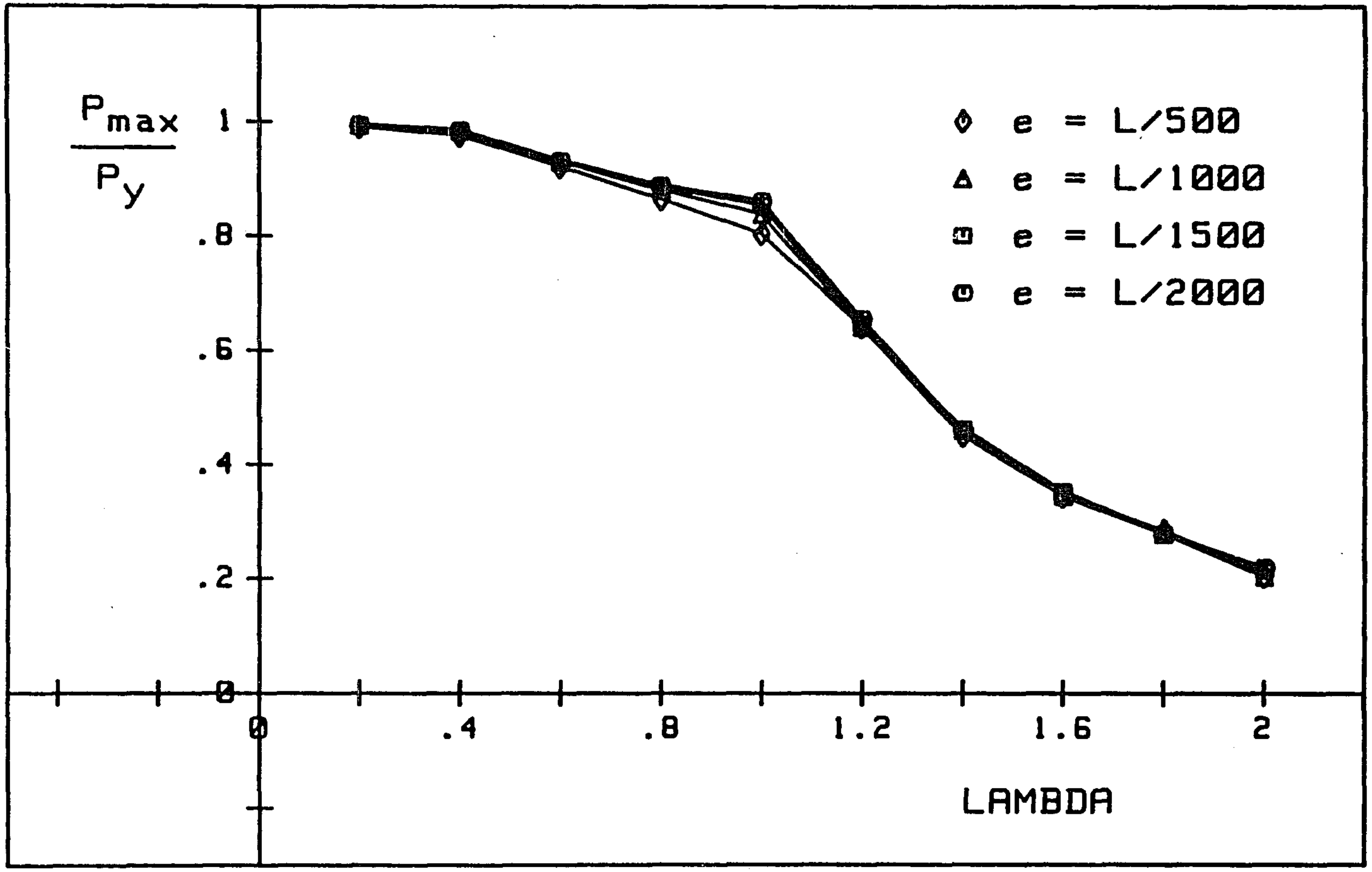

Fig. 6.94. Maximum strength column curves for shape H 20 x 354 (50 ksi steel, 70 ksi electrodes) and x-axis bending.

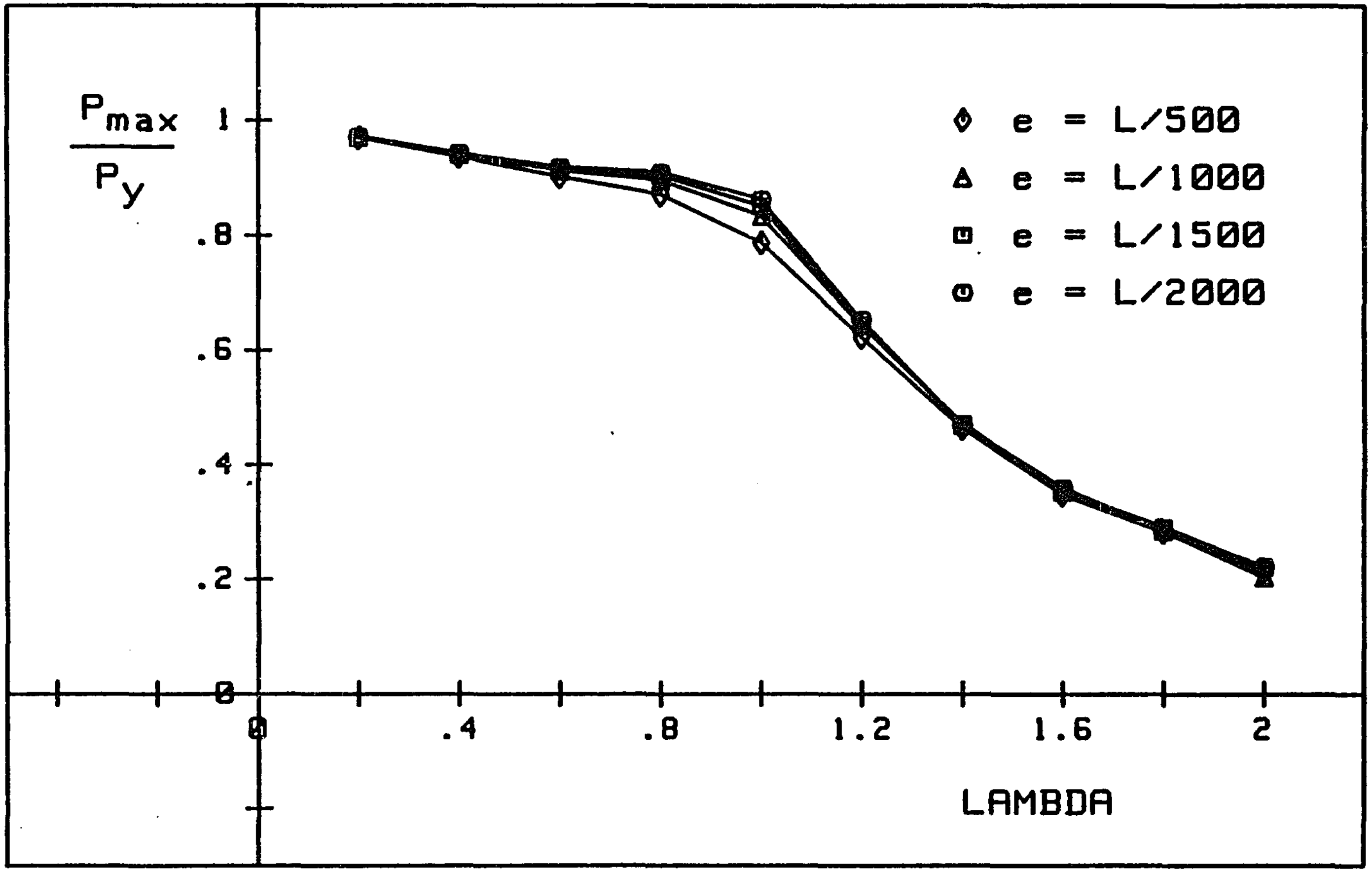

Fig. 6.95. Maximum strength column curves for shape H 20 x 354 (50 ksi steel, 70ksi electrodes) and y-axis bending.

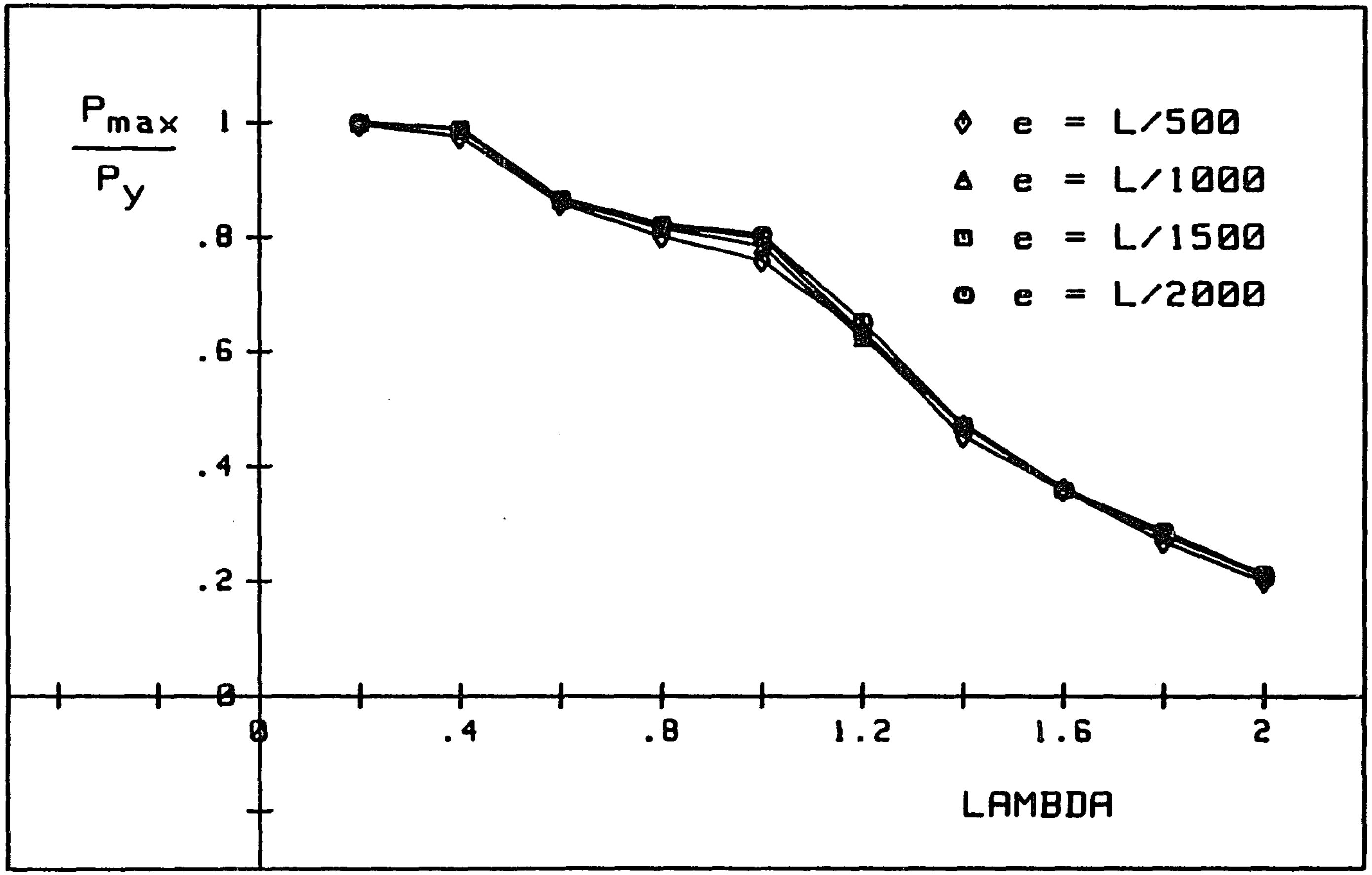

Fig. 6.96. Maximum strength column curves for shape H 20 x 354 (50 ksi steel, 100 ksi electrodes) and x-axis bending.

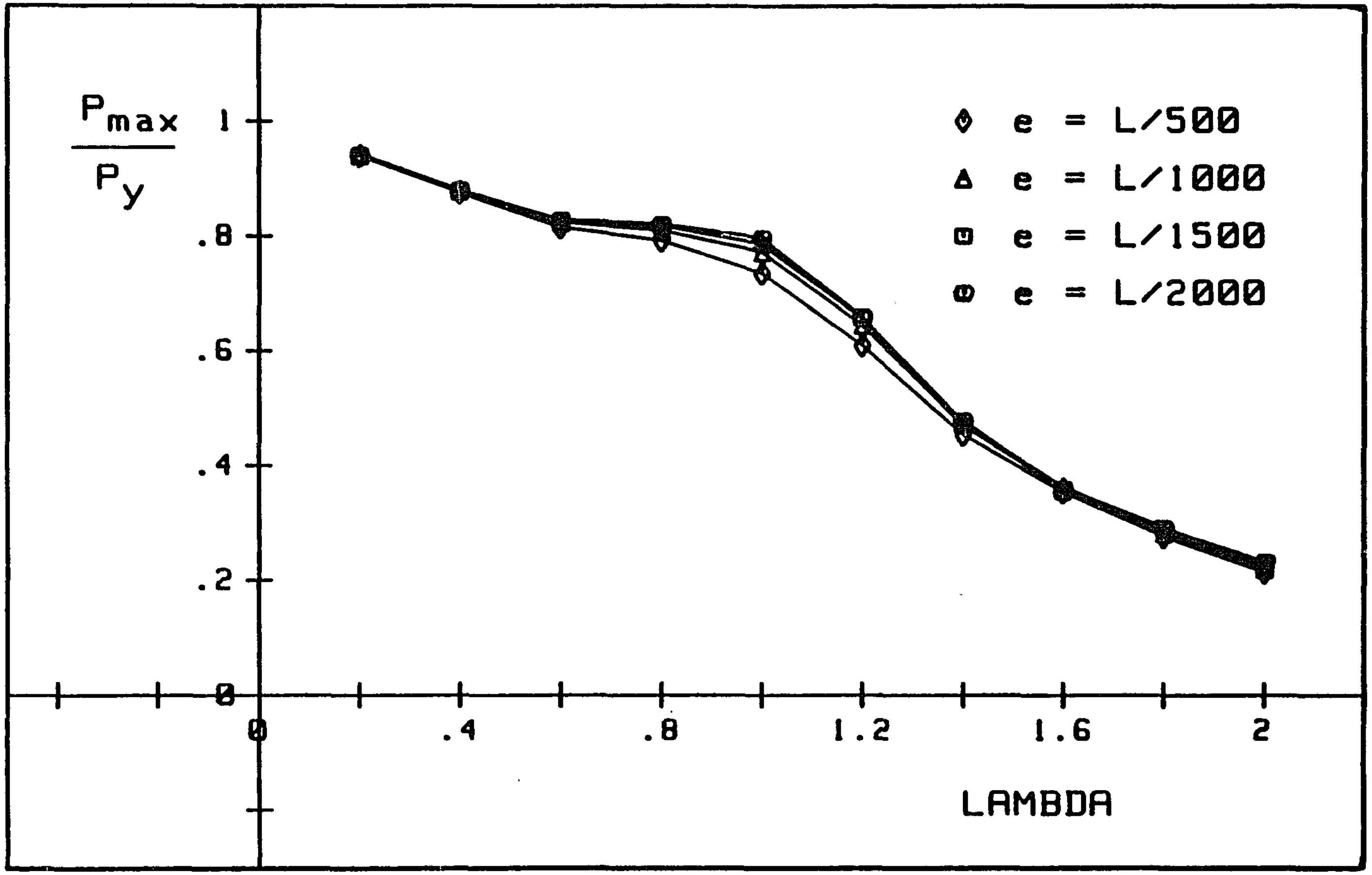

Fig. 6.97. Maximum strength column curves for shape H 20 x 354 (50 ksi steel, 100 ksi electrodes) and y-axis bending.

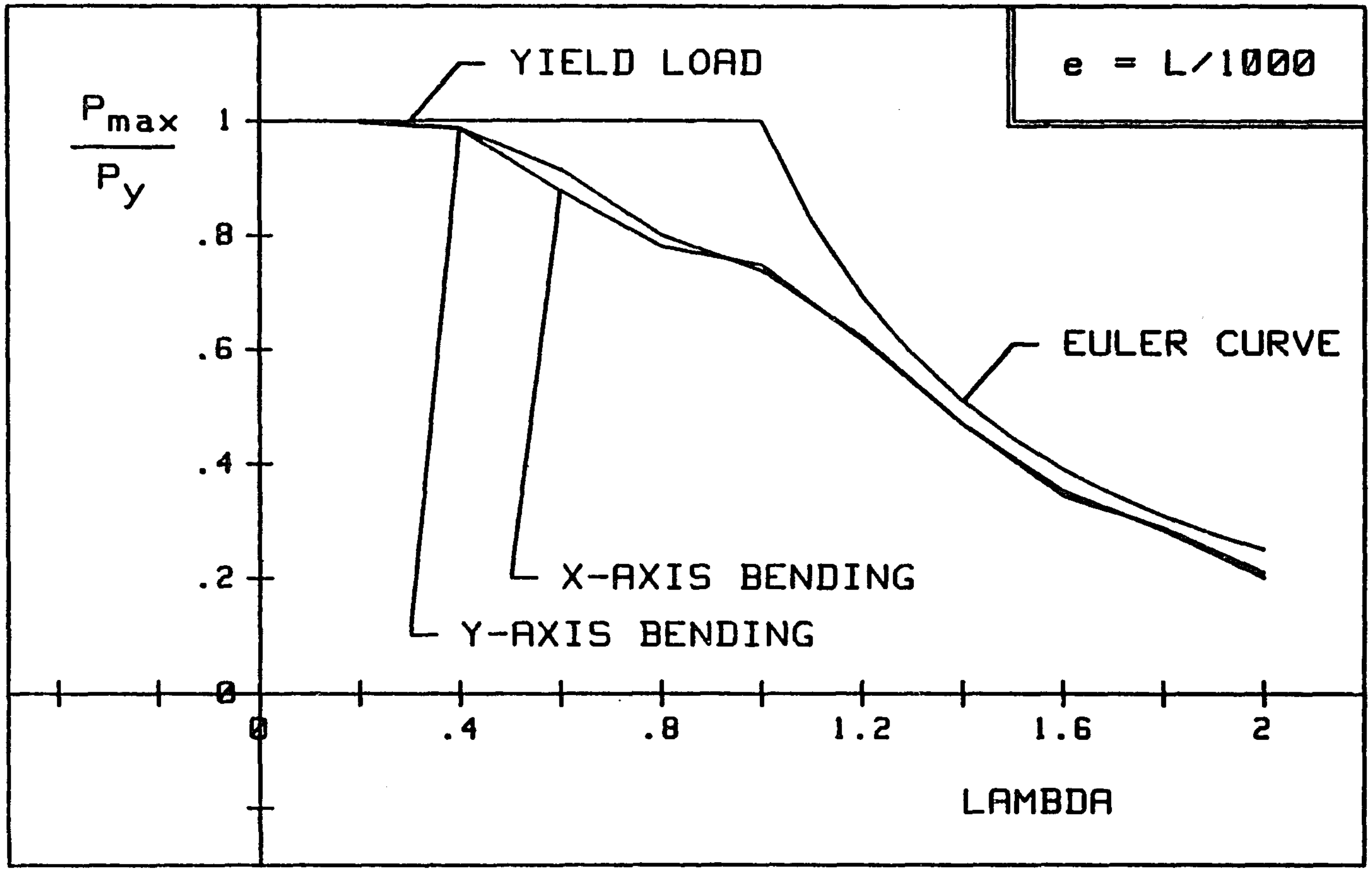

Fig. 6.98. x- and y-axis maximum strength column curves for shape H 20 x 354 (36 ksi steel, 70 ksi electrodes).

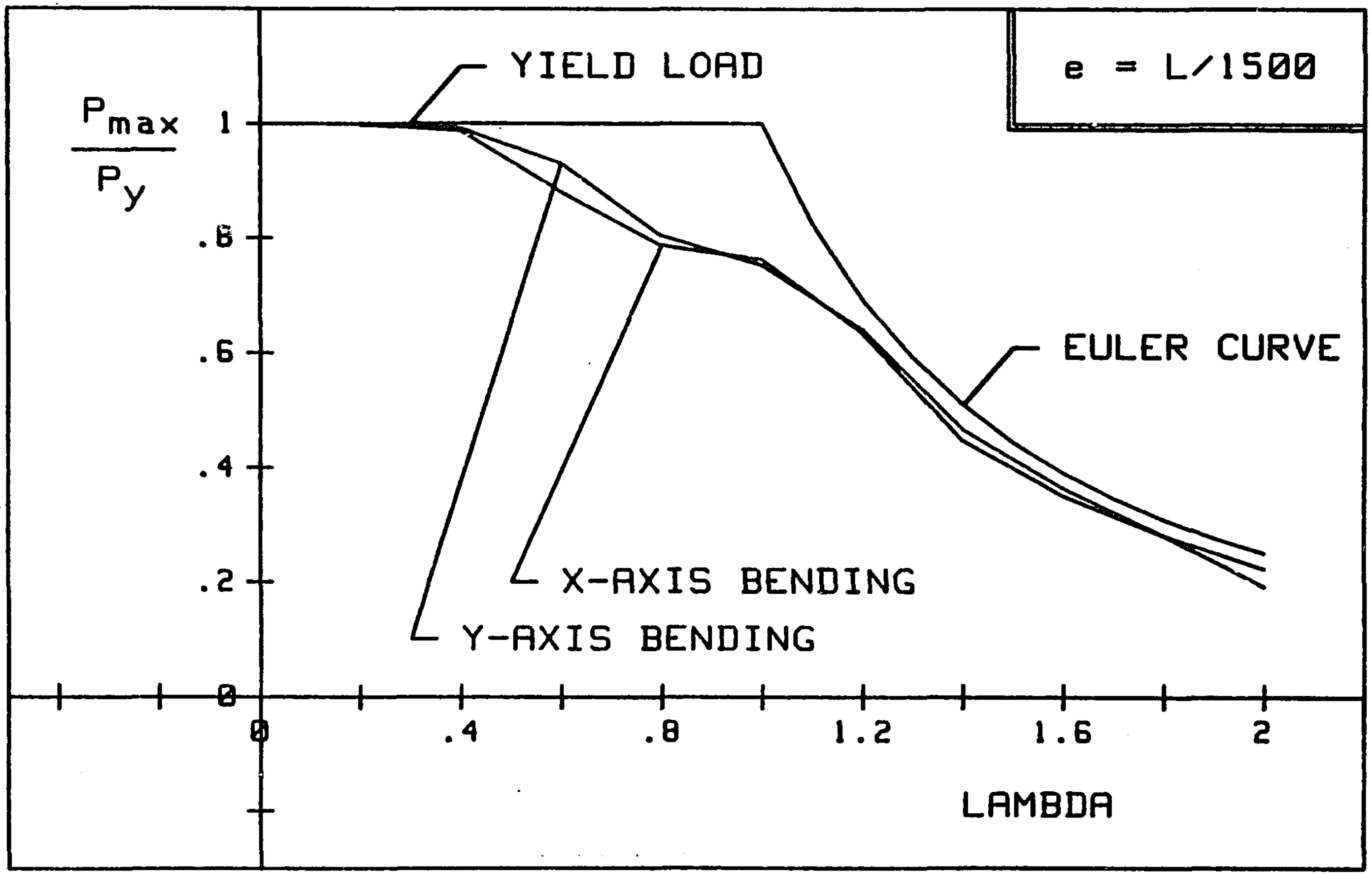

Fig. 6.99. x- and y-axis maximum strength column curves for shape H 20 x 354 (36 ksi steel, 70 ksi electrodes).

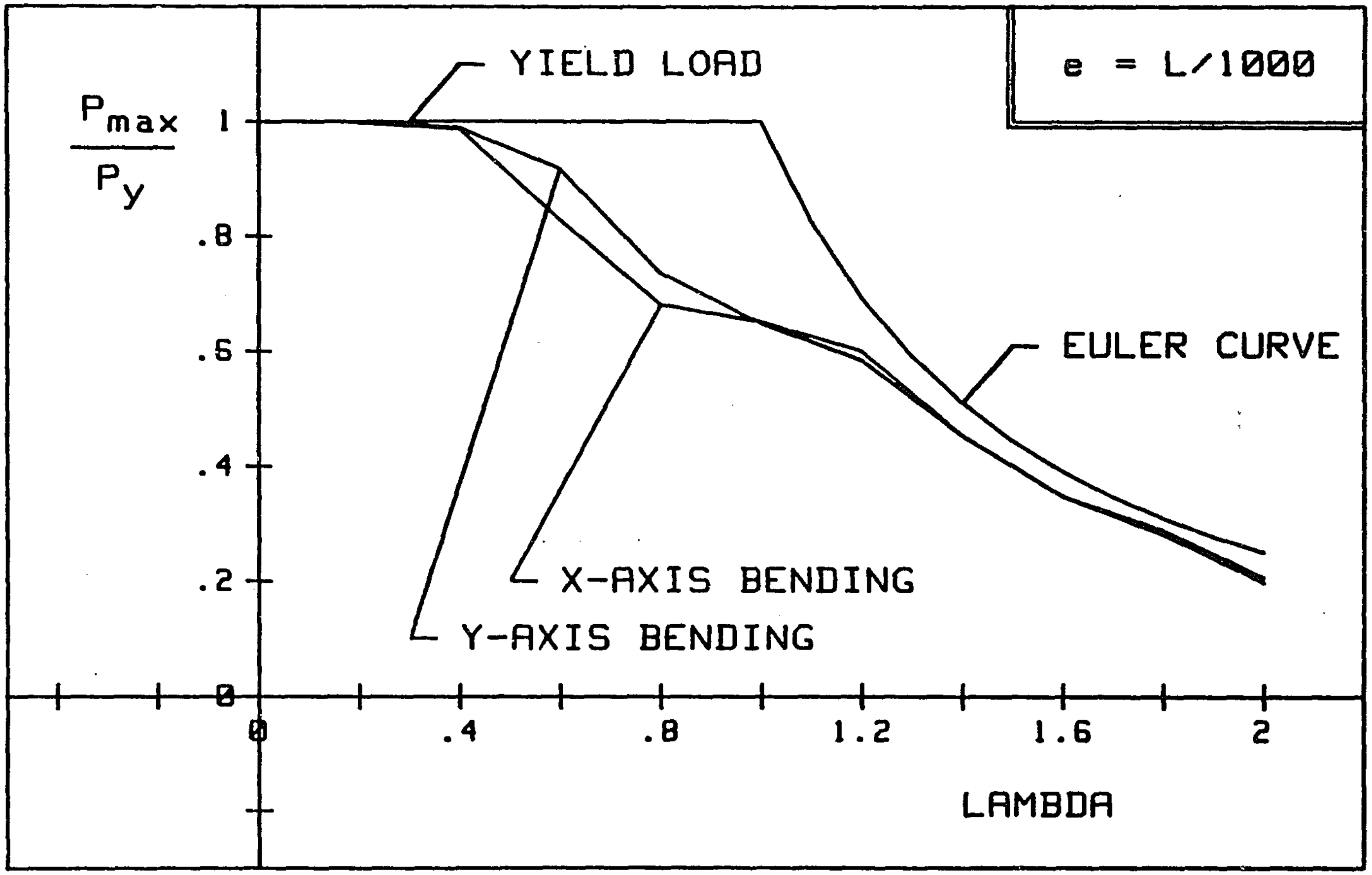

Fig. 6.100. x- and y-axis maximum strength column curves for shape H 20 x 354 (36 ksi steel, 100 ksi electrodes).

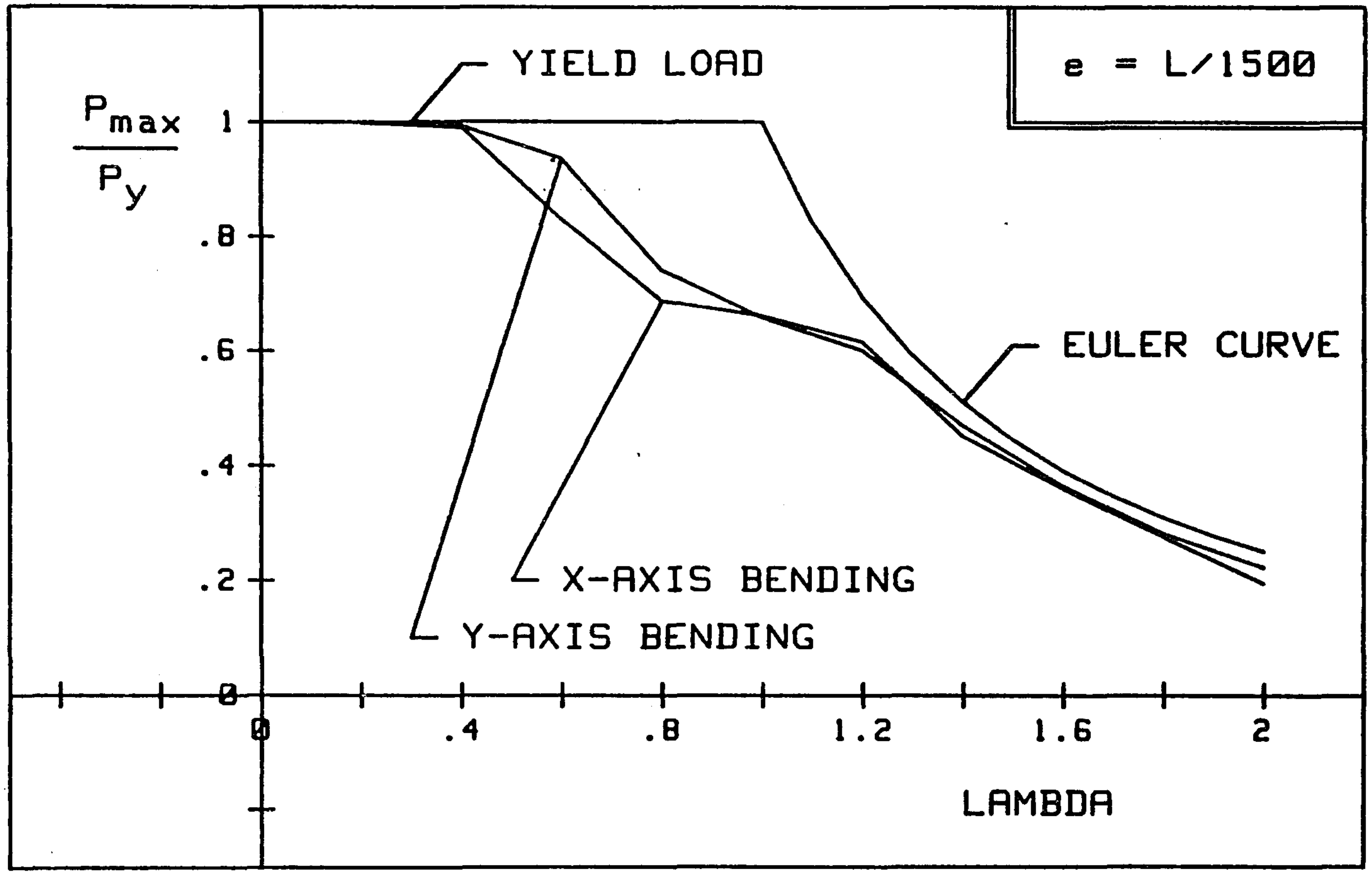

Fig. 6.101. x- and y-axis maximum strength column curves for shape H 20 x 354 (36 ksi steel, 100 ksi electrodes).

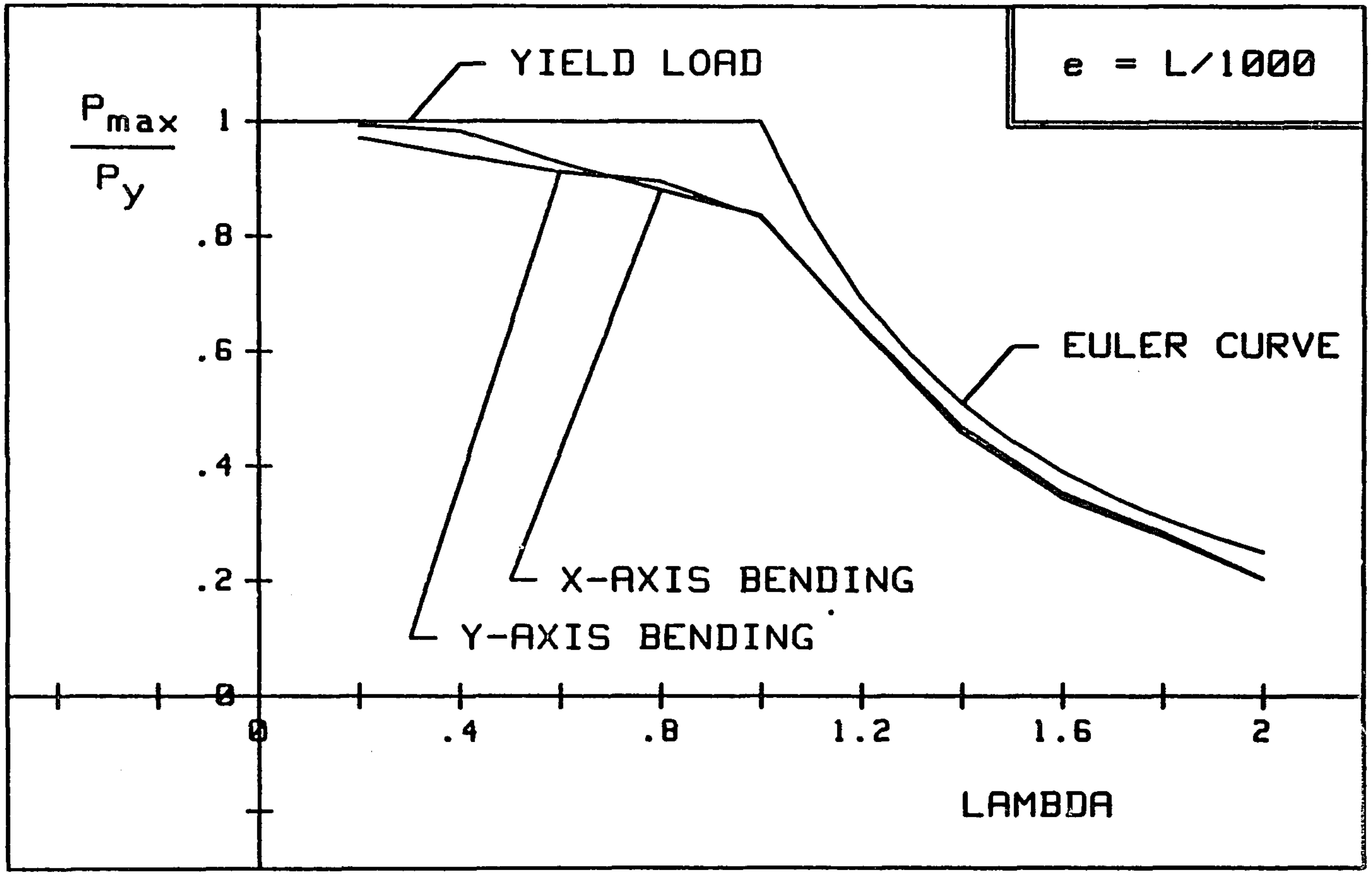

Fig. 6.102. x- and y-axis maximum strength column curves for shape H 20 x 354 (50 ksi steel, 70 ksi electrodes).

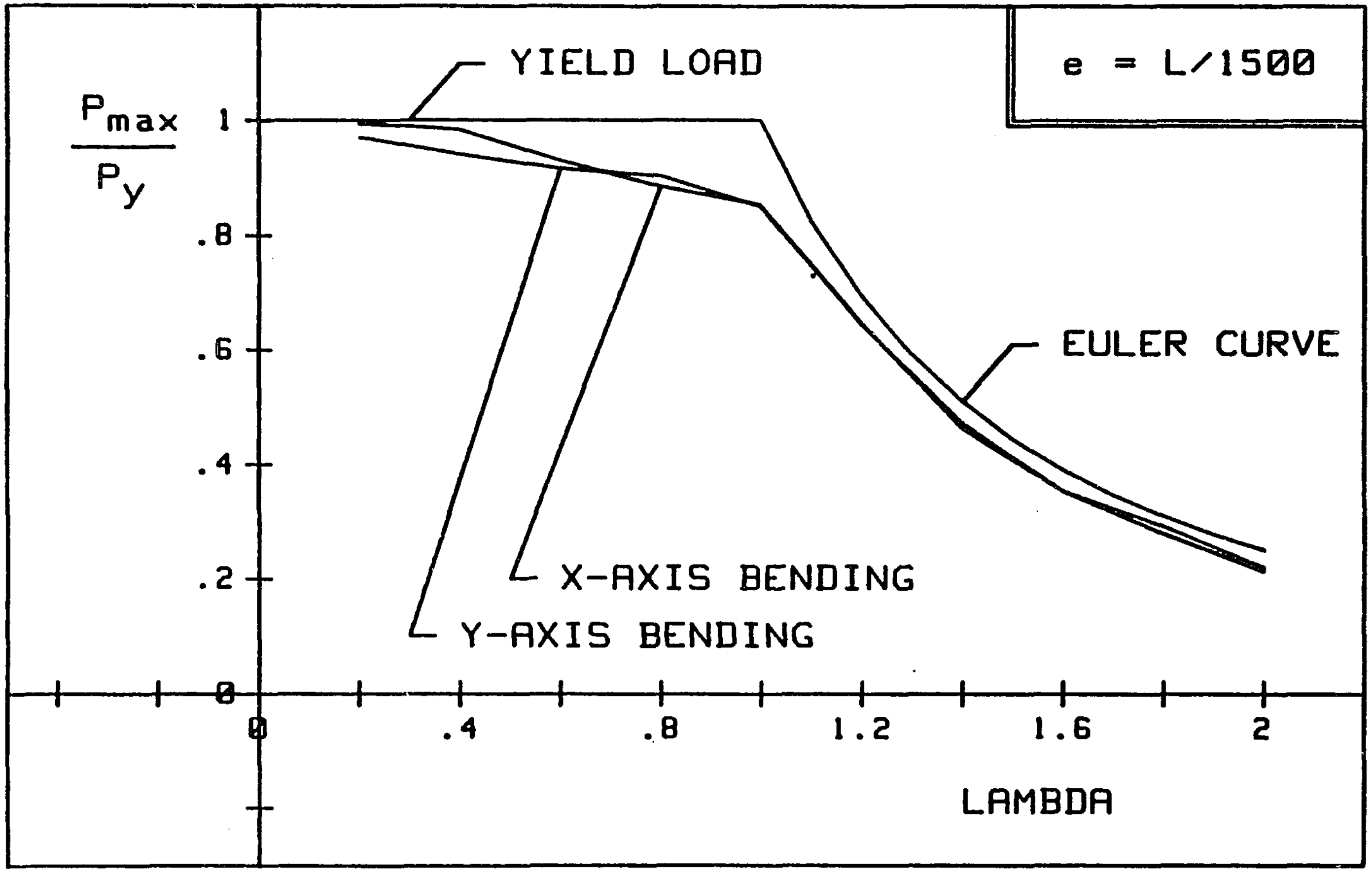

Fig. 6.103. x- and y-axis maximum strength column curves for shape H 20 x 354 (50 ksi steel, 70 ksi electrodes).

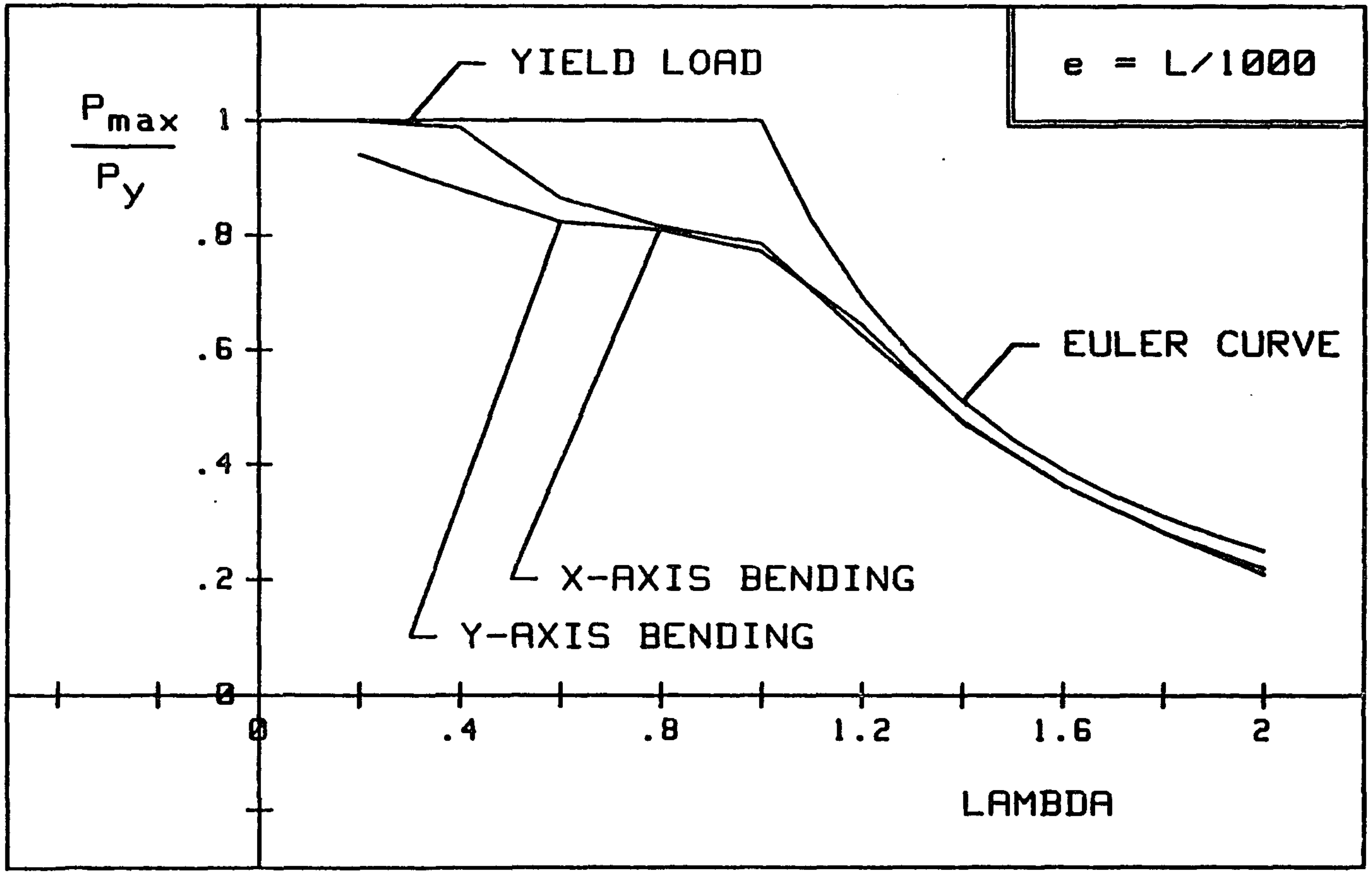

Fig. 6.104. x- and y-axis maximum strength column curves for shape H 20 x 354 (50 ksi steel, 100 ksi electrodes).

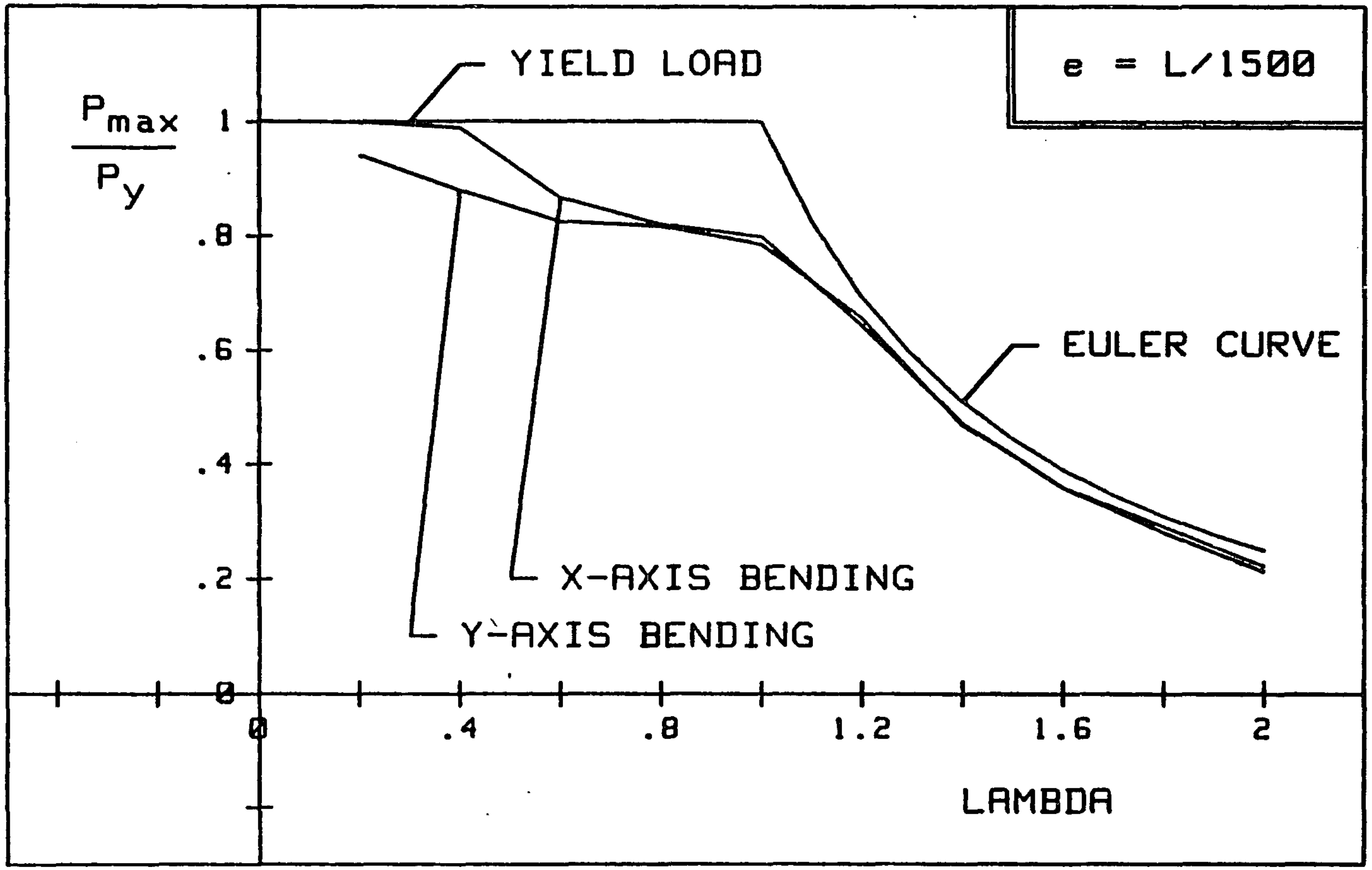

Fig. 6.105. x- and y-axis maximum strength column curves for shape H 20 x 354 (50 ksi steel, 100 ksi electrodes).

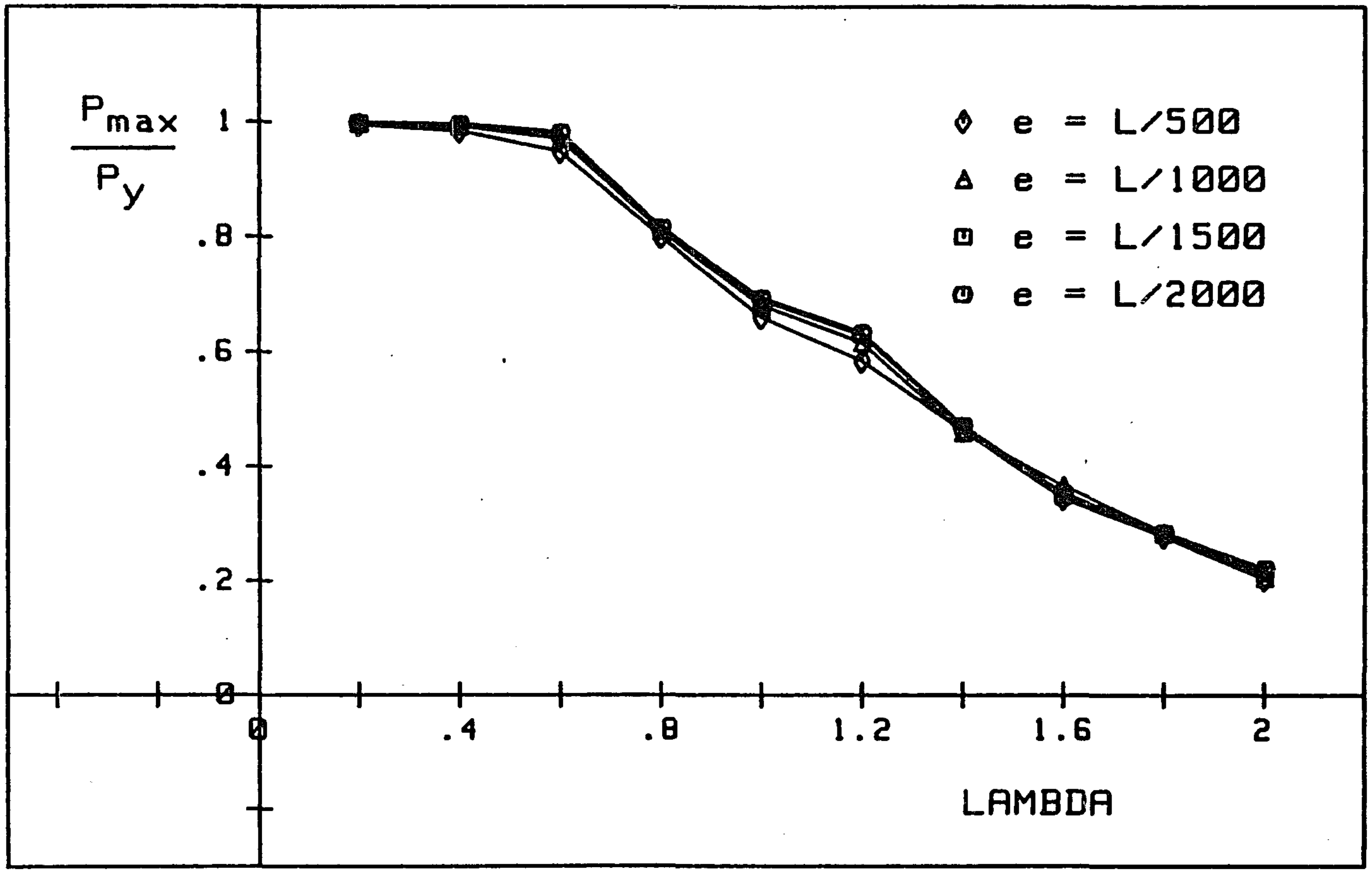

Fig. 6.106. Maximum strength column curves for shape H 24 x 428 (36 ksi steel, 70 ksi electrodes) x-axis bending.

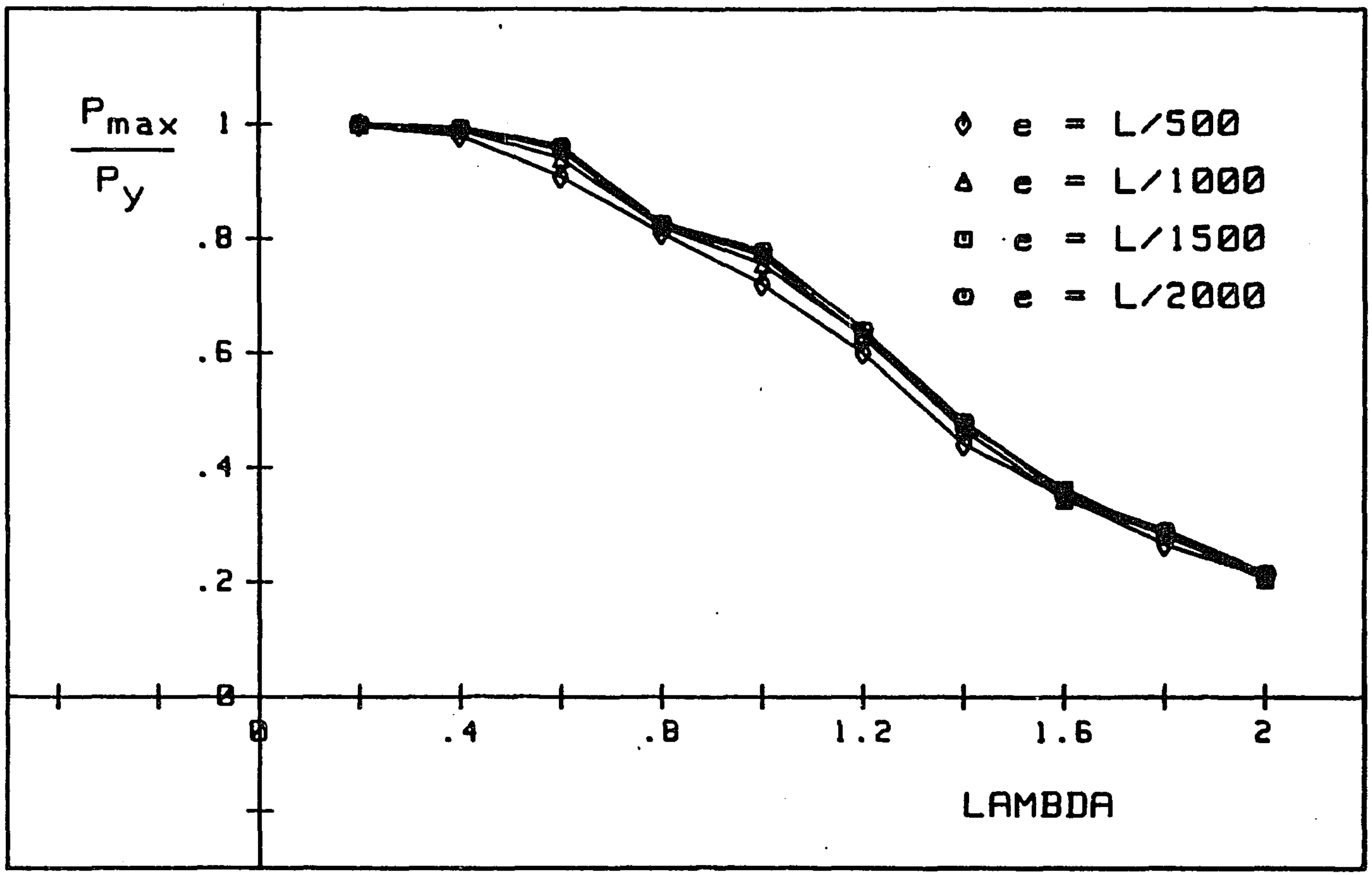

Fig. 6.107. Maximum strength column curves for shape H 24 x 428 (36 ksi steel, 70 ksi electrodes) and y-axis bending.

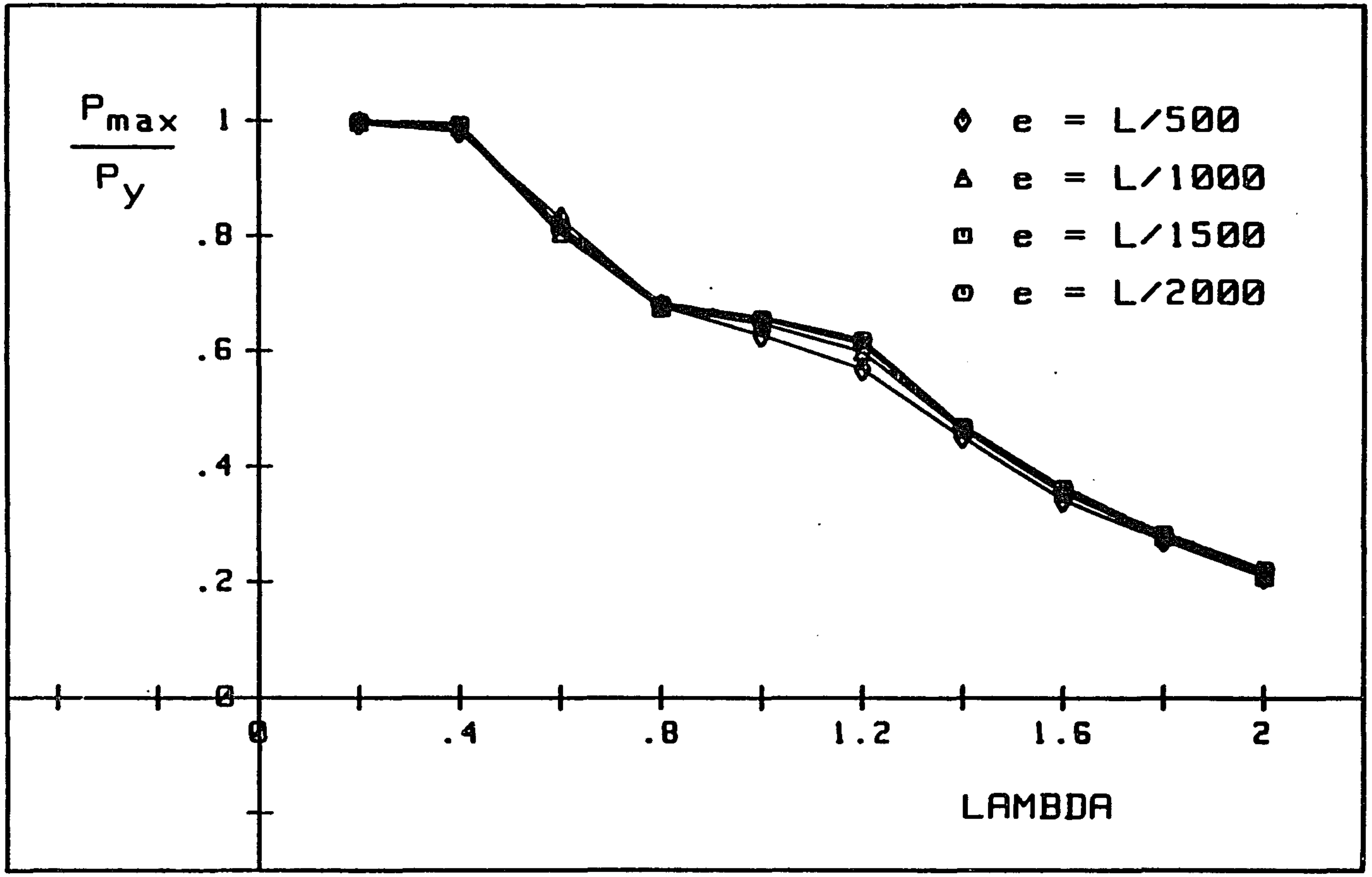

Fig. 6.108. Maximum strength column curves for shape H 24 x 428 (36 ksi steel, 100 ksi electrodes) and x-axis bending.

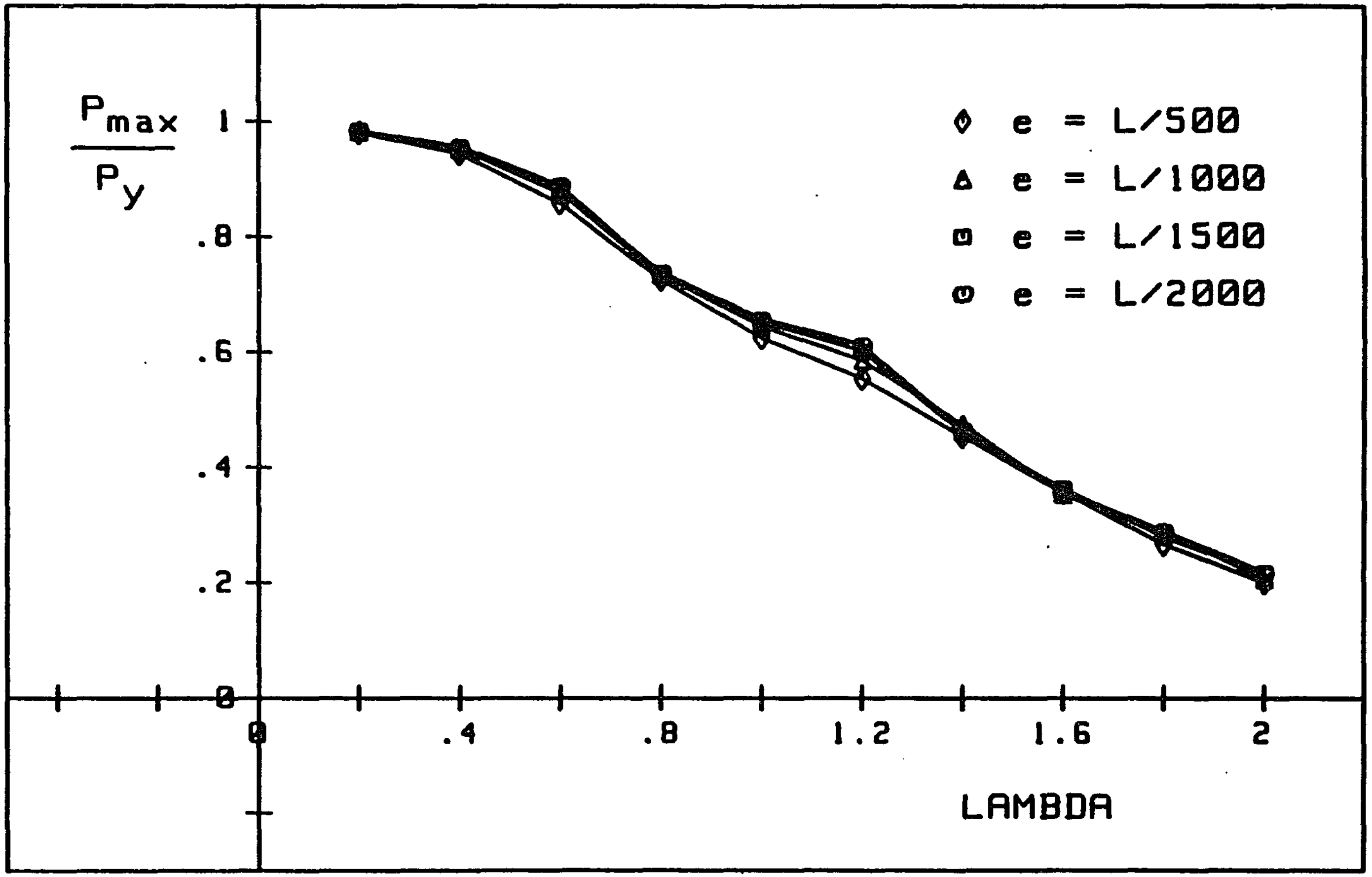

Fig. 6.109. Maximum strength column curves for shape H 24 x 428 (36 ksi steel, 100 ksi electrodes) and y-axis bending.

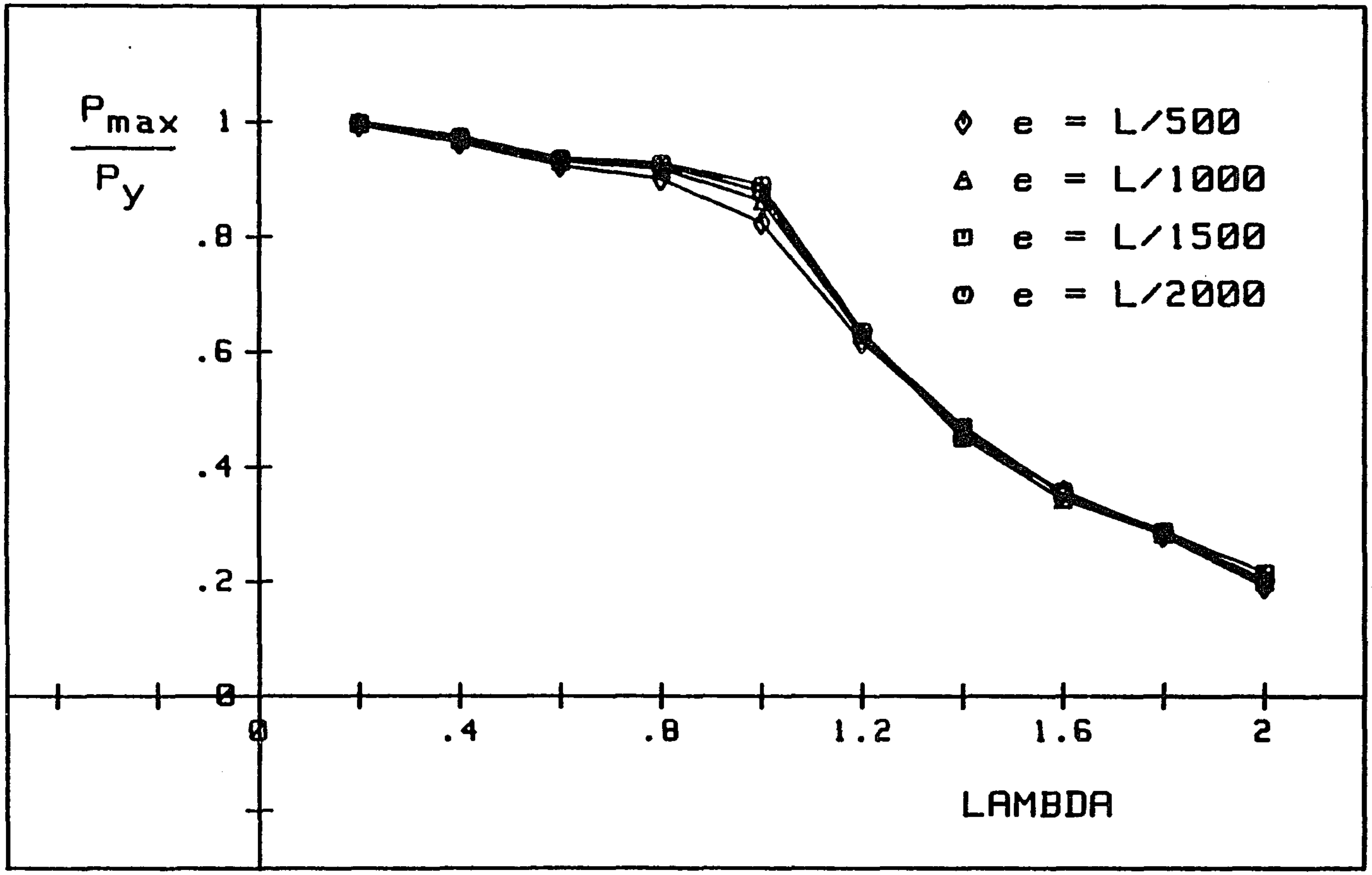

Fig. 6.110. Maximum strength column curves for shape H 24 x 428 (50 ksi steel, 70 ksi electrodes) and x-axis bending.

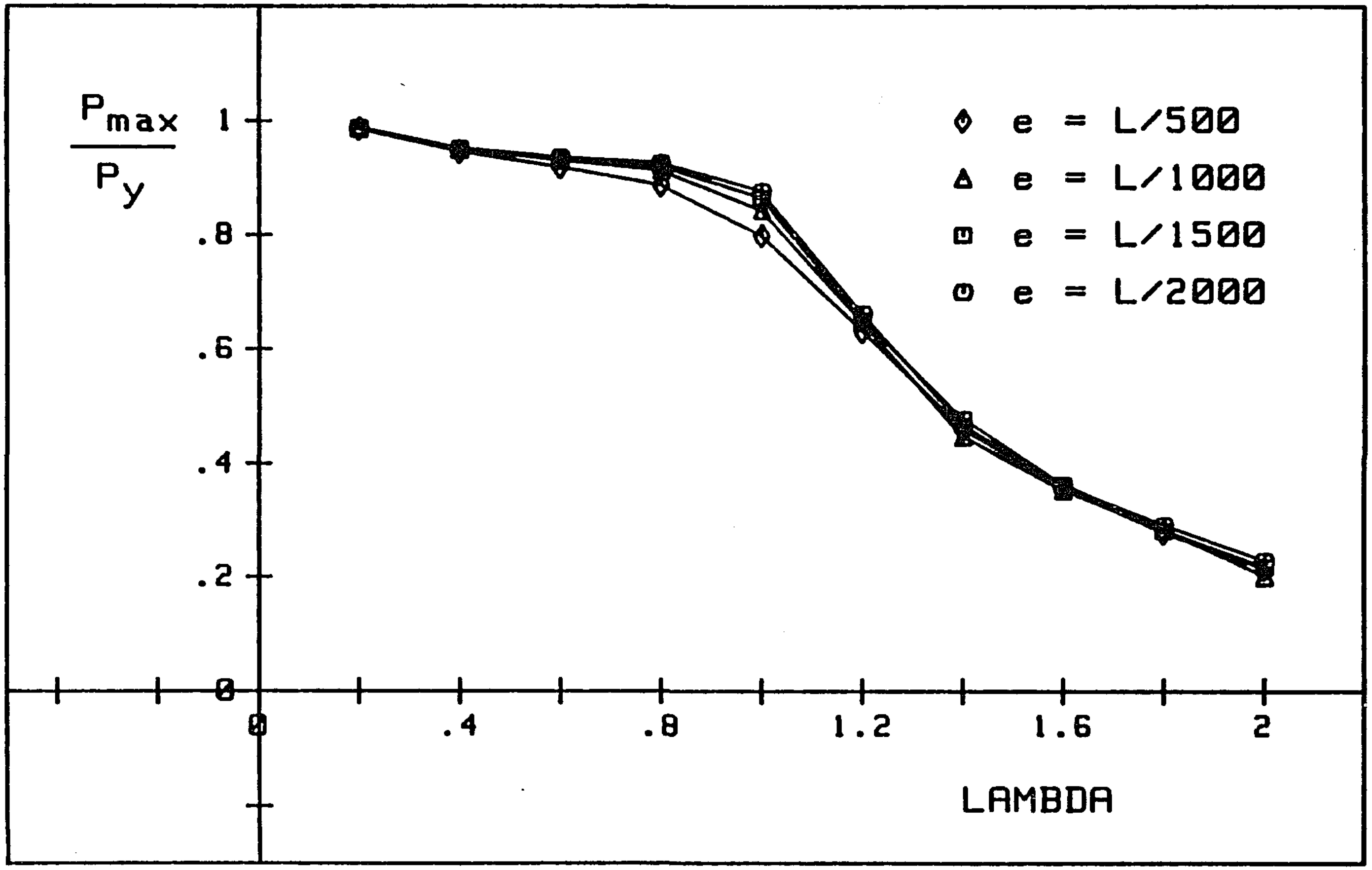

Fig. 6.111. Maximum strength column curves for shape H 24 x 428 (50 ksi steel, 70 ksi electrodes) and y-axis bending.

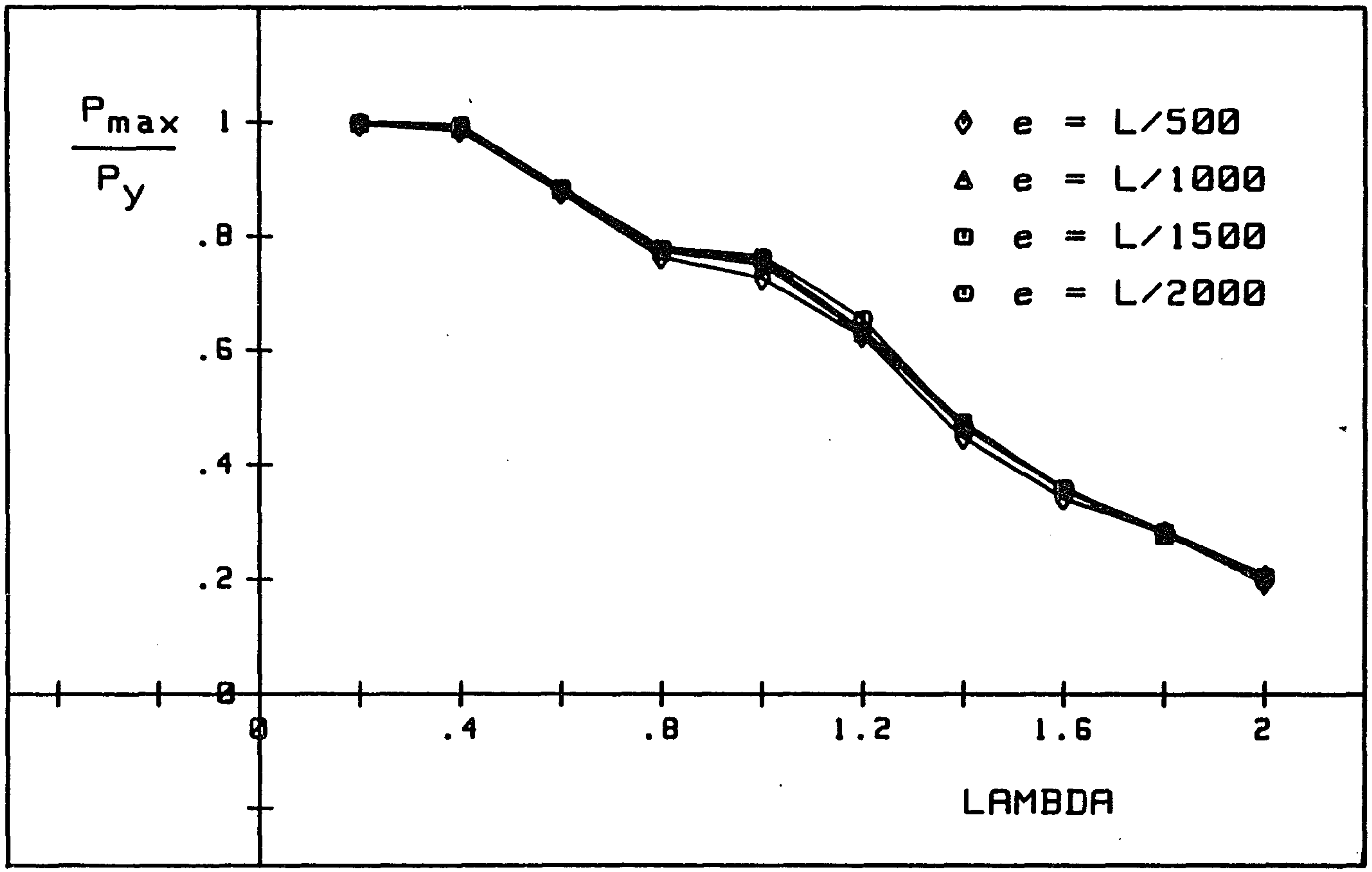

Fig. 6.112. Maximum strength column curves for shape H 24 x 428 (50 ksi steel, 100 ksi electrodes) and x-axis bending.

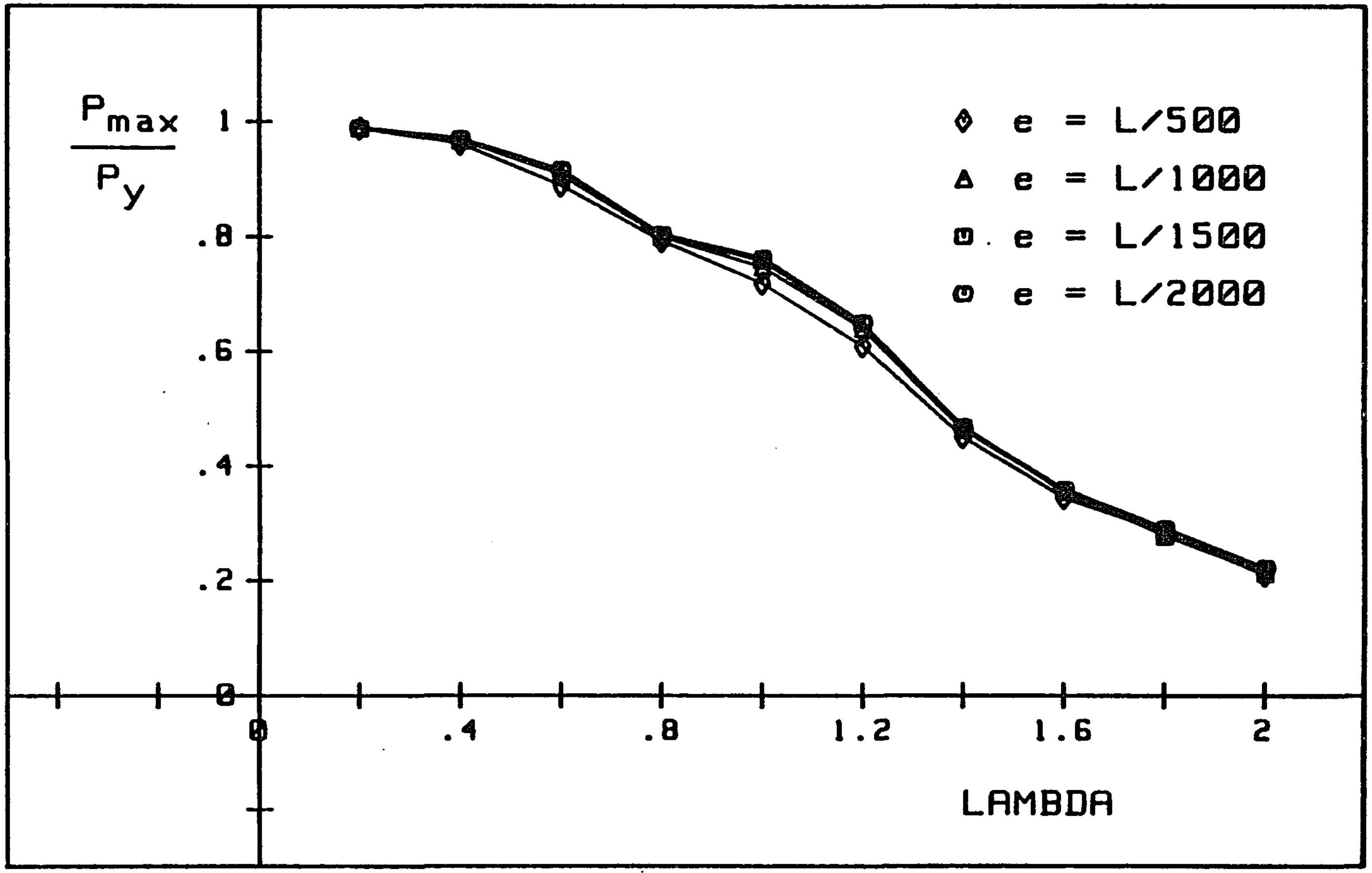

Fig. 6.113. Maximum strength column curves for shape H 24 x 428 (50 ksi steel, 100 ksi electrodes) and y-axis bending.

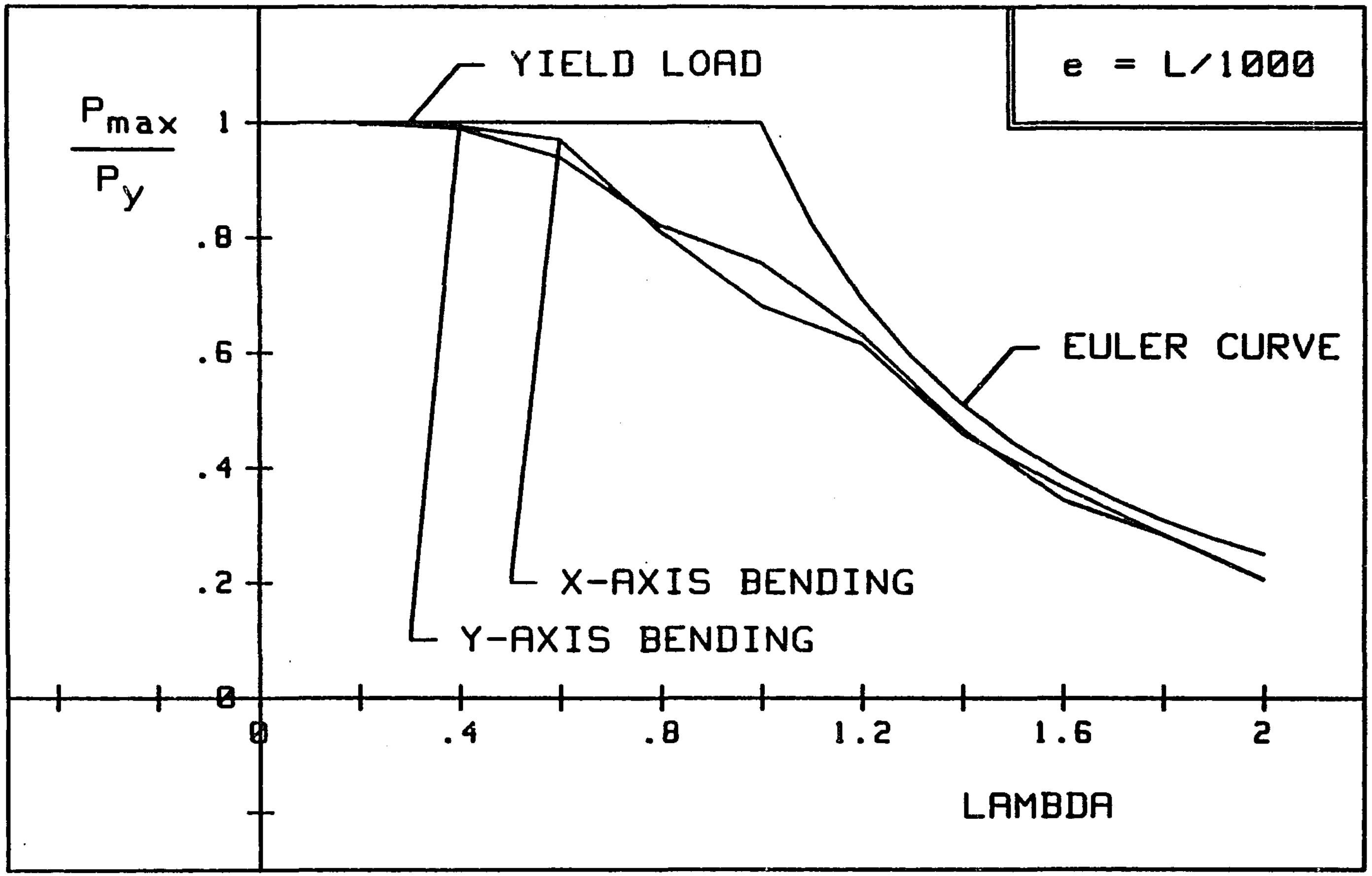

Fig. 6.114. x- and y-axis maximum strength column curves for shape H 24 x 428 (36 ksi steel, 70 ksi electrodes).

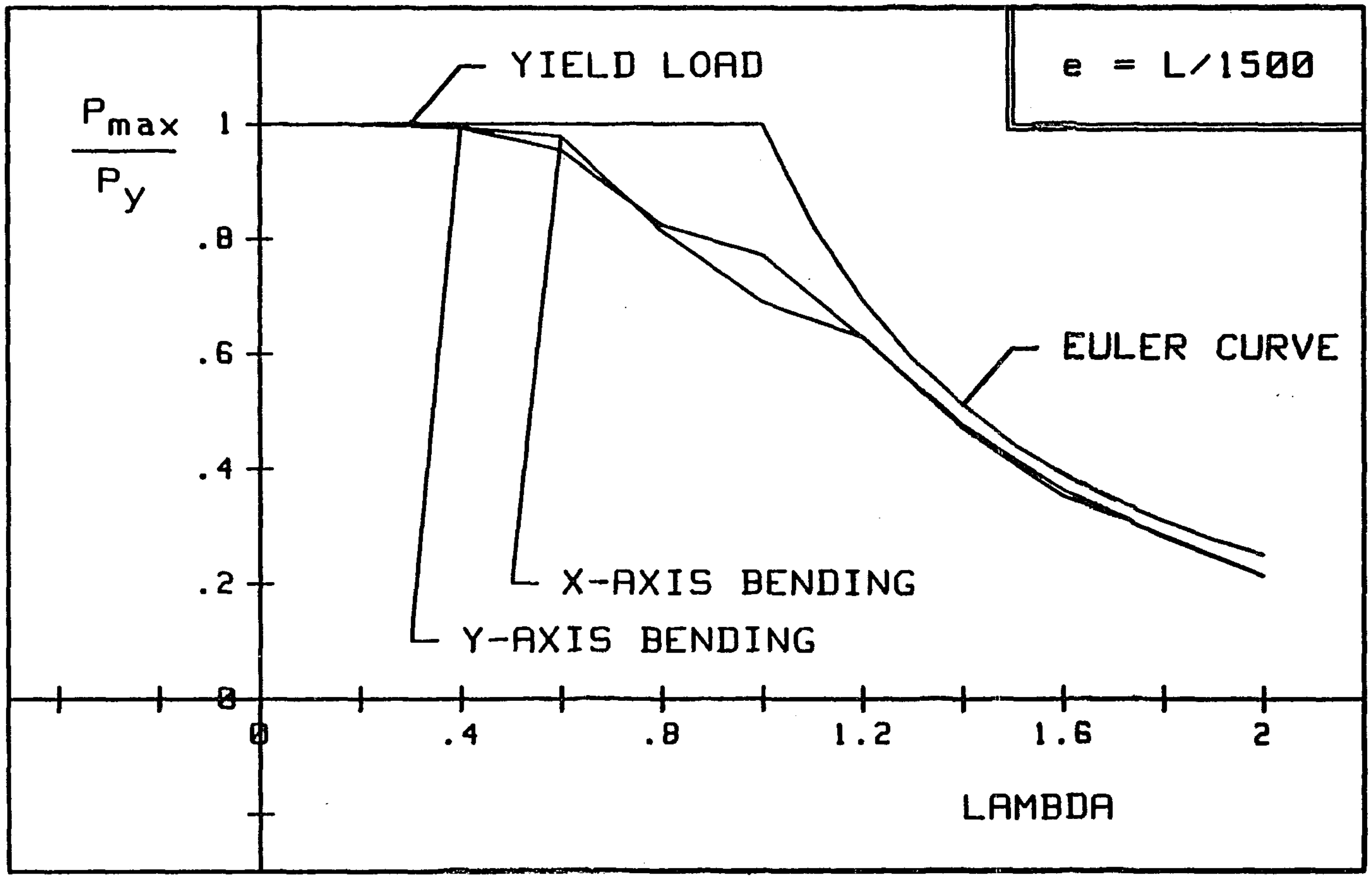

Fig. 6.115. x- and y-axis maximum strength column curves for shape H 24 x 428 (36 ksi steel, 70 ksi electrodes).

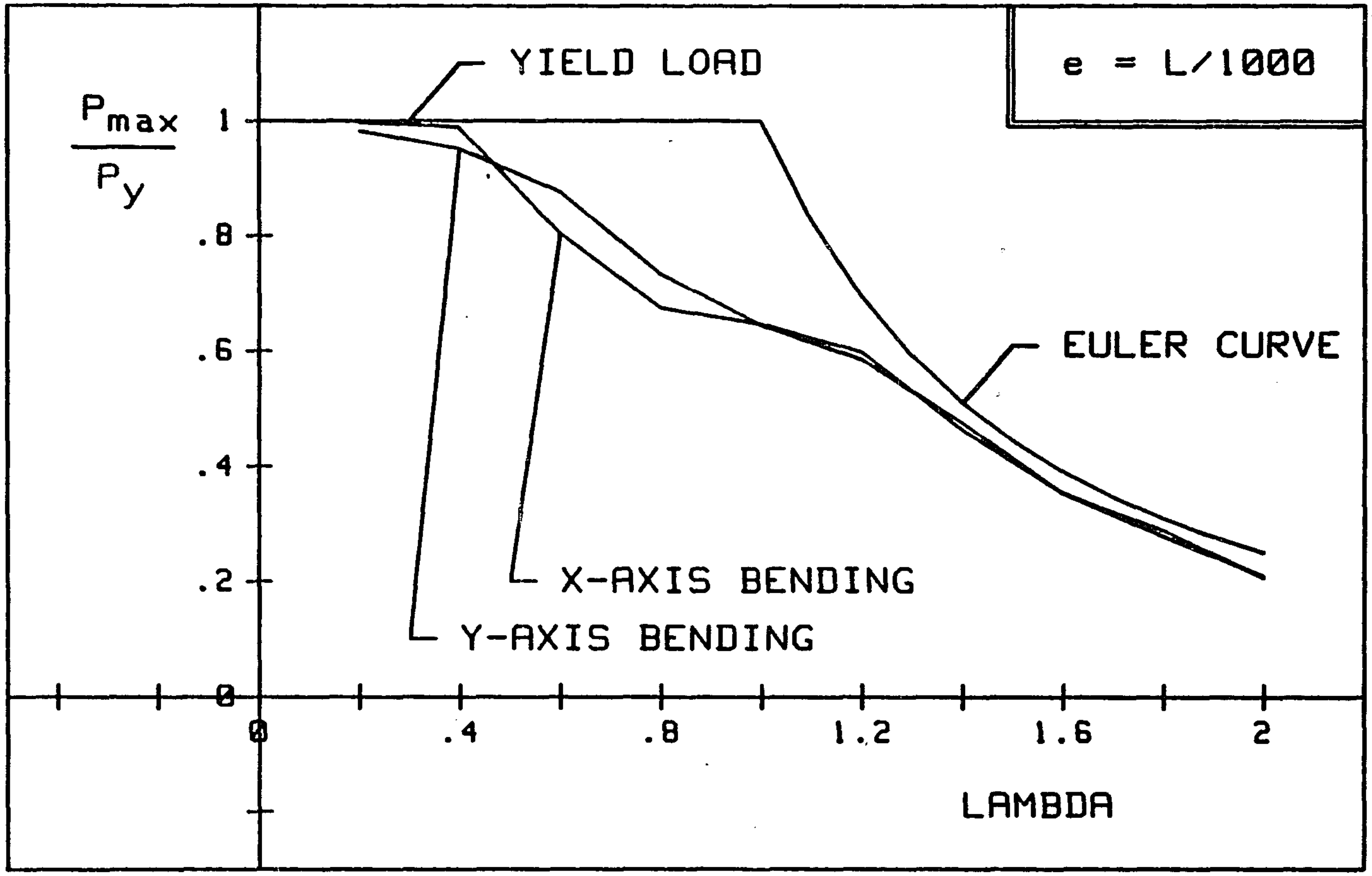

Fig. 6.116. x- and y-axis maximum strength column curves for shape H 24 x 428 (36 ksi steel, 100 ksi electrodes).

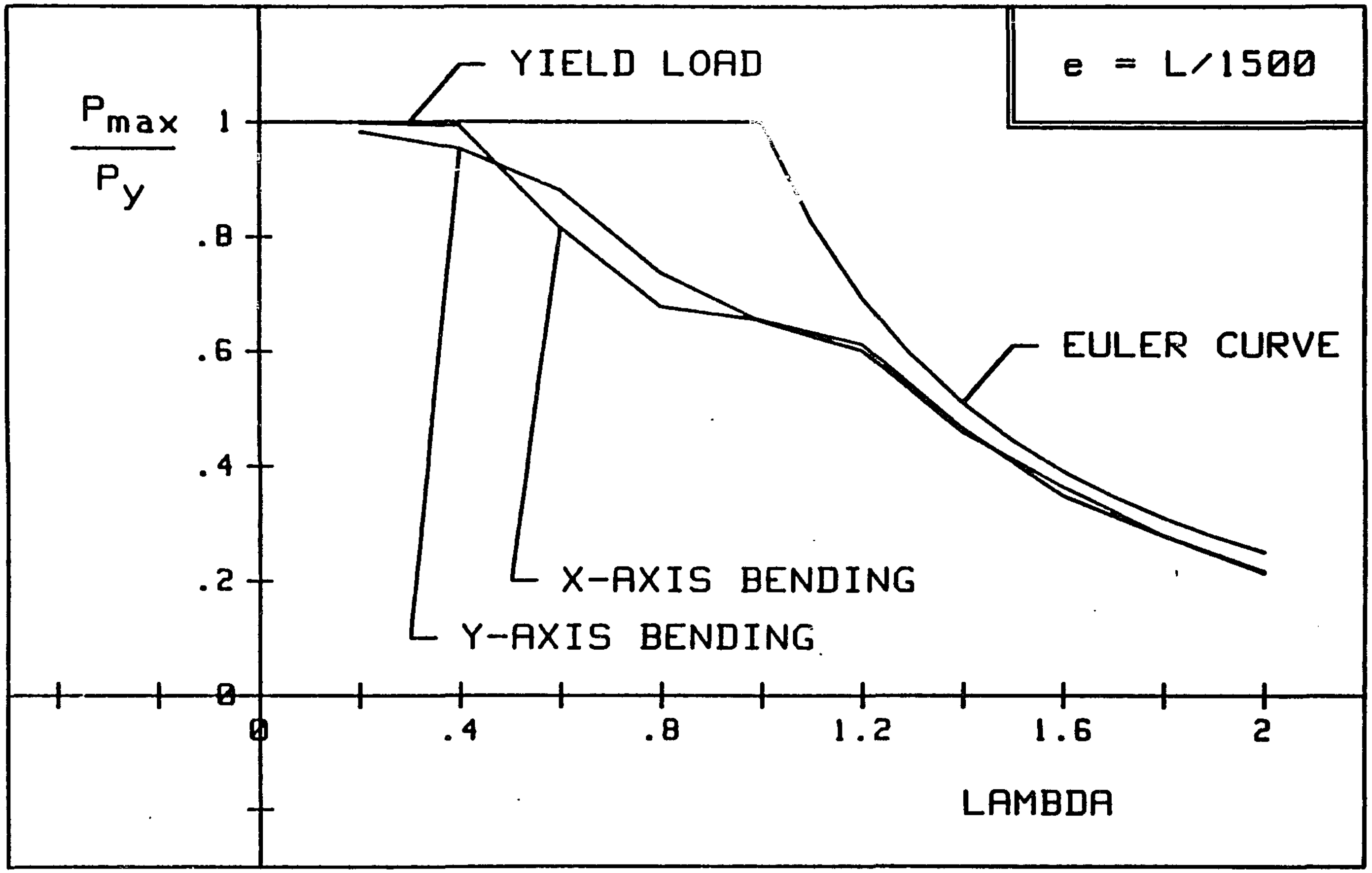

Fig. 6.117. x- and y-axis maximum strength column curves for shape H 24 x 428 (36 ksi steel, 100 ksi electrodes).

178

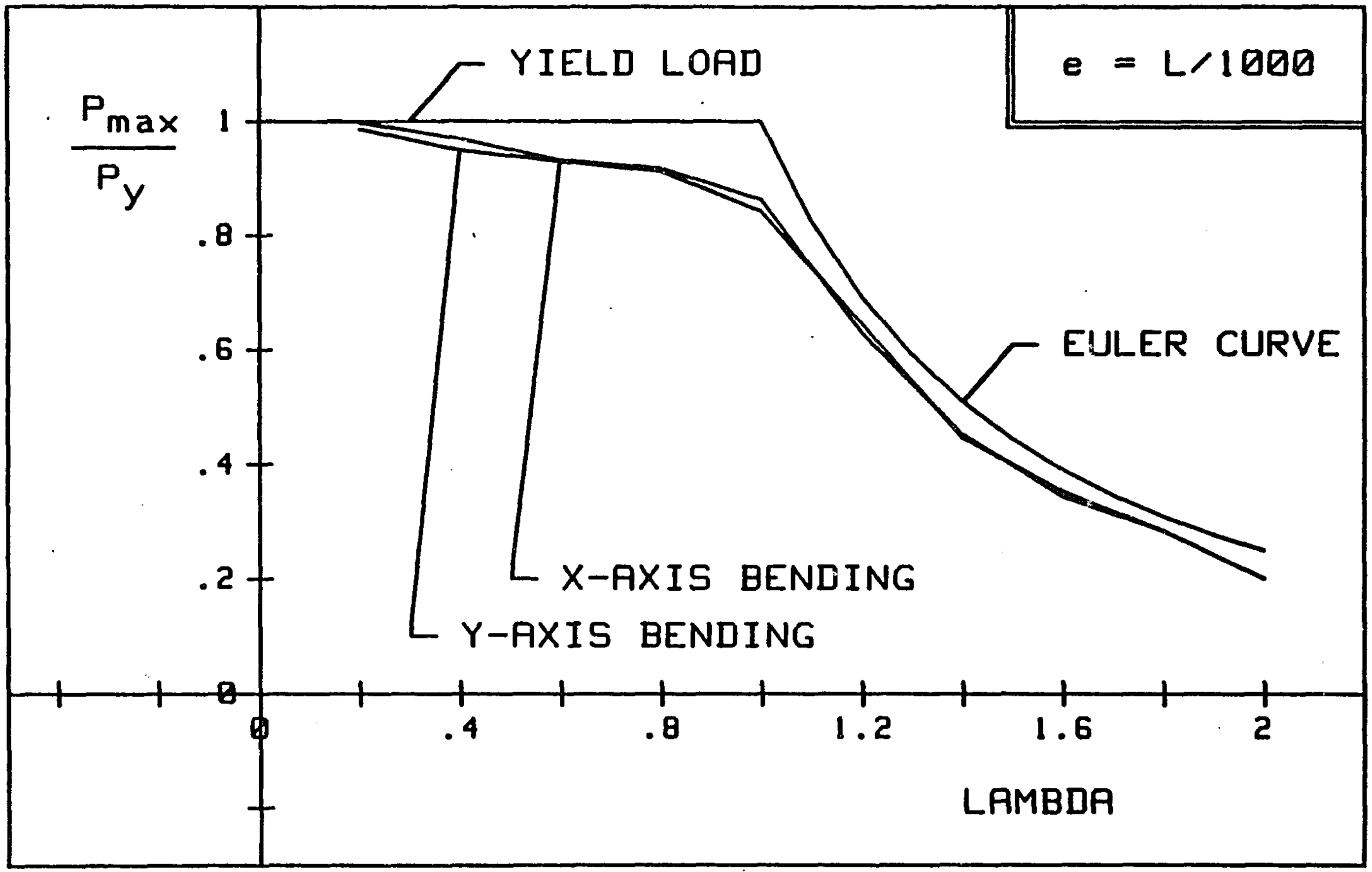

Fig. 6.118. x- and y-axis maximum strength column curves for shape H 24 x 428 (50 ksi steel, 70 ksi electrodes).

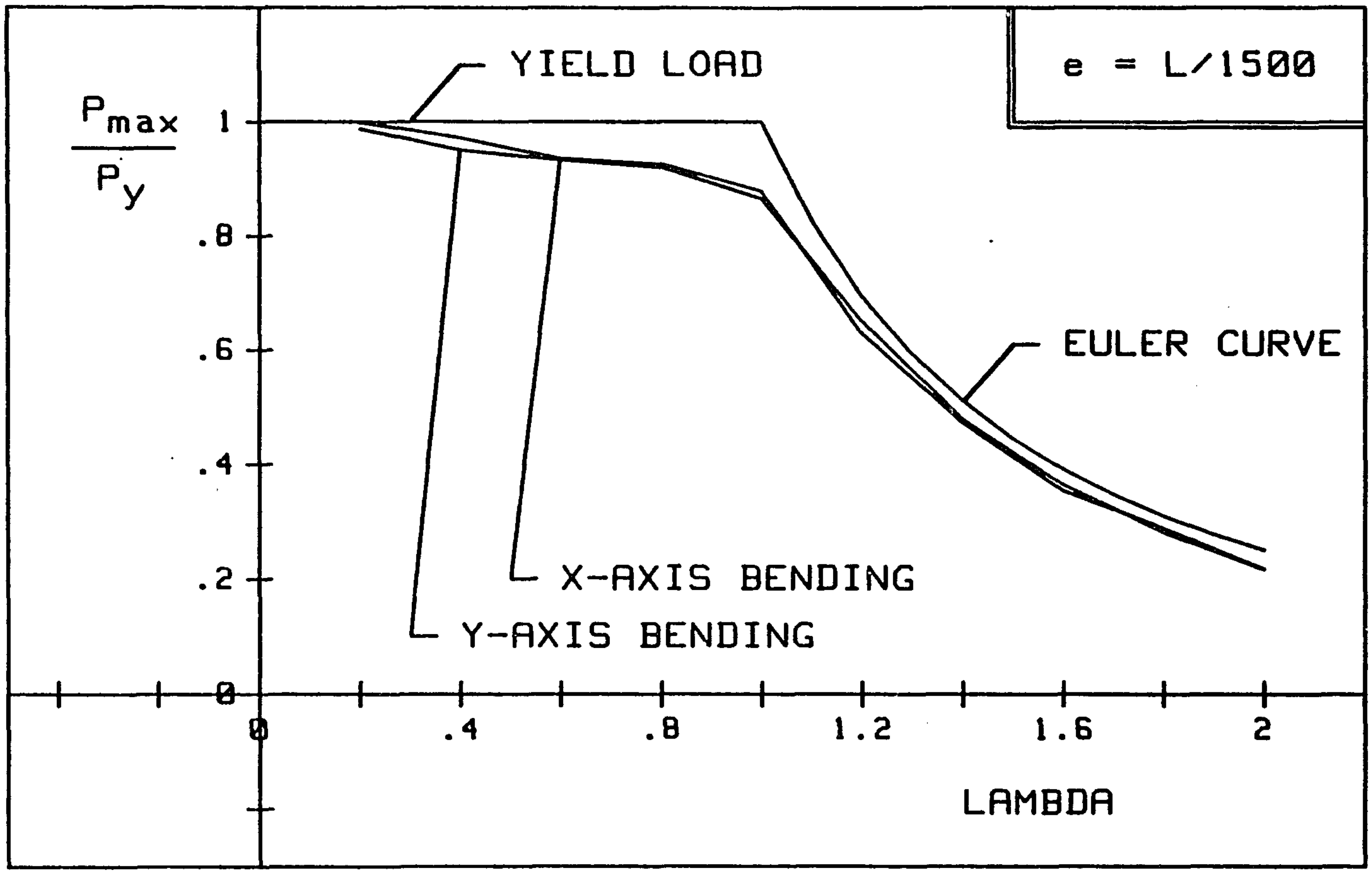

Fig. 6.119. x- and y-axis maximum strength column curves for shape H 24 x 428 (50 ksi steel, 70 ksi electrodes).

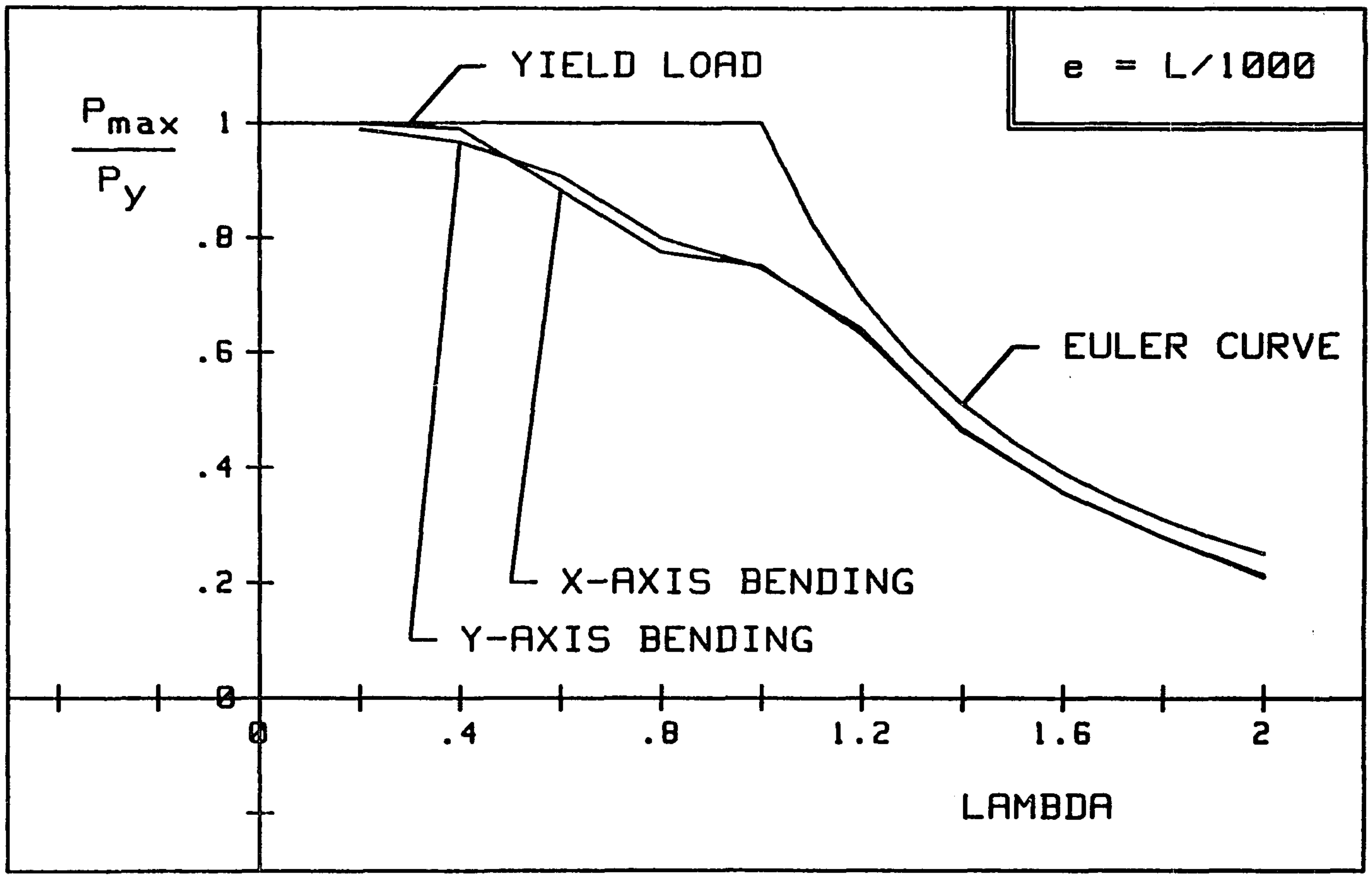

Fig. 6.120. x- and y-axis maximum strength column curves for shape H 24 x 428 (50 ksi steel, 100 ksi electrodes).

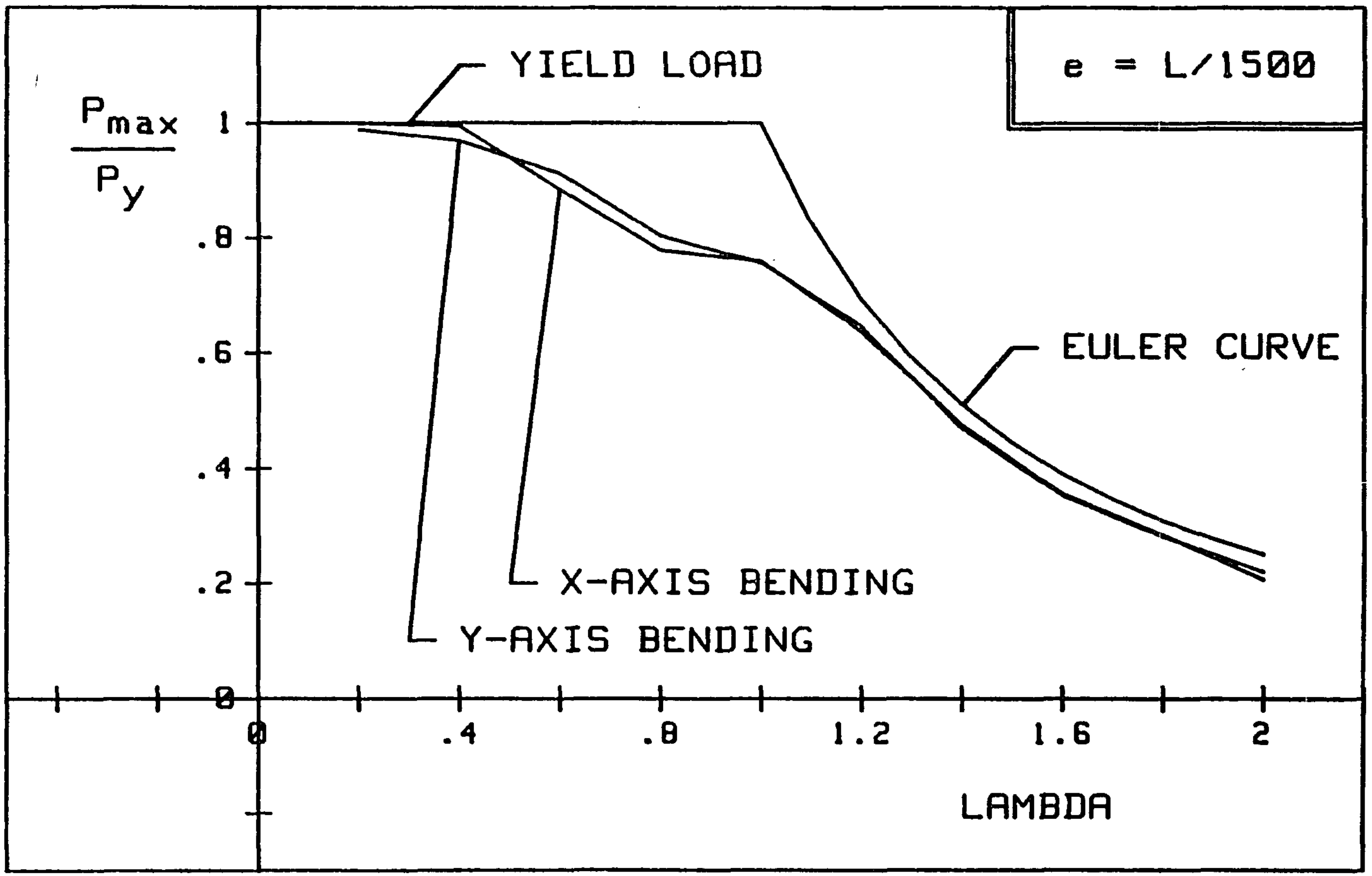

Fig. 6.121. x- and y-axis maximum strength column curves for shape H 24 x 428 (50 ksi steel, 100 ksi electrodes).

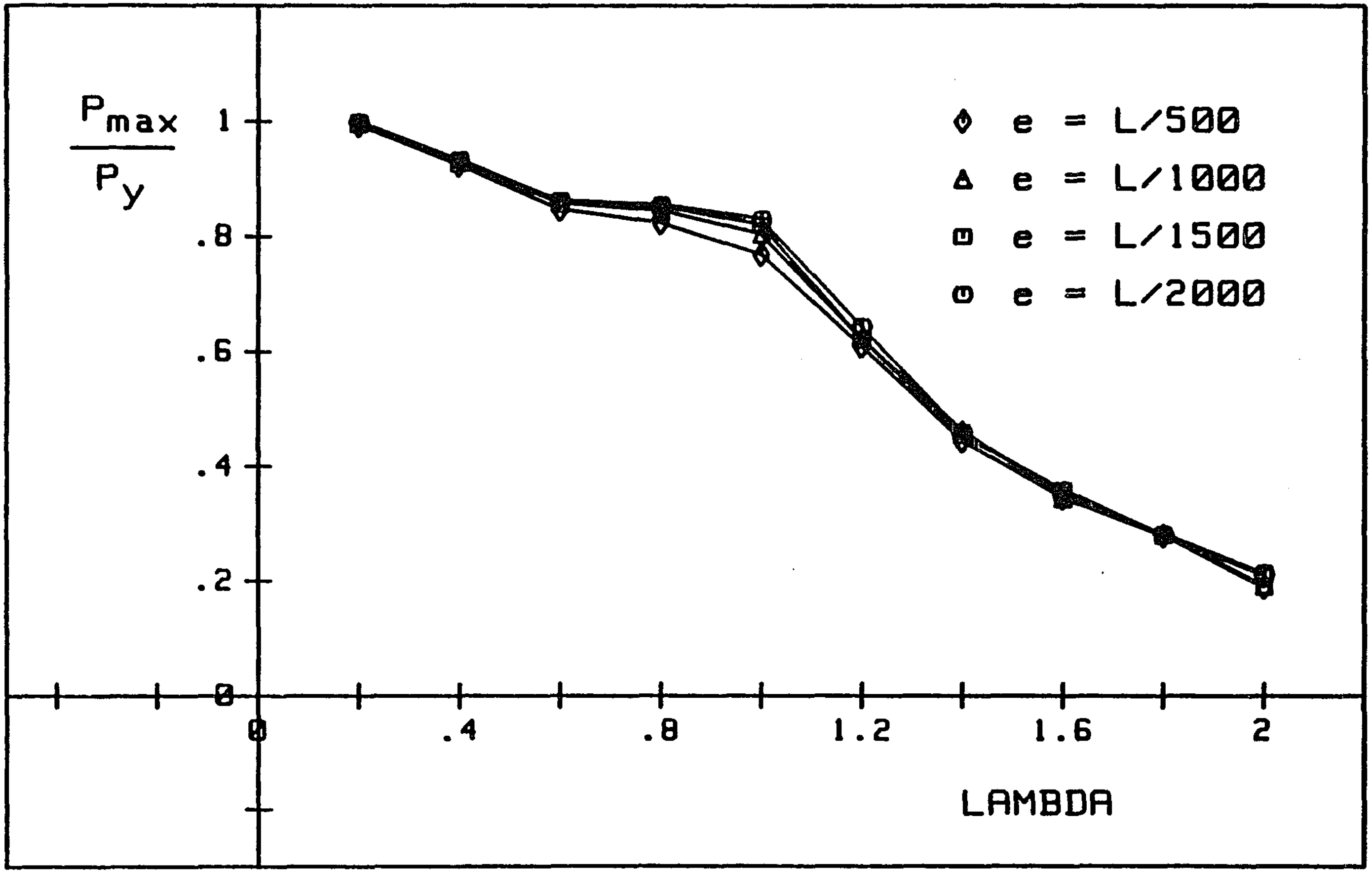

Fig. 6.122. Maximum strength column curves for shape H 24 x 1122 (36 ksi steel, 70 ksi electrodes) and x-axis bending.

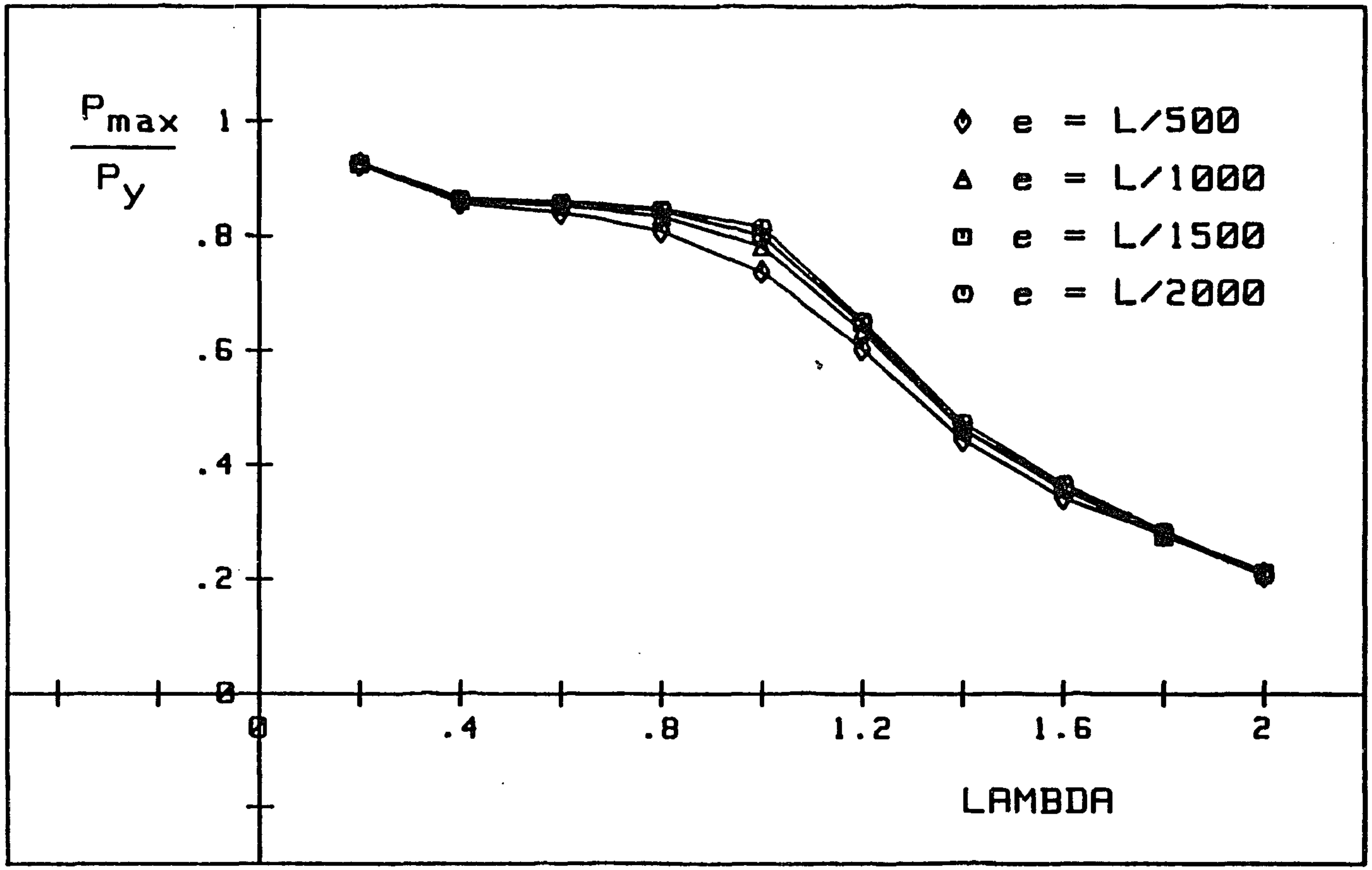

Fig. 6.123. Maximum strength column curves for shape H 24 x 1122 (36 ksi steel, 70 ksi electrodes) and y-axis bending.

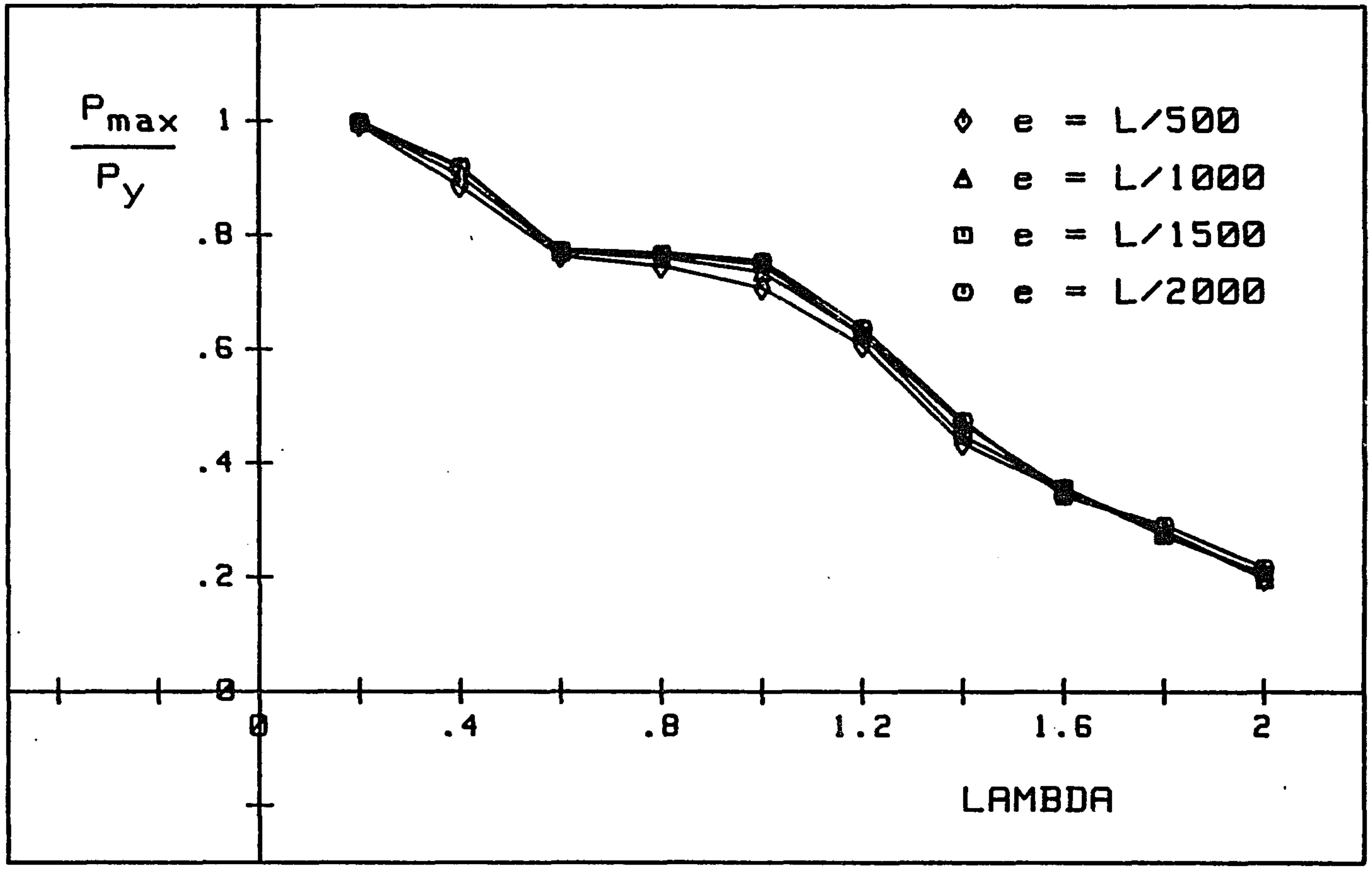

Fig. 6.124. Maximum strength column curves for shape H 24 x 1122 (36 ksi steel, 100 ksi electrodes) and x-axis bending.

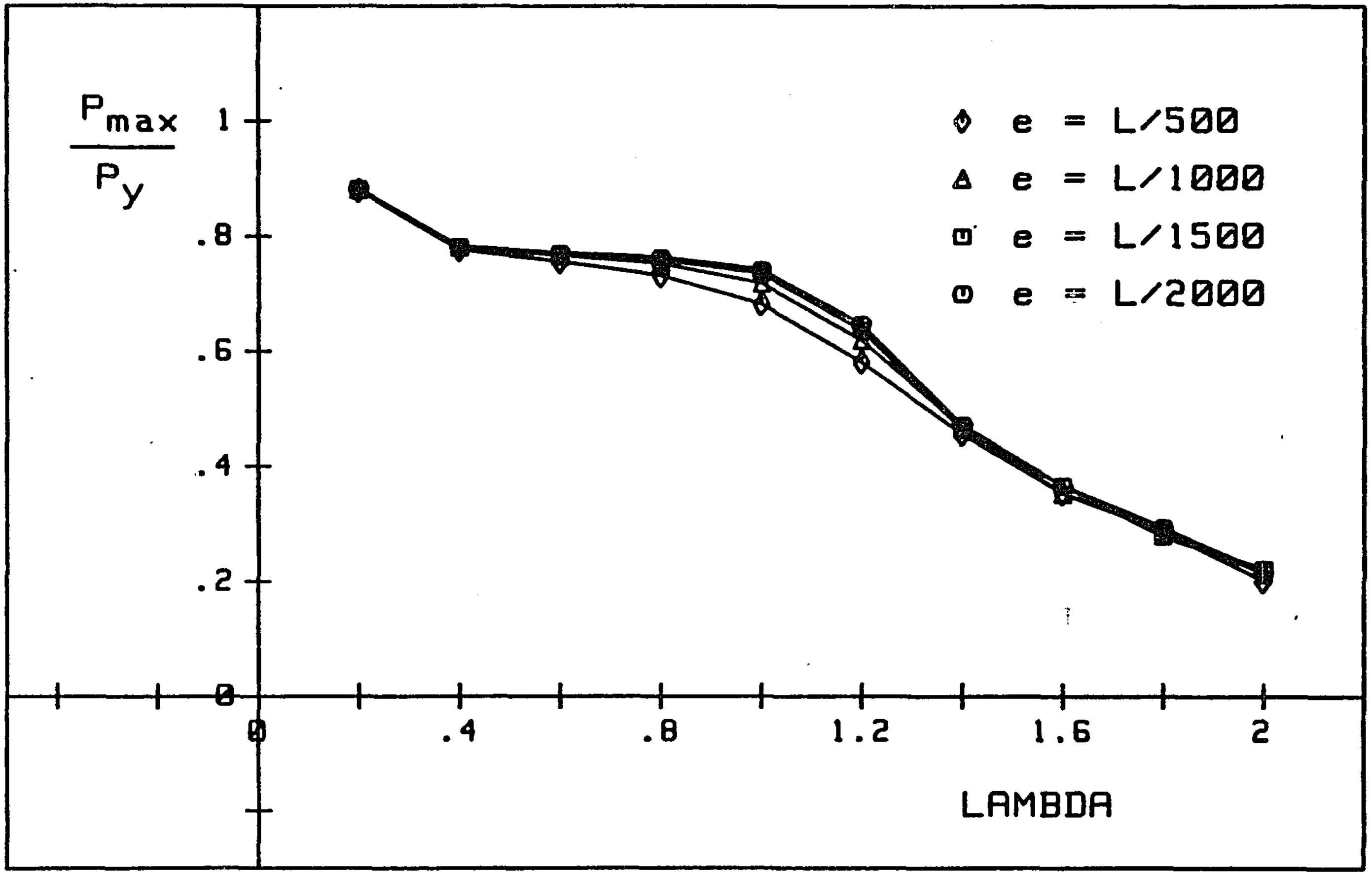

Fig. 6.125. Maximum strength column curves for shape H 24 x 1122 (36 ksi steel, 100 ksi electrodes) and y-axis bending.

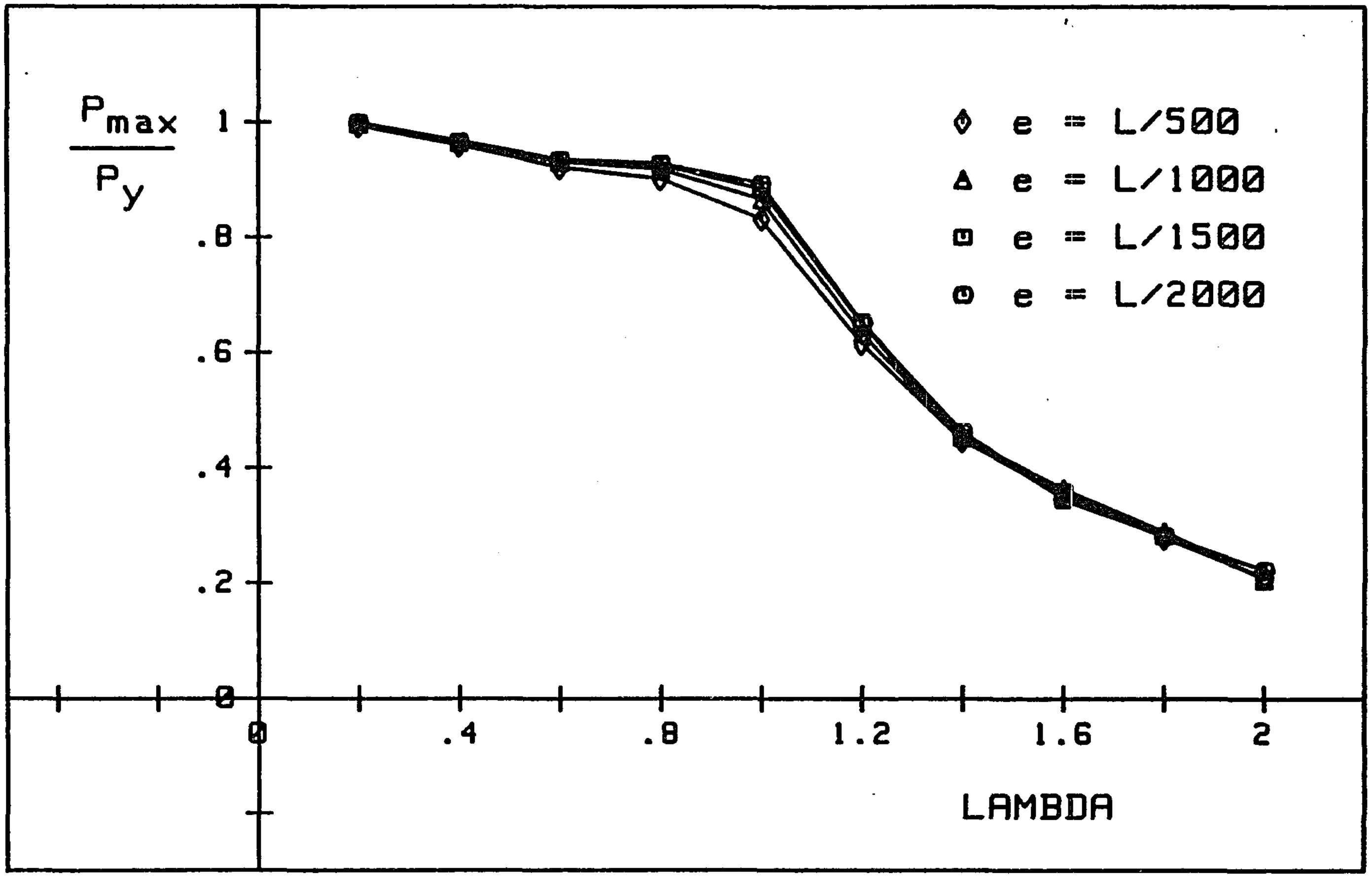

Fig. 6.126. Maximum strength column curves for shape H 24 x 1122 (50 ksi steel, 70 ksi electrodes) and x-axis bending.

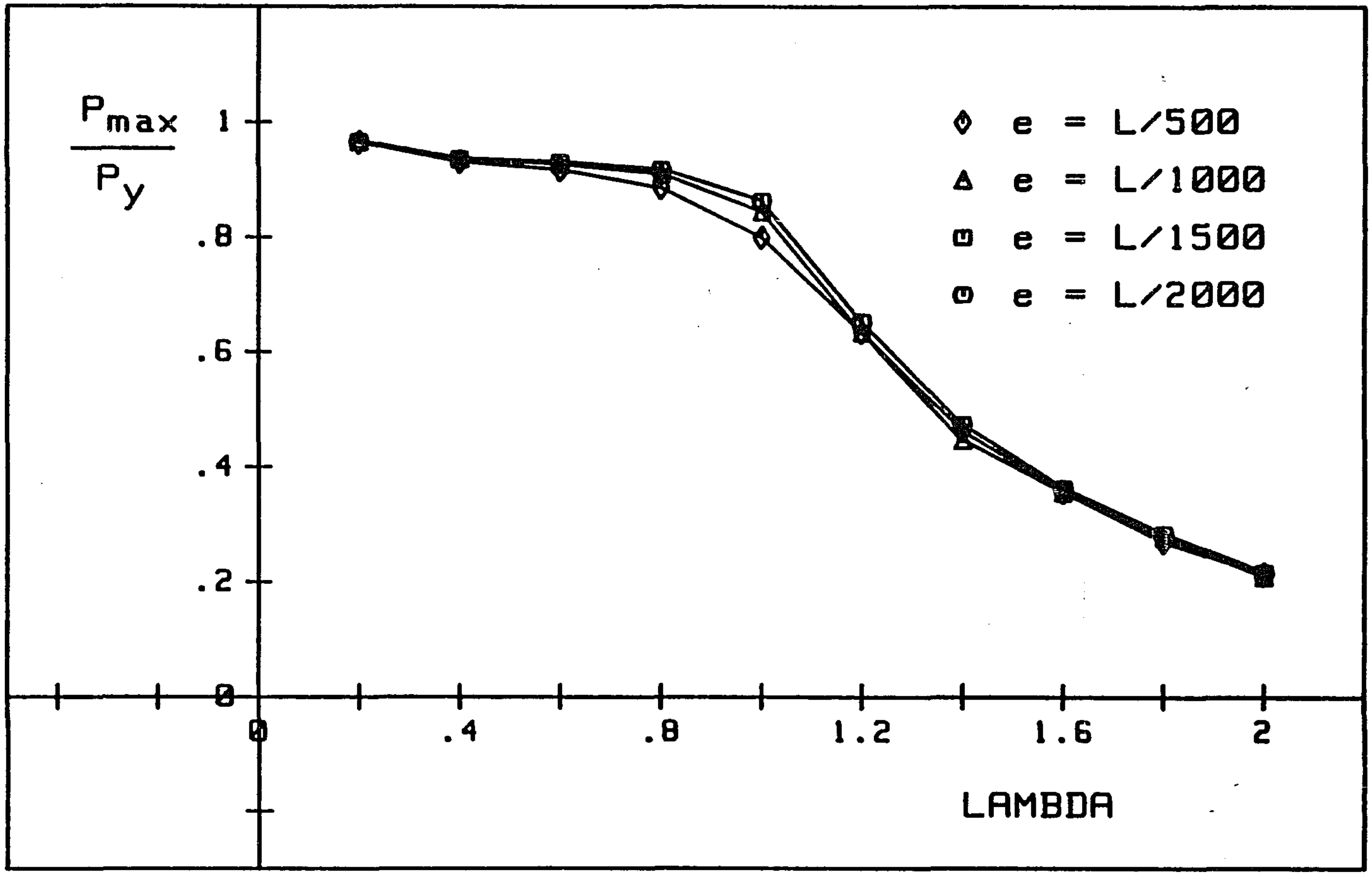

Fig. 6.127. Maximum strength column curves for shape H 24 x 1122 (50 ksi steel, 70 ksi electrodes) and y-axis bending.

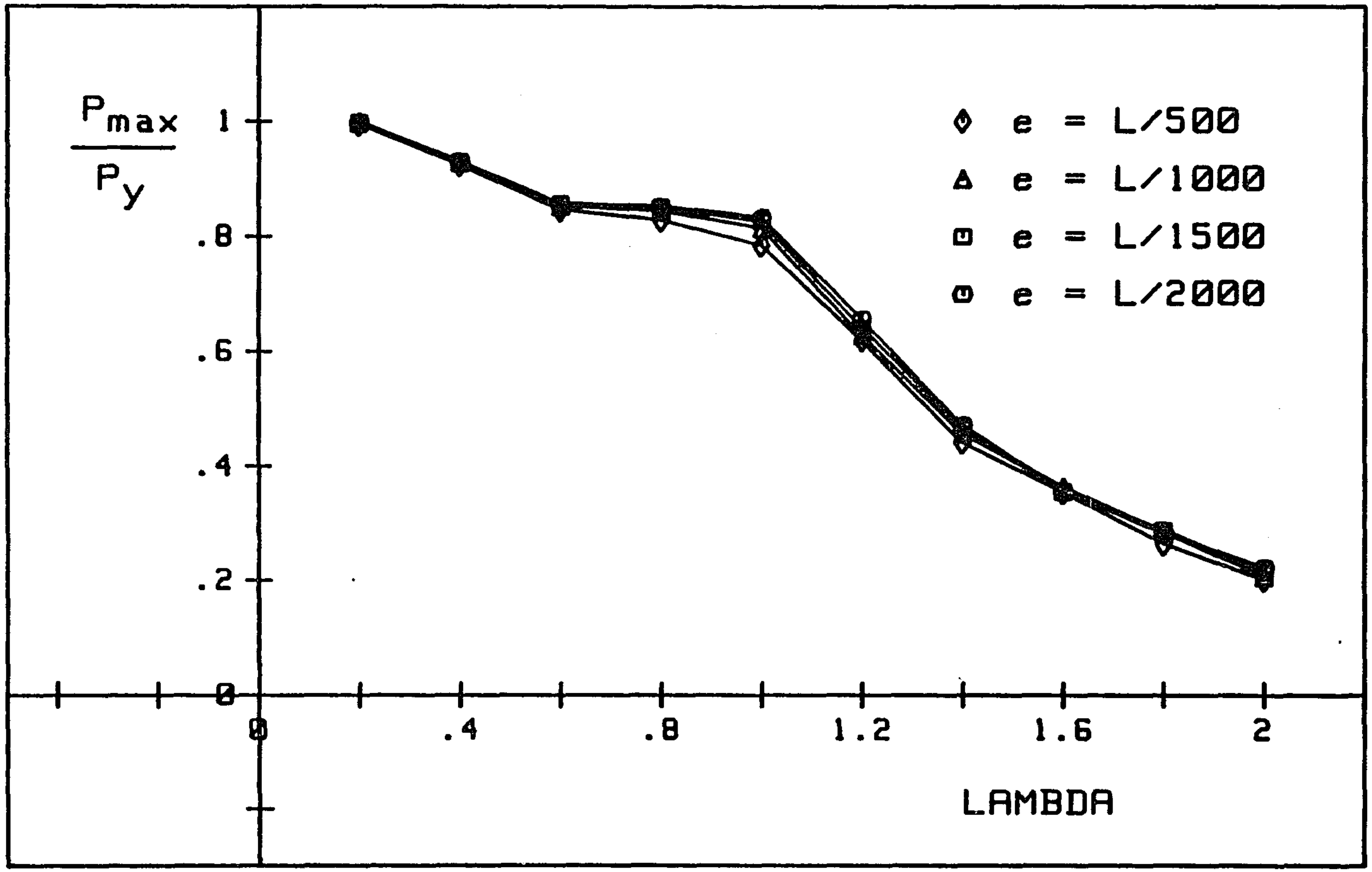

Fig. 6.128. Maximum strength column curves for shape H 24 x 1122 (50 ksi steel, 100 ksi electrodes) and x-axis bending.

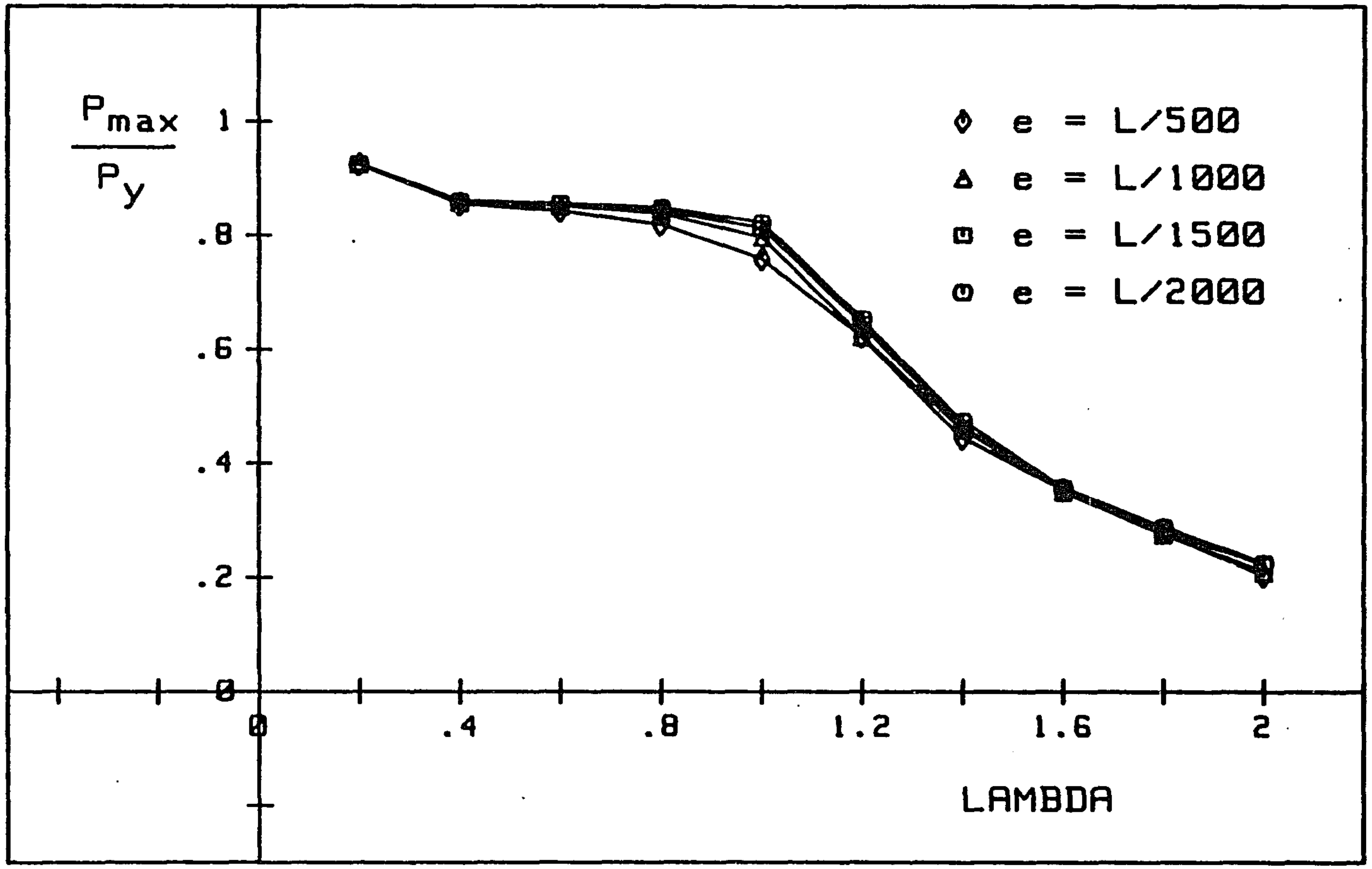

Fig. 6.129. Maximum strength column curves for shape H 24 x 1122 (50 ksi steel, 100 ksi electrodes) and y-axis bending.

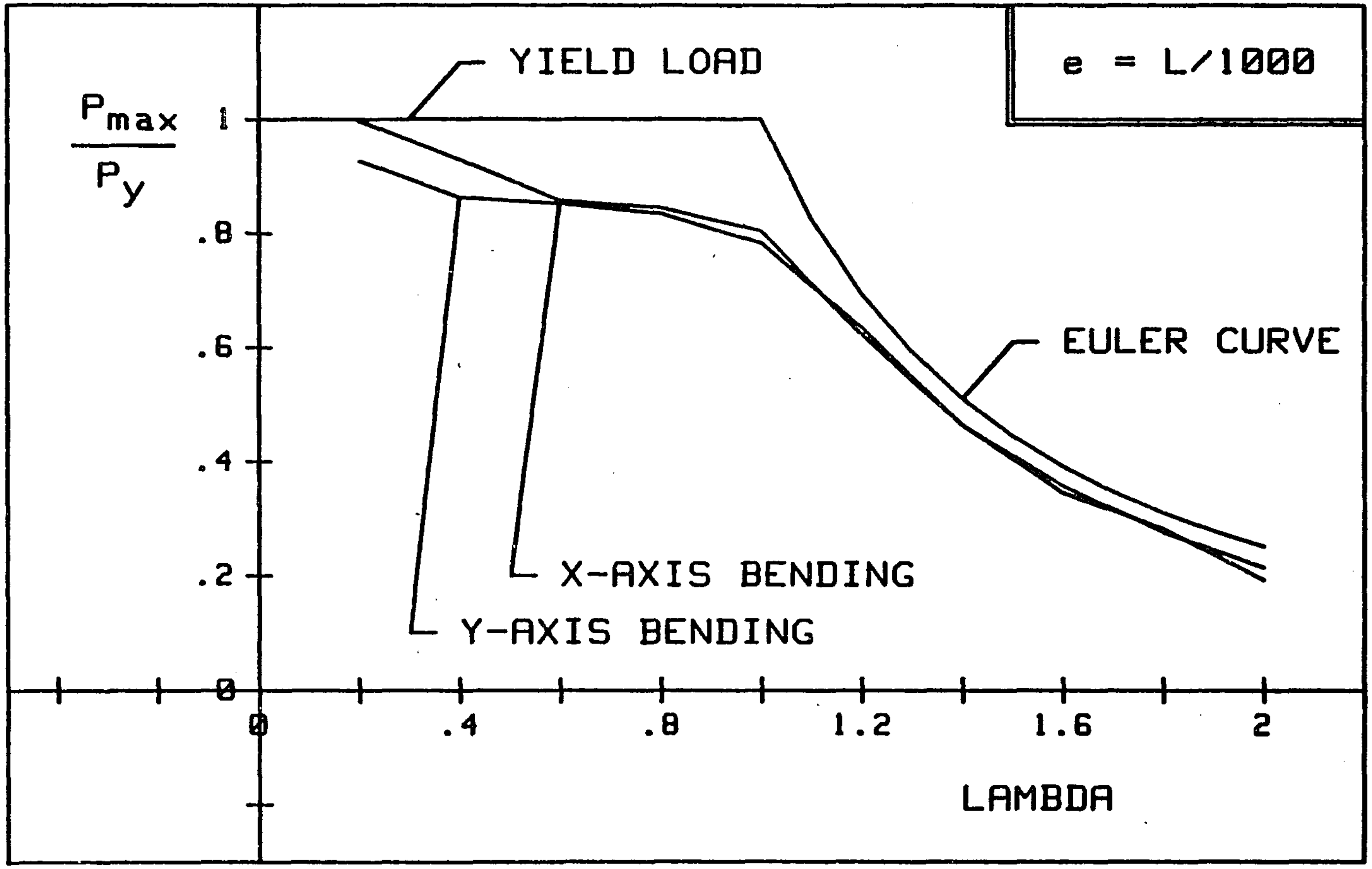

Fig. 6.130. x- and y-axis maximum strength column curves for shape H 24 x 1122 (36 ksi steel, 70 ksi electrodes).

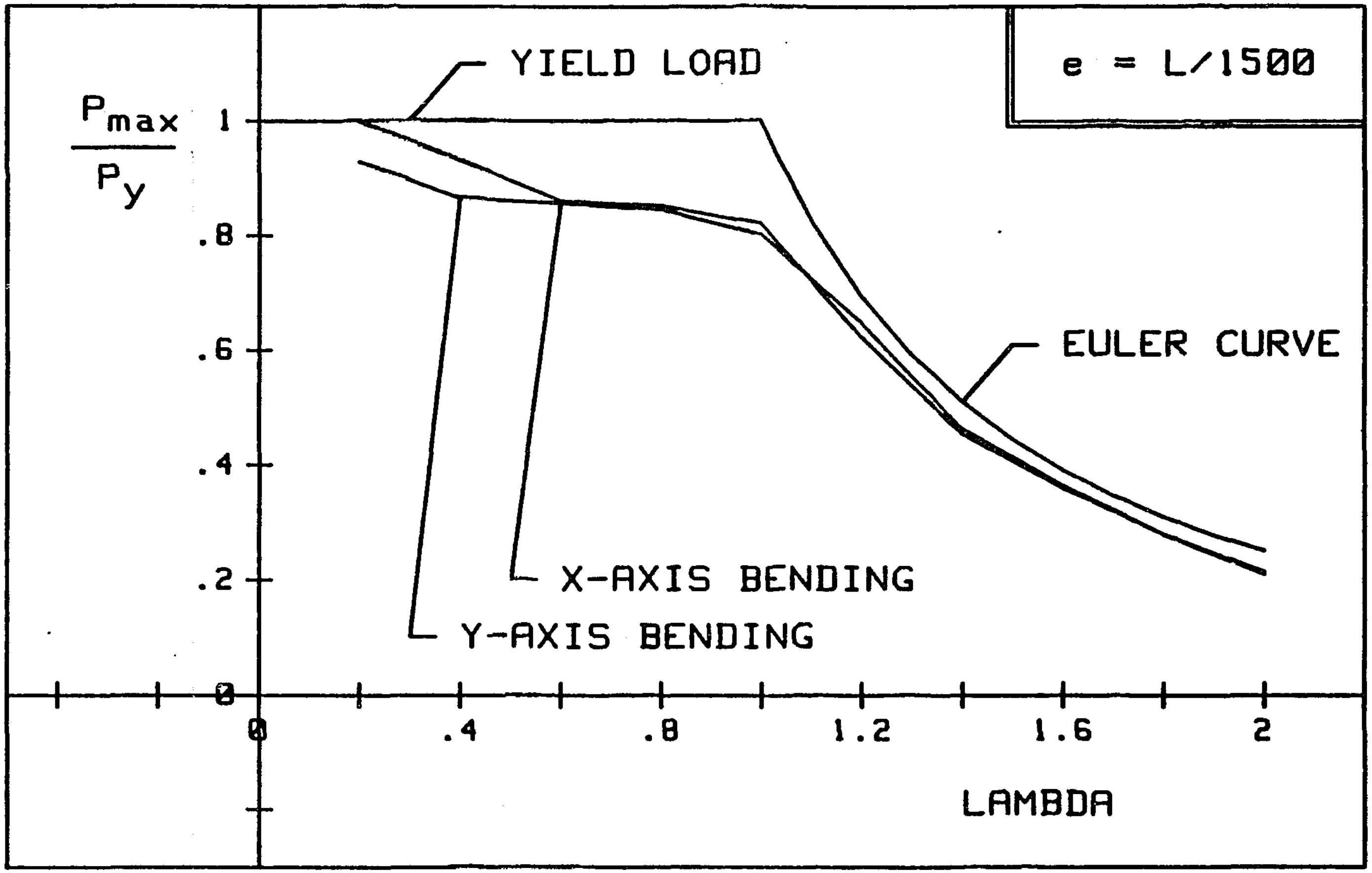

Fig. 6.131. x- and y-axis maximum strength column curves for shape H 24 x 1122 (36 ksi steel, 70 ksi electrodes).

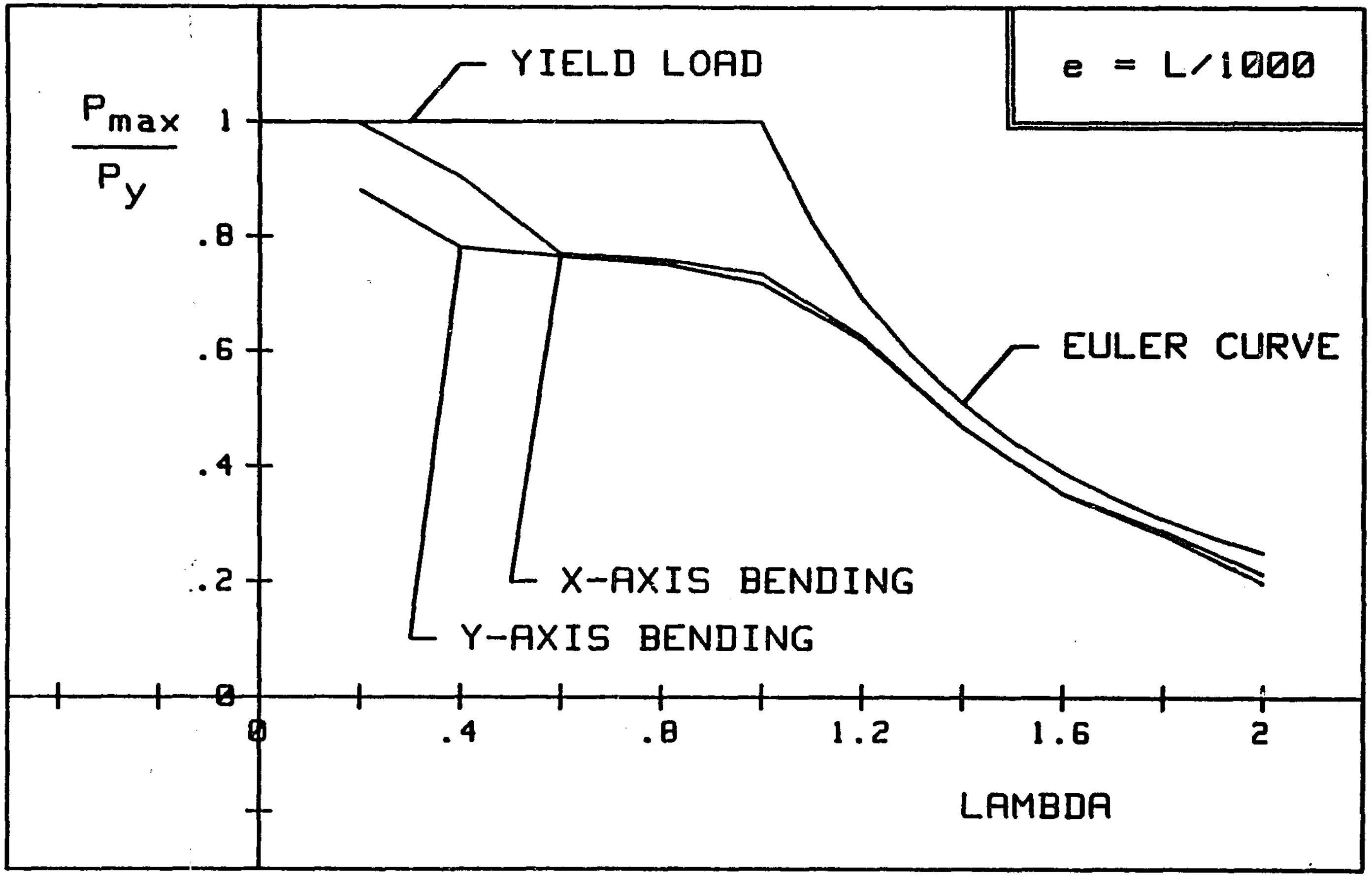

Fig. 6.132. x- and y-axis maximum strength column curves for shape H 24 x 1122 (36 ksi steel, 100 ksi electrodes).

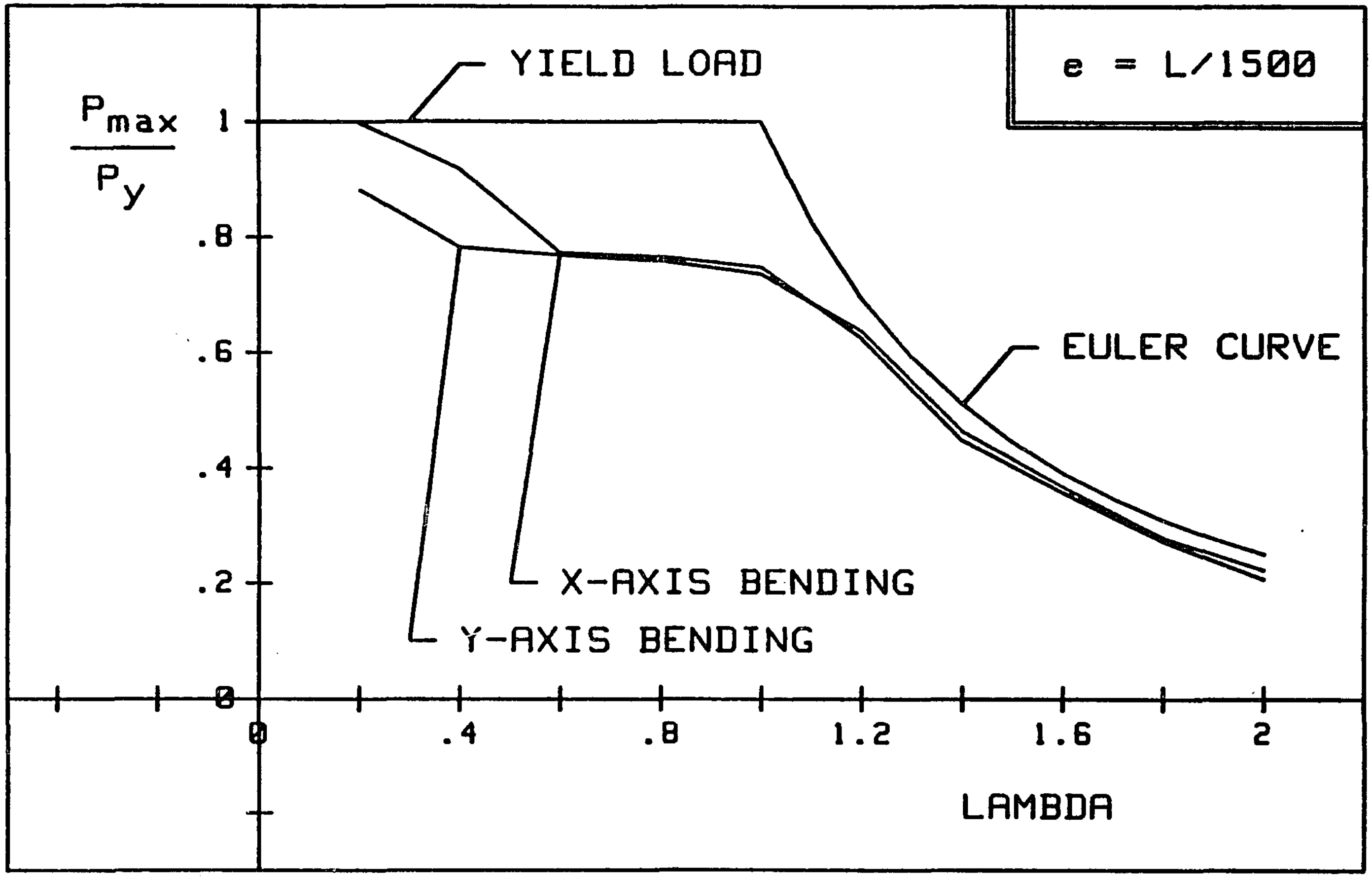

Fig. 6.133. x- and y-axis maximum strength column curves for shape H 24 x 1122 (36 ksi steel, 100 ksi electrodes).

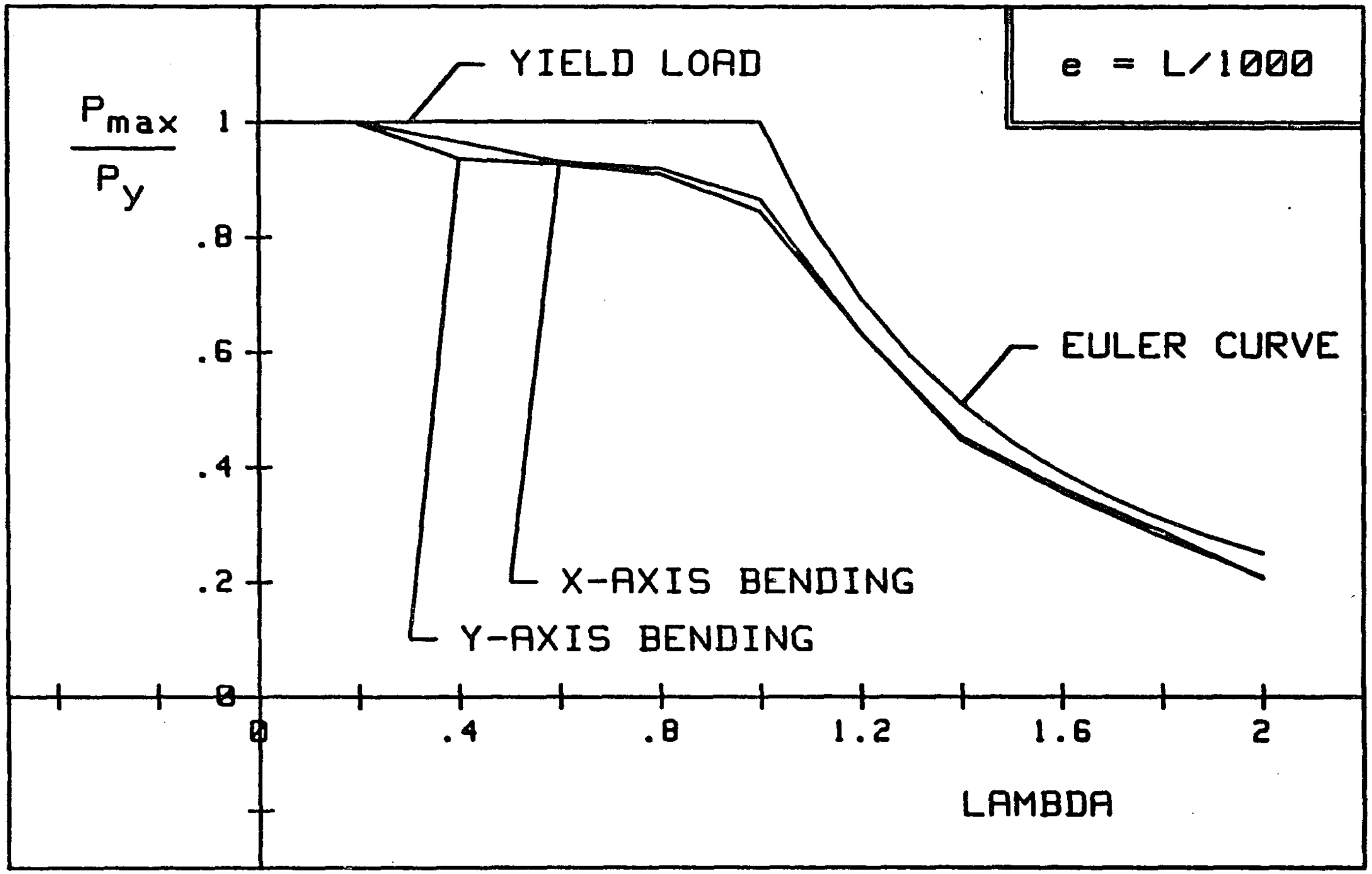

Fig. 6.134. x- and y-axis maximum strength column curves for shape H 24 x 1122 (50 ksi steel, 70 ksi electrodes).

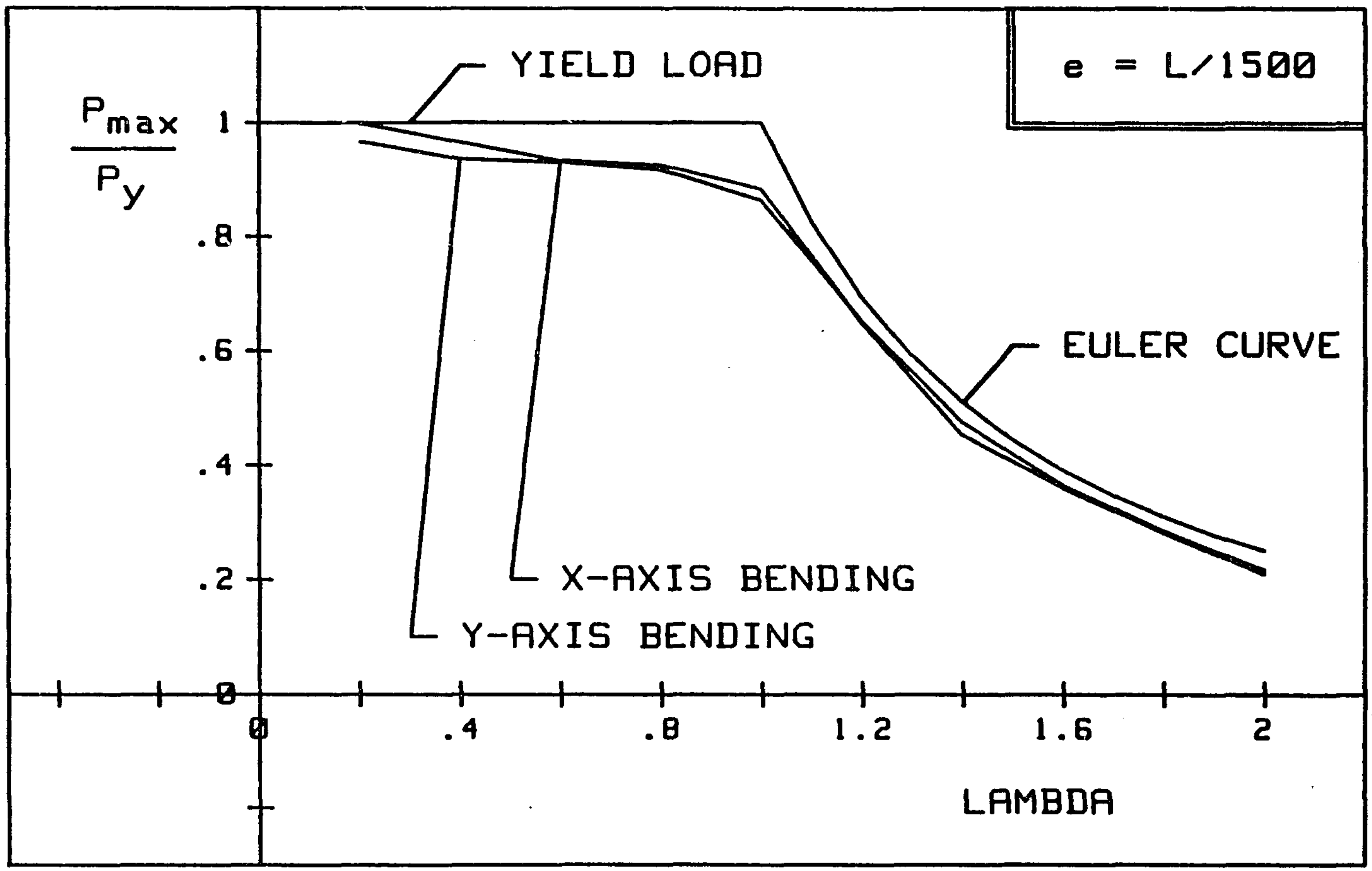

Fig. 6.135. x- and y-axis maximum strength column curves for shape H 24 x 1122 (50 ksi steel, 70 ksi electrodes).

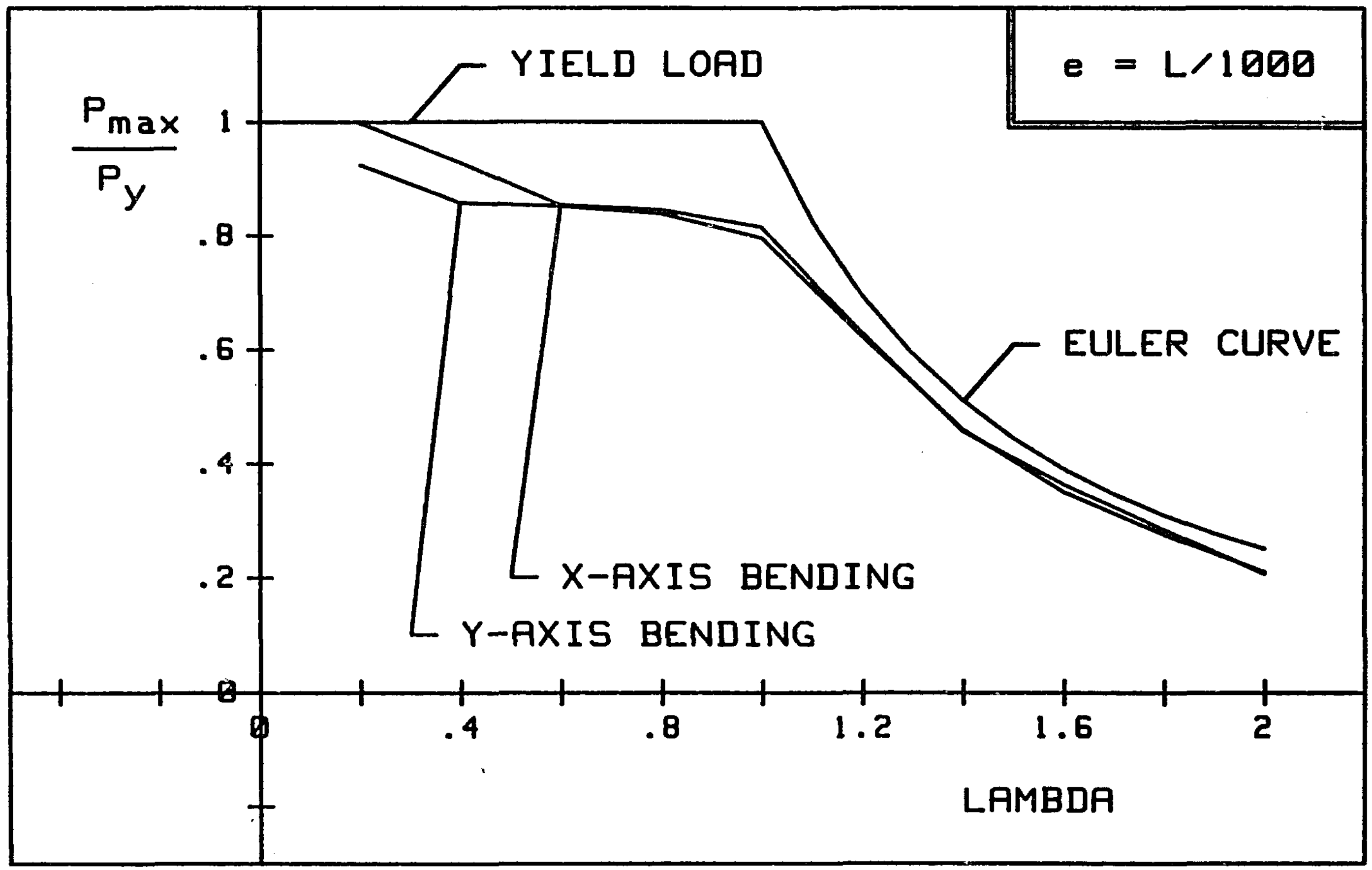

Fig. 6.136. x- and y-axis maximum strength column curves for shape H 24 x 1122 (50 ksi steel, 100 ksi electrodes).

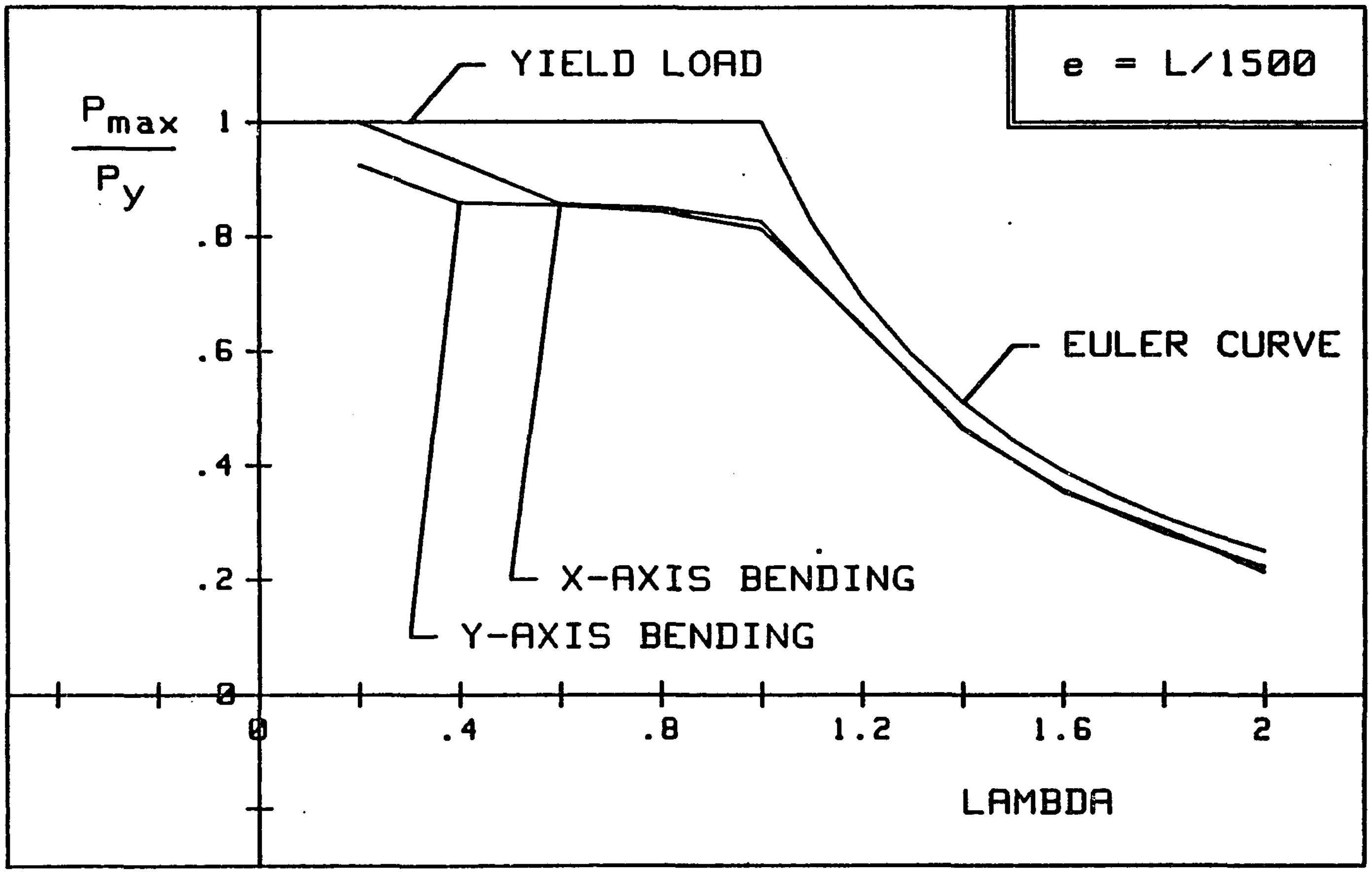

Fig. 6.137. x- and y-axis maximum strength column curves for shape H 24 x 1122 (50 ksi steel, 100 ksi electrodes).

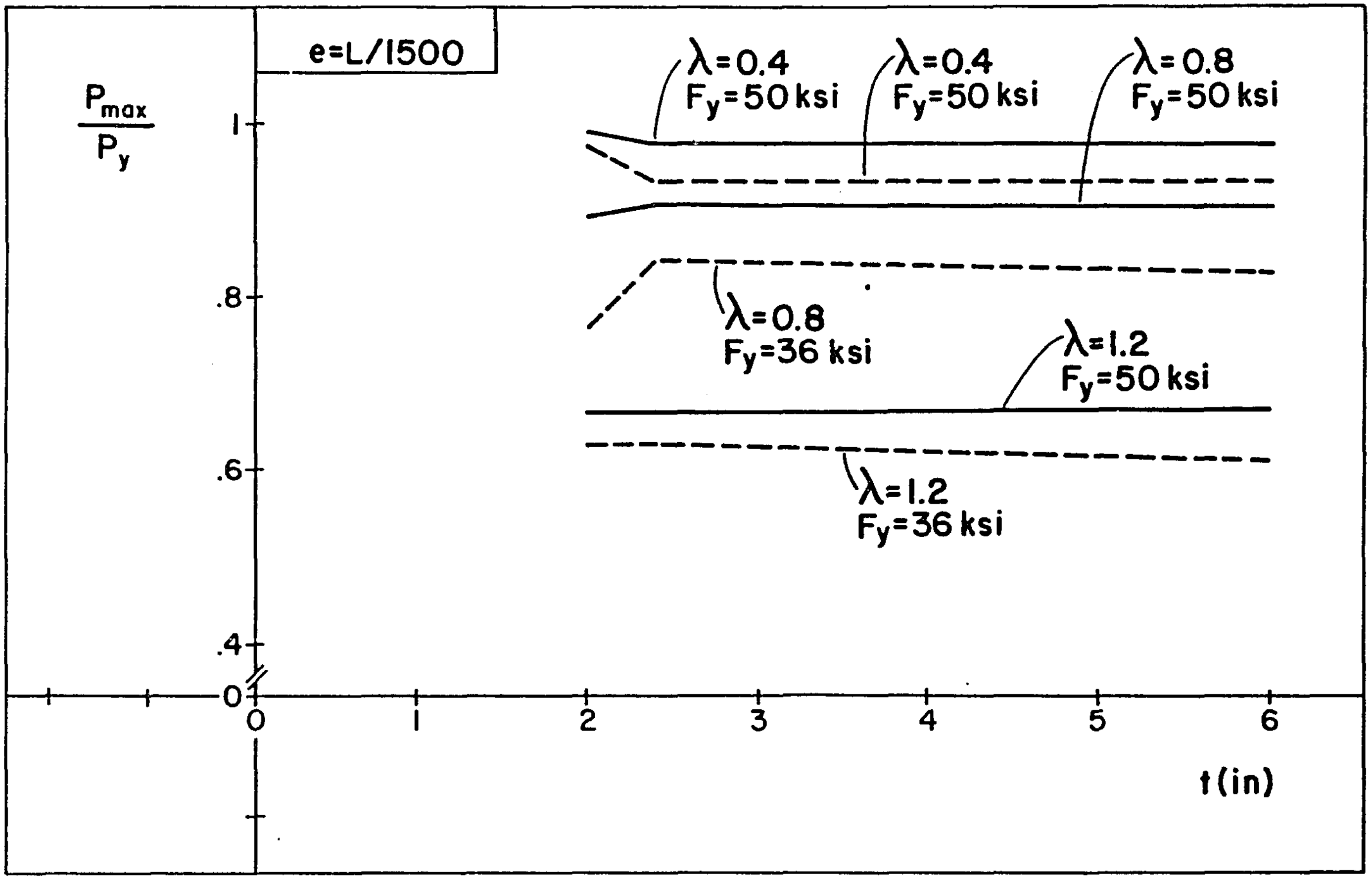

Fig. 6.138. Relationship between maximum column strength and flange thickness for welded built-up wide-flange shapes (36 and 50 ksi steel; 70 ksi electrodes) (x-axis bending).

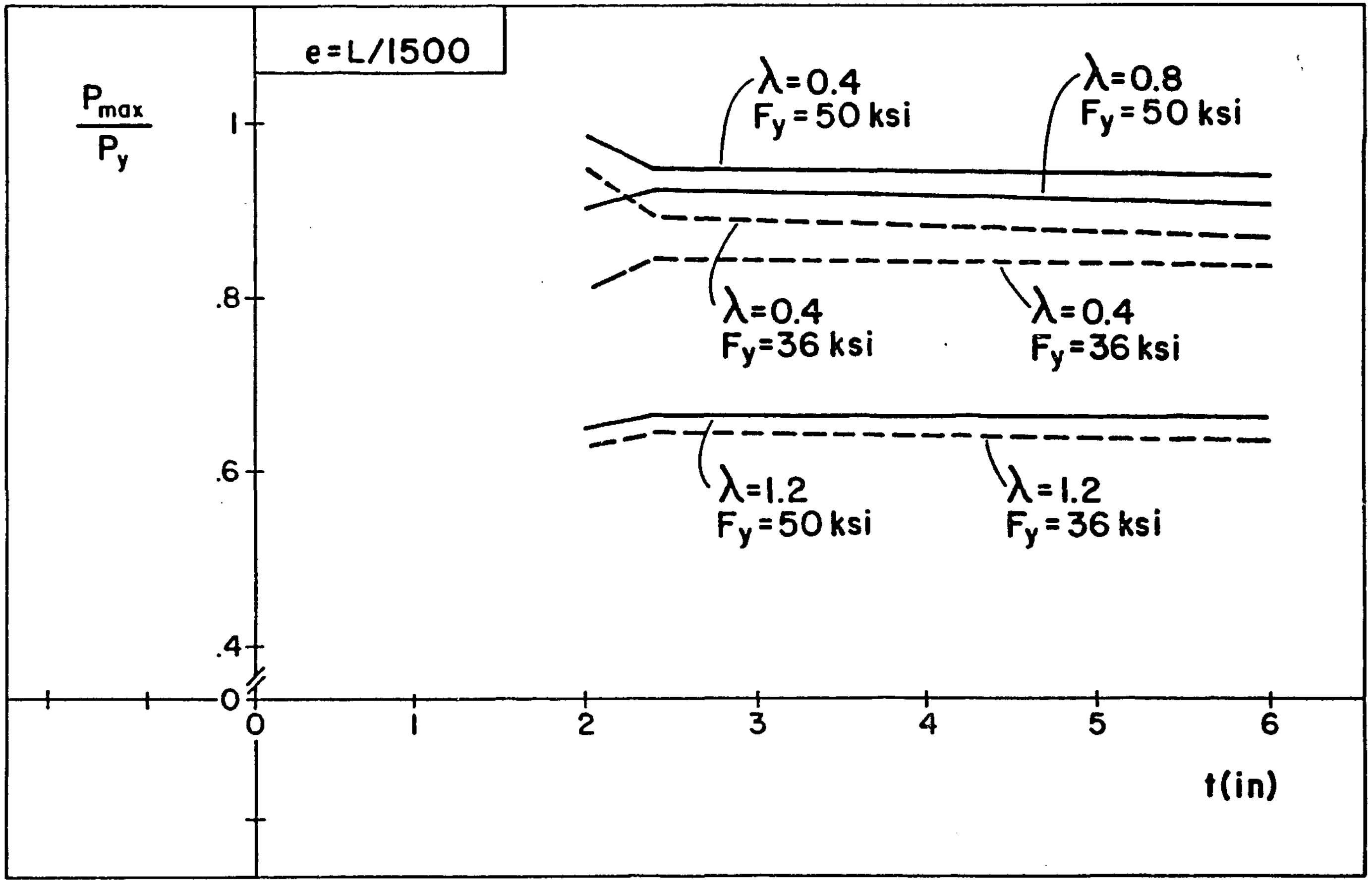

Fig. 6.139. Relationship between maximum column strength and flange thickness for welded built-up wide-flange shapes (36 and 50 ksi steel; 70 ksi electrodes) (y-axis bending).

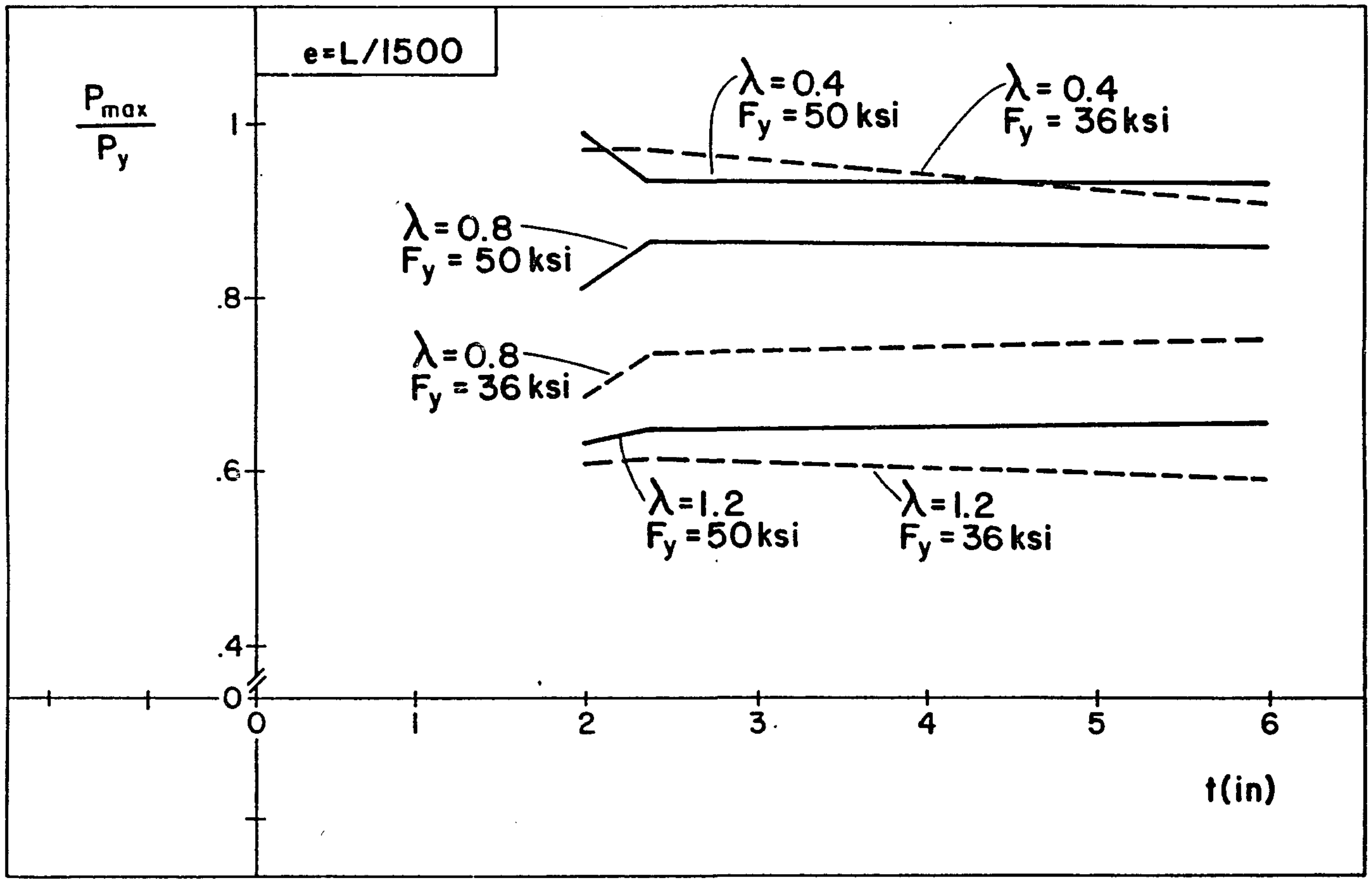

Fig. 6.140. Relationship between maximum column strength and flange thickness for welded built-up wide-flange shapes (36 and 50 ksi steel; 100 ksi electrodes) (x-axis bending).

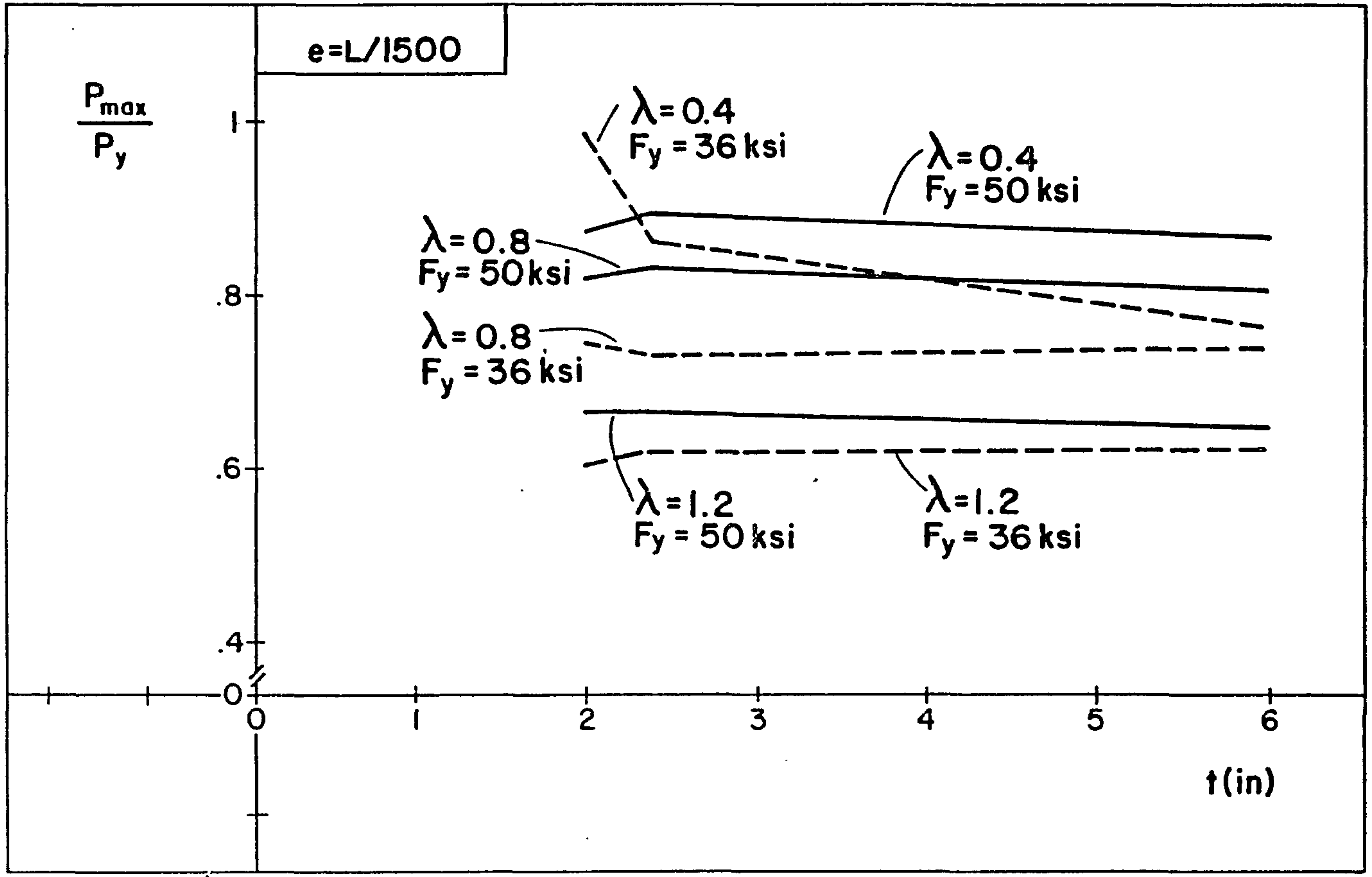

Fig. 6.141. Relationship between maximum column strength and flange thickness for welded built-up wide-flange shapes (36 and 50 ksi steel; 100 ksi electrodes) (y-axis bending).

CHAPTER 7

SUGGESTED DESIGN CONSIDERATIONS

It has been observed that the relative strength of heavy hot-rolled wide-flange shapes has a direct correlation with the flange thicknesses. As it increases to about 3 inches, the corresponding relative strength decreases, and then increases as the thickness is further increased. For the intermediate column length range, which is the most sensitive one as far as column strength reductions are concerned, the loss in relative strength is approximately 14 percent, on the average. It is somewhat less for higher strength steel (about 11 percent on the average).

Further studies are needed for welded built-up shapes to verify the details of the above conclusions. At this stage, the data are not clear for such shapes; however, the strength seems to be significantly less influenced by thickness variations. This is correct for shapes made with flame-cut as well as universal mill plates. It was observed that the short and long column relative strength is constant and not much affected by the flange thickness variations. Intermediate columns show an increase of relative strength as t goes to 2.5 inches and then remains constant as it increases to 6 inches.

The influence of the thickness variation is on the order of a maximum of about 13% in the most important λ-range. It was previously thought that 1 inch was the limiting thickness (in terms of separating light from heavy shapes); it is now clear that the transition is gradual. This is as would be expected. Flange thicknesses on the order of 2.5 to 3.5 inches seem to indicate the low points; for larger thicknesses it appears that the size of the cross-sectional area overcomes the negative effects of the increased thickness.

For practical design purposes, it is felt that using an ultimate strength approach as in Load and Resistance Factor Design (LRFD), along with an appropriate resistance factor, is the best solution. In all likelihood, this will be sufficient to overcome the strength reductions that are caused by the larger t-values.

CHAPTER 8

SUMMARY AND CONCLUSIONS

A theoretical study has been conducted to examine the maximum strength of heavy hot-rolled and welded built-up wide-flange shapes. It was undertaken to alleviate the current lack of data on the behavior and strength of such shapes, and included the effects of initial crookedness, residual stresses, and the variation of the yield stress throughout the cross section.

A mathematical model based on the maximum strength concept was used to simulate the behavior of pinned-end, prismatic columns, taking into account all of the relevant column strength parameters. The numerical iterative solution procedure has been used in a computer program that was developed previously.

Four initial out-of-straightness values were used for the computations, namely, $\ell/500$, $\ell/1000$, $\ell/1500$, and $\ell/2000$. Actual residual stress data were used; these had been found in studies by other researchers. Only longitudinal residual stresses were considered, and it was assumed that they were constant through the thickness of the component plates of the cross section. This is a slightly conservative assumption as far as the shown strength is concerned.

Five hot-rolled and five welded built-up steel shapes were included in this investigation. The hot-rolled members were assumed to have a constant yield stress throughout the cross section. For the welded shapes, however, the yield stress increases in the weld metal and at the flame-cut edges were taken into account.

Column strength curves were generated for different combinations of residual stress, initial curvature, yield stress, and different axes of bending (major, minor). The welded built-up shapes also utilized different values of the weld metal strength. The analysis was carried out for 36 and 50 ksi yield stress levels for the base metal, in addition to the values that were reported by the various reports. For example, the European shapes that were included were analyzed with yield stresses of 25 and 28 ksi.

The following conclusions have been arrived at through the investigation:

1. The relative strength of heavy hot-rolled shapes has a clear correlation with the flange thickness. It decreases as t goes to about 3 inches and then increases as t is further increased. This applies to all slenderness ratios, but most significantly in the intermediate range.

2. Welded built-up members appear to be less influenced by the component plate thickness, and short and long columns have an almost constant relative strength as the component plate thickness goes up to 6 inches. Some relative strength increases for intermediate column lengths are found for thicknesses up to approximately 2.5 inches, but then remains constant.
3. The initial out-of-straightness value of $\ell/1000$ appears to be a fair straightness requirement. This confirms the results of previous investigations.
4. Increasing the yield stress of the steel has the same effect for both hot-rolled and welded built-up shapes. The relative strength increases as yield stress goes up. This is pronounced for intermediate columns.
5. Welded built-up shapes that use flange plates with flame-cut edges occasionally show weak axis strength higher than that for the strong axis. This happens because the high yield stress flange tips contain high tensile residual stress. Welded built-up members with universal mill edges show the same behavior as hot-rolled shapes.
6. At this time, data regarding heavy welded built-up shapes are incomplete. Therefore, further studies are required to investigate their strength and

behavior as they are influenced by the different imperfections.

APPENDIX A

MAXLD PROGRAM

MAXLD PROGRAM

A.1 Introduction

The computer program "MAXLD" provides an iterative, incremental solution for the maximum strength of pinned-end, prismatic, initially curved, centrally loaded columns. The principle for determining the maximum strength is to find the axial load which for a given deflection , δ, at the column mid-height, will cause a state of equilibrium between the internal and external forces and moments.

The whole cross section is discretized into individual segments. The column strength parameters are assigned for each element and assumed to be constant along the width and through the thickness. Residual stresses are adjusted in order to satisfy equilibrium in the cross section for zero external load and before iteration begins. The initial crookedness is incorporated using this mathematical model. The output data give the necessary information for plotting relative strength versus non-dimensionalized slenderness ratio, λ, as well as data for the load-deflection curve.

A.2 Variable Definitions

Card No.	Input Variable	Definition
1	NPROB	Problem number.
	TITLE	Problem title.
2	NSHAPE	Flag, if NSHAPE = 1 then member is a wide flange, if NSHAPE = 2 then a box shape.
3	NF	No. of flange elements.
	NW	No. of web elements.
	B	Flange width.
	T	Flange thickness.
	D	Web depth.
	DRD1	Flange steel grade.
	GRD2	Web steel grade.
	GRD3	Weld electrode yield stress (for welded shapes).
4	NA	Flag, if NA = 1 then flange element width is generated internally; otherwise it is input.
5	DX(J)	Flange element widths; necessary if NA $\neq$ 1.

Card No.	Input Variable	Definition
6	NB	Flag, if NB = 2 then web element depths are generated internally, otherwise they are input.
7	DY(J)	Web element depths, necessary if NB $\neq$ 2.
8	NC	Flag, if NC = 3 then element yield stresses are generated internally.
9	SYF(J)	Flange element (normalized) yield stress, if NC = 3 then SYF(J) = 1.0.
10	SYW(J)	Web element (normalized) yield stress if NC = 3 then SYW(J) = 1.0.
11	RSTF1(J)	Residual stress input for flange 1.
12	RSTW1(J)	Residual stress input for web 1.
13	RSTF2(J)	Residual stress input for flange 2.
14	RSTW2(J)	Residual stress input for web 2 (box shape).
15	NCYCLE	No. of iterations necessary for a given deflection to find the equilibrium force acting on the column.

Card No.	Input Variable	Definition
	IMAX	No. of deflection increments needed to reach P_{max}.
	YS	Average cross-sectional yield stress.
	E	Modulus of elasticity.
16	AXIS	If AXIS = 4, then the strength is evaluated for x-axis buckling; if AXIS = 7, then it is found for y-axis buckling.
17	LINCR	Increment increase of λ.
	LSTART	Initial value of λ.
	NLAM	No. of values of λ.
18	NEOL	No. of initial curvature values to be used.
	EIL(J)	Value of initial curvatures.
19	OPT	Flag, if OPT = 8 then P-δ values are output; otherwise no such output is provided.

A.3 Program Listing

```
      PROGRAM  MAXLD
      DIMENSION RESTF1(50),RESTW1(50),RESTF2(50),RESTW2(50)
     1,ALAM(50),EIL(50),Y1MAX(50,10),X2(50,10),NCO(50,50),NTE(50,50)
      DIMENSION X1(50,50),Y1(50,50),NUMA(50)
      COMMON/AR/ RSTF1(50),RSTF2(50),RSTW1(50),RSTW2(50),NW,NF,OUT
      COMMON/BR/ SF,MOMENT,BASTR,PHI,YSTR,SWITCH
      COMMON/CR/ NSHAPE
      COMMON/DR/ DX(50),DY(50),X(50),Y(50),XI,YI,XA,YA,AREA,D,B
      COMMON/ER/ XAA(50),YAA(50),XAAM(50),YAAM(50)
      COMMON/FR/ NYT,NYC
      COMMON/GR/ W,T,SYF(50),SYW(50),ASY
      REAL LINCR,LSTART,LAM,LAMDA
      REAL L,MOMLD,MOMENT
      REAL M,MU
      REAL LAMA,LAMB(50),POPY(50)
      INTEGER OUT,SWA,SWB,GRD1,GRD2,GRD3
      INTEGER AXIS,OPT
      EQUIVALENCE (RESTF1,LAMB),(RESTF2,POPY)
       CHARACTER TITLE*70

C******  OPEN INPUT,OUTPUT FILE NAMES
       CHARACTER*50 INNAME,OUTNAME
       WRITE(5,*,ERR=1000) 'WHAT IS THE INPUT FILE NAME ?  '
 1000  ACCEPT 1001,INNAME
 1001  FORMAT(A)
       OPEN(UNIT=12,FILE=INNAME,STATUS='OLD',READONLY)
       WRITE(5,*,ERR=1107) 'CHOOSE THE OUTPUT FILE NAME !  '
 1107  ACCEPT 1001,OUTNAME
       OPEN(UNIT=16,FILE=OUTNAME,STATUS='NEW')
       WRITE(*,*) 'INPUT & OUTPUT FILE NAMES ACCEPTED '

      READ(12,533) NPROB,TITLE
 533  FORMAT(I1,A)
      WRITE(OUT,534)NPROB,TITLE
 534  FORMAT(1H1,//,4X,'PROBLEM NO. =',I2,'  TITLE: ',A)
      READ(12,*)NSHAPE,RNAME
      IF(NSHAPE .EQ. 1) GOTO 4
      IF(NSHAPE .EQ. 2) GO TO 14
 4    WRITE(OUT,114) NSHAPE,RNAME
 114  FORMAT(/////,30X,'THIS SHAPE IS A WIDE FLANGE SHAPE',//,
     130X,'NO. USED FOR WF SHAPES IS =',2X,I2,//,30X,'DESIGNATION
     2 OF THE CROSS-SECTION IS =',2X,F9.4)
      GOTO 69
 14   WRITE(OUT,115) NSHAPE,RNAME
 115  FORMAT(/////,30X,'THIS SHAPE IS A BOX GIRDER',//,30X,'NO.
     1USED FOR BOX IS =',2X,I2,//,30X,'DESIGNATION SHAPE IS =',2X,
     2F9.4)

 69    READ(12,*)NF,NW,B,T,D,W,GRD1,GRD2,GRD3

      DO 9100 J=1,NW
 9100 RSTW2(J)=0.
C
C     GENERATE THE WIDTH OF ELEMENTS IN FLANGE
      READ(12,*)NA
       IF(NA .EQ. 1) GO TO 9101

      READ(12,*) (DX(J),J=1,NF)
      WRITE(OUT,1717) (DX(J),J=1,NF)
 1717 FORMAT(////,10X,'LEGTH(DX) OF BOTH FLAGES IS :',//,2X,20(1X,F5.2))
```

```
      GOTO 9102
 9101 DO 9103 J=1,NF
      RNF=NF
 9103 DX(J)=B/RNF
      WRITE(OUT,1710)
 1710 FORMAT(////,10X,'ELEMENT LENGTH (DX) GENERATED INTRNALLY BY
     1 (B/NW) NA FLAG = 1',/)
      WRITE(OUT,1718)   (DX(J),J=1,NF)
 1718 FORMAT(///,10X,'LENGTH OF EACH ELEMENT (DX) OF BOTH FLANGES
     1 IS :',//,2X,20(1X,F5.2))
C
 9102 READ(12,*)NB
       IF(NB .EQ. 2) GO TO 9104
      READ(12,*)  (DY(J),J=1,NW)
      WRITE(OUT,1719)  (DY(J)  ,J=1,NW)
 1719 FORMAT(///,30X,'WEB=',1X,F5.2)
      GOTO 9105
 9104 DO 9106 J=1,NW
      RNW=NW
 9106 DY(J)=D/RNW
      WRITE(OUT,1711)
 1711 FORMAT(//,10X,'ELEMENT DEPTH (DY) GENRATED AUTOMATICALLY BY
     1 (D/NW) NB FLAG = 2',//)
      WRITE(OUT,1720)  (DY(J),J=1,NW)
 1720 FORMAT(/,15X,'DEPTH OF WEB ELEMENT(DY)=', F5.2)
C
C
C****** READ DATA FOR VARIATION OF YIELD STRENGTH IN FLANG AND WEB
C
 9105 READ(12,*)NC
C
       WRITE(OUT,1721) NA,NB,NC
 1721  FORMAT(///,10X,'FLAGS OF CALCULATIONS ARE :',//,5X,'NA =',2X,I1,
     1 /,5X,'NB =',2X,I1,/,5X,'NC =',2X,I1)
       IF(NC .EQ. 3) GO TO 9107
C
      READ(12,*)  (SYF(J),J=1,NF)
      WRITE(OUT,1735)  (SYF(J),J=1,NF)
 1735 FORMAT(20X,'YIELD STRESS FOR FANGES ELEMENTS IS :',//,2X,
     120(1X,F5.0))
      READ(12,*)  (SYW(J),J=1,NW)
      WRITE(OUT,1722)  (SYW(J),J=1,NW)
 1722 FORMAT(20X,'(WEB STRESS)',F5.0)

      GOTO 9108
C
 9107 DO 9109 J=1,NF
 9109 SYF(J)=1.
      DO 9110 J=1,NW
 9110 SYW(J)=1.0
      WRITE(OUT,1712)
 1712 FORMAT(///,10X,'AVERAGE YIELD STRESS IS =1.0  NC= 3',/)
 9108 XA=0.
       IF(NSHAPE.EQ.2) XA=B*.5-W*.5
      YA=.5*(D+T)
       IF(NSHAPE.EQ.2)     YA=.5*(D+T)
C
C***** CHECK THE LAY OUT AND CHECK THE RESULT
C
```

```
      CALL LAYOUT(X,DX,NF,B)
      CALL LAYOUT(Y,DY,NW,-D)
      CHECK=X(NF)+DX(NF)*.5-X(1)-DX(1)*.5
      IF(CHECK-B.GT..01) GOTO 9111
      CHECK=-Y(NW)-DY(NW)*.5+Y(1)+DY(1)*.5
      IF(CHECK-D.GT..01) GOTO 9112

      AREA=2.*B*T+D*W
       IF (NSHAPE.EQ.2)     AREA=2.*B*T+2.*D*W
C
C******READ RESIDUAL STRESS
C
      READ(12,*)      (RSTF1(J),J=1,NF)
      READ(12,*)      (RSTW1(J),J=1,NW)
      READ(12,*)      (RSTF2(J),J=1,NF)
C
      WRITE(OUT,1723)  (RSTF1(J),J=1,NF)
 1723 FORMAT(///,10X,'FLANGE 1 RESIDUAL STRESSES DISTRIBUTION IS :',
     1//,18F7.2,//)
      WRITE(OUT,1724)  (RSTW1(J),J=1,NW)
 1724 FORMAT(/,37X,'WEB',2X,F5.2)
      WRITE(OUT,1725)  (RSTF2(J),J=1,NF)
 1725 FORMAT(//,10X,'FLANGE2 RESIDUAL STRESSES:',//,18F7.2,//)
      IF(NSHAPE .EQ. 1) GO TO 311
      IF(NSHAPE.EQ.2) READ(12,*)     (RSTW2(J),J=1,NW)
      WRITE(OUT,2346)   (RSTW2(J),J=1,NW)
 2346 FORMAT(/,37X,'WEB2',2X,F5.2)

 311  READ(12,*)    NCYCLE,IMAX,YS,E
C1001 FORMAT(I2,1X,I2,2F10.0)
      SY=YS
C
C********* COMPUTE THE AVERAGE YIELD LOAD AND ANERAGE YIELD STRENGH
      PYF=0.
      PYW=0.
      DO 8114 J=1,NF
 8114 PYF=SYF(J)*SY*DX(J)*T+PYF
      DO 8115 J=1,NW
 8115 PYW=SYW(J)*SY*DY(J)*W+PYW

      PY=2.0*PYF+PYW
       IF(NSHAPE.EQ.2)     PY=2.0*(PYF+PYW)
      ASY=PY/AREA
C
C******** ADJUST THE GIVEN DISTRIBUTION OF YIELD STRENGTH YO SY/ASY
C
      FACT=SY/ASY
      DO 9114 J=1,NF
 9114 SYF(J)=SYF(J)*FACT
      DO 9115 J=1,NW
 9115 SYW(J)=SYW(J)*FACT
      WRITE(OUT,1604)
 1604 FORMAT(///,1H1,//,10X,'MAX.STRENGTH ANALYSIS OF A CENTRALL LOADED
     1COLUMN',//,1H-,9X,'CROSS-SECTIONAL AND MATERIAL PROPERTIES',//)
      WRITE(OUT,1605)GRD1,GRD2
 1605 FORMAT(1H0,10X,'STEEL GRADE',10X,'FLANGE GRADE IS A',I3,10X,'WEB
     1 GRADE IS A',I3)
      WRITE(OUT,948)B,D,T,W,AREA,YS,ASY,PY,E,NSHAPE,NCYCLE,IMAX,NF,NW
 948  FORMAT(//1H-,9X,'CROSS-SECTIONAL PROPRTIES',///,10X,'FLANGE WIDTH
     1',13X,'B =',F10.3,//,10X,'NET DEPTH OF WEB',9X,'D =',F10.3,//,10X,
```

```
     2'FLANGE THIKCNESS',9X,'T =',F10.3,//,10X,'WEB THICKNESS',12X,'W
     3=',F10.3,//,10X,'AREA OF CROSS-SECTION',4X,'A =',F10.3,////,10X,'
     4MATERIAL PROPERTIES',///,10X,'YIELD STREGTH',11X,'YS =',F10.3,//,
     510X,'AVERAGE YIELD STREGTH',3X,'ASY =',F10.3,//,10X,'YIELD LOAD',1
     65X,'PY =',F10.3,//,10X,'MODULUS OF ELASTICITY',4X,'E =',F10.1,//,
     725X,'SHAPE=',2X,I1,//,20X,'NO. OFCYCLE=',2X,I2,//,20X,'MAX ITER=
     8',2X,I2,//,20X,'FALANGE ELEMENT',2X,'NF =',2X,I2,//,20X,'WEB ELE
     9MENT',2X,'NW =',2X,I2,/)

C
C******* PRINT THE DATA OF THE DISTRIBUTION OF THE YIELD STRENGTH
C
      WRITE(OUT,951)
 951  FORMAT(///,1H1,'YIELD STRENGTH DISTRIBUTION (SYN/ASY)',/)
       IF(NC .NE. 3) GO TO  9113
      WRITE(OUT,9151)
 9151 FORMAT(1HO,'CONSTANT',/)
      GOTO 333
 9113 WRITE(OUT,9251) (SYF(J)  ,J=1,NF)
 9251 FORMAT(1HO,'FLANGE =',20F6.3)
      WRITE(OUT,952) (SYW(J), J=1,NW)
 952  FORMAT(20X,'WEB=',F9.3)
 333  PI=4.0*ATAN(1.0)
      C=1./AREA
      YSTR=ASY/E

C
C*********** ADJUST THE RESIDUAL STRESS DISTRIBUTION FOR EQUILIBRIUM
C
      CALL ADJUST
      IF(SWITCH .EQ. 1.0) CALL EXIT
      YS=ASY
C
C******* NON-DIMENSIONALIZE THE RESIDUAL STRESS DISTRIBUTION
C
      DO 6 J=1,NF
      RESTF2(J)=-RSTF2(J)/YS
 6    RESTF1(J)=-RSTF1(J)/YS
      DO 5 J=1,NW
      RESTW2(J)=-RSTW2(J)/YS
 5    RESTW1(J)=-RSTW1(J)/YS

      READ(12,*) AXIS
      IF(AXIS .EQ. 4) R=XI
      IF(AXIS .EQ. 7) R=YI
      R=SQRT(R/AREA)
      CONST=R*PI*SQRT(E/ASY)

      READ(12,*) LINCR,LSTART,NLAM
      WRITE(OUT,1759)LINCR,LSTART,NLAM,AXIS,CONST,R
 1759 FORMAT(///,30X,'INCREMENT=',2X,F8.3,//,30X,'START=',5X,F8.3,//,
     130X,'NO. OF LAMDA=',2X,I2,/,30X,'AXIS OF BENDING=',3X,I1,//,30X
     2,'CONSTANT=',2X,F8.3,//,35X,'R =',3X,F8.3,/)

      LAM=LSTART-LINCR
      DO 9116 J=1,NLAM
      LAM=LAM+LINCR
      ALAM(J)=LAM
 9116 CONTINUE
C
```

```
C******* READ THE VALUE OF INITIAL DEFLECTION FOR WHICH COLUMN CURVES
C         ARE TO BE COMPUTED
C
      READ(12,*) NEOL,(EIL(J),J=1,NEOL)
      READ(12,*) OPT
      WRITE(OUT,759) OPT,NEOL,(EIL(J),J=1,NEOL)
 759  FORMAT(///,30X,'FLAG OPT=', I1,/,30X,'NO. OF INI. OUT OF STRAIT.=
     1',I2,/,30X,'VALUES OF NEOL=',7F10.5,/)

      LOOP1=0
 9120 LOOP1=LOOP1+1
      IF(LOOP1.GT.1.AND.OPT.EQ.8) GOTO 2222
 8884 IF(LOOP1.GT.NEOL)CALL EXIT
      EOL=EIL(LOOP1)
      WRITE(OUT,955)GRD1,GRD2,AXIS,EOL,GRD3
 955  FORMAT(1H1,7X,'STEEL GRADES ARE',2X,2I10,//,7X,'AXIS BENDING',
     12X,I2,//,7X,'INITIAL OUT OF STRAITNESS(VO/L)=',F10.5,10X,'WELD
     2 GRADE IS',2X,I3,//)
      WRITE(OUT,950)
 950  FORMAT(1H0,6X,'LAMDA   P/PY',8x,'L',8X,'P',8X,'V',7X,'VO',
     14X,'NO. OF STEPS',/)
      LOOP2=0
 939  LOOP2=LOOP2+1
      IF(LOOP2.GT.NLAM) GOTO 9120
      LAMDA=ALAM(LOOP2)
      L=LAMDA*CONST
C
C******  INITIALIZE THE VALUES OF VARIABLE USED IN ITERATION
C
      DINCR=0.08
  1   NYC=0
      NYT=0
      DINCR=.5*DINCR
      BASTR=0.
      VO=EOL*L
      V=0.
      AXLOAD=0.
      DEFL=VO
      VINCR=DINCR
      NUM=0
 10   NUM=NUM+1
      NCO(NUM,LOOP2)=NYC
      NTE(NUM,LOOP2)=NYT
      Y1(NUM,LOOP2)=AXLOAD
      X1(NUM,LOOP2)=V
      IF(NUM.EQ.1) GOTO 88

      CHECK1=Y1(NUM-1,LOOP2)
      IF(NUM.EQ.IMAX)  GOTO 9126
      IF(AXLOAD.LE.CHECK1) GOTO 8
C
C********* SELECT VALUE OF VINCR ACCORDING TO THE VALUE OF LAMDA
C
      IF(LAMDA .LE. 1.) GO TO 9117
      IF(LAMDA .GT. 2.) GO TO 9118
      IF(AXLOAD .LT. .15) GO TO 9119
      GOTO 88
 9117 IF(AXLOAD .LT. .4) GO TO 9119
      GOTO 88
 9118 IF(AXLOAD .LT. .05) GO TO 9119
```

```
      GOTO 88
 9119 VINCR=2.*VINCR
 88   DEL=.05
      BASTR=BASTR+.05
      V=V+VINCR
      PHI=PI*PI*V/(L*L)
      DEFL=VO+V
      SWA=0
      IC=0
      M=0.0
      MU=0.0
      ITER=0
C
C******* START ITERATION TO OBTAIN P/PY FOR A SPECFIC VALUE OF V
C
 11   ITER=ITER+1

      IF(ITER .GE. NCYCLE) GO TO 26
C
C****** INTEGRATE ALONG SHAPE TO OBTAIN INTERNAL MOMENT AND FORCES
C****** BENDING ABOUT Y_AXIS
C
C      IF(AXIS.EQ.XAX) GOTO 40
       IF(AXIS .EQ. 4)   GO TO 40
      CALL SUMSTR(RESTF1,X,SYF,DX,NF,T)
      CALL SUMSTE(RESTW1,XAA,SYW,DY,NW,W)
      CALL SUMSTE(RESTF2,X,SYF,DX,NF,T)
       IF(NSHAPE.EQ. 2)    CALL SUMSTE(RESTW2,XAAM,SYW,DY,NW,W)
      GOTO 200
C
C******** BENDING ABOUT X-AXIS
C
 40   CALL SUMSTR(RESTW1,Y,SYW,DY,NW,W)
      CALL SUMSTE(RESTF1,YAA,SYF,DX,NF,T)
       IF(NSHAPE.EQ. 2)    CALL SUMSTE(RESTW2,Y,SYW,DY,NW,W)
      CALL SUMSTE(RESTF2,YAAM,SYF,DX,NF,T)
 200  MOMLD=-(MOMENT/DEFL)*C
      AXLOAD=SF*C
C
C******** CHECK EQUILIBRIUM CONDITION
C******** IF ACCURACY IS SUFFICINT GOTO THE NEXT VALUE OFV
C
      DELTA=AXLOAD-MOMLD
      IF(ABS(DELTA) .LE. .002) GO TO 10
      IF(MOMLD .EQ. 0.)GO TO 26
      IF(AXLOAD .GT. 1.) GO TO 26
C
C****** THE FOLLOWING STATEMENT CONTROLS THE ITERATION PROCEDURE AND
C       CHANGE THE VALUES OF BASTR AT EVERY ITERATION CYCLE SUCH THAT
C       FAST CONVERGENCE IS OBTAINED
C
      IF(SWA) 50,60,50
 50   IF(DELTA) 70,81,81
 70   SWB=-1
      GOTO 91
 81   SWB=1
 91   IF(SWB-SWA) 103,104,103
 60   IF(DELTA)111,120,120
 111  SWA=-1
      GOTO 101
```

```
 120  SWA=1
 101  IF(M) 300,301,300
 301  IF(DELTA) 100,100,90
 90   M=-1.0
      GOTO 300
 100  M=1.0
 300  BASTR=BASTR+DEL*M
      GOTO 11
 103  IF(IC) 106,105,107
 104  IF(IC)107,101,106
 106  MU=1.0
      GOTO 108
 107  MU=-1.0
      GOTO 108
 105  IF(M) 109,112,112
 109  IC=-2
      GOTO 106
 112  IC=1
      GOTO 107
 108  DEL=DEL/2.
      BASTR=BASTR+MU*DEL
      GOTO 11
C
C******* PRINT THE RESULT OF THE COMPUTATION
C
 8    IF(NUM .LT. 4) GO TO 1
      Y1MAX(LOOP2,LOOP1)=CHECK1
      X2(LOOP2,LOOP1)=LAMDA
      NUMA(LOOP2)=NUM
      PMAX=CHECK1*PY
      WRITE(OUT,957) LAMDA,CHECK1,L,PMAX,X1(NUM-1,LOOP2),VO,NUM
 957  FORMAT(6X,2F8.3,2F10.2,F8.3,F8.5,I10)
      GOTO 939
C
C******* PRINT THE DATA OF THE LOAD DEFLECTION CURVE
C
 2222 WRITE(OUT,9000)
 9000 FORMAT(1H1)
      DO 1555 J=1,NLAM
      WRITE(OUT,1108) ALAM(J)
 1108 FORMAT(1HO,'VALUES OF LOAD-DEF. CURVE FOR LAMDA=',F10.3)
      NUM=NUMA(J)
      WRITE(OUT,1199) (X1(I,J),Y1(I,J),NCO(I,J),NTE(I,J),I=1,NUM)
 1199 FORMAT(///,3X,'V=',F7.3,2X,'P/PY=',F7.3,5X,I10,2X,'ELEMEN YIEL.
     1IN COPR.',I10,2X,'1N TENSION',/)
 1555 CONTINUE
      GOTO 8884
C
C****** ERROR MESSAGE
C
 9111 WRITE(OUT,1002) B
 1002 FORMAT(1HO,'ERROR NUMBER 1.. ERROR IN LAYOUT(X-DIRECTION),B='
     1,F10.3)
      WRITE(OUT,1003) (DX(J),J=1,NF)
 1003 FORMAT(1HO,'DX(J)=',20F6.3)
      WRITE(OUT,1004) (X(J),J=1,NF)
 1004 FORMAT(1HO,'X(J)=',20F6.3)
      CALL EXIT
 9112 WRITE(OUT,1005) D
 1005 FORMAT(1HO,'ERROR NUMBER 1.. ERROR IN LAY OUT(Y-DIRECTION),D='
```

```
     1,F10.3)
      WRITE(OUT,1006)  (DY(J),J=1,NW)
 1006 FORMAT(1HO,'DY(J)=',20F6.3)
      WRITE(OUT,1007)  (Y(J),J=1,NW)
 1007 FORMAT(1HO,'Y(J)=',20F6.3)
      CALL EXIT
 9996 WRITE(OUT,5555) NUM
 5555 FORMAT(1HO,'ERROR NUMBER2.. DEFLECTION INCREMENT TOO LARGE'/
     11HO,'MAXIMUM LOAD OBTAINED AFTER',I10,'STEPS',/)
      GOTO 4444
 9126 WRITE(OUT,1100) IMAX
 1100 FORMAT(1HO,'ERROR NUMBER 2..NUMBER OF DEFLECTION INCREMENT TOO
     1SMALL',/,1HO,'MAXIMUM LOAD NOT OBTAINED AFTER',I10,'STEPS',/)
 4444 WRITE(OUT,1108)LAMDA
      NUM1=NUM-1
      WRITE(OUT,1109)  (X1(J,LOOP2),Y1(J,LOOP2),J=1,NUM1)
 1109 FORMAT(1HO,'V=',F10.3,' P/PY=',F10.3)
      CALL EXIT
 26   WRITE(OUT,1900) ITER,LAMDA,V,BASTR,MOMLD,AXLOAD,DELTA
 1900 FORMAT(1HO,'ERROR NUMBER 4.. CONVERGENCE NOT OBTAINED AFTER',I10,
     1'CYCLES,LAMDA=',F10.3/
     21HO,'V=',F10.3,'BASTR=',F10.3,'MOMLD=',F10.3,' AXLOAD=',F10.3,
     3'DELTA=',F10.3)
      CALL EXIT

       END

      SUBROUTINE SUMSTR(RESTR,X,SY,DX,N,T)
C
C******** THIS PERFORMS NUMERICAL INTEGRATINO OF STRESS
C         ALONG THE COMPONENT PLATE OF THE SHAPE TO OBTAIN INTERNAL MOMENT
C         AND FORCE. IT ALSO COMPUTES THE ELEMEMTS YIELDED IN TENSION
C         COPMRESSION
C
      COMMON/BR/ SF,MOMENT,BASTR,PHI,YSTR,SWITCH
      COMMON/FR/ NYT,NYC
      DIMENSION RESTR(50),X(50),DX(50),SY(50)
      REAL MOMENT
      SF=0.0
      MOMENT=0.0
      NYT=0
      NYC=0
      ENTRY SUMSTE(RESTR,X,SY,DX,N,T)
      C=PHI/YSTR
      DO 20 J=1,N
      ELSTRN=RESTR(J)+BASTR-C*X(J)
      ELYSTR=SY(J)
      IF(ELSTRN.LT.-ELYSTR) GOTO 60
      IF(ELSTRN.GT.ELYSTR)  GOTO 70
      STRESS=ELSTRN
      GOTO 10
 60   STRESS=-ELYSTR
      NYT=NYT+1
      GOTO 10
 70   STRESS=ELYSTR
      NYC=NYC+1
 10   FELE=STRESS*DX(J)*T
      SF=SF+FELE
      DELMOM=FELE*X(J)
```

```
 20   MOMENT=MOMENT+DELMOM
      RETURN
      END


      SUBROUTINE ADJUST
C
C********THIS COMPUTES OUT OF EQUILIBRIUM MOMENT AND FORCES
C          AND STRESS OF THE RESUDUAL STRESS DISTRIBUTION
C          THE RESIDUAL STRESS IS THEN ADJUSTED FOR EQUIL.
C
      COMMON/AR/ RSTF1(50),RSTF2(50),RSTW1(50),RSTW2(50),NW,NF,IOUT
      COMMON/BR/ SF,MOMENT,BASTR,PHI,YSTR,SWITCH
      COMMON/CR/NSHAPE
      COMMON/DR/ DX(50),DY(50),X(50),Y(50),XI,YI,XA,YA,AREA,D,BA
      COMMON/ER/ XAA(50),YAA(50),XAAM(50),YAAM(50)
      COMMON/FR/ NYT,NYC
      COMMON/GR/ W,T,SYF1(50),SYW1(50),ASY
      DIMENSION SYW(50),SYF(50)
      REAL MOMENT
C
C******** COMPUTE THE MOMENT OF INERTIA
C
      T1=2.*T
      W1=W
       IF(NSHAPE.EQ.2 )    W1=2.*W
      CALL MINERT(YI,DX,X,NF,D,XA,W1,T1)
      CALL MINERT(XI,DY,Y,NW,BA,YA,T1,W1)
      WRITE(IOUT,1600) XI,YI
 1600 FORMAT(1HO,'IX=',F10.3,10X,'IY=',F10.3,2X,'INCH4')
      WRITE(IOUT,1400)
 1400 FORMAT(1H1,'ACTUAL RESIDUAL STRESS DISTRIBTION',/,2X,'KSI',/)
      CALL OUTPUT
      BASTR=0.0
      PHI=0.0
      SWITCH=0.0
      DO 30 J=1,NW
      XAA(J)=XA
      XAAM(J)=-XA
 30   SYW(J)=SYW1(J)*ASY
      DO 31 J=1,NF
      YAA(J)=YA
      YAAM(J)=-YA
 31   SYF(J)=SYF1(J)*ASY
C
C******** COMPUTE THE MOMENT ABOUT THE AXES AND THE AXIAL FORCE
C
      CALL SUMSTR( RSTF1,X,SYF,DX,NF,T)
      CALL SUMSTE( RSTW1,XAA,SYW,DY,NW,W)
      CALL SUMSTE( RSTF2,X,SYF,DX,NF,T)
      IF(NSHAPE .EQ. 2)    CALL SUMSTE(RSTW2,XAAM,SYW,DY,NW,W)
      SUMF=SF
      SUMY=MOMENT
      CALL SUMSTR(RSTW1,Y,SYW,DY,NW,W)
      CALL SUMSTE(RSTF1,YAA,SYF,DX,NF,T)
      IF(NSHAPE .EQ. 2)  CALL SUMSTE(RSTW2,Y,SYW,DY,NW,W)
      CALL SUMSTE(RSTF2,YAAM,SYF,DX,NF,T)
      SUMX=MOMENT
      IF(NYT.EQ.0.AND.NYC.EQ.0) GOTO 20
```

```
      WRITE(IOUT,1710) NYT,NYC
 1710 FORMAT(1HO,'ERROR NUMBER 3=RESIDUAL STRESS EXCEEDS YIELD STRESS
     1(TENSION) IN',I10,'ELEM.',/,5X, '(COMPR.) IN',I10,' ELEM.',/)
 20   WRITE(IOUT,1700) SUMF
 1700 FORMAT(1HO,'OUT OF EQUILIBRIUM FORCE=',F10.5)
      SUMS=SUMF/AREA
      WRITE(IOUT,1800) SUMS
 1800 FORMAT(1HO,'OUT OF EQULIBRIUM STRESS=',F10.5)
      WRITE(IOUT,1900) SUMY
 1900 FORMAT(1HO,'OUT OF EQUILI. MOMENT MY=',F10.5)
      WRITE(IOUT,2000) SUMX
 2000 FORMAT(1HO,'OUT OF EQUILI. MOMENT MX=',F10.5)
      CALL EQUILI(RSTF1,RSTF2,SUMY,YI,X,NF)
      BJA=SUMS+SUMY/YI*XA
      BJB=SUMS-SUMY/YI*XA
      DO 70 J=1,NW
      RSTW1(J)=RSTW1(J)-BJA
       IF(NSHAPE.EQ. 2)   RSTW2(J)=RSTW2(J)-BJB
 70   CONTINUE
      CALL EQUILI(RSTW1,RSTW2,SUMX,XI,Y,NW)
      BJC=SUMS+SUMX/XI*XA
      BJD=SUMS-SUMX/XI*XA
      DO 80 J=1,NF
      RSTF1(J)=RSTF1(J)-BJC
 80   RSTF2(J)=RSTF2(J)-BJD
      WRITE(IOUT,2100)
 2100 FORMAT(1H1,'RESIDUAL STRESS_DISTRIBUTION ADJUSTED FOR EQUILIBRIUM
     1',/,5X,'KSI',/)
      CALL OUTPUT
      RETURN
      END


      SUBROUTINE MINERT(XI,D,X,N,B,XA,T,W)
C
C******** THIS IS TO FIND THE MOMENT OF INERTIA OF THE CROSS SECTION
C
      DIMENSION D(50),X(50)
      XI=0.0
      DO 10 J=1,N
 10   XI=XI+W*D(J)*X(J)*X(J)
      XI=XI+XA*XA*B*T
      RETURN
      END


      SUBROUTINE EQUILI(RST1,RST2,SUMM,XI,X,N)
C
C******** THIS SUBROUTINE IS USED TO ADJUST THE RESIDUAL STRESS DISTR.
C         FOR EQUILI..
C
      DIMENSION RST1(50),RST2(50),X(50)
      BJE=SUMM/XI
      DO 10 J=1,N
      RST1(J)=RST1(J)-BJE*X(J)
 10   RST2(J)=RST2(J)-BJE*X(J)
      RETURN
```

```
      END

      SUBROUTINE OUTPUT
C
C********* THIS PRINTS THE RESIDUAL STRESS IN ACERTAIN PATTERN
C
      COMMON/AR/ RSTF1(50),RSTF2(50),RSTW1(50),RSTW2(50),NW,NF,IOUT
      COMMON/CR/NSHAPE
      NF02=(NF+1)/2
      WRITE(IOUT,2000) (RSTF1(J),J=1,NF02)
 2000 FORMAT(1HO,'(FLANGE)',18F7.2)
      IF(NSHAPE .EQ. 1)  GO TO 1
      WRITE(IOUT,3000) (RSTW2(J),J=1,NW)
 3000 FORMAT(1HO,'(WEB)',F7.2)
      GOTO 2
 1    WRITE(IOUT,5000) (RSTW1(J),J=1,NW)
 2    WRITE(IOUT,2000) (RSTF2(J),J=1,NF02)
      WRITE(IOUT,4000)
 4000 FORMAT(1H1)
      WRITE(IOUT,2000) (RSTF1(J),J=NF02,NF)
      IF(NSHAPE .EQ. 1)  GO TO3
      WRITE(IOUT,5000)  (RSTW1(J),J=1,NW)
 5000 FORMAT(50X,'(WEB)',F7.2)
 3    WRITE(IOUT,2000) (RSTF2(J),J=NF02,NF)
      RETURN
      END

      SUBROUTINE LAYOUT(X,D,N,B)
      DIMENSION X(50),D(50)
      REAL M
      M=1.
      IF(B.LT.0.) M=-1.
      XA=0.
      B1=0.5*B
      DO 10 J=1,N
      XA=XA+D(J)*.5
      X(J)=M*XA-B1
      XA=XA+D(J)*.5
 10   CONTINUE
      RETURN
      END
```

REFERENCES

1. Kuzmanovic, Bogdan O. and Willens, Nicholaas W., "Steel Design for Structural Engineers," Prentice-Hall, Inc., 2nd Edition, 1983.

2. Euler, L., "Sur La Force Des Colonnes (On the Strength of Columns)," Academie Royale des Sciences et Belles Lettres de Berlin, Mein., Vol. 13, 1759. English translation by J. A. Van den Brock, American Journal of Physics, Vol. 15, No. 4, 1947.

3. Johnston, B. G. (Ed.), "Guide to Stability Design Criteria for Metal Structures," John Wiley and Sons, Inc., 3rd Edition, 1974.

4. McCormac, Jack C., "Structural Steel Design," Harper and Row, Publishers, New York, 3rd Edition, 1981.

5. Bjorhovde, R., "Deterministic and Probabilistic Approaches to the Strength of Steel Columns," Ph.D. Dissertation, Lehigh University, May 1972.

6. Ballio, G. and Mazzolani, F. M., "Theory and Design of Steel Structures," Published by Chapman and Hall Ltd., New York, 1983.

7. Gaylord, Edwin H., "Design of Steel Structures," Published by McGraw-Hill, Inc., 2nd Edition, 1972.

8. Alpsten, G. A., "Thermal Residual Stresses in Hot-rolled Steel Members," Fritz Engineering Laboratory Report No. 337.3, Lehigh University, Dec. 1968.

9. Fujita, Y., "Ultimate Strength of Columns with Residual Stresses," Journal of the Society of Naval Architecture of Japan, 102 (1958) and 107 (1960).

10. Osgood, W. R., "The Effect of Residual Stresses on Column Strength," Proceedings, First U. S. National Congress on Applied Mechanics, June 1951.

11. Alpsten, G. A., "Residual Stresses, Yield Strength and Column Strength of Hot-Rolled and Roller-Straight End Steel Shapes," Coll. on International Column Strength, Paris, France, Nov. 1972.

12. Brozzetti, J., Alpsten, G. A., and Tall, L., "Residual Stresses in a Heavy Rolled Shape 14 WF 730," Fritz Engineering Laboratory Report No. 337.10, Lehigh University, Jan. 1970.

13. Alpsten, G. A., and Tall, L., "Residual Stresses in Heavy Welded Shapes," Fritz Engineering Laboratory Report No. 337.12, Lehigh University, Jan. 1969.

14. Bjorhovde, R., Brozzetti, J., Alpsten, G. A. and Tall, L., "Residual Stresses in Thick Welded Plates," Fritz Engineering Laboratory Report No. 337.13, Lehigh University, June 1971.

15. Batterman, R. H. and Johnston, B. G., "Behavior and Maximum Strength of Metal Columns," Journal of the Structural Division, ASCE, Vol. 93, No. ST2, April 1967 (pp. 205-230).

16. Beer, H., and Schultz, G., "Theoretical Bases for the European Column Buckling Curves," Construction Metallique, Paris, France, No. 3, 1970.

17. Canadian Standards Association (CSA), "Steel Structures for Buildings--Limit States Design," Canadian Standards Association (CSA), CSA Standard No. S 16.1-1974, Rexdale, Ontario, Canada, 1974.

18. American Institute of Steel Construction (AISC), "Load and Resistance Factor Design Specification for Structural Steel Buildings," Chicago, Illinois, 1986.

19. Osgood, W. R. (Ed.), "Residual Stresses in Metal and Metal Structures," New York, Reinhold Pub. Corp., 1954.

20. Van de Walle, Larry J. (Ed.), "Residual Stresses for Designers and Metallurgists," Proceedings of a conference held 9-10 April, Chicago, IL, 1980. Sponsored by the American Society for Metals, Highway and Off-Highway Vehicles Activity of the Materials Systems and Design Division.

21. Masubuchi, Koichi, "Analysis of Welded Structures, Residual Stresses Distortion and Their Consequences," Pergamon Press Ltd., New York, 1980.

22. Tebedge, Negussie, Alpsten, Goran A., and Tall, Lambert, "Measurement of Residual Stresses: A Study of Methods," Fritz Engineering Laboratory Report, No. 337.8, Lehigh University, Feb. 1971.

23. Tall, L., "Welded Built-up Columns," Fritz Engineering Laboratory Report No. 249.29, Lehigh University, April, 1966.

24. American Society for Testing and Materials (ASTM), "1971 Annual Book for ASTM Standards, Part 4," ASTM, 1916 Race Street, Philadelphia, PA, 1971.

25. Odar, Enver, Nishino, Fumio and Tall, Lambert, "Residual Stresses in Rolled-Treated 'T-1' Shapes," Welding Research Council Bulletin No. 121, New York, April 1967 (pp. 30-36).

26. Arbed, S. A. and the Stahlwerke Peine-Salzgitter Companies, "Buckling of the Thick-Flanged I-section Columns," Joint research program of the ARBED S.A. and the Stahlwerke Peine Salzgitter Companies. ARBED-Recherches, Feb. 9, 1982.

27. Marcus, Samuel H., "Basics of Structural Steel Design," 2nd Edition, Reston, VA: Reston Pub. Co., 1981.

28. Morris, L. J. (Ed.), "Inestability and Plastic Collapse of Steel Structures," Proceedings of Michael R. Home Conference Organized by the University of Manchester with co-sponsor, the Institution of Structural Engineers, 1983.

29. Tall, Lambert (Ed.), "Structural Steel Design," Ronald Press Company, New York, 2nd Edition, 1974.

30. Nishino, F., Tall, L., and Okumura, T., "Residual Stresses and Torsional Buckling Strength of H and Cruciform Column," Japan Society of Civil Engineers, Trans., No. 160, Dec. 1968.

31. Beedle, L. S., "Plastic Design of Steel Frames," published by John Wiley and Sons, Inc., 3rd Edition, 1964.

32. Trahair, N. S., "The Behavior and Design of Steel Structures," Distributed by Halted Press, a Division of John Wiley, 1st Edition, 1977.

33. Davison, Thomas A., "A Theoretical Investigation of the Column Behavior of Hollow Structural Steel Sections," Masters Thesis, University of Toronto, 1977.

34. Structural Stability Research Council, "Determination of Residual Stresses in Structural Shapes," Structural Stability Research Council, Task Group 6, Experimental Techniques, Vol. 5, No. 3, 4-7, Sept. 1981.

35. Young, B. W., "Residual Stresses in Hot-Rolled Members," Coll. on International Column Strength, Paris, France, Nov. 1972.